



Terms and Conditions of Use of Digitised Theses from Trinity College Library Dublin

Copyright statement

All material supplied by Trinity College Library is protected by copyright (under the Copyright and Related Rights Act, 2000 as amended) and other relevant Intellectual Property Rights. By accessing and using a Digitised Thesis from Trinity College Library you acknowledge that all Intellectual Property Rights in any Works supplied are the sole and exclusive property of the copyright and/or other IPR holder. Specific copyright holders may not be explicitly identified. Use of materials from other sources within a thesis should not be construed as a claim over them.

A non-exclusive, non-transferable licence is hereby granted to those using or reproducing, in whole or in part, the material for valid purposes, providing the copyright owners are acknowledged using the normal conventions. Where specific permission to use material is required, this is identified and such permission must be sought from the copyright holder or agency cited.

Liability statement

By using a Digitised Thesis, I accept that Trinity College Dublin bears no legal responsibility for the accuracy, legality or comprehensiveness of materials contained within the thesis, and that Trinity College Dublin accepts no liability for indirect, consequential, or incidental, damages or losses arising from use of the thesis for whatever reason. Information located in a thesis may be subject to specific use constraints, details of which may not be explicitly described. It is the responsibility of potential and actual users to be aware of such constraints and to abide by them. By making use of material from a digitised thesis, you accept these copyright and disclaimer provisions. Where it is brought to the attention of Trinity College Library that there may be a breach of copyright or other restraint, it is the policy to withdraw or take down access to a thesis while the issue is being resolved.

Access Agreement

By using a Digitised Thesis from Trinity College Library you are bound by the following Terms & Conditions. Please read them carefully.

I have read and I understand the following statement: All material supplied via a Digitised Thesis from Trinity College Library is protected by copyright and other intellectual property rights, and duplication or sale of all or part of any of a thesis is not permitted, except that material may be duplicated by you for your research use or for educational purposes in electronic or print form providing the copyright owners are acknowledged using the normal conventions. You must obtain permission for any other use. Electronic or print copies may not be offered, whether for sale or otherwise to anyone. This copy has been supplied on the understanding that it is copyright material and that no quotation from the thesis may be published without proper acknowledgement.

The modulation of microglia by astrocytes; a role for CD200.

F. Fionnuala Cox



**Thesis submitted to University of Dublin for the degree of
Doctor of Philosophy.**

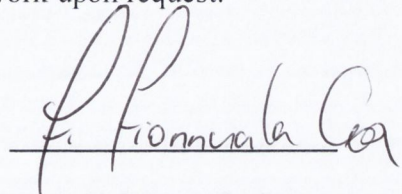
September 2010



Thesis 9709

Declaration of Authorship

This thesis is submitted by the undersigned for the degree of Doctor of Philosophy at the University of Dublin. I declare that this thesis is entirely my own work. This work has not been submitted in whole or in part to this or any other university for any other degree. The author gives permission to the library to lend or copy this work upon request.

A handwritten signature in black ink, appearing to read 'F. Fionnuala Cox', written over a horizontal line.

F. Fionnuala Cox

Abstract

Glial cell activation is believed to play a critical role in the pathogenesis of neurodegenerative diseases, impairing neuronal function and ultimately leading to cognitive decline. Epidemiological studies have advocated the benefit of anti-inflammatory drugs in decreasing the risk of developing, or delaying the onset of, dementia. The objective of this thesis was to investigate the consequences of modulating glial cell activity with two different compounds, FGL and a CD200 fusion protein. First, the ability of the NCAM-mimetic peptide, FGL, to attenuate LPS and A β -stimulated changes on primary mixed glial cells and isolated microglia was investigated. Next, the dependence of the action of FGL on expression of the immunosuppressive molecule CD200 was examined, using glia prepared from wildtype and CD200^{-/-} animals. Finally, the modulatory effects of CD200Fc on LPS- and aged-induced deficits in LTP and in markers of inflammation in hippocampus were explored.

FGL attenuated the LPS- and A β -induced increase in the pro-inflammatory cytokine IL-1 β , in mixed glial cells and this action was blocked when mixed glia were exposed to the FGFR-1 antagonist, SU5402. FGL also decreased the LPS-induced increase in IL-1 β release, but not transcription, in isolated microglial cells. Interestingly, basal IL-1 β was greater in the isolated cultures compared with mixed glial preparations. An increase in markers of microglial activation was also found in mixed glia prepared from CD200^{-/-} animals. They displayed increased basal levels of CD11b and CD68, compared with glia cultured from their wildtype counterparts. Additionally, glia cultured from CD200^{-/-} mice exhibited an exaggerated response to LPS, with increased CD40 and ICAM-1 mRNA expression, as well as, enhanced IL-1 β , TNF- α and IL-6 transcription and release, indicating that the loss of CD200 increased inflammatory markers. The markers of glial cell activation were attenuated by FGL in mixed glia prepared from wildtype, but not CD200^{-/-}, mice. It was demonstrated that CD200 was expressed on a CD11b-negative population in a mixed glial preparation and CD200 expression was increased on isolated astrocytes after incubation in FGL. Moreover, exposing microglia to a membrane fraction prepared from isolated astrocytes, previously incubated in FGL, decreased the LPS-stimulated increase in pro-inflammatory cytokine production from these isolated cells. Finally, acute intrahippocampal administration of CD200Fc reversed the LPS- and age-related deficit in LTP in the perforant path-granule cell synapses. There was an age-related decrease in CD200, and CD200Fc reduced the age-associated increase in markers of microgliosis, astrogliosis and oxidative stress in hippocampus, while also enhancing concentration of the neuroprotective hormone IGF-1 and phosphorylation of its down-stream signalling molecule AKT.

One of the central findings of this study was that primary astrocytes express CD200 and in turn can modulate the activity of microglial cells, which bear the receptor. *In vitro* analysis demonstrated that, in the absence of CD200, primary microglia display markers of activation, which are potentially destructive *in vivo*. Senescence is the primary risk factor for developing certain neurodegenerative diseases, particularly Alzheimer's disease. The findings of this thesis reveal an age-related increase in markers of inflammation and concomitant decrease in CD200 in hippocampus, which may contribute to the risk of developing a neurodegenerative disease like AD. CD200Fc reversed the age-related neuroinflammatory changes and enhanced synaptic function, characterised by LTP. Thus up-regulating endogenous CD200 or administering an exogenous source could maintain glial cells in a quiescent state and support neuronal integrity.

Acknowledgements

I wish to express my gratitude to Professor Marina Lynch for her help and guidance over the past three years. I would also like to acknowledge all in MAL Lab for creating an enjoyable work environment. Finally, I thank my friends and family for their support and encouragement.

Abbreviations

AD	Alzheimer's Disease
ANOVA	Analysis of variance
AP5	(2R)-amino-5-phosphonovaleric acid
APC	Antigen presenting cell
BSA	Bovine serum albumin
Ca ²⁺	Calcium
CaCl ₂	Calcium Chloride
CaMK II	Calcium/Calmodulin-dependent protein kinase II
cAMP	Cyclic adenosine monophosphate
CD	Cluster of differentiation
CIA	Collagen induced arthritis
CNS	Central nervous system
CREB	cAMP response element-binding
CSF	Cerebrospinal fluid
DAB	Diaminobenzidine
DAG	Diacylglycerol
DAMP	Damage associated molecular pattern
dH ₂ O	Deionised water
DMSO	Dimethyl sulfoxide
DNA	Deoxyribonucleic acid
DOK	Downstream of tyrosine kinase
DPX	Di-N-butyle phthalate in xylene
EAE	Experimental-autoimmune encephalomyelitis

EAU	Experimental autoimmune uveitis
ECL	Enhanced chemiluminescence
EDTA	Ethylenediaminetetraacetic acid
EGTA	Ethylene glycol tetraacetic acid
ELISA	Enzyme-linked immunosorbent assay
EPSP	Excitatory post-synaptic potential
ERK	Extracellular-signal-regulated kinase
F3	Fibrinectin type III
FACS	Fluorescence-Activated Cell Sorting
FADD	FAS-associated death domain
FBS	Fetal bovine serum
FCS	Fetal calf serum
FGF	Fibroblast growth factor
FGFR	Fibroblast growth factor receptor
FGL	Fibroblast growth loop
g	Grams
x g	acceleration due to gravity
GAP 43	Growth Associated Protein 43
GFAP	Glial fibrillary acidic protein
GM-CSF	Granulocyte-macrophage colony-stimulating factor
gp	Glycoprotein
GPI	Glycosylphosphatidylinositol
HCl	Hydrochloric acid
HFS	High-frequency stimulation

HIV	Human immunodeficiency virus
H ₂ O ₂	Hydrogen Peroxide
HRP	Horseradish peroxidase
Hz	Hertz
ICAM	Intercellular cell adhesion molecule
icv	Intracerebroventricular
IFN	Interferon
Ig	Immunoglobulin
ih	Intrahippocampal
IKK	Inhibitor of κ B kinase
IL	Interleukin
IL-1R	Interleukin-1 receptor
ip	Intraperitoneal
IP ₃	Inositol 1,4,5-trisphosphate
IRAK	Interleukin-1 receptor-associated kinase
JNK	Jun N-terminal kinases
K ⁺	Potassium ion
KCl	Potassium Chloride
kDa	Kilodalton
kg	Kilograms
LAMP	Lysosomal associated membrane protein
LFA	Lymphocyte function associated molecule
LPS	Lipopolysaccharide
LTP	Long-term potentiation

M	Molar
MAP	Mitogen-activated protein
MCP-1	Monocyte chemoattractant protein-1
MEK	Mitogen-activated protein kinase kinase
μg	microgram
MHC	Major histocompatibility complex
μl	microlitre
ml	millilitre
μM	micromolar
MOG	Myelin Oligodendrocyte Glycoprotein
MRI	Magnetic resonance imaging
mRNA	Messenger ribonucleic acid
ms	Millisecond
MS	Multiple sclerosis
Myd88	Myeloid differentiation primary response gene 88
n	Number
NaCl	Sodium Chloride
NCAM	Neural cell adhesion molecule
NF-κB	Nuclear factor κ-light-chain-enhancer of activated B cells
NIK	NF-κB-inducing kinase
NMDA	N-methyl-D-aspartate
NMR	Neuclear magnetic resonance
NO	Nitric Oxide
NT	Neurotrophin

pAKT	Phosphorylated AKT
PAMP	Pathogen associated molecular pattern
PBS	Phosphate buffered saline
PBS-T	Phosphate buffered saline-Tween
PCR	Polymerase chain reaction
PIP ₃	Phosphatidylinositol (3,4,5)-triphosphate
PKA/C	Protein Kinase A/C
PLC	Phospholipase C
PSA	Poly-salic acid
PTB	Phosphotyrosine-binding
Q-PCR	Quantitative real-time polymerase chain reaction
RasGAP	Ras GTPase activating protein
RIP	Receptor interacting protein
RNA	Ribonucleic acid
ROS	Reactive oxygen species
rpm	Revolutions per minute
s	Second
SDS	Sodium Dodecyl sulphate
SEM	Standard error of the mean
SHIP	SH2-containing inositol 5-phosphatase
SIRP	Signal-regulatory protein
STAT	Signal transducer and activation of transcription
Strep	Streptavidin
TBS	Tris buffered saline

TGF	Transforming growth factor
Th	T helper
TIR	Toll/Interleukin-1 receptor
TLR	Toll-like receptor
TNF	Tumor necrosis factor
TNF-R	Tumor necrosis factor-receptor
TRADD	TNF-R associated death domain
TRAF	Tumor necrosis factor-receptor associated factor
Tris	Tris(hydroxymethyl)aminomethane
V	Volts
°C	Degree Celsius
6-OHDA	6-hydroxydopamine
8-OHdG	8-Oxo-2'-deoxyguanosine

List of Figures

Chapter 1

- 1.1. Activation of Microglia.
- 1.2. Signalling pathway leading from LPS activation of TLR4.
- 1.3. The structure of NCAM on the cell membrane.
- 1.4. Signalling pathways leading from PSA-NCAM activation of FGFR-1.
- 1.5. Activation of CD200R by CD200.

Chapter 3

- 3.1. FGL significantly attenuated the LPS-induced increase in CD40 mRNA expression in cultured mixed glia.
- 3.2. FGL attenuated the LPS-induced increase in CD11b mRNA expression in cultured mixed glia.
- 3.3. FGL significantly attenuated the LPS-induced increase in IL-1 β mRNA expression and release in mixed glial cultures.
- 3.4. FGL significantly attenuated the LPS-stimulated increase in IL-6 concentration in cultured mixed glia.
- 3.5. FGL significantly attenuated the LPS-induced increase in IL-1 β release, but not mRNA expression, in isolated microglial cultures.
- 3.6. SU5402 blocked the ability of FGL to attenuate the LPS-induced increase in IL-1 β mRNA expression and release.
- 3.7. A β increased IL-1 β mRNA expression and release in cultured mixed glia.
- 3.8. A β increased MHC II mRNA expression in cultured mixed glia.
- 3.9. FGL attenuated the A β -stimulated increase in IL-1 β , but not CD40, mRNA expression in cultured mixed glia.

Chapter 4

- 4.1. CD11b and CD68 mRNA expression was enhanced in mixed glia prepared from CD200^{-/-}, compared with wildtype, mice.
- 4.2. FGL attenuated the LPS-induced increase in CD40, ICAM-1 and CD11b mRNA in glia prepared from wildtype but not CD200^{-/-} mice.

- 4.3. FGL attenuated the LPS-induced increase in IL-1 β mRNA and release in glia prepared from wildtype but not CD200^{-/-} mice.
- 4.4. FGL attenuated the LPS-induced increase in TNF- α mRNA and release in glia prepared from wildtype but not CD200^{-/-} mice.
- 4.5. FGL attenuated the LPS-induced increase in IL-6 mRNA and release in glia prepared from wildtype but not CD200^{-/-} mice.
- 4.6. CD200 expression on CD11b-negative cells in a mixed glial prepared from wildtype mice.
- 4.7. FGL enhanced CD200 expression in cultured astrocytes.
- 4.8. CD200 is expressed in an astrocytic membrane extract that contains minimal GFAP expression, compared with a cytosolic fraction.
- 4.9. LPS induced an increase in IL-1 β mRNA expression in isolated microglia. Pre-incubation with an astrocytic membrane fraction attenuated the LPS-induced changes.
- 4.10. LPS induced an increase in TNF- α mRNA expression and release in isolated microglia. Pre-incubation with an astrocytic membrane fraction attenuated the LPS-induced changes.
- 4.11. LPS induced an increase in IL-6 mRNA expression and release in isolated microglia. Pre-incubation with an astrocytic membrane fraction attenuated the LPS-induced changes.
- 4.12. An LDH assay confirmed that exposure to LPS or an astrocytic membrane fraction did not compromise cell viability.

Chapter 5

- 5.1. CD200Fc attenuated the LPS-induced increase in mRNA expression and release of pro-inflammatory cytokines in mouse primary glial cells.
- 5.2. CD200Fc attenuated the LPS-induced increase in nitrite concentration in primary rat mixed glia.
- 5.3. CD200Fc rescues LPS-induced impairment of LTP.
- 5.4. CD200Fc rescues the age-induced impairment of LTP.
- 5.5. Synaptophysin expression decreases in hippocampus with age.
- 5.6. CD200 expression decreases in hippocampus with age.
- 5.7. CD200Fc attenuated the age-induced increase in MHC II mRNA expression in hippocampus.

- 5.8.** CD200Fc attenuated the age-related increase in hippocampal MHC II expression.
- 5.9.** CD200Fc attenuated the age-induced increase in GFAP mRNA in hippocampus.
- 5.10.** iNOS mRNA expression was increase in hippocampus with age.
- 5.11.** CD200Fc attenuated the age-related increase in hippocampal 8-OHdG expression.
- 5.12.** CD200Fc increased IGF-1 concentration in hippocampus.
- 5.13.** CD200Fc attenuated the age-related decrease in pAKT in hippocampus.

CHAPTER 1. INTRODUCTION.....	1
1.1 THE IMMUNE SYSTEM.....	1
1.1.1 <i>Inflammation</i>	1
1.1.2 <i>The Immune system and the CNS</i>	2
1.2 IMMUNE-COMPETENT CELLS OF THE CNS.....	4
1.2.1 <i>Microglia</i>	4
1.2.2 <i>Astrocytes</i>	7
1.3 <i>Membrane markers of activation</i>	8
1.3.1 <i>MHC II</i>	8
1.3.2 <i>CD40</i>	9
1.3.3 <i>CD11b</i>	10
1.3.4 <i>ICAM-1</i>	11
1.3.5 <i>CD68</i>	12
1.4 CYTOKINES.....	12
1.4.1 <i>Interleukin-1</i>	13
1.4.2 <i>Interleukin-6</i>	15
1.4.3 <i>Tumor necrosis factor-α</i>	16
1.5 <i>LPS: a model for inflammation</i>	17
1.6 NEURAL CELL ADHESION MOLECULE.....	20
1.6.1 <i>NCAM Homophilic Binding</i>	20
1.6.2 <i>NCAM Heterophilic Binding</i>	21
1.7 FIBROBLAST GROWTH FACTORS AND THEIR RECEPTORS.....	23
1.8 FIBROBLAST GROWTH LOOP.....	27
1.8.1 <i>Inhibition of FGL by SU5402</i>	29
1.8.2 <i>Administration of FGL in humans</i>	30
1.9 IMMUNE-MODULATION; A ROLE FOR CD200.....	30
1.9.1 <i>CD200 Signalling</i>	33
1.10 THE CNS; AN ANATOMICAL VIEW.....	35
1.11 LONG-TERM POTENTIATION; A BIOLOGICAL SUBSTRATE FOR MEMORY.....	37
1.11.1 <i>Signalling molecules involved in LTP</i>	38
1.11.2 <i>Age-related impairment in LTP</i>	39
1.12 OBJECTIVES.....	40
CHAPTER 2. METHODS.....	43
2.1 <i>IN VITRO</i> STUDIES.....	43
2.1.1 <i>Preparation of cultured mixed glia</i>	43
2.1.2 <i>Preparation of cultured microglia and astrocytes</i>	44
2.1.3 <i>Isolation of cell membrane from astrocytes</i>	45
2.1.4 <i>Preparation of culture media and test compounds</i>	45
2.2 ANIMALS.....	47
2.2.1 <i>Treatment with LPS</i>	47
2.2.2 <i>Treatment with CD200Fc</i>	47
2.2.3 <i>Induction of LTP in vivo</i>	48
2.2.4 <i>Dissection and preparation of tissue</i>	48
2.2.5 <i>Protein Quantification</i>	49
2.3 ANALYSIS OF CYTOKINE EXPRESSION BY ELISA.....	49
2.3.1 <i>Preparation of rat tissue for cytokine analysis</i>	50

2.3.2 General ELISA protocol	50
2.4 ANALYSIS OF mRNA EXPRESSION	51
2.4.1 Preparation of tissue for RNA isolation	51
2.4.2 Protocol for RNA isolation	52
2.4.3 Reverse Transcription for cDNA synthesis	52
2.4.4 Quantitative real time PCR	53
2.5 WESTERN IMMUNOBLOT ANALYSIS	55
2.5.1 General protocol for western immunoblotting	55
2.6 FLOW CYTOMETRY	57
2.7 ANALYSIS OF NITRITE CONCENTRATIONS (GREISS ASSAY).....	57
2.8 IMMUNOHISTOCHEMISTRY	58
2.8.1 Preparation of tissue sections for immunohistochemistry.....	58
2.8.2 Immunohistochemical staining	58
2.8.3 Microscopy	59
2.9 STATISTICAL ANALYSIS	60
CHAPTER 3. RESULTS.....	61
3.1 INTRODUCTION	61
3.2 METHODS	64
3.3 RESULTS	65
3.3.1 Investigating the action of FGL on LPS-stimulated primary glia.....	65
3.3.2 Investigating the action of FGL on A β ₂₅₋₃₅ -stimulated primary glia.....	67
3.4 DISCUSSION	87
CHAPTER 4. RESULTS.....	95
4.1 INTRODUCTION	95
4.2 METHODS	97
4.3 RESULTS	98
4.3.1 Mixed glia prepared from wildtype mice have an activated phenotype compared with glia from CD200 ^{-/-} mice.	98
4.3.2 CD200 is expressed on astrocytes	99
4.4 DISCUSSION	125
CHAPTER 5. RESULTS.....	131
5.1 INTRODUCTION	131
5.2 METHODS	133
5.3 RESULTS	135
5.3.1 CD200Fc attenuated an LPS-induced increase in pro-inflammatory cytokines and Nitrate production in mixed glial cells.	135
5.3.2 CD200Fc rescues LPS- and aged-induced impairment in LTP	135
5.3.3 Aged-related changes in hippocampus	136
5.3.4 CD200Fc attenuated age-induced markers of glial activity in hippocampus	136
5.3.5 CD200Fc increases AKT phosphorylation.....	138
5.4 DISCUSSION	165
CHAPTER 7. BIBLIOGRAPHY	181

Chapter 1. Introduction

1.1 The Immune System

The immune system is the body's defence mechanism against foreign pathogens and deviant native cells. It can be described as a collection of biological processes that is divided into innate and adaptive responses, however there is much cross-talk between the two. The objective of the innate immune system is damage limitation, eliciting rapid, non-specific responses, whereas adaptive immunity relies on the recognition of a pathogen and generation of specific antibodies to combat it.

Cells involved in innate immunity include granulocytes (natural killer cells, mast cells, basophils and eosinophils) and phagocytes (neutrophils and monocytes), which are carried in the blood and translocate to the site of insult or injury when required. In addition, dendritic cells and macrophages survey the tissue in which they reside performing several innate immune functions including phagocytosis, antigen presentation, and production of pro-inflammatory cytokines (Becher *et al.*, 2000). B and T lymphocytes are the primary cells of the adaptive immune system; B cells mediate humoral responses and generate memory cells after antigen exposure, while T cells possess homing receptors to mediate cellular responses (Becher *et al.*, 2000). The two branches of the immune system are functionally intertwined; the innate system activates the adaptive through antigen presentation in the lymph tissue, while the adaptive immune system uses effector mechanisms of innate immune cells to eradicate targeted material.

1.1.1 Inflammation

Inflammation is a quintessential innate immune response, aiming to destroy pathogens and remove debris. The word has been used for centuries, however, its meaning and our understanding of it has evolved in tandem with advances in scientific method. One of the first descriptions of inflammation was in the first century AD; the hallmarks described as rubor, tumor, calor and dolor, meaning redness, swelling, heat and pain, which are the unmistakable

visual manifestation of a subcutaneous inflammatory response (George, 2006). Prior to the 19th century definitions and concepts of this process were primitive, relying on mere observation not investigation. Inflammation is now described as a cellular- and humoral-based process that can arise in any tissue; the expression of rubor, tumor, calor and dolor are no longer an obligatory part. Thus modern science has largely extinguished the fire that previously epitomised inflammation.

An inflammatory response is induced in tissue as it reacts to trauma, infection or auto-immunity (Nathan, 2002). Such stimuli can activate resident immune cells and increase infiltration of blood-borne leukocytes and lymphocytes to the site of injury. Pathogen-associated molecular patterns (PAMPs) are extracellular molecular structures that have been conserved between microbial pathogens. PAMPs are recognised by germ-line encoded pattern recognition receptors located on phagocytic cells, allowing the innate immune system to discriminate self from pathogen-associated non-self matter (Medzhitov & Janeway, 1998). Activation of this receptor initiates a generic inflammatory reaction, rapidly recruiting phagocytes and lymphocytes. Toll-like receptors (TLRs) are a subset of PAMP receptors containing an extracellular leucine-rich repeat domain and a cytoplasmic signalling domain with homologies to the cytoplasmic domain of the IL-1 receptor, thus is termed Toll/IL-1R (TIR) domain (Kopp & Medzhitov, 1999). Many PAMPs have been classified and their respective TLR identified, for example lipopolysaccharide (LPS) attaches to TLR4.

1.1.2 The Immune system and the CNS

The brain was once thought to be an 'immune-privileged' organ. It was reasoned that an immune response, in an effort to destroy potentially harmful matter, could be destructive to nearby irreplaceable, postmitotic neurons. This assumption was compounded by the lack of lymphatic drainage and the presence of a blood-brain barrier; a complex system of tight junction between endothelial cells in the CNS, which could prevent the penetration of peripheral immune cells and humoral signals into the brain parenchyma (Risau & Wolburg, 1990). Today the passage of cells and signals through the blood-brain barrier is no longer considered an insurmountable event (Carson & Sutcliffe, 1999). Immunocompetent T cells have been found to traverse the blood-brain barrier and the recruitment of peripheral immune

cells to the CNS can be beneficial in combating infection, with no long-term collateral damage (Merrill & Benveniste, 1996). Therefore, it is now accepted that the CNS is continually surveyed by the immune system and there are bidirectional interactions between the immune and nervous system (O'Donnell *et al.*, 2000). Furthermore, the CNS has a resident macrophage population known as microglial cells, which play a central role as the effector cells during engulfment of pathogens and cellular debris (Feuer, 2007).

In addition to immune cell transversing the blood-brain barrier, inflammatory molecules and signals from the periphery can elicit central effect (Cunningham 2005). The discovery that such signals activate the hypothalamic-pituitary-adrenal (HPA) axis initiated a new understanding of interactions between the periphery and the CNS. The HPA axis is formed by a complex set of feedback interactions between neuroendocrine organs; the hypothalamus and pituitary gland, which are located in the brain, and the adrenal gland, positioned above the kidney. Circulating inflammatory mediators in the periphery, for example IL-1 β , IL-6 and TNF- α (see section 1.4), can directly stimulate the hypothalamus and pituitary gland, inducing secretion of adrenocorticotrophic hormone, this in turn induces release of glucocorticoids from the adrenal glands (Chrousos 1995). Glucocorticoids are considered stress hormones and have a potent anti-inflammatory action, thus allowing immune signals to drive an anti-inflammatory response (Sandi 2004). This classical negative feedback loop prevents prolonged inflammation, which can be destructive to the host, while deficits in this axis are associated with increased susceptibility to disease (Morand & Leech 2001).

Inflammation as an acute response is a critical component of tissue repair, involving activation and cross-talk between many cells, however, the consequences of prolonged inflammation can be detrimental (Nathan 2002). The powerful anti-inflammatory action of exogenous glucocorticoids, which reflect the endogenous hormones produced by the adrenal glands, is currently being developed to treat chronic autoimmune diseases, for example Rheumatoid arthritis, an autoimmune disease that effects joints and surrounding tissue (Morand & Leech 2001). Glucocorticoids, derived from steroids, integrate immune responses with metabolic regulation. They are responsible for catabolising energy reserves, in addition to suppressing inflammation, forming the cornerstone of 'The Fight or Flight Response' (Chrousos 1995). Nonsteroidal anti-inflammatory drugs (NSAIDs) have also been developed for clinical use.

These compounds target a diverse array of receptors expressed on immune cells, thus suppressing their activity independently of enhancing glucocorticoid-related activity. The current study focuses on potential targets for novel NSAIDs. However, before targets receptors are discussed the immune cells involved must be considered.

1.2 Immune-competent cells of the CNS

1.2.1 Microglia

There are resident populations of myeloid cells within all tissues; these include alveolar macrophages found in the lungs, Kupffer cells in the liver and microglia in the CNS. While these cells are tailored to their microenvironment, they are essentially responsible for regulating both non-specific and antigen-specific inflammatory actions. Macrophages are specialised in pathogen recognition, engulfment of foreign matter or cellular debris via phagocytic receptors, digestion of the intake by lysosomal machinery and finally, displaying the digested material to other immune cells (Napoli & Neumann, 2009). Microglia serve this function in the brain, spinal cord and retina. Although the exact origin of microglia is unknown, there is little debate that they are derived from myeloid progenitor cells (Soulet & Rivest, 2008). It has been hypothesised that microglia originate from the neuroectodermal matrix, while others suggest they originate in the periphery, like other hematopoietic cells, and populate the CNS during early pre- and post-natal development (Hanisch & Kettenmann, 2007; Soulet & Rivest, 2008). Unlike neurons, microglia can proliferate during infection or injury and it is believed that over 95% of microglia are generated after birth (Soulet & Rivest, 2008). There is still controversy over whether these cells are derived from progenitor cells already present in the CNS or from circulating precursor cells that infiltrate the blood-brain barrier.

Parenchymal microglia are found throughout the brain, although there is heterogeneity between brain regions. Microglia within the hippocampus express greater levels of TNF- α mRNA, while microglia in the cerebral cortex express higher levels of the neurotrophin NT-3 (Elkabes *et al.*, 1996; Ren *et al.*, 1999). There are also distinct populations of perivascular and

meningeal microglia that act as the first line of defence against foreign invaders and can influence the integrity of the blood-brain barrier. Microglia in a non-inflammatory state are often referred to as 'resting', however, these cells are not dormant (see Figure 1.1). During non-pathological conditions, microglial processes actively survey their microenvironment. Nimmerjahn and colleagues (2005) elegantly used two-photon microscopy and fluorescently labelled microglia to visualise highly mobile microglial processes. They demonstrated how microglia continually withdraw and extend their arborisations, suggesting careful navigation by these immune cells through fine-wired neuronal structures. Indiscriminate scanning can rapidly switch to targeted movement towards a site of injury or infection, when microglia detect a change in the extracellular milieu. This directional guidance is achieved through a variety of cell surface receptors that detect chemokines and purines, which can re-orientate the microglia within seconds (Davalos *et al.*, 2005; Figure 1.1).

There is a countless number of molecules and conditions that could threaten the structure and function of the CNS, many of which trigger the transformation of a quiescent, surveying microglia into a reactive, effector cell. Microglia, like other macrophages, are equipped to detect a wide variety of potentially harmful materials through PAMP receptors, which identify exogenous threats and damage associated molecular pattern (DAMP) receptors that recognise endogenous debris (Olson & Miller, 2004; Soulet & Rivest, 2008). Once 'activated' microglia morph from a ramified cell with a small soma and long processes to a rounder, amoeboid form, expressing an array of cell surface proteins (Figure 1.1). Microglia differ to peripheral macrophages as they do not constitutively express the same array of cell surface proteins that are essential for inducing or mediating a typical immune response, for example CD45 and major histocompatibility complex (MHC) II (Kreutzberg, 1996). It is hypothesised that this tight regulation and restriction of inflammatory activity is aimed to preserve an immunologically tranquil environment around post-mitotic neurons. To further bolster this tight immune regulation, there is constitutive immunosuppressive signalling between microglia and adjacent cells, including neurons, endothelia, astrocytes and T cells, via CD200-CD200R, Fractalkine and its receptor and SIRP α -CD47 (Hoek *et al.*, 2000; Cardona *et al.*, 2006). Nevertheless once stimulated, microglia respond promptly in a context-dependent manner, up-regulating expression of cytokines, chemokines and surface markers of activation

that perpetuate an immune response directed towards tissue repair and elimination of the ‘danger signal’ (Hesselgesser & Horuk, 1999; Aloisi, 2001).

Although the initial premise of microglia is one of neuroprotection, evidence supports the concept that unregulated activation can propagate neuronal injury due to the barrage of toxic molecules that they sequester. Inflammation is a common denominator in a diverse array of neurodegenerative diseases and activated microglia the common thread (Block & Hong, 2005).

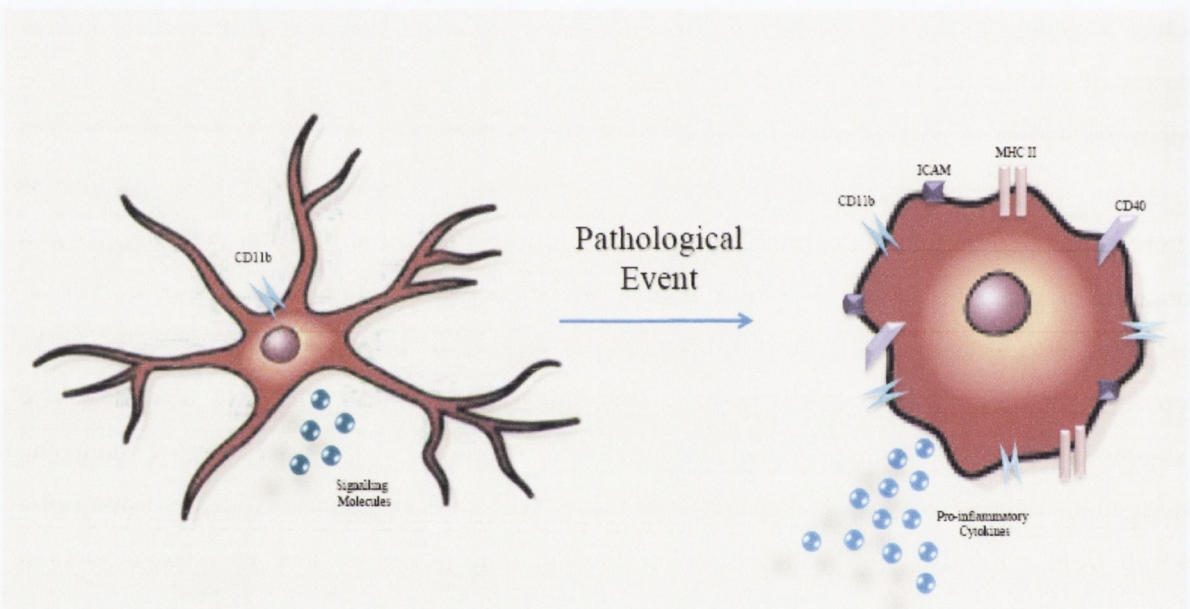


Figure 1.1. Activation of Microglia.

Microglia are activated in response to pathological events such as disease or injury, and change from a quiescent, ramified cell to an amoeboid morphology. This enables them to migrate to the site of injury. In the course of microglial activation, various receptors and co-stimulatory molecules are expressed (MHC II, CD40, ICAM), allowing microglia to interact with other cell types. Activated microglia secrete pro-inflammatory cytokines (IL-1 β , IL-6, TNF- α), which also perpetuate an immune response. Quiescent microglia are not ‘passive’, they express low levels of CD11b to aid motility and secrete signalling molecules (IL-4, IGF-1) while surveying the CNS. Abbreviations: CD, Cluster of Differentiation; ICAM, Intercellular adhesion molecule; MHC, Major histocompatibility complex.

1.2.2 Astrocytes

In 1893, Michael Von Lenhossék coined the word astrocyte, from the Greek meaning star cell, for stellate-shaped glia that had been previously visualised by Ramón y Cajal. This name soon became universally accepted and is still used today. However, it was not until the end of the 19th century that the roles for these cells and their possible interactions with nerve cells were considered. In recent years, knowledge of astrocytic activity and their function as immune effector cells is increasingly perceived to be an essential part of understanding brain function during health and disease.

Advancements in microscopy and use of fluorescent dyes have established astrocytes as highly complex, process-bearing cells with heterogeneous morphology. Protoplasmic astrocytes, found in gray matter, have multiple branching processes with end-feet, while fibrous astrocytes in the white matter have unbranched processes (Zerlin *et al.*, 1995). Both subtypes appear to have an ordered arrangement that is established in the early postnatal brain in tandem with neurons and vasculature, and there is minimal overlap between the cells (Bushong *et al.*, 2002). Astrocytes serve a variety of house-keeping roles, maintaining a viable milieu for nerve cells to function. Firstly, they regulate the ionic environment of the extracellular space, particularly after intense synaptic activity, by buffering surplus K^+ ions and mopping-up excess neurotransmitter (Karwoski *et al.*, 1989). Secondly, astrocytes respond to the metabolic needs of neurons directly, by metabolising glycogen and releasing lactate, and indirectly, by regulating blood flow in accordance with neuronal activity (Poitry-Yamate *et al.*, 1995; Zonta *et al.*, 2003). In addition to regulation of blood flow via induction of functional hyperaemia, astrocytes have been implicated in the maintenance of blood-brain barrier integrity, which can impact significantly on the outcome of both acute and chronic immune activity (Wang & Bordey, 2008).

Astrocytes function as a syncytium within the cerebral cortex and hippocampus. This is achieved by the presence of over 50,000 gap junctions, which serve as direct conduits of ions and small signalling molecules, connecting each astrocyte to its neighbour (Yamamoto *et al.*, 1990). This network aids in the redistribution of K^+ ions after synaptic activity and can mediate intracellular calcium oscillations that influence the dynamics of adjacent neurons

(Pasti *et al.*, 1997). Therefore, despite not being electrically excitable, astrocytes exhibit neurotransmitter receptors aiding them to monitor and adequately respond to neuronal activity. They can also release modulatory substances, for example growth factors and cytokines, which in turn alter the activity of neurons and other glial cells, including microglia (Cotrina & Nedergaard, 2002).

Astrocytes are commonly identified by the presence of intermediate filaments (glial fibrils), a major component of which is glial fibrillary acidic protein (GFAP), and is thought to be specific to astrocytes within the CNS (Eng *et al.*, 1971). GFAP, as a cytoskeletal protein, provides structural stability to astrocytic processes allowing modulation of their shape and movement. Similar to microglia, astrocytes exhibit a profound response to neuronal injury and undergo a series of metabolic and morphological changes. This astrogliosis, as it is known, has been reported in a variety of neurodegenerative diseases including multiple sclerosis (MS) and Alzheimer's disease (AD) (Schipper, 1996). Astrogliosis is, in part, characterised by a rapid increase in GFAP expression and although the pro-inflammatory function of microglia is more prominent, astrocytes also respond to and secrete cytokines during an immunologically challenge (Aloisi, 1999; Eng *et al.*, 2000). Even in the absence of disease, astrocytes in the brains of aged individuals display an elevated content of GFAP (Nichols, 1999). It has been suggested that the increase in GFAP may be a response to the enhanced inflammatory and oxidative profile of the aging brain (Cotrina & Nedergaard, 2002). Bearing in mind the integral role astrocytes play in the CNS, an alteration in their dynamics during aging may affect synaptic function and neuronal survival, perhaps in turn, contributing to cognitive decline.

1.3 Membrane markers of activation

1.3.1 MHC II

MHC molecules are a set of immune recognition molecules present on all nucleated cells and impart the property of self. The complete sequence of MHC was published in 1999 and it was found to include an expansive genomic region on chromosome 6, unique to each individual,

which allows the immune system to recognise native cell (1999). The exclusivity of each person's MHC contributes to complications after organ transplantation, as recipients reject and attack the foreign tissue. In contrast, the absence of MHC molecules on red blood cells permits blood transfusion with ease. MHC class II (MHC II) molecules are heterodimeric peptide-binding proteins expressed on antigen presenting cells (APC). Following engulfment of a pathogen, APC can present extracellular components of the pathogen to T cells via its MHC II binding domain (Carson & Sutcliffe, 1999) Unlike classical macrophages and APCs that constitutively express MHC II, microglia express very low levels of MHC II while in a ramified state, thus going undetected by T cells (Wekerle *et al.*, 1986). However, MHC II expression can rapidly be up-regulated on both microglia and astrocytes upon an inflammatory stimulus, as the cells gain immune function (Kreutzberg, 1996; De Keyser *et al.*, 2010).

Almost all neurodegenerative diseases, including MS, AD and Parkinson's disease, are associated with signs of neuroinflammation and a concurrent up-regulation in microglial MHC II expression (Neumann, 2001). It is noteworthy that although presence of an MHC II complex on microglia can alert T cells, additional co-stimulatory molecules are required for T cell activation (Kreutzberg, 1996). Co-stimulatory molecules are expressed on microglia upon stimulation and can amplify and shape the differentiation of T cell effector phenotypes (Carson & Sutcliffe, 1999).

1.3.2 CD40

CD40 is a co-stimulatory molecule found on APCs in the periphery and microglia within the CNS. It is a member of the tumor necrosis factor (TNF) receptor superfamily and its cognate ligand (CD40L) is expressed predominantly on T cells (Harnett, 2004). Ligation of CD40 is imperative for a productive immune response, enhancing MHC II and CD40 expression in a positive feedback fashion, in addition to inducing cytokine and chemokine release (Qin *et al.*, 2005). Qin (2005) found that LPS enhanced microglial CD40 expression and reported that the up-regulation is reliant on activation of the transcription factors NF- κ B and signal transducer and activation of transcription-1 α (STAT-1 α). Furthermore, Town and colleagues (2001) have proposed a series of intracellular events occurring in microglia upon CD40 ligation. Initial binding of CD40L activates Src-family kinases, which are non-receptor tyrosine kinases and,

once activated, can phosphorylate the mitogen-activated protein kinase MEK1/2, targeting p44/42 and allowing it to translocate to the nucleus, thus promoting gene transcription (Town *et al.*, 2001). These events can up-regulate pro-inflammatory cytokine transcription and subsequent release, for example TNF- α , thus further promoting an inflammatory response.

Activation of this intracellular cascade is transient, as chronic activation could be more detrimental than beneficial to surrounding tissue. In fact, persistently high levels of CD40 and CD40L have been implicated in the pathogenesis of neurodegenerative diseases (Town *et al.*, 2001; Tan *et al.*, 2008).

1.3.3 CD11b

CD11b is constitutively expressed on myeloid cells and its exclusivity to microglia within the CNS allows these cells to be identified in brain tissue and mixed glial perorations (Cowley *et al.*, 2010). CD11b is classified as an integrins, which are cell surface receptors that regulate cell-cell adhesion, migration and two-way signal transduction with the extracellular matrix (Solovjov *et al.*, 2005). Solovjov reported that the action of this heterodimer is reliant on the integration of activities of its two functionally distinct subunits; α and β . The α subunit is responsible for recognition of a broad spectrum of ligands, including fibrinogen, intercellular cell adhesion molecule-1 (ICAM-1) and the inactivated complement fragment iC3b, while supporting firm adhesion. In contrast, the β subunit has a more limited repertoire of ligands and displays poor adhesion, but can mediate cell migration. The signalling mechanism responsible for the increased CD11b expression during inflammation is still unknown; however, it is thought that nitric oxide (NO), which is sequestered from stimulated microglia, could play an instrumental role (Roy *et al.*, 2006). Increased expression of CD11b is prevented when microglia are stimulated in the presence of a NO scavenger. Similar to other markers of microglial activation, it has been reported that during a neuroinflammatory disease there is an increase in the cell-surface expression of CD11b, and this corresponds to the degree of microglial activation (Roy *et al.*, 2008).

1.3.4 ICAM-1

Cell adhesion molecules are cell surface structures that mediate cell-cell and cell-substratum interactions. ICAM-1 is a 90kDa cell adhesion molecule, containing five (immunoglobulin) Ig-like domains. It plays a critical role in the arrest and transmigration of leukocytes out of the brain's vasculature and their diapedesis into the tissue. ICAM-1 is expressed on a variety of cells including leukocytes, endothelial cells, astrocytes and microglia, while soluble forms of ICAM-1 have been found in the serum and cerebrospinal fluid (Lee & Benveniste, 1999). Endothelial cells constitutively express ICAM-1, while astrocytes and microglia display aberrant expression when activated (Sobel *et al.*, 1990). The primary leukocyte ligand that ICAM-1 interacts with is Lymphocyte Function Associated molecule (LFA)-1, which is an integrin consisting of an $\alpha\beta$ heterodimer. It shares the same $\beta 2$ integrin subunit as CD11b as well as having a homologous α subunit (Huang & Springer, 1995). ICAM-1 also interacts with CD11b as well as partaking in homophilic binding.

In addition to playing an important role in cell migration, ligation of ICAM-1 can induce signalling cascades that perpetuate an immune response. Recent studies have identified ICAM-1 as a co-stimulatory molecule during T cell-mediated immune activation (Huang & Springer, 1995). While homophilic engagement of ICAM-1 molecules on astrocytes have been reported to induce the pro-inflammatory cytokines IL-1 β , IL-6 and TNF- α via ERK1/2 and p38 MAPK; signalling transduction pathways that are distinct from those induced during glia-endothelium interactions (Lee *et al.*, 2000). Phosphorylation of the cytoskeletal-associated protein cortactin in brain microvessel endothelial cells by ICAM-1 reveals a possible role for this molecule in cytoskeletal reorganisation (Durieu-Trautmann *et al.*, 1994). Several studies have associated increased expression of membrane bound and soluble ICAM-1 during CNS pathologies, for example MS, the animal model for MS experimental-autoimmune encephalomyelitis (EAE) and AD, suggesting a possible role for this molecule in these disorders (Lee *et al.*, 2000).

1.3.5 CD68

Microglia are the primary effector cells of phagocytosis in the CNS, a process by which immune cells engulf and digest harmful matter. Digestion occurs in the lysosome, an organelle that contains highly acidic enzymes with the ability to degrade and denature protein (Majumdar *et al.*, 2007). CD68, also known as macrosialin in mice, is a highly glycosylated protein expressed on the lysosomal membrane of cells with phagocytic activity, especially peripheral macrophages and monocytes (Davey *et al.*, 1988). The major structural contributors to the lysosomal membrane are by the lysosomal associated membrane protein (LAMP) family, of which CD68 is a member (Holness & Simmons, 1993). Although CD68 is predominantly an intracellular protein, cell surface expression representing 10-15% of the total protein has been described and this is rapidly internalised and exchanged with intracellular stores (Kurushima *et al.*, 2000). The function of CD68 has yet to be fully described, but roles in antigen presentation and protection of the lysosomal membrane against acidic hydrolase proteins have been suggested due to its location and glycosylation state (Kurushima *et al.*, 2000).

Rabinowitz and Gordon (1991) reported differential expression and altered pattern of glycosylation of CD68 in macrophages following an inflammatory stimulus. Moreover, CD68 expression has been co-localised with MHC II in the rat brain 1-3 days post lesion (Cho *et al.*, 2006). However, this study found that the expression of CD68 persisted on cells long after the attenuation in MHC II, perhaps suggestive of different states of microglial activity.

1.4 Cytokines

Cytokines are small signalling molecules released from immune cells and used expansively to mediate immune responses. They stimulate early inflammatory reactions and are major determinants of the state of cellular activation. In general, cytokines act locally, binding to cell surface receptors of neighbouring cells. These receptors display a very high affinity for their ligand and with an extremely low dissociation constant ($10^{-10} - 10^{-12} M$) even a small amount can induce an intense biological response. Most cytokines are pleiotropic, eliciting their effects locally or systemically in an autocrine or paracrine manner. While orchestrating an

immune response, cytokines are involved in both synergistic and antagonistic interactions (Feghali & Wright, 1997). Pro-inflammatory cytokines, including IL-1 β and TNF- α , endeavour to heighten an immune response, while the anti-inflammatory cytokine IL-4 seeks to suppress it. Shifting the equilibrium of these two counteractive forces is essential for the attainment of homeostasis during health and disease (Nathan, 2002).

1.4.1 Interleukin-1

IL-1 was one of the first cytokines described and believed to act as an endogenous pyrogen (Rothwell, 1991). When successfully cloned in 1984 it was found to contain two distinct proteins, IL-1 α and IL-1 β , the genes of which are located on the long arm of chromosome 2 (Webb *et al.*, 1986). Expression of these genes are NF- κ B-responsive and are induced by various pro-inflammatory stimuli, including bacterial and viral products, cellular injury and hypoxia (Allan, 2005). TNF- α , can induce IL-1 transcription as well as IL-1 itself, acting in a positive-feedback loop. Despite having only a 30% sequence homology, both variants can bind to the same IL-1 receptor and mediate biological responses (Feghali & Wright, 1997; Allan, 2005). Although, in recent years several new IL-1 family members have been identified, based on gene homology, gene location and receptor binding, much attention is still focused on the role of IL-1 β in the CNS under both physiological and pathological conditions.

IL-1 β is the most rapidly-expressed cytokine in response to insult or injury within the CNS, while IL-1 α plays a minimal role (Davies *et al.*, 1999; Gosselin & Rivest, 2007). Translation results in pro-IL-1 β , a dormant form of the cytokine that remains in the cytosol until enzymatically cleaved. The pro form of IL-1 β is cleaved by caspase-1, which relies on the formation of a complex of protein known as the inflammasome to gain enzymatic activity, before IL-1 β can be released to the extracellular environment (Thornberry *et al.*, 1992; Dinarello, 1996). Under normal conditions IL-1 β release and mRNA expression are tightly regulated within the CNS. The lack of tonic stimulation and the swiftness of IL-1 β amplification during pathology contribute to its finesse as a pro-inflammatory cytokine. IL-1 β is synthesised by microglia (Giulian *et al.*, 1986), astrocytes (Lieberman *et al.*, 1989), oligodendrocytes and neurons (Takao *et al.*, 1990) within the CNS. In addition, non-resident

cell for example infiltrating T cells are also believed to be a source of pro-inflammatory cytokines during certain pathological conditions (Murphy *et al.*).

Once released, IL-1 β has a diverse assortment of actions. It can enhance immune cell responsiveness and T cell proliferation, increase vascular permeability and contribute to 'sickness behaviour' (Allan *et al.*, 2005). IL-1 β mediates its responses through activation of the type I IL-1 receptor (IL-1R1), an 80kDa protein containing a synaptic domain of 215 amino acids in length. A type II IL-1 receptor has also been described and it is thought to act as a 'decoy' receptor, containing a significantly smaller cytoplasm domain (29 amino acids) lacking the capacity to initiate signal transduction events (Sims *et al.*, 1993). The presence of IL-1R1 has been shown in many brain areas, with a high level of expression in the hippocampus and hypothalamus (Ban *et al.*, 1991) that increases with age (Murray & Lynch, 1998). Also, IL-1R1-immunoreactive vessels have been demonstrated throughout (Konsman *et al.*, 2004).

One of the principal ways by which IL-1 β regulates gene transcription is via NF κ B activation. In brief, IL-1 β binds to IL-1R1, which is complexed with the IL-1 receptor accessory protein, this leads to recruitment of IL-1 receptor associated kinase (IRAK). IRAK associates with TRAF6, leading to activation of I κ B kinase and the subsequent phosphorylation of I κ B. This cascade finally results in the transcription of NF κ B responsive genes (O'Neill & Greene, 1998). Other biochemical cascades that have been strongly implicated in IL-1 signalling are the MAP kinases, which include ERK, p38 MAP kinases and (c-Jun N-terminal kinases) JNK. Elucidating the roles of these kinases in IL-1 β signalling has been greatly aided by the availability of MAP kinase specific inhibitors (Alessi *et al.*, 1995; Cuenda *et al.*, 1995). Downstream targets of MAP kinases include the transcription factors c-fos and c-jun and well as many non-nuclear targets, for example microtubule-associated proteins (Fukunaga & Miyamoto, 1998). Therefore, not only can IL-1 affect the transcription of up to 90 genes, from cytokines and acute phase proteins to growth factors and adhesion molecules, it can activate cytoplasmic targets that mediate rapid effects.

Chronic up-regulation of IL-1 β can be destructive, inducing neuronal injury and compromising the blood-brain barrier. O'Donnell and colleagues (2000) reported that an age-

related deficit in LTP is coupled with an increase in hippocampal IL-1 β concentration and enhanced activity of the stress-activated MAP kinases JNK and p38. Several other studies have implicated high concentrations of IL-1 β in mediating both acute neurodegeneration and chronic neurodegenerative disease ranging from AD to HIV-associated dementia (Allan & Pinteaux, 2003) (Fogal & Hewett, 2008). However, it is important to note that IL-1 β not only plays a role during infection and inflammation but also during non-pathological processes including sleep. Krueger and colleagues (1998) revealed IL-1 β to be a somnogenic cytokine, playing a role rapid eye movement sleep. Also, despite reports of IL-1 β impairing LTP, low levels of the cytokine are required, and antagonising IL-1R1 has been shown to reversibly block the maintenance of LTP *in vivo* and *in vitro* (Schneider *et al.*, 1998). Although IL-1 β is often associated with destructive and damaging signalling cascades, complete inhibition of its activity could also be detrimental to normal function; therefore researchers persistently strive to understand how homeostasis of this cytokine can be maintained.

1.4.2 Interleukin-6

The cytokine interleukin-6 (IL-6) is an important mediator of immune and inflammatory responses. It was first identified in 1985 for its stimulatory action in peripheral B cell proliferation, but is now believed to have a more multifaceted purpose in immunity (Gruol & Nelson, 1997). Although synthesised by both neurons and microglia, it is hypothesised that astrocytes are the primary source of IL-6 within the CNS (Van Wagoner *et al.*, 1999). However, similar to IL-1 β , IL-6 is found in only trace amounts in the healthy CNS, displaying a marked, yet transient, increase hours after injury (Yan *et al.*, 1992). This concomitant pattern of activation with IL-1 β is suggestive of a role for IL-6 in early inflammatory mechanisms.

IL-6 is sequestered from cells after acute IL-1 or LPS stimulation and exerts its actions via binding to specific IL-6 receptors (Heinrich *et al.*, 1995). The IL-6R is made up of two subunits; an extracellular binding protein (gp80) and a signalling-transducing domain (gp130), which are members of the hematopoietic-receptor superfamily (Bazan, 1990; Heinrich *et al.*, 1995). Binding of IL-6 to gp80 activates gp130, causing it to dimerise and initiate a signal transduction pathway (Murakami *et al.*, 1993). In addition, the external domain of the membrane-bound receptor can be cleaved resulting in a soluble IL-6R. The soluble subunit

forms a complex with IL-6 and has the ability to antagonise the signal-transduction subunit gp130, if exposed at the cell surface (Heinrich *et al.*, 1995). Dimerisation of gp130 leads to phosphorylation of its associated Janus kinases, JAK1 and JAK2, which have the potential to phosphorylate (Signal Transducers and Activators of Transcription) STAT-1 α and STAT-3 (Van Wagoner & Benveniste, 1999). Upon activation, the STAT proteins can translocate to the nucleus and bind to IL-6 response elements and induce transcription. Activation of gp130 by IL-6 has also been shown to enhance MAP kinase activity with subsequent gene transcription (Taga & Kishimoto, 1997; Van Wagoner & Benveniste, 1999). Once the IL-6/gp80 complex is bound to gp130 it becomes internalised, thus the IL-6 receptor becomes down regulated by its ligand to protect against over-stimulation.

Studies have shown IL-6 to be both beneficial and destructive within the CNS. Some of the effects include inhibiting TNF- α and providing negative feedback to limit acute inflammation, as well as being implicated in the protection of neurons from ischemic insult (Feghali & Wright, 1997; Loddick *et al.*, 1998). On the contrary, dysregulation and over expression of IL-6 may contribute to the neuropathology related to dysfunction of the blood-brain barrier and neurodegenerative disease (Campbell *et al.*, 1993; Van Wagoner & Benveniste, 1999).

1.4.3 Tumor necrosis factor- α

TNF- α , originally recognised for its tumor fighting activity, was not detected in the CNS until the late 1980s (Spriggs *et al.*, 1987). TNF- α is a pro-inflammatory cytokine with the ability to enhance IL-1 β and IL-6, thereby perpetuating the inflammatory response through a cascade of signalling molecules with over-lapping properties. TNF- α is synthesised by activated microglia and astrocytes as a membrane-bound precursor of 26kDa, which is cleaved to an active 17kDa signalling molecule and shed from the membrane (Brenner *et al.*, 1993; Gosselin & Rivest, 2007).

This multipotent cytokine can oxymoronically stimulate apoptosis in some cells while evoking growth and proliferation in others. These opposing effects may be partially explained by two distinct signalling pathways of TNF- α , mediated through TNF receptor 1 (TNF-R1; p55) and TNF receptor 2 (TNF-R2; p75; Arnett 2001). Both p55 and p75 are members of the TNF-R

superfamily, related by a conserved cysteine-rich repeat in their extracellular domain and, although their intracellular domains are unrelated, p55 and p75 do share similarities in their signal-transduction (Declercq *et al.*, 1998). Binding of TNF- α to p55 induces the formation of a complex between the receptors death domain (TRADD) and TNF-R associated factor 2 (TRAF2); concurrently FAS-associated death domain protein (FADD) and the death domain kinase receptor interacting protein (RIP) can also be recruited to interact with TRADD (Gosselin & Rivest, 2007). Aggregation of the FADD and TRADD plays a dominant role in TNF- α induced apoptosis via caspase-8, while RIP and TRAF2 direct activity of NF- κ B and JNK (Declercq *et al.*, 1998). Activation of p75 by TNF- α predominates with TRAF2 interactions and downstream signalling leading to NF- κ B and MAP kinase activation. TNF- α is a potent stimulator of trophic proteins; including the NF- κ B regulated monocyte chemoattractant protein-1 (MCP-1), those promoting B-cell proliferation and oligodendrocyte regeneration (Chaplin & Fu, 1998; Arnett *et al.*, 2001; Gosselin & Rivest, 2007). However like p55, p75 activity may trigger apoptosis, but through a different mechanism (Declercq *et al.*, 1998). Indeed, expression of p75 is up-regulated on neurons and astrocytes following an ischemic insult, and ligation of this receptor induces apoptosis via caspase-3 rather than caspase-8 activity (Angelo *et al.*, 2009).

TNF- α supports an elaborate array of inflammatory events, thus it must be stringently regulated; inhibiting TNF- α in the CNS can reduce oedema, while promoting neuronal survival and maintenance of integrity following traumatic brain injury (Shohami *et al.*, 1996). Furthermore, evidence supports the concept that TNF- α is involved in neurodegenerative disease. It has been reported that AD patients have exceptionally elevated levels of TNF- α in their cerebrospinal fluid (CSF) that correlates with clinical deterioration, making TNF- α a potential target for therapeutics (Tobinick *et al.*, 2006).

1.5 LPS: a model for inflammation

LPS is an endotoxin found on the cell wall of all gram negative bacteria, making it an ideal PAMP. LPS is a potent activator of the immune system and is therefore often used experimentally to investigate inflammatory responses. Upon ligation, TLR4 induces an intracellular signalling cascade that promotes transcription of genes involved in inflammation.

This cascade of events has been extensively described by Kopp and colleagues (1999; Figure 1.2). In brief, activation of TLR4 recruits the adaptor protein myeloid differentiation primary response gene 88 (MyD88) to the receptor complex. The TIR domains of MyD88 and TLR4 interact, while MyD88's death domain binds to the death domain of IL-1R-associated kinase (IRAK) leading to IRAK phosphorylation. The signal is propagated via the adaptor molecule tumor necrosis factor-receptor associated factor 6 (TRAF6), ultimately activating nuclear factor- κ B (NF- κ B) and MAP kinases. Once the transcription factors translocate to the nucleus, pro-inflammatory cytokines are up-regulated, forming the basis of an innate immune response. LPS is a prototypical inflammatory stimulus used experimentally to activate immune cells *in vivo* and *in vitro*, inducing up-regulation of the aforementioned surface proteins and cytokines.

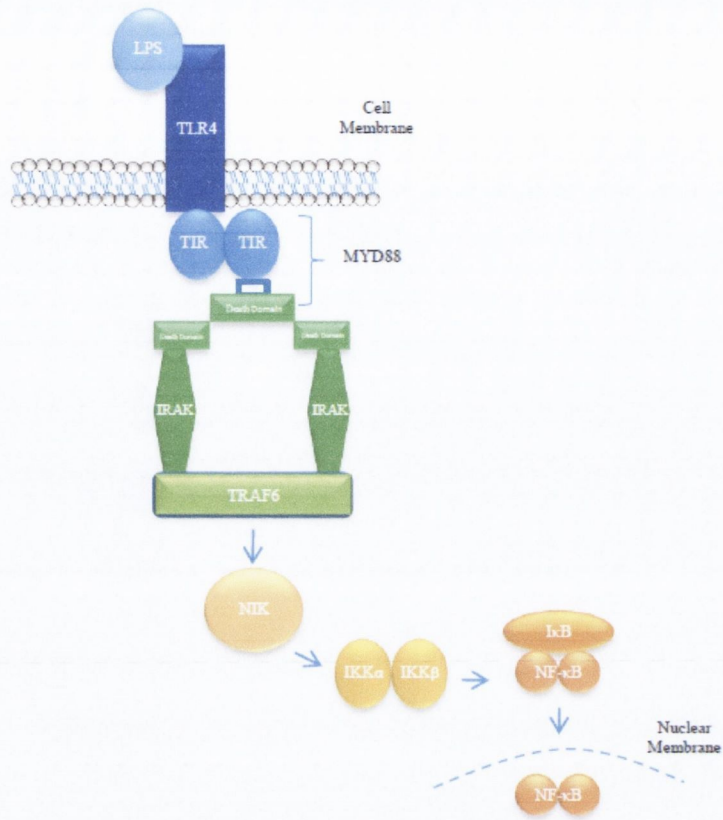


Figure 1.2. Signalling pathway leading from LPS activation of TLR4.

Upon ligation the TIR domain of TLR4 interacts with the TIR domain of MyD88, while MyD88's Death Domain recruits IRAK to the receptor complex. Upon recruitment IRAK is autophosphorylated. IRAK may then dissociate from the receptor complex and associate with TRAF6. TRAF6 interacts with and activates NIK. Activated NIK phosphorylates and activates IKKs, which in turn phosphorylate IκB. Phosphorylated IκB is ubiquitinated and degraded thus releasing NF-κB for translocation to the nucleus. Once in the nucleus NF-κB induces transcription of many genes associated with inflammation. Abbreviations: IKK, Inhibitor of κB kinase; IRAK, Interleukin-1 receptor-associated kinase; MyD, Myeloid differentiation primary response gene; NF-κB, Nuclear factor κ-light-chain-enhancer of activated B cells; NIK, NF-κB-inducing kinase; TIR, Toll/Interleukin-1 receptor; TLR, Toll-like Receptor; TRAF, TNF receptor-associated factor.

1.6 Neural Cell Adhesion Molecule

NCAM was first described as a membrane glycoprotein and termed D2 in 1974 (Jacque *et al.*, 1974). Its characteristic role in cell-cell adhesion during neural development was soon documented in studies using the chick embryo, making it the first cell adhesion molecule to be identified and thus renaming it NCAM (Thiery *et al.*, 1977). NCAM is a member of the immunoglobulin (Ig) superfamily and its extracellular region contains five N-terminal Ig domains, in addition to two fibronectin-type III (F3) modules, see Figure 1.3. It is expressed throughout the CNS, being found on both neurons and glial cells. Thus far the structures of the first three Ig domains and the second F3 module have been determined by nuclear magnetic resonance (NMR) and x-ray crystallography (Jensen *et al.*, 1999; Atkins *et al.*, 2001; Kiselyov *et al.*, 2003). The ectodomain is consistent for the three main isoforms NCAM-120, NCAM-140 and NCAM-180, the numbers referring to their relative molecular weight. These isoforms are generated due to differential slicing of pre-mRNA that is encoded by the same NCAM gene (Owens *et al.*, 1987). It is the intracellular domains of the different NCAMs that make them structurally unique. NCAM-120 lacks a cytoplasmic tail and is secured by a glycosylphosphatidylinositol (GPI) anchor, while NCAM-140 and -180 have cytoplasmic domains of different lengths. Soluble forms of NCAM also exist due to truncation, proteolysis and shedding (Olsen *et al.*, 1993).

1.6.1 NCAM Homophilic Binding

Homophilic interactions between NCAM molecules are fundamental to its role in cell-cell or cell-substratum adhesion and this is largely dependent on the Ig domains of these molecules (Figure 1.3). The Ig1 and Ig2 domains on the same cell can dimerise to form a strong *cis*-bond, this arrangement then permits contact with opposing cells. The adhesion between opposing cells leads to the formation of a weak *trans*-bond and is mediated via the Ig3 domains, in addition to simultaneous Ig1 and Ig2 binding (Soroka *et al.*, 2003). Soroka (2003) proposes a novel zipper mechanism for homophilic adhesion that is supported by x-ray crystallography. On examination it was found that the Ig3 domain on NCAM is orientated at approximately a 45° angle to the Ig1-Ig2 axis, thus adding support to a possible 'zipper' formation between NCAMs during adhesion. Homophilic interactions play an essential role in the developing

CNS and have been implicated in a variety of developmental processes as diverse as cell positioning, tissue patterning and compartmentalisation, axon guidance and synaptogenesis (Thiery, 2003). It has been demonstrated that NCAM-deficient rodents have impaired migration of neural precursor cells during development leading to a marked reduction in brain weight (Ono *et al.*, 1994).

1.6.2 NCAM Heterophilic Binding

Under favourable conditions NCAM can undergo post-transcriptional modification in the Golgi apparatus, leading to the attachment of polysialic acid (PSA) to N-glycosylation sites on the fifth Ig domain (Nelson *et al.*, 1995). Polysialylation of NCAM, producing PSA-NCAM, can modulate the distance between cells due to its hydrated volume. The high degree of hydration leads to enhanced steric repulsion between cell membranes, thus decreasing the efficiency of *trans*-bonds and regulating the overall ability of cells to interact (Johnson *et al.*, 2005; Figure 1.3). PSA-NCAM creates a permissive environment that prevents homophilic interaction and promotes NCAM engaging with growth factor receptors, for example the fibroblast growth factor receptors (FGFR). Interacting with growth factor receptors is important for neuronal differentiation, postnatal myelination, post-mitotic migration of precursor cells and refinement to brain-circuitry during development (Markram *et al.*, 2007). PSA deficiency, although not fatal, can result in mistimed neuronal differentiation, ectopic synapse sprouting and general distortion of the neuronal architecture (El Maarouf & Rutishauser, 2003). For many cells, reaching their final destination is accompanied by a loss of PSA, perhaps to facilitate the establishment of stable synapses (Seki & Rutishauser, 1998). Although overall levels of PSA are reduced in the adult brain, compared with the embryonic brain, high levels still persist in distinct regions that retain some neurogenic capacity, for example the hippocampus, and it is believed to be central to the maintenance of synaptic plasticity in these areas (Seki & Arai, 1991). Many researchers have demonstrated that perturbation of PSA levels can influence synaptic strength at a cellular level, and memory acquisition and consolidation at a functional level (Markram *et al.*, 2007).

In contrast to PSA enhancing NCAM-FGFR binding, the presence of ATP in the extracellular fluid can inhibit phosphorylation of the growth factor receptor by NCAM (Skladchikova *et al.*,

1999). ATP is a prevalent neurotransmitter, found in abundance in the vicinity of synapses. Using surface plasmon resonance (SPR), Skladchikova and colleagues (1999) reported that the NCAM sites binding to fibroblast growth factor receptor (FGFR) and ATP overlapped, indicating that ATP probably regulates the NCAM-FGFR interaction. With this in mind Kiselyov (2005) hypothesised that when a growth cone reaches its target and a new synaptic contact is formed, the presence of ATP may inhibit growth extension, switching NCAM from the signalling mode to a mode promoting adhesion.

It is evident that NCAM has a plethora of diverse and dynamic roles within the CNS. Studies using NCAM knock-out mice have demonstrated that, in addition to impairing CNS development, blockade of this system can induce deficits in spatial learning and inhibit induction or early maintenance of LTP *in vivo*, indicating a pivotal role of NCAM in neuronal plasticity throughout life (Ronn *et al.*, 1995; Becker *et al.*, 1996). Studies investigating the pattern of PSA-NCAM immunoreactivity demonstrate a marked decrease in its expression on both glia and neurons in the dentate gyrus with age (Fox *et al.*, 1995). It has been implied that this decline correlates with diminished cognitive ability that can accompany the aging process (Regan & Fox, 1995).

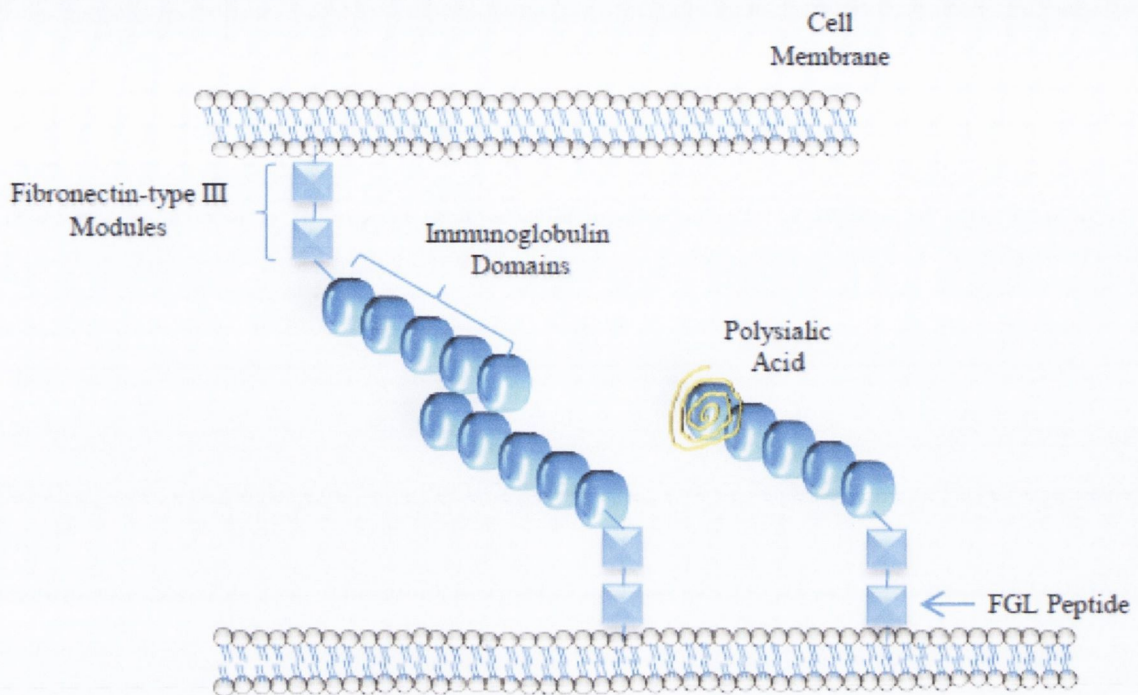


Figure 1.3. The structure of NCAM on the cell membrane.

The seven-domain protein, contains five immunoglobulin domains and two fibronectin-type III (F3) modules. Homophilic binding between identical NCAM molecules occurs at opposing membranes to form cell-cell junctions. PSA-NCAM is modified with up to two linear polysialic acid chains, which are negatively charged and prevent homophilic binding, thus favouring interaction with other receptors, for example FGFR-1. FGL mimics a fifteen amino acid chain on the second F3 module. Abbreviations: FGL, Fibroblast growth Loop.

1.7 Fibroblast Growth Factors and their receptors

Fibroblast growth factors (FGF) were the first family of growth factors to be identified and, like NCAM, play a central role in many developmental processes. There are twenty-two FGF, ten of which have been identified in the CNS. All FGF molecules contain a conserved 120 amino acid core region that shares 30-60% homology across the family and a heparin sulphate

proteoglycan binding domain, which is an obligatory co-factor in activation of FGFR by FGF (Ornitz *et al.*, 1996; Ornitz & Itoh, 2001).

While the bulky addition of PSA to NCAM can decrease NCAM-NCAM homophilic interactions, it enhances NCAM heterophilic binding (outlined in Figure 1.3). Moreover, removal of PSA can inhibit NCAM-mediated neuronal development (Doherty *et al.*, 1990). Evidence suggests that under these conditions NCAM is involved in *cis*-interactions with FGFR via the NCAM F3 region (Kiselyov *et al.*, 2003). FGFR are a family of four receptors with intrinsic tyrosine kinase activity. These receptors contain three Ig-like domains and a heparin-binding sequence in their extracellular region. Alternative splicing of FGFR mRNA produces receptors with different carboxyl terminal halves of the Ig3 domain, which in turn influences ligand-receptor binding specificity (Johnson & Williams, 1993). Expression studies indicate differential expression of the FGF receptors throughout the CNS and this pattern changes during the stages of development. FGFR-1 is expressed most abundantly throughout life. FGFR-2 and -3 display a localised pattern of expression, which is highly dynamic and adapts with the architecture of the developing CNS. While FGFR-4 is the most elusive within the CNS, its expression has been confirmed but a detailed localisation of this expression has yet to be mapped (Ford-Perriss *et al.*, 2001). Studies using FGFR knock-out mice have not been of great benefit in establishing the exact role of these receptors in the developing CNS as deletion of these receptors is lethal prior to the development of the CNS (Ford-Perriss *et al.*, 2001).

Interaction between NCAM and FGFR was first noted in 1994 and was proposed to be required for NCAM-induced neurite outgrowth (Williams *et al.*, 1994). Williams (1994) identified a domain in the FGFR family that was homologous to that found on the F3 region of NCAM. Antibodies that bind to this domain specifically inhibit neurite outgrowth stimulated by NCAM. Further studies by Williams and colleagues confirmed that NCAM directly induces phosphorylation of FGFR, thus activating a variety of down-stream signalling cascades. On the other hand, expression of a dominant negative FGFR in a transgenic model inhibits NCAM-stimulated axonal development. The affinity for NCAM for FGFR is approximately 10^6 less than the attraction between FGFR and its cognate ligand, FGF (Kiselyov *et al.*, 2005). However, NCAM is one of the most abundant molecules in the brain,

in contrast with FGF that only appears transiently and in nanomolar concentrations. Moreover, the polysialylation of NCAM may act as a switch to increase probability of NCAM-FGFR binding. Due to concentration and temporal differences in the expression of NCAM and FGF it is suggested that these molecules activate FGFR in distinctly different ways. Figure 1.4 delineates a complex and diverse array of signalling cascades that are activated after ligation of FGFR-1 by NCAM.

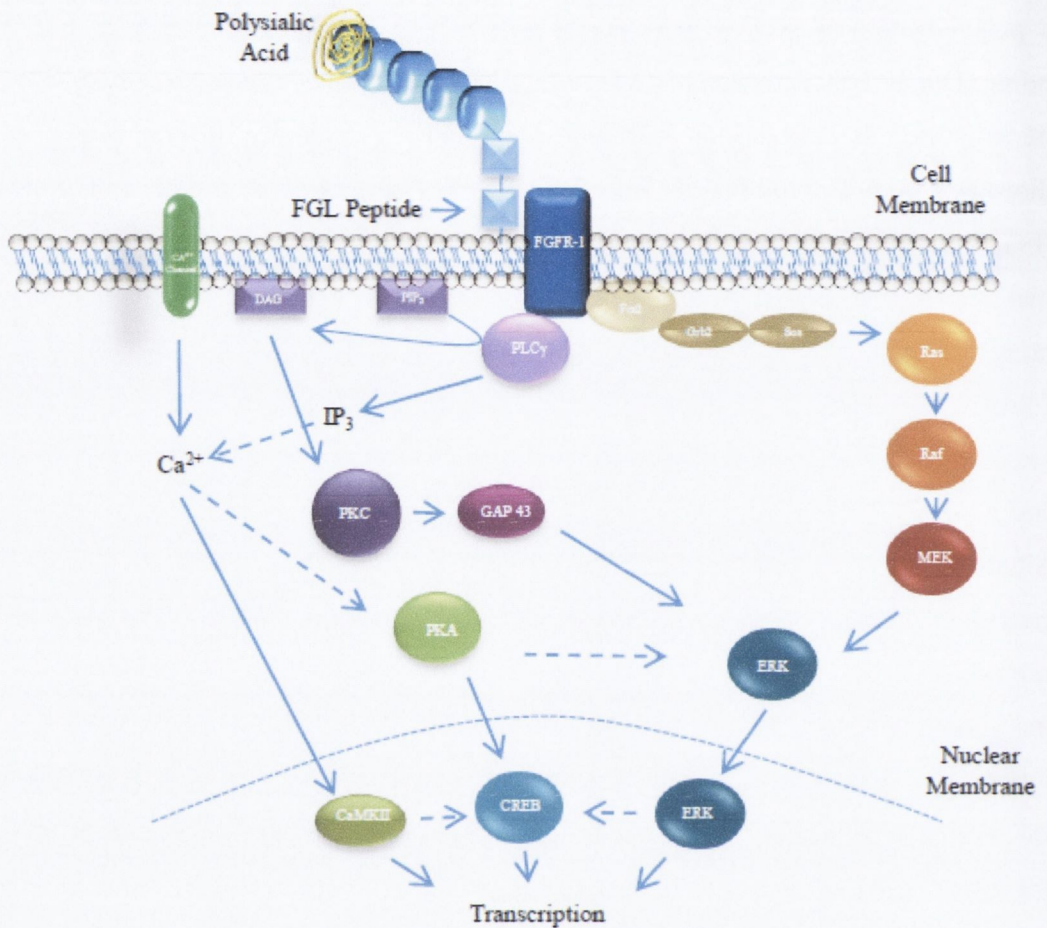


Figure 1.4. Signalling pathways leading from PSA-NCAM activation of FGFR-1.

FGFR-1 activation by PSA-NCAM leads to autophosphorylation and propagation of intracellular signalling cascades, including the Ras/MAPK pathway, PI3 kinase/Akt pathway, and the PLC γ /Ca²⁺ pathway. There is much cross-talk between cascades, which is indicated with dotted arrows. The Ras/MAPK cascade is activated by binding of Grb2 to phosphorylated FRS2. The subsequent formation of a Grb2/SOS complex leads to the activation of Ras. Various routes by which FGFR-1 can activate the PI3 kinase/Akt pathway are indicated. The PI3 kinase-regulatory subunit can bind to a phosphorylated tyrosine residue of the FGFR-1. Alternatively, activated Ras can induce membrane localization and activation of a catalytic subunit of PI3 kinase. All of the depicted pathways lead to an up-regulation in the transcription factors CaMKII, CREB or ERK, which are associated with cell proliferation and pro-survival molecules. Abbreviations: See list page iv.

1.8 Fibroblast Growth Loop

Fibroblast growth loop (FGL) is an NCAM-mimetic peptide that emulates the interaction of NCAM with FGFR-1. The FGL peptide is a fifteen amino acid long chain, encompassing the F and G β -strands and interconnecting loop of the second F3 domain of NCAM. SPR was used to confirm that the interaction between NCAM and FGFR was dependant on the F3 domain, while NMR spectroscopy allowed the distinct structure of the active binding site to be determined (Kiselyov *et al.*, 2003).

Since the 1970s NCAM has been intensively investigated and research has facilitated our understanding of the mechanisms underlying enduring synaptic modifications and memory storage. Its role in cognitive processes has been demonstrated by studies that interfere with NCAM function and more recently attention has been drawn to the possible benefits, whereby enhancement of NCAM expression could boost LTP and aid memory formation. The progression of this research has been facilitated by advancements in NMR spectroscopy, which allows molecules to be visualised, and combinatorial chemistry, allowing specific mimetic molecules to be constructed. Kiselyov and colleges (2003) identified the small peptide loop that represents the FGFR-1 binding site of NCAM and confirmed the importance of this peptide by demonstrating the ability of this NCAM region to activate the receptor and stimulate neurite outgrowth.

The first study revealing the therapeutic potential of FGL was published by Cambon and colleagues in 2004. This study demonstrated the ability of FGL to facilitate memory consolidation and enhance presynaptic function. Contextual fear conditioning, a hippocampal-dependent memory task, demonstrated that treatment with FGL could enhance memory consolidation. This finding was substantiates previous work which also used contextual fear conditioning and proposed that NCAM participates in the establishment of long-term memory in this particular learning paradigm (Merino *et al.*, 2000). Consistent with the importance of synaptic plasticity in memory formation, Cambon and colleagues (2004) demonstrated the proclivity of FGL to up-regulate transmitter release in primary cultured hippocampal neurons and to promote synapse formation, as measured by synaptophysin-positive staining. FGL has also been shown to increased neurite length in a dose-dependent manner and protect against a

variety of toxic insults, including 6-Hydroxydopamine (6-OHDA) and amyloid- β ($A\beta$) *in vitro* (Neiiendam *et al.*, 2004). The data suggest that the neuroprotective and proliferative effects of FGL depend of activation of MAP kinases and phosphoinositide 3-kinase (PI-3 kinase) through FGFR phosphorylation.

A protective role for the peptide was also established by demonstrating that incubation with FGL could prevented cell damage in hippocampal organotypic slice cultures subjected to oxygen-glucose deprivation (OGD) and the presence of FGL maintained metabolic activity in these slices (Skibo *et al.*, 2005). The same authors tested the neuroprotective actions of FGL *in vivo* using a transient global ischemia model. They found that sub-optical administration of FGL prior to clamping the carotid artery protected the hippocampal neurons; their survival increased from 12.5% to 36.6%. These results challenge previous studies that have used the OGD model and targeted FGFR through use of FGF, which lead to increased cell loss with the treatment (Lobner & Ali, 2002). One explanation for the loss of activity after FGF administration may relate to the possibility that FGL-mediated phosphorylation of FGFR induces a spatio-temporally specific response that differs from stimulation by FGF.

A number of studies have assessed the ability of FGL to ameliorate the effects of $A\beta$. $A\beta_{1-42}$ is the primary component of senile plaques found in the brains of AD patients, however, the sequence from 25-35 has been referred to as a toxic core fragment of the 42 amino-acid long peptide (Pike *et al.*, 1995). It was shown that while intracerebroventricular (icv) administration of pre-aggregated $A\beta_{25-35}$ induced a time-dependent increase in $A\beta$ -immunoreactivity in the cingulate cortex and hippocampus, this immunoreactivity was decreased in animals that received FGL intracisternally post- $A\beta_{25-35}$ injection (Klementiev *et al.*, 2007). $A\beta$ induced a decline in cognitive function, in a social recognition test that requires short-term memory, whereas administration of FGL following the $A\beta$ injection decreased the deficit.

Klementiev (2007) also investigated the effects of FGL on $A\beta_{25-35}$ -induced changes in neuronal morphology, tau phosphorylation, microgliosis and astrogliosis. Immunohistochemical analysis revealed that $A\beta_{25-35}$ administration led to neuronal atrophy and enhanced tau phosphorylation in the hippocampus and these changes were abrogated by administration of FGL after $A\beta$ exposure. It is well documented that inflammation plays an

integral role in neurodegeneration and, in addition to neuronal atrophy, A β ₂₅₋₃₅ increased microglial and astrocytic activity as assessed by CD11b and GFAP immunoreactivity in hippocampus. This increase was attenuated in hippocampus of animals that received FGL, highlighting the anti-inflammatory capabilities of the peptide.

The anti-inflammatory effects of FGL were also reported by Downer and colleagues (2007); in this study the anti-inflammatory action of FGL was observed in hippocampus of aged rats, as chronic treatment with the peptide over a 3 week period attenuated the age related increase in hippocampal IL-1 β , CD86 and ICAM-1 expression. FGL also reversed the age-related impairment in LTP, measured at the perforant path-granule cell synapse in the dentate gyrus. The data suggested that, through the activation of MAP kinases, FGL enhanced neuronal CD200 expression and increase release of the anti-inflammatory cytokine IL-4. A subsequent study by Downer and colleagues (2009) set out to delineate the mechanism by which FGL modulates neuroinflammatory changes *in vivo* and *in vitro*. The study demonstrated that FGL attenuated the age-related decrease in insulin like growth factor-1 (IGF-1) at an mRNA and protein level. Consistent with this, exposure to FGL amplified IGF-1 expression in primary neuronal cultures. It is of note that IGF-1 is one of the most potent stimulators of the AKT/PI-3 kinase signalling cascade, which is fundamental in cell survival, growth and proliferation. *In vivo* analysis shows that changes in AKT activation parallel those of IGF-1. In this study there was a concomitant age-related decrease in AKT phosphorylation, which was reversed by FGL treatment.

1.8.1 Inhibition of FGL by SU5402

The activity of FGL can be antagonised by the compound SU5402 (3-[(3-(2-carboxyethyl)-4-methylpyrrol-2-yl) methylene]-2-indolinone), which specifically inhibits the catalytic domain of FGFR-1 (Mohammadi *et al.*, 1997). SU5402 has been utilised in a variety of studies to demonstrate that the effects of FGL are dependent on activation of the FGF receptor. This specific antagonist prevents the FGL induced enhancement of neurite outgrowth and transmitter release from hippocampal neurons *in vitro* (Cambon *et al.*, 2004; Neiiendam *et al.*, 2004). SU5402 also blocked the neuroprotective action of FGL on cultured cerebellar granule neurons subjected to a low KCl environment (Neiiendam *et al.*, 2004). Skibo (2005) reported

that incubating cells in the presence of FGL and SU5402, abrogated the neuroprotective effects of FGL in cultured neurons subjected to OGD, thus further signifying that the activity of FGL depends on activation of FGFR.

1.8.2 Administration of FGL in humans

The first report on human exposure to the NCAM-mimetic FGL was published in 2007. The study, based in Switzerland, was designed to test the tolerability, safety and pharmacokinetics of ascending doses of FGL in healthy male volunteers. The study evaluated 24 subjects that received a single intranasal dose of FGL (25, 100 or 200mg), as FGL is a peptide it cannot be administered orally. The three doses of FGL were well tolerated and caused no clinically notable abnormalities. However, three of the subjects that received the highest dose experienced transient, mild adverse effects, including a burning sensation in the nose and shorted-lived epiphora. The pharmacokinetic analysis revealed quantifiable plasma concentrations of FGL at 1 hour for the 100mg dose and at 1 and 4 hours for the 200mg dose, the 25mg dose was undetectable. FGL was not quantifiable at 8 or 24 hours post dose. The maximum serum concentration (C_{max}) and the area under the plasma concentration-time curve up to 24 hours post-dose (AUC_{24}) showed no significant increase in systemic exposure with increasing dosage from 100-200mg. This inaugural study, exposing humans to FGL, found that intranasal administration of FGL was well tolerated in healthy males and further studies are warranted to examine the relationship between intranasal dosage and CNS activity, before moving on to a clinical population.

1.9 Immune-modulation; a role for CD200

In 1982, CD200 was purified and characterised using an OX 2 monoclonal antibody (Barclay & Ward, 1982). It was found to have a specific, rather than ubiquitous distribution on thymocytes, neurons, dendritic cells, vascular endothelium, smooth muscle and B cells, indicating a distinct, but yet unknown, biological function. CD200 was characterised as a 41-47 kDa cell surface glycoprotein, bearing two Ig superfamily domains, a single transmembrane domain and a short cytoplasmic tail (Clark *et al.*, 1985). By binding

fluorescent beads to the extracellular domains of OX 2, a chimeric protein was produced, which allowed CD200 receptor/ligand interactions to be identified (Preston *et al.*, 1997). Further analysis and use of high affinity antibodies led to the CD200 receptor (CD200R) being isolated from the rat spleen and its expression recognised on all cells of the myeloid lineage (Wright *et al.*, 2000). Similar to CD200, CD200R contains two Ig superfamily domains, but a considerably larger cytoplasmic domain with signalling capacity.

It was noted that the CD200 and its receptor had a similar distribution pattern to that of CD47, and its receptor, SIRP- α , which also is found predominantly on myeloid cells (Kharitononkov *et al.*, 1997). With the knowledge that interaction between CD47 and SIRP- α can inhibit myeloid cell activity, the quest to uncover a function for CD200 within the immune system became more credible. One of the first studies to suggest an immunosuppressive role for CD200 was conducted by Gorczynski and colleagues on murine graft survival (Gorczynski, Chen *et al.* 1998). They reported that increasing CD200 expression could enhance allograft survival, while later work revealed that this could be reversed by use of a monoclonal antibody specific for CD200 (Gorczynski *et al.*, 2000). The proclivity for CD200 to provide an inhibitory signal to myeloid cells was further confirmed through use of CD200^{-/-} mice. Mice deficient in CD200 were developed by Sedgwick and colleagues (2000). In brief, an *Eco*-47III-*Sal* 1 fragment of a CD200 genetic clone was used to create a targeting construct in which the *Nco* 1 fragment was replaced with a PGK-neo^r cassette. The construct was used to transfect C57BL/6 embryonic stem cells that were microinjected into BALB/c blastocytes. Chimeras were mated with C57BL/6 mice and CD200^{-/-} progeny generated by co-breeding offspring expressing the deleted germ-line DNA (Hoek *et al.*, 2000). CD200-deficient mice are essentially indistinguishable from their wildtype counterparts; they are fertile and have a normal lifespan. However, disruption to CD200 expression leads to increased populations of macrophages in the spleen and lymph nodes and amplification in CD11b and CD45 expression on microglia. The microglia in these mice also displayed a more amoeboid morphology and clustered in aggregates, particularly in the spinal cord. With the apparent dysregulation of these cells, it was hypothesised that in the absence of CD200 there is a shift in the 'resting' state myeloid cells to a more tonically active state (Hoek *et al.*, 2000).

The assertion that myeloid cells from CD200^{-/-} mice expressed a more activated phenotype was tested in three autoimmune models; myelin oligodendrocyte glycoprotein (MOG)-induced EAE, collagen-induced arthritis (CIA), a model for rheumatoid arthritis and experimental autoimmune uveoretinitis (EAU), a murine model for uveitis. All three experimentally-induced diseases had a more rapid onset in CD200^{-/-} animals, compared with wildtype mice (Campbell *et al.*, 2000; Hoek *et al.*, 2000; Copland *et al.*, 2007). The studies revealed enhanced expression of nitric oxide (NO), a potent immune regulator with antimicrobial activity, in EAE and EAU treated CD200^{-/-} mice, compared with their wildtype counterparts. NO production has been shown to induce microgliosis and is implicated in the perpetuation of an immune response, therefore enhanced NO production in these animals makes them more vulnerable to bystander tissue damage, which further increases the severity of the disease (Roy *et al.*, 2006). Next the function of CD200 during viral infection was investigated. Snelgrove and colleagues (2008) reported that CD200-deficient mice had enhanced sensitivity to influenza infection. They reported excessive production of NO and pro-inflammatory cytokines, which resulted in delayed resolution of inflammation and an enhancement in collateral tissue damage. The authors emphasised that alveolar macrophages innately have higher CD200R expression, compared with macrophages in other tissue, to maintain a high threshold of immune ignorance to innocuous antigens, thus preventing an excessive host response and destruction of delicate respiratory tissue (Snelgrove *et al.*, 2008). It is also of note that the immune activity of microglia within the CNS must also be tightly regulated, to avoid damaging post-mitotic neurons. Like the in the lungs a quiescent environment is maintained through high CD200R expression on microglia that engages with CD200 that is abundant on neurons and endothelia (Hoek *et al.*, 2000).

While a deficit in CD200 can intensify an inflammatory response, it has been reported that enhancing CD200R ligation by gene manipulation or administration of a CD200R agonist can be beneficial. Interestingly, in contrast to CD200^{-/-} mice displaying an increased susceptibility to EAE, a spontaneously-occurring strain of mice, called Wld^s, which express elevated levels of neuronal CD200, are less vulnerable to the experimentally-induced disease (Chitnis *et al.*, 2007). Furthermore, it has been reported that skin and cardiac allografts are readily accepted in transgenic mice, which over express CD200. However, endogenous levels of CD200 are sufficient to maintain viability of the graft after two weeks of induced tolerance (Gorzynski *et*

al., 2009). With a less invasive approach than gene manipulation, the immunological consequences of small soluble CD200R agonists have been shown to modulate graft rejection and inflammatory disease. In the case of EAU, it was found that a CD200R monoclonal antibody (DX109) suppressed macrophage activation and resulted in an earlier resolution of the disease when administered either systemically or locally (Copland *et al.*, 2007). Similarly, it was found that a CD200 fusion protein (CD200Fc), containing the ectodomain of CD200 bound to a murine IgG2a module, decreased the severity of established CIA, both clinically and histologically, and diminished mast cells mediators in targeted joints without obvious systemic immunosuppressive effects (Simelyte *et al.*, 2008). CD200Fc was also beneficial in preventing inflammatory lung disease and bystander tissue damage, while not affecting viral clearance, in influenza infected mice (Snelgrove *et al.*, 2008). These findings present a compelling case for the therapeutic potential of CD200-CD200R manipulation. In fact, immunohistochemical studies have examined CD200 and CD200R expression in the CNS of AD and MS patients. A decrease in both ligand and receptor was found in hippocampus of AD patients, compared with non-demented controls, at an mRNA and protein level (Walker *et al.*, 2009). While a decreased in CD200 immunoreactivity was also observed in MS lesions (Koning *et al.*, 2009). Thus suggesting the CD200-CD200R axis may be perturbed in these conditions.

1.9.1 CD200 Signalling

CD200 interacts with its cognate receptor via their N-terminal Ig-like domains and the functional consequences of this engagement requires downstream signalling events in the cell bearing the receptor, which in turn leads to immune-suppression (Hatherley & Barclay, 2004). The cytoplasmic tail of CD200R contains three conserved tyrosine residues, while CD200 is not known to possess any signalling motifs (Wright *et al.*, 2000). Mahrshahi and colleagues (2009) investigated the molecular mechanisms of CD200R in human myeloid cells, which is outlined in Figure 1.5. They reported that the third tyrosine residue of CD200R, located most distal to the membrane, contains a phosphotyrosine-binding (PTB) domain that recruits the PTB domain of the downstream of tyrosine kinase 2 (DOK-2) adaptor proteins, upon receptor ligation. Once phosphorylated, DOK-2 recruits RAS p21 protein activator 1 (RasGAP), which in turn can inhibit Ras-ERK signalling pathways. The critical involvement of DOK-2 in

CD200R signalling was confirmed by use of RNA interference and DOK-2 knockdown experiments, thus the hierarchy of interactions established through quantitative biochemistry were consistent with functional data (Mihirshahi *et al.*, 2009). Previous studies using murine mast cells advocate recruitment and phosphorylation of both DOK-1 and DOK-2 in CD200R activation (Zhang & Phillips, 2006). The receptor is highly conserved between species and Mihirshahi (2009) found that DOK-1 recruitment occurs once DOK-2 was phosphorylated; however, its activation was not integral to CD200-induced myeloid cells regulation. Although some discrepancies remain regarding the exact signalling induced by engagement of CD200 with its receptor, there is agreement that its modulatory activity is unique. Unlike other myeloid cell inhibitory receptors that recruit phosphatases through inhibitory motifs, it has been established the CD200R signalling relies on tyrosine phosphorylation rather than dephosphorylation (Mihirshahi *et al.*, 2009).

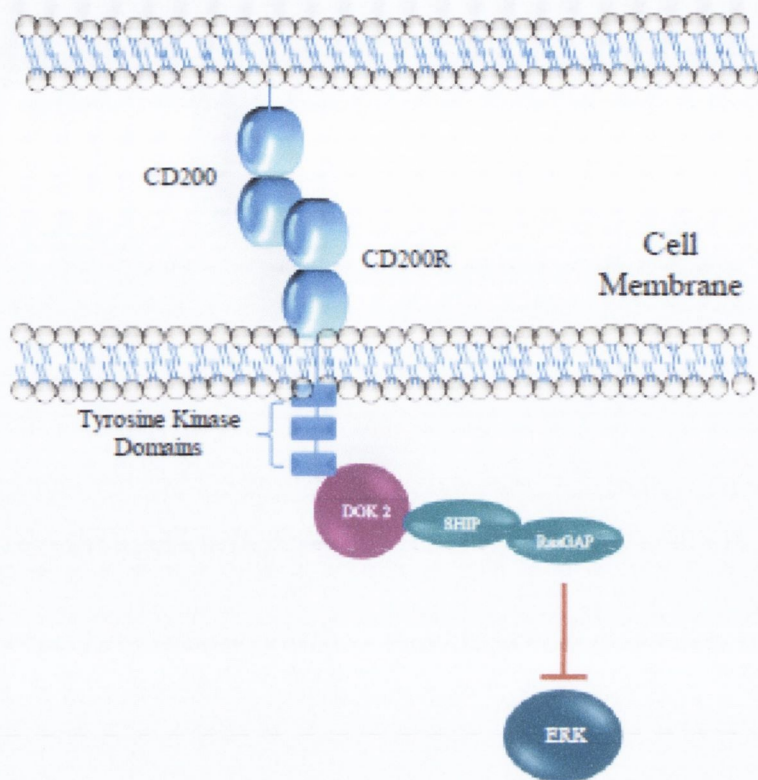


Figure.1.5. Activation of CD200R by CD200

Interaction between the immunoglobulin domains of CD200 and CD200R initiates a downstream signalling cascade that inhibits the Ras-ERK pathway. It is proposed that upon ligation the third tyrosine residue of CD200R recruits the adaptor protein DOK-2. Phosphorylation of DOK-2 activates RasGAP via SHIP, which eventually results in immune cell modulation. Abbreviations: CD, Cluster of Differentiation; DOK, Downstream of tyrosine kinase; RasGAP, Ras GTPase activating protein; SHIP, SH2-containing inositol 5-phosphatase.

1.10 The CNS; an anatomical view

The Central Nervous System (CNS) integrates information allowing it to coordinate the functions of all organs. Despite Aristotle's notions that the brain was merely a blood cooler, and the heart a command centre, the importance of the brain in controlling body function and bearing the seat of intelligence has been advocated since the Archaic Period of Ancient

Greece. The oldest and, up until recently, most widely used method for investigating the CNS was anatomical analysis of both large scale and microscopic structures. The Roman physician Galen elegantly demonstrated the association between the brain and the periphery via branching networks of nerves. The Renaissance saw the return of artistic depictions of neuro-anatomy; and the development of the Golgi Stain in the late 1800s revealed networks of distinct neurons with unique dendritic structures and patterns of connectivity.

Today, neurons are defined by their ability to transmit rapid electrical signals. This involves the conduction of action potentials down an axon to a presynaptic terminal, depolarisation of the terminal, release of neurotransmitters and subsequent excitation of connecting neurons, thus propagating the signal. In the late 1800s it was recognised that many cells in the brain lack this ability and these cells were referred to as glia (Wang & Bordey, 2008). Such cells include, but are not restricted to, astrocytes, microglia, oligodendrocytes, Schwann cells and ependymal cells. Glia are highly conserved between species and account for over 90% of cells in the human brain, as they surround and ensheath neuronal cell bodies, axons and synapses.

Glia were originally alluded to as 'brain glue' by Rudolph Virchow in the mid 1800's. He referred to these cells as an inert scaffold, essentially there as a structural support for neurons, in a paper published in the German Medical Journal (1856). This disregard for the role of glia in CNS activity became entrenched and it is only in recent years that their complex function is beginning to be unravelled. We now know that the lipid-rich, myelin sheath that insulates and enhances neuronal conductance is formed by oligodendrocytes, Schwann cells serving a similar function on peripheral nerve fibres; radial glia guide the migration of nerve cells in the embryonic brain and ependymal cells form the lining of the cerebral ventricles, producing and secreting cerebrospinal fluid.

In addition to the microscopic depiction of different cell types, the functional and anatomical associations between brain regions were also being elucidated. Post-mortem dissection of an aphasic patient by Paul Broca revealed a lesion in the ventroposterior region of the frontal lobe, now known as the Broca's area and deemed the speech producing centre. Similarly, Carl Wernicke described a patient with deficits in language comprehension, who was later found to have damage to his posterior superior temporal gyrus. This region is now referred to as

Wernicke's area and known to be required for semantical speech output. However, no lesion study has been more extensively documented, or indeed contributed more to the structure-function relationship of brain regions, than that of patient H.M. This patient, suffering from intractable epilepsy, underwent a bilateral medial temporal lobectomy in order to prevent debilitating tonic-clonic seizures, or more commonly known as grand mal seizures. After the surgery H.M. suffered from severe anterograde amnesia and was unable to commit new events to long-term memory (Scoville & Milner, 1957). From this point our understanding of the organisation of memory was revolutionised and the hippocampus took centre stage.

1.11 Long-Term Potentiation; a biological substrate for Memory

It is almost universally accepted that the hippocampus, located in the medial temporal lobe, plays a critical function in spatial memory and there are many well-developed protocols substantiating this. One of the most widely accepted is the Morris water maze, a memory test where hippocampal-lesioned animals display impairments (Morris *et al.*, 1982). While specific brain structures and neuronal circuits have been considered essential for particular forms of learning and memory, the exact molecular and cellular mechanisms that are required have yet to be determined. There is a plethora of evidence to suggest that memory is a form of synaptic plasticity and the Hebbian theory (1949) proposes a basic mechanism for plasticity, whereby an increase in synaptic efficacy occurs from one cell's repeated and persistent stimulation of another, thus strengthening the connection. In an effort to establish an association between synaptic plasticity and memory, models for synaptic strengthening are used, the most prominent being long-term potentiation (LTP).

LTP was first described by Bliss and Lomo in 1973 when it was discovered that brief trains of high-frequency stimulation (HFS) to a monosynaptic excitatory pathway in rabbit hippocampus, resulted in an abrupt and sustained enhancement in synaptic transmission. LTP has three defined characteristics: cooperativity, associativity and input specificity (Bliss & Collingridge, 1993). Cooperativity describes the intensity and pattern of tetanic stimulation required to induce LTP. Associativity is the property that synapses will only undergo potentiation in response to a subthreshold stimulation if activated in tandem with a strong tetanus on a separate synapse of the same cell, which is an implicit property of the Hebbian

theory (Levy & Steward, 1979). Finally, input specificity refers to the phenomenon that when LTP is induced in one set of cells the adjacent cells that did not receive tetans will not undergo potentiation (Lynch *et al.*, 1977). In the 1980s the role of *N*-methyl-D-aspartate (NMDA) receptors in the consolidation of LTP became apparent. The NMDA receptor is a dually-gated Ca^{2+} channel that requires membrane depolarisation and binding of glutamate to promote opening. It acts as a molecular coincidence detector displaying characteristics of activation that eloquently explain the properties of cooperativity, associativity and input specificity of LTP (Bliss & Collingridge, 1993).

1.11.1 Signalling molecules involved in LTP

Once activated, NMDA receptors act as Ca^{2+} channels, transiently permitting an influx of calcium ions into post-synaptic spines. NMDA receptor activation and the subsequent increase in intracellular Ca^{2+} concentration are critical for LTP induction. Blocking NMDA receptors competitively with AP5, or non-competitively with MK801, or chelating Ca^{2+} in the post-synaptic cell using EGTA, prevents induction of LTP (Lynch *et al.*, 1983; Coan & Collingridge, 1987; Errington *et al.*, 1987). The same antagonists can also impair acquisition and memory retention in the Morris water maze (Morris *et al.*, 1986). The elevation in intracellular Ca^{2+} concentration triggers phosphorylation of Ca^{2+} /calmodulin-dependent protein kinase II (CaMKII), which remains active after induction of LTP due to autophosphorylation at threonine-286. Substitution of this threonine with alanine, thus preventing activation, leads to impairment in LTP and can similarly, attenuate performance in spatial learning tasks (Giese *et al.*, 1998). Downstream of CaMKII phosphorylation a variety of signaling molecules have been identified that are critical in the maintenance of LTP, many of which are stimulated by an increase in cyclic adenosine monophosphate (cAMP), as a result of activation of protein kinase A (PKA) (Huang & Kandel, 1994). Huang and Kandel demonstrated that unlike CaMKII these molecules were not required for the induction of LTP, but inhibiting PKA attenuated the maintenance of LTP. Data also indicate that cAMP can stimulate extracellular-signal-regulated kinases (ERK), a mitogen-activated protein (MAP) kinase, possibly via TrkB or indeed PKA (Martin *et al.*, 1997; Adams & Sweatt, 2002). The fundamental involvement of ERK in early- and late-phase LTP was initially established through the finding that antagonising ERK with a specific inhibitor (PD98059) suppressed

LTP in the dentate gyrus (McGahon *et al.*, 1999). In addition, an increase in ERK phosphorylation has been consistently reported in the hippocampus following induction of LTP and this has been associated with enhanced glutamate release (Davis *et al.*, 2000; Gooney *et al.*, 2002). Furthermore, through the use of specific inhibitors, the role of ERK in spatial memory was confirmed (Selcher *et al.*, 1999; Hebert & Dash, 2002). ERK appears to be a point of convergence for several signalling cascades, resulting in an array of changes following its activation, which involve its translocation to the nucleus and induction of transcription (Gooney *et al.*, 2002).

1.11.2 Age-related impairment in LTP

In contrast to impairing the induction and maintenance of LTP with exogenous chemicals, endogenous factors can induce deficits and one of the most prominent risk factor for impairing LTP is age. For many years an age-related decline in cognitive function has been recognised and more recently deficits in spatial memory have been correlated with impairment in LTP (Bach *et al.*, 1999). There is general agreement that maintenance of LTP is impaired with age, but the underlying causes for this deficit have yet to be fully elucidated (Barnes, 1979; de Toledo-Morrell & Morrell, 1985; McGahon *et al.*, 1997). Initially, a plausible explanation for the deficit could be due age-related neuronal loss; however, there is much debate as to whether a significant amount of atrophy occurs with age. Many studies have reported no age-related cell loss in the hippocampus or entorhinal cortex, while others have detected a lower density of neurons in these areas (Rapp & Gallagher, 1996; McLay *et al.*, 1999; Merrill *et al.*, 2001). Although this debate continues, the age-related deficit in LTP is believed to be more complex than mere cell counts can explain. Studies have reported a variety of age-related changes that could in-part explain a deficit, these include decreased membrane fluidity due to lipid peroxidation, reduced glutamate release in the hippocampus, diminished capacity for NMDA receptor binding, disruption to Ca^{2+} homeostasis and a decline in ERK signalling (Lynch, 2004). It has been suggested that the impairment may be a consequence of the alterations in membrane characteristics, which could impact on membrane function and decreased synaptic plasticity has been negatively correlated with an increase in oxidative stress induced by reactive oxygen species (ROS) (Vereker *et al.*, 2001). Vereker and colleagues found that the increase in ROS in the hippocampus was closely coupled with an increase in the pro-

inflammatory cytokine interleukin-1 β (IL-1 β). Up-regulation in IL-1 β concentration has persistently been shown to inhibit LTP and evidence suggests that age-related enhancement of the inflammatory profile in the hippocampus contributes to impairment in plasticity (Lynch, 1998; Murray & Lynch, 1998; Kelly *et al.*, 2001). Furthermore, immune-active molecules have the ability to modulate learning and memory process and there is a plethora of data indicating cognitive function is disrupted by neuroinflammation (Maier & Watkins, 1995; Pugh *et al.*, 1998).

1.12 Objectives

The aims of this study were:

1. To examine the modulating action of FGL on LPS- and A β ₂₅₋₃₅-induced changes in primary mixed glia. An *in vitro* approach was used to delineate the effect of FGL on specific cell populations within the CNS, namely astrocytes and microglia. Cells were pre-treated with LPS, a gold-standard inflammatory stimulus, to mirror the pro-inflammatory profile and activation state of glial cells that has been described in the aged brain (Lynch *et al.*, 1998). An A β peptide was also used as an inflammatory stimulus. In addition to a pro-inflammatory phenotype, the accumulation of A β is associated with the pathogenesis of the age-related neurodegenerative disease AD (Tan *et al.*, 2001). The A β ₂₅₋₃₅ peptide was chosen because it has been demonstrated to be the toxic core fragment of the full-length A β ₁₋₄₂ peptide, found in the CNS of AD patients. Moreover, previous work has shown FGL to attenuate the pro-inflammatory action of this peptide *in vivo* (Klementiev *et al.*, 2007).
2. To examine if the anti-inflammatory action of FGL in primary mixed glia is dependent on CD200 expression. Mixed glial cultures were prepared from wildtype and CD200^{-/-} mice to determine the modulating effect of FGL on LPS-stimulated glial cells in the presence and absence of CD200.
3. To investigate non-neuronal (astrocytic) CD200 expression *in vitro*. Previous work has focused on neuronal CD200 expression and its ability to regulate the phenotype of

microglial cell (Lyons *et al.*, 2007). In this study, primary cell culture allowed the investigation of CD200 expression on isolated astrocytes and the role of astrocytes in the modulation of microglia *in vitro*.

4. To assess the modulating effect of CD200Fc on LPS- and age-induced impairment of LTP in perforant path-granule cell synapses. Induction and maintenance of LTP measures the functional integrity of the hippocampus, an area of the brain susceptible to age-associated inflammatory changes (Lynch *et al.*, 1998). It has been demonstrated that CD200Fc has an immunosuppressive action on experimentally induced inflammatory disease in the periphery, leading to reduced disease burden (Gorczyński *et al.*, 2001). The current study investigated the ability of CD200Fc to reverse the negative impact of a pro-inflammatory profile in the CNS. Previous studies have revealed acute administration of LPS can induce impairment in LTP, similar to an age-related deficit (Lynch 2010). The age-associated decline in plasticity has been correlated with a pro-inflammatory phenotype, therefore, age-related changes in inflammatory markers in hippocampus were examined and their modulation by CD200Fc assessed.

Chapter 2. Methods

2.1 *In vitro* studies

2.1.1 Preparation of cultured mixed glia

Primary cortical mixed glia were established from postnatal one-day old Wistar rats, supplied by BioResources Unit in Trinity College Dublin. All instruments required for dissection were sterilised in 70% ethanol. Rats were decapitated, the cortices dissected free and the meninges removed. The cortices were chopped bi-directionally using a sterile scalpel and incubated in warm filter sterilised Dulbecco's modified Eagle medium (DMEM; Sigma Aldrich, UK) supplemented with fetal calf serum (FCS, 10%; Gibco, UK), penicillin (100U/ml; Gibco, UK) and streptomycin (100U/ml; Gibco, UK) for 5 minutes at room temperature. Tissue was triturated using a sterile Pasteur pipette, filtered through a nylon mesh filter (40µl; BD Biosciences, USA) and centrifuged at 2,000rpm for 3 minutes at 20°C. The pellet was re-suspended in DMEM and cell counts were performed by diluting cells (normally 1:50 or 1:10) with Trypan Blue (Sigma, UK). An aliquot (10µl) of the cell suspension was loaded onto a haemocytometer (Hycor Biomedical, UK). The numbers of viable cells, which appear white under a light microscope, were counted. Glia (2×10^6 cells/ml) were plated onto each well of a 6-well plate (Sarstedt, Germany) and allowed to adhere for at least 2 hours in a humidified incubator, 5% CO₂, 95% air at 37°C, before each well was supplemented with 1.5ml of warm DMEM. Media was changed every 2-3 days. Glia were grown for approximately 14 days before treatment. Flow cytometry was used to determine purity of mixed glial cultures. Cultures contained approximately 70% astrocytes and 30% microglia (Cowley *et al.*, 2010).

Mouse mixed glia were prepared from dissecting and cross chopping the whole brain from neonatal C57BL/6 or CD200^{-/-} mice. The rest of the protocol is as described for the preparation of cultured rat mixed glia.

2.1.2 Preparation of cultured microglia and astrocytes

Primary cortical microglia and astrocytes were prepared from one-day old Wistar rats (BioResources Unit, Trinity College Dublin) using the same method for primary cortical glial cells, as described above, except resuspended glia from each neonate were plated into two separate T25 flasks (Sarstedt, Germany) using a Pasteur pipette. Glia were incubated for 2 hours (5% CO₂, 95% air, 37°C), allowing cells to adhere before being flooded with 8ml of culture media. The following day media was removed and replaced with culture media enriched with mononuclear phagocyte colony stimulating factor (M-CSF; 20ng/ml, R&D Systems, USA) and granulocyte macrophage colony stimulating factor (GM-CSF; 10ng/ml, R&D Systems, USA). Every three days, media was removed and replaced with enriched culture media. On day 13 flasks were wrapped with Parafilm (Alcan, USA), making an air-tight seal around neck and cap, and placed on an orbital shaker (110rpm) for 2 hours at room temperature. Flasks were taken back into the hood, tapped 10 times, the contents containing suspended microglia was poured into a 50ml falcon tubes and spun at 2,000rpm for 5 minutes. The resulting pellet is a microglial cell pellet. The supernatant was removed and the pellet resuspended in 1ml DMEM. Resuspended microglial cells were pipetted onto poly-L-lysine-coated (60µg/ml) cover slips in 24-well plates. Cover-slips enhance microglial cell adherence and were prepared as follows. Glass cover-slips (10mm diameter) were sterilised in 70% ethanol for 1 hour and dried overnight in a fume hood, under a sterilising UV light. The following day cover slips were incubated at 37°C in sterile ploy-L-lysine (1mg/ml; diluted in sterile H₂O). After incubation the cover slips were dried and placed in 24-well plates. After plating, microglial cells were incubated for an hour before addition of warm DMEM (400µl). Cells were treated the following day.

Astrocytes, which remain adhered to the flask, were incubated in 1ml of Trypsin-ethylenediaminetetraacetic acid (Trypsin-EDTA; Sigma, UK) for 15 minutes at 37°C before the flask was tapped and contents poured into a 50ml falcon tube. The suspension was centrifuged at 2,000rpm for 3 minutes at 20°C, supernatant removed and resulting pellet resuspended in standard culture media. Resuspended astrocytes were plated (200µl/well of 6 well plate), allowed to adhere for 2 hours in 5% CO₂ at 37°C before being flooded with 1.5ml of culture media. Cells were treated the following day.

Primary microglia and astrocytes were prepared from neonatal C57BL/6 mice (BioResources Unit, Trinity College Dublin) using the same method for primary rat microglia and astrocytes, as described above.

2.1.3 Isolation of cell membrane from astrocytes

Cell membranes were isolated from cultured astrocytes prepared from C57BL/6 mice using a subcellular protein fractionation kit (Thermo Scientific, USA). Confluent astrocytes were incubated in 1ml of Trypsin-EDTA for 15 minutes at 37°C before the flask was tapped and contents poured into a 50ml falcon tube. The suspension was centrifuged at 500 x g for 5 minutes and the cell pellet washed with ice-cold PBS. Cells were re-suspended in 1ml of PBS, centrifuged at 500 x g for 3 minutes before the supernatant was discarded. The remaining pellet was re-suspended in ice-cold Cytoplasmic Extraction Buffer, containing 1:100 dilution of protease inhibitors (100µl, Thermo Scientific, USA) and incubated at 4°C for 10 minutes before being centrifuged at 3,000 x g for 5 minutes. The supernatant was removed and pellet re-suspended in ice-cold Membrane Extraction Buffer, containing 1:100 dilution of protease inhibitors (100µl, Thermo Scientific, USA) before incubating at 4°C for 10 minutes, with gentle mixing. The mixture was centrifuged at 3,000 x g for 5 minutes and supernatant, containing the membrane extract, transferred to a clean tube. A Bradford Microassay (BioRad, USA) was carried out on the membrane fraction to quantify protein concentration.

2.1.4 Preparation of culture media and test compounds

All agents used to treat cells were diluted to required concentration in pre-warmed supplemented DMEM and all solutions were filter-sterilised through a syringe with a 0.2µm cellulose acetate membrane filter. A Lactate Dehydrogenase (LDH) assay was performed on cells after test compound exposure to confirm that compounds did not alter cell viability.

Lipopolysaccharide (LPS; Alexis Biochemicals, UK) was prepared as a stock solution in sterile phosphate-buffered saline (PBS) and diluted to a final concentration of 1µg/ml in media. Cells were treated for 24 hours with LPS.

A stock solution of amyloid- β_{25-35} ($A\beta_{25-35}$; BAChem, Switzerland) was prepared in sterile PBS and aggregated at 37°C for 72 hours. Formation of aggregates was confirmed by microscopy. $A\beta_{25-35}$ was diluted to a final concentration (1-50 μ M) in media and cells were treated for 24 hours.

Fibroblast growth-loop (FGL; ENKAM Pharmaceuticals, Denmark) was prepared as a stock solution in sterile H₂O and diluted to a final concentration (10-100 μ g/ml) in media. Cells were treated with FGL 24 hours prior to LPS or $A\beta_{25-35}$ exposure.

SU5402 (Calbiochem, USA) was prepared as a stock solution in sterile DMSO and diluted to a final concentration (10-50 μ g/ml) in media. Cells were incubated in the presence of SU5402 for 30 minutes prior to FGL exposure.

Astrocytic membrane fractions were prepared from isolated C57Bl/6 primary astrocytes. Isolated microglia, cultured from C57Bl/6 mice were treated with the astrocytic membrane fraction (20ng protein/ml) for 2 hours prior to LPS exposure.

CD200Fc (R&D Systems, USA) was prepared as a stock solution in sterile PBS and diluted to a final concentration (2.5 μ g/ml) in media. Cells were treated with CD200Fc 2 hours prior to LPS treatment.

Following indicated treatments; supernatants were removed into fresh tubes and stored at -80°C until required for analysis of cytokine concentration. Cells used for polymerase chain reaction (PCR) were harvested by washing once in PBS, lysed in RA1 buffer (Nucleospin RNA II, Macherey-Nagel, USA) containing 1% β -mercaptoethanol (Sigma-Aldrich, UK) and stored at -80°C, in RNase free tubes for later analysis of messenger ribonucleic acid (mRNA) expression. Cells used for Western Immunoblotting were harvested by washing once in PBS, lysed in ice-cold lysis buffer (composition in mM: Tris-HCl 10, NaCl 50, Na₄P₂O₇.H₂O 10, NaF 50, 1% IGEPAL[®], Na₃VO₄ 1, PMSF1, Protease Inhibitor cocktail) for 15 minutes, scraped off and added to fresh tubes. Cells in lysis buffer were stored at -80°C until required.

2.2 Animal

Groups of specific pathogen-free male Wistar rats aged 3-4 months (young) and 18-22 months (aged), weighing approximately 250-300g and 550-600g respectively, were used. Animals were supplied by Harlan (UK) and maintained in the BioResources Unit, Trinity College Dublin. The animals were housed in groups of four, maintained under veterinary supervision in an ambient temperature of 22°-23°C, under a 12-hour light-dark cycle. Food, standard laboratory chow, and water were available *ad libitum*.

All animal experimentation was performed under a license granted by the Minister for Health and Children (Ireland), with approval from the local ethical committee and in compliance with the Cruelty to Animals act, 1876 and the European Community Directive, 86/609/EC, and every effort was made to minimise stress to the animals.

2.2.1 Treatment with LPS

Rats were anaesthetised by intraperitoneal (ip) injection of urethane (1.5g/kg, 33% w/v). The depth of anaesthesia was determined by the absence of a pedal reflex, and if required a further top-up dose of urethane was administered (to a maximum of 2.5g/kg). Once anaesthetised, the animals were divided into four groups (n=6): control rats that received saline ip and intrahippocampally (ih; 3mm posterior, 0.8mm lateral and 3.5mm dorsoventral to Bregma), rats which received an ip injection of lipopolysaccharide (LPS; 100 µg/kg; Sigma-Aldrich, U.K.) and saline ih, rats which received CD200Fc ih (2µg/µl; 5 µl infusion volume) and saline ip, and rats which received both LPS (ip) and CD200Fc (ih). Three hours after treatment, the ability to sustain LTP in perforant path-granule cell synapses, in response to tetanic stimulation of the perforant path was assessed.

2.2.2 Treatment with CD200Fc

Once anaesthetised, young and aged animals were randomly assigned into treatment groups (n=6 young or aged animals per group). Young and aged control animals received an

intrahippocampal infusion with sterile saline (5µl; 0.9% NaCl). Young and aged CD200Fc treated animals received CD200Fc (2µg/µl; 5µl infusion volume) intrahippocampally, using the above coordinates.

2.2.3 Induction of LTP in vivo

Following Urethane anaesthetisation rats were placed in a stereotaxic instrument with the isobars set 2mm below the ear bars to ensure the skull was flat. The scalp was incised along the midline and retracted. A drill was used to bore-holes for the electrodes, using Bregma and the midline as reference points. A bipolar stimulating electrode stereotaxically positioned in the perforant path (4.4mm lateral to Bregma) and a unipolar recording electrode in the dorsal cell body region of the dentate gyrus (2.5mm lateral and 3.9mm posterior to Bregma) were used to induce and record LTP. Following a period of stabilisation, test shocks were delivered at 30 second intervals and responses recorded over 10 minutes to establish stable baseline recordings. This was followed by delivery of 3 trains of high-frequency stimuli (HFS; 250Hz for 200ms; 30 second inter-train interval). Recording at test shock frequency resumed for 45 minutes. The slope of the excitatory post-synaptic potential (EPSP) was used as a measure of excitatory synaptic transmission in the dentate gyrus. A post tetanic change in the EPSP slope was used to indicate excitatory synaptic transmission and changes were expressed as a percentage of control baseline recordings prior to tetanus.

2.2.4 Dissection and preparation of tissue

In all studies, animals were sacrificed four hours post-treatment by decapitation. The brains were quickly removed and placed on ice. From the mid-line a sagittal section (5mm) was taken, placed on cork, covered in OCT[®] (Tissue-Tek, USA) and snap frozen in isopropanol which had been pre-chilled on dry ice for immunohistochemical staining. The remaining hippocampus and cerebral cortices were dissected free. One quarter of the hippocampus was snap frozen on dry ice, in an RNase-free tube and frozen at -80°C for later analysis of mRNA. The rest of the hippocampal and cortical tissue was sliced bi-directionally, placed in fresh tubes and rinsed in Krebs buffer (composition of Krebs buffer in mM: NaCl 136, KCl 2.54, 48

KH₂PO₄ 1.18, Mg₂SO₄·7H₂O 1.18, NaHCO₃ 16, glucose 10, pH 7.5) containing CaCl₂ (2mM, Sigma Aldrich, UK). The slices were allowed to settle before being rinsed twice more in Krebs buffer containing CaCl₂ and finally immersed in Krebs buffer containing CaCl₂ and 10% Dimethylsulphoxide (DMSO). Samples were stored in this solution at -80°C until required for further analysis.

2.2.5 Protein Quantification

Tissue slices were thawed on ice and rinsed three times in ice-cold Krebs buffer containing CaCl₂, before homogenising with two separate 5 second pulses with a Polytron homogeniser (PT 1200E, Kmematica, Switzerland). Protein concentration, in the homogenate, was assessed using the Bradford Microassay (BioRad, USA). Briefly, standards (0-7.5µg/100µl) were prepared in Bovine Serum Albumin (BSA; 1mg/ml; Sigma-Aldrich, UK) dissolved in Krebs buffer containing CaCl₂. Samples were diluted 1:100 in dH₂O and Bradford reagent (BioRad, USA) diluted 1 in 2.5, also in dH₂O. Triplicate standards and samples (100µl) were pipetted into a 96-well plate (Sarstedt, Germany) to which 100µl of working reagent was added. The plate was read immediately at 570nm (Labsystem Multiskan RC, UK), the standard curve was made by plotting the standards against absorbance. Protein concentrations were calculated from the standard curve and protein concentrations were equalised by dilution in ice-cold Krebs buffer containing CaCl₂ to concentrations of 1mg/ml.

2.3 Analysis of cytokine expression by ELISA

The concentrations of IL-1β and IL-6 were assessed by ELISA in supernatant from primary rat mixed glial cultures. The concentration of IL-1β, IL-6 and TNF-α were assessed by ELISA in the supernatant of mixed glia prepared from neonatal wildtype and CD200^{-/-} mice, and also isolated microglia prepared from wildtype mice. IGF-1 concentration was analysed in hippocampal homogenate prepared from young and aged rats that received CD200Fc intrahippocampally, or saline as a control.

2.3.1 Preparation of rat tissue for cytokine analysis

Tissue slices were thawed on ice, rinsed three times and homogenised in 500µl of ice-cold Krebs buffer containing CaCl₂ using a Polytron homogeniser (PT 1200E, Kmematica, Switzerland). Protein concentration in homogenates were equalised to 1mg/ml using the Bradford Microassay, see section 2.2.5.

2.3.2 General ELISA protocol

In all cases 96-well plates (Nunc-Immuno plate with Maxisorp surface, Denmark) were coated with capture antibody (see Table 2.1 for details) and incubated overnight at 4°C. The plates were washed three times in PBS (137mM NaCl, 2.7mM KCl, 8.1mM Na₂HPO₄ and 1.5mM KH₂PO₄, pH 7.2-7.4) containing 0.05% Tween-20 (PBS-T; pH 7.2-7.4), and incubated for 1 hour at room temperature in blocking buffer (100µl assay diluent; see Table 2.1 for details). Following the 1 hour incubation plates were washed three times in PBS-T. A standard curve was prepared using serial dilutions of the appropriate recombinant protein in DMEM, or Krebs Buffer in the case of tissue homogenate, (Table 2.1). Triplicate samples and standards (50µl) were added to each well and incubated for 2 hours at room temperature. At the end of the incubation period, plates were washed three times in PBS-T and detection antibody (50µl; see Table 2.1 details) was added to each well for a further 2 hours at room temperature. Plates were washed three times and incubated for 20 minutes at room temperature with streptavidin-horseradish peroxidase conjugate (strep-HRP; 100µl; 1:200 dilution in assay diluent; Table 2.1). Plates were washed three further times before addition of substrate solution (100µl; 1:1 H₂O₂: tetramethylbenzidine; R&D Systems, USA) and incubated in the dark for 40 minutes or until a blue colour appeared. The reaction was terminated using a stop solution (50µl; 1M H₂SO₄) and plates were read at 450nm immediately (Labsystem Multiskan RC, UK). The standard curve was constructed by plotting the standards against their absorption (GraphPad Prism v4.0 Macintosh; GraphPad Software, USA) and the results were expressed as pg cytokine/ml for supernatant or pg IGF-1/mg as tissue homogenate was used.

Species	Cytokine	Diluent	Capture Antibody	Standards	Detection Antibody
Rat	IGF-1	5% Tween-20 in PBS	Mouse anti-human 4µg/ml in PBS	0-2ng/ml	80ng/ml in diluent
	IL-1β	1% BSA in PBS	Goat anti-rat 0.8µg/ml in PBS	0-2ng/ml	350ng/ml in 2% goat serum/diluent
	IL-6	10% FBS in PBS	Mouse anti-rat 4µg/ml in 0.1M Na ₂ CO ₃ /PBS	0-4ng/ml	400ng/ml in diluent
Mouse	IL-1β	1% BSA in PBS	Rat anti-mouse 4µg/ml in PBS	0-1ng/ml	600ng/ml in 2% goat serum/diluent
	IL-6	10% FBS in PBS	Rat anti-mouse 2µg/ml in PBS	0-2ng/ml	200ng/ml in diluent
	TNF-α	10% FBS in PBS	Goat anti-mouse 0.8µg/ml in PBS	0-2ng/ml	200ng/ml in diluent

Table 2.1 Cytokine analysis protocols

2.4 Analysis of mRNA expression

2.4.1 Preparation of tissue for RNA isolation

RNA was extracted from snap frozen hippocampal tissue. Cell lysis master mix (353.5µl; RA1 buffer containing 1% β-mercaptoethanol; Nucleospin RNA II, Macherey-Nagel, Germany) was added to hippocampal samples snap frozen in RNase-free tubes. Samples were

homogenised with two 5 second pulses with the Polytron homogeniser (PT 1200E; Kmematica, Switzerland). Cells from *in vitro* studies were lysed on the day of harvest in 200µl of cell lysis master mix (Nucleospin RNA II, Macherey-Nagel, Germany) for extraction of RNA.

2.4.2 Protocol for RNA isolation

Samples were filtered using a NucleoSpin Filter, collected in a 2ml tube and centrifuged (11,000 x g, 1 minute). Ethanol (70%, 350µl) was added to the filtrate and samples were mixed and loaded onto NucleoSpin RNA II columns. Tubes were centrifuged (8,000 x g, 3 minutes) allowing the RNA to bind to the column. The silica membrane was desalted by addition of membrane desalting buffer (350µl) and centrifuged (11,000 x g, 1 minute), to dry the membrane. To digest the DNA, DNase reaction mixture (95µl) was added to the column and incubated at room temperature for 15 minutes. The silica membrane was washed and dried. RNA was eluted by adding RNase-free H₂O and centrifuged (11,000 x g, 1 minute). RNA concentration was quantified using a NanoDrop[®] spectrophotometer (Thermo Scientific, USA).

2.4.3 Reverse Transcription for cDNA synthesis

Total mRNA (1µg) was reverse-transcribed into cDNA using high-capacity cDNA archive kit (Applied Biosystems, Darmstadt, Germany) according to the protocol provided by the manufacturer. In brief, an equal concentration of RNA was added to fresh tubes containing to appropriate volume of nuclease-free H₂O, to make up a 20µl volume. A 2x master mix was prepared containing the appropriate volumes of 10x RT buffer, 25x dNTPs and 10x random primer multiscrite reverse transcriptase (50U/µl). The master mix (20µl) was added to the RNA and nuclease free H₂O. Tubes were incubated for 10 minutes at 25°C, followed by 2 hours at 37°C on a thermocycler (PTC-200, Peltier Thermal Cycler, MJ Research, Biosciences, Ireland).

2.4.4 Quantitative real time PCR

Quantitative real time PCR (Q-PCR) is used to amplify and quantify targeted gene expression. Primers and probes were delivered as “TaqMan[®] Gene Expression Assays” for the mouse and rat genes listed in Table 2.2 (Applied Biosystems, Germany). Q-PCR was performed on Applied Biosystems ABI Prism 7300 Sequence Detection System v1.3.1 in 96-well format and using a 25µl reaction volume per well. TaqMan Universal PCR master mix (Applied Biosystems, Germany) was mixed with cDNA (200pg/well) and the respective target gene assay. Mouse or rat β-actin RNA (Applied Biosystems, Germany) was used as a reference. Forty cycles were run with the following conditions: 2 minutes at 50°C, 10 minutes at 95°C and for each cycle 15 seconds at 95°C to denature and 1 minute at 60°C for transcription. Analysis of gene expression values was performed using the efficiency-corrected comparative CT method, determining target gene expression relative to β-actin endogenous control expression and relative to the control sample.

Species	Gene Name	TaqMan Gene Expression Assay Number	Genebank Accession Number
Rat	CD11b	Rn00709342_m1	NM_012711.1
	CD40	Rn01423583_m1	NM_134360.1
	CD40L	Rn00584362_m1	NM_053353.1
	CD68	Rn01495631_g1	NM_001031638.1
	FGFR-1	Rn00577234_m1	NM_024146.1
	GFAP	Rn00566603_m1	NM_017009.2
	IL-1 β	Rn00580432_m1	NM_031512.2
	IL-6	Rn00561420_m1	NM_012589.1
	iNOS	Rn00561646_m1	NM_012611.3
	MHC II	Rn01768597_m1	NM_198741.1
	TNF- α	Rn99999017_m1	NM_012675.2
Mouse	CD11b	Mm01271265_m1	NM_000632.3
	CD40	Mm00441891_m1	NM_001250.1
	CD68	Mm03047341_m1	NM_009853.1
	ICAM-1	Mm00516027_g1	NM_010493.2
	IL-1 β	Mm00434228_m1	NM_008361.3
	IL-6	Mm00446190_m1	NM_031168.1
	TNF- α	Mm00443258_m1	NM_013693.2

Table 2.2 Q-PCR TaqMan Gene Expression Assays.

2.5 Western Immunoblot Analysis

The concentrations of a variety of proteins, including β -actin, were assessed from crude hippocampal homogenate and lysed cultured glia by gel electrophoresis and immunoblotting. Throughout the experiment all samples and buffers were kept on ice, to minimise denaturing of proteins, and all instruments rinsed with appropriate buffers.

The hippocampal homogenate was stored in modified Krebs buffer and cultured glia in lysis Buffer, a Bradford Microassay assay (BioRad, USA; see section 2.2.5) was carried out to ascertain the amount of protein present in each sample. The samples were equalised and diluted to a final concentration of 1mg protein/ml with NuPAGE LDL sample buffer (Invitrogen, UK) containing NuPAGE reducing agent, heated at 70°C for 10min and loaded onto 12% NuPAGE Novex Bis-Tris gels (Invitrogen, UK). Proteins were separated by application of a 130V (PowerPac Basic, Bio-Rad, UK) constant for 90 minutes in the presence of NuPAGE MOPS SDS running buffer (Invitrogen, UK). The separated proteins were transferred (XCell II Blot module: Invitrogen, UK) on to nitrocellulose membrane (Whatman, Germany) at 30V constant for 75 minutes in the presence of NuPAGE transfer buffer (Invitrogen, UK). Nitrocellulose membranes were immunoblotted with the appropriate antibody.

2.5.1 General protocol for western immunoblotting

The following describes a general protocol used to identify proteins of interest, which was carried out directly following transfer of proteins onto the nitrocellulose membrane. The specific details for every protein assessed by Western Immunoblotting are presented in Table 2.3. The nitrocellulose membranes were incubated at 4°C, overnight, in blocking buffer (5% powdered milk in TBS-T (20mMTris-HCl, 150Mm NaCl; pH 7.4 containing 0.05% Tween-20), to block non-specific antibody binding. The membrane was washed in TBS-T (3 x 15 minutes) and incubated in the appropriate concentration of primary antibody diluted in TBS-T containing 2% milk. Membranes were washed (3 x 15 minute washes in TBS-T) and incubated in the appropriate concentration of secondary antibody conjugated to horseradish peroxidase (HRP; TBS-T 2%; Jackson, USA) for 2 hours at room temperature. Membranes

were washed (3 x 15 minute washes in TBS-T). Protein complexes were visualised after 5 minute incubation with enhanced chemiluminescence (ECL) system (2ml; ECL Western Blotting Analysis System, Amersham, UK). The proteins were visualised using a Fujifilm Intelligent Dark Box and quantified using ImageJ analysis software. The nitrocellulose membranes were stripped with antibody stripping solution (1:10 dilution in dH₂O; Reblot Plus Strong antibody stripping solution; Chemicon, USA) and re-probed for β -actin as a loading control.

Target Protein (Source)	Supplier	1° Antibody Dilution	2° Antibody Dilution	Protein Band (kDa)
β -Actin (Mouse)	Sigma, UK	1:10,000; 2 hours @ RT	1:10,000; 2 hours @ RT	42
CD200 (Goat)	Santa Cruz, USA	1:500; o/n @ 4°C	1:5,000; 2 hours @ RT	47
pAKT (Rabbit)	Cell Signalling, USA	1:1,000; o/n @ 4°C	1:5,000; 2 hours @ RT	60
Synaptophysin (Mouse)	Sigma, UK	1:5,000; o/n @ 4°C	1:5,000; 2 hours @ RT	38
GFAP (Rabbit)	Invitrogen, USA	1:1,000; o/n @ 4°C	1:2,000; 2 hours @ RT	56

Table 2.3 Western Immunoblotting protocol

2.6 Flow Cytometry

CD200 expression was assessed in primary mixed glial cells by flow cytometry (DAKO CyAN_{ADP} Flow Cytometer). The flow cytometer was calibrated using Flow-Check Fluorospheres (Beckman Coulter, Ireland). Mixed glial cells were lysed in Trypsin-EDTA for 5 minutes at 37°C before the plates were tapped and cells removed to sterile tubes. The suspension was centrifuged at 1,200rpm for 5 minutes at 20°C and the Trypsin-EDTA removed. The resulting pellet was washed in FACS buffer (PBS containing 2% FCS and 0.1% NaN₃) and centrifuged at 1,200rpm for 5 minutes. The pellet was resuspended in 1ml of FACS block (FACS buffer containing 50% FCS), incubated for 15 minutes and washed twice. Cells were suspended in fluorescent-tagged antibodies, CD200 (BD Biosciences, USA), CD11b (Serotec, UK) and comparison beads to compensate between fluorescent channels (BD Biosciences, USA), and allowed to incubate for 30 minutes, in the dark. Cells were washed twice in FACS buffer (1,200rpm for 5 minutes) and immunofluorescence analysed using Summit software.

2.7 Analysis of nitrite concentrations (Griess assay)

The production of nitrite by cultured glial cells was measured using a Griess assay. Nitric oxide is an unstable compound which is rapidly broken down into two stable and non-volatile substrates, nitrite and nitrate, and so since nitric oxide cannot be measured directly the Griess assay is a way of determining its production in cells in an indirect manner. An 18mM stock solution of sodium nitrite (NaNO₂) was prepared by dissolving 62mg of NaNO₂ in 50ml dH₂O. Standards (0μM to 180μM) were prepared by carrying out serial dilutions of the NaNO₂ stock solution in DMEM. Aliquots (100μl) of each standard and sample were plated out onto a 96-well plate in triplicate. Griess Reagent I (1% Sulphanilamide in 85% orthophosphoric acid; 50μl) was added to each well and the plate was incubated at room temperature for 10 minutes. Griess Reagent II (0.1% N-(1-naphthyl-ethylenediamine dihydrochloride); 50μl) was then added to each well and the plate incubated at room temperature for a further 10 minutes. The absorbance was read at 450 nanometres (Labsystem Multiskan RC, UK). The standard curve was constructed by plotting the standards against their absorption (GraphPad Prism v4.0 Macintosh; GraphPad Software, USA) and the total

nitrite concentration for each of the samples was calculated by comparison against the standard curve.

2.8 Immunohistochemistry

2.8.1 Preparation of tissue sections for immunohistochemistry

Slices for immunohistochemistry were prepared from tissue obtained from young and aged CD200Fc treated animals. For cryostat sectioning, a sagittal slice from left hemisphere of each brain was placed onto a cork disk coated in OCT[®] compound (R.A. Lamb, UK). The brain was covered with this compound and snap-frozen in isopropanol which had been pre-chilled on dry ice. Brains were stored at -80°C until required for sectioning. Pre-subbed slides (Thermo Scientific, USA) were used for sectioning, as they provided a suitable surface to which the section could adhere. On the day of sectioning the brain was allowed to equilibrate to -20°C for 30 minutes. Sagittal sections (10µm) were cut, and periodically stained with 1% toluidine blue solution until the hippocampus was visible on the section. Toluidine blue was added for 30 seconds and sections were viewed by light microscopy (Nikon Labophot, Nikon Instech Co., Japan). When the hippocampus became visible, 60 sections (10µm) were cut from each animal onto 20 pre-subbed slides (3 sections per slide), making sure that one section from the outside, middle and inside of the brain hemisphere was added to each slide. Sections were allowed to dry for 20 minutes and stored at -20°C until required.

2.8.2 Immunohistochemical staining

Sections were left at room temperature for 30 minutes to allow the temperature to equilibrate. Individual brain sections were surrounded in a hydrophobic well using a cremation pen (Dako, UK). Following fixation in ice-cold ethanol for 5 minutes, brain slices were washed three times for 5 minutes in TBS. In the case of 8-hydroxy-2'-deoxyduanosine (8-OHdG), sections were permeabilised with Triton[®] X-100 (Sigma, UK) for 5 minutes. To block unspecific antibody binding the slices were incubated in the appropriate animal serum (Vector, UK; see

Table 2.4) prepared in TBS containing 4% BSA (Sigma, UK). Sections were incubated overnight at 4°C in primary antibody solution (table 2.4; in TBS containing 2% BSA). Negative controls were incubated in an isotype matched IgG (Sigma, UK) in TBS containing 2% BSA, to verify specific antibody binding. Sections were washed three times in TBS and incubated in biotin-conjugated secondary antibody (anti-mouse; 1:200 in TBS containing 2% BSA; Vector, UK) for 2 hours at room temperature. Sections were washed three times in TBS. Endogenous peroxidases were blocked by incubating the sections in 0.3% H₂O₂ in TBS for 15 minutes. Sections were washed 3 times in TBS, before being incubated in a pre-made avidin: biotinylated enzyme complex (Vector, UK) for 1 hour and washed a further 3 times with TBS. Diaminobenzidine (DAB solution; Vector, UK, 2µl H₂O₂/ml) was applied to the sections and incubated for approximately 10 minutes. The colour development was monitored and stopped with distilled water. The sections were counterstained for 30 seconds in the case of toluidine blue (Sigma, UK) or 2 minutes in the case of methyl green (Sigma, UK), rinsed with distilled water, dehydrated through a series of graded alcohols (70%, 95%, 100%; Sigma, UK) and cleared by immersion in xylene (Sigma, UK). Coverslips were applied using DPX (R.A. Lamb, UK) as the mount, and slides were left overnight to set in a fume hood.

2.8.3 Microscopy

Light microscopy staining was viewed using an Olympus XD51 microscopy and images were captured with analysis D software.

Antibody (Source)	Supplier	Block	Dilution
MHC II (Mouse)	Serotec, USA	Normal Horse Serum	1:100
8-OHdG (Mouse)	QED Bioscience, USA	Normal Goat Serum	1:1,000

Table 2.4 Immunohistochemistry protocol

2.9 Statistical Analysis

Data are expressed as means \pm standard error of mean (SEM). Analysis of variance (ANOVA) was performed to determine whether significant differences existed between conditions. If this indicated significance ($p < 0.05$), the appropriate a post-hoc test was used to determine which conditions significantly differ from each other. Two-tailed unpaired Students *t*-tests were also performed, where indicated, to compare treatment groups; significance was set as $p < 0.05$.

Chapter 3. Results

3.1 Introduction

Neural Cell Adhesion Molecule (NCAM) is a cell surface macromolecule involved in the establishment, maintenance and modification of neural circuitry within the CNS. The extra-cellular region of NCAM contains five Ig-like domains and two fibronectin-type III (F3) modules. Homophilic interactions occur between Ig-like domains and play an important role in cell positioning and axon guidance, particularly during embryonic development (Ono *et al.*, 1994). NCAM can be modified post-transcriptionally in the Golgi apparatus, with the addition of polysialic acid to the fifth Ig-like domain, resulting in PSA-NCMA. This bulky addition inhibits homophilic binding and favours heterophilic interactions, for example between the F3 modules and fibroblast growth factor (FGF) receptors (Nelson *et al.*, 1995). PSA-NCAM is ubiquitously expressed on neurons and glial cells (Markram *et al.*, 2007). During development it is required for neuronal differentiation and post-mitotic migration however, in the adult brain, its expression is limited to areas of ongoing synaptic plasticity including the hippocampus (Sandi, 2004). While deficits in NCAM, particularly PSA-NCAM, have been shown to impair memory and LTP, it is only in recent years that the possible benefit of enhancing NCAM-related signalling has been examined (Seki & Rutishauser, 1998).

Advancements in molecular modelling allowed a peptide derived from NCAM, which targets FGFR-1, to be identified and constructed (Kiselyov *et al.*, 2003). The fifteen amino acid peptide, FGL, was shown to bind FGFR-1 by nuclear magnetic resonance and surface plasmon resonance analysis. Within the CNS, FGFR-1 is expressed on astrocytes and microglia, in addition to neural cells, and inactivation of this receptor is lethal in early life leading to defective patterning of the neural tube (Magnusson *et al.*, 2007). Ligation of FGFR-1 by FGL induces autophosphorylation of the receptor and activation of a variety of intracellular signalling cascades (Kiselyov *et al.*, 2003). FGL is in clinical development to treat disorders associated with neurodegeneration and the aim of this study is to identify the cellular and molecular mechanisms underlying the previously-reported beneficial effects. *In vitro* FGL has the proclivity to induce neurite outgrowth in primary dopaminergic and hippocampal neurons,

protect hippocampal cultures following oxygen/glucose deprivation, promote synaptogenesis and enhance pre-synaptic function (Cambon *et al.*, 2004; Neiiendam *et al.*, 2004; Skibo *et al.*, 2005). While *in vivo*, studies have found FGL to enhance performance in hippocampal-dependent memory tasks, protect hippocampal neurons in an ischemic model, reduce cognitive impairments and neuropathology induced by A β , and attenuate the age-related increase in microglial activation and accompanying deficit in LTP (Cambon *et al.*, 2004; Skibo *et al.*, 2005; Klementiev *et al.*, 2007; Downer *et al.*, 2008). The above studies reveal FGL to be neuroprotective, however, the mechanism of this has yet to be elucidated.

It is well established that increased inflammatory activity can be detrimental to neuronal activity and contribute to the pathology of many degenerative conditions, from AD to Parkinson's disease. Moreover, enhanced microglial activation is believed to drive this progression (Block & Hong 2005). Quiescent microglia continually survey the CNS, systematic scanning can convert to targeted movement in response to brain insult or injury leading to either containment or aggravation of the disease process (Hanisch & Kettenmann 2007). Astrocytes have also been shown to become activated in response to immunological challenges, although this activity not as prominent (Aloisi 1999). When a pro-inflammatory phenotype dominates both cells contribute to inflammation-mediated destruction and, although the triggers of various degenerative diseases are diverse, this dysregulated immunological mechanism driving neuronal damage and synaptic impairment shares a common thread. It is hypothesised that inhibiting immune cell activation and release of pro-inflammatory mediators, which are potentially cytotoxic, may be beneficial in controlling disease progression (Block & Hong 2005). The objective of the following set of experiments is to determine if FGL can act as an anti-inflammatory agent in primary microglia and astrocytes, which have been stimulated with LPS or A β_{25-35} .

LPS is a gold-standard inflammatory stimulus, which induces a pro-inflammatory phenotype in glial cells that parallels many aspects of glial cell activation *in vivo* (Quan *et al.*, 1994). Previous work in this laboratory has demonstrated FGL to attenuate age-related neuroinflammatory changes *in vivo* (Downer *et al.*, 2008). The following *in vitro* experiments further examine the pro-inflammatory phenotype of activated glial cells, which is typified by enhanced pro-inflammatory cytokine production and cell surface markers of activation. How

this profile is specifically altered by exposure to FGL is of particular interest. A β was also chosen as an inflammatory stimulus. This peptide is associated with the pathogenesis of AD. It has been shown to recruit and activate microglia, inducing release of a plethora of neurotoxic factors (Tan *et al.*, 1999). Furthermore, inhibition of glial cell activation in animal models of AD was shown to attenuate neuronal damage and synaptic degeneration (McGeer & Mc Geer 1996). The 25-35 fragment of A β (A β_{25-35}) is a toxic core fragment of the full-length A β_{1-42} (Pike *et al.*, 1995). At a functional level, intracerebroventricular administration of FGL was reported to reduce A β_{25-35} -induced impairment in short-term memory (Klementiev *et al.*, 2007). The current study aims to investigate if FGL has an anti-inflammatory effect on A β_{25-35} -stimulated glia *in vitro*, as this containment of glial cells activation could be mediating the beneficial action of FGL on reversing cognitive impairment.

3.2 Methods

Mixed glial cells and isolated microglia were prepared from 1 day old Wistar rats and cultured for 14 days before treatment (see section 2.1 for details). In the case of FGL (1µg/ml-100µg/ml), cells were exposed to the peptide for 24 hours before being incubated in the presence or absence of LPS (1µg/ml) or the presence or absence of Aβ₂₅₋₃₅ (1µM-50µM) for a further 24 hours. Cells treated with SU5402 (1-50µM) were incubated in the presence of the inhibitor for 30 minutes prior to FGL exposure. Concentration of cytokines in supernatant was determined by ELISA and mRNA expression of surface proteins was assessed by Q-PCR (see section 2.3 and 2.4). Data are expressed as means ± SEM. Students *t*-test or ANOVA were performed to determine whether significant differences existed between treatment groups and Newman-Keuls post-hoc tests were applied where appropriate.

3.3 Results

3.3.1 Investigating the action of FGL on LPS-stimulated primary glia

It has previously been reported that FGL exerts an anti-inflammatory effect *in vivo*; chronic administration of the drug attenuated an aged-related increase in markers of microglial activation in hippocampus and decreased microgliosis and astrogliosis in A β treated animals (Klementiev *et al.*, 2007; Downer *et al.*, 2008). The aim of the following set of experiments was to evaluate the effect of FGL in primary glial cells subjected to two different inflammatory stimuli. The stimuli chosen were LPS, a prototypical endotoxin that readily induces an inflammatory response and A β_{25-35} ; the toxic core fragment of the A β peptide found in the plaques of AD patients (Pike *et al.*, 1995). The mean values \pm SEM for all parameters are presented Appendix I.

Communication between different cell types is an integral part of the inflammatory process, allowing interactions between cells and the amplification of signals. During inflammation, cells display various markers indicative of their activation state, thus communicating their status to other cells. Microglia express surface molecules associated with antigen presentation, as well as co-stimulatory molecules that engage with and activate T cells. LPS induced a significant increase in mRNA expression of the co-stimulatory molecule CD40 in primary mixed glial cultures, compared with control-treated glia (** $p < 0.001$; ANOVA; $F_{(5,29)} = 6.76$, Figure 3.1). Pre-treatment with FGL (10 μ g/ml) did not significantly alter CD40 mRNA expression, compared with control treated cells (non-significant; ANOVA), however, FGL (1-100 μ g/ml) dose-dependently attenuated the LPS-induced increase in CD40 mRNA ($^{++}p < 0.01$; $^{+++}p < 0.001$; ANOVA). In subsequent experiments, 10 μ g/ml FGL was used to evaluate the effects of this peptide on LPS- and A β_{25-35} -induced changes *in vitro*. CD11b is another marker of inflammation, it is a cell surface protein that is up-regulated during an inflammatory response and, within the CNS, it is specific to microglia (Cowley *et al.*, 2010). CD11b mRNA was up-regulated in LPS-treated mixed glia, compared with control-treated glia (** $p < 0.001$; ANOVA; $F_{(3,28)} = 14.61$, Figure 3.2), this increase was attenuated by pre-incubation in the presence of FGL (* $p < 0.05$; ANOVA).

Cytokines are a group of small signaling molecules that exhibit a diverse array of biological actions involved in managing and manipulating immune and inflammatory activity. Microglia and astrocytes are the primary source of cytokines within the CNS. Pro-inflammatory cytokines, for example IL-1 β , are of particular interest in this study, as they are imperative in the initiation and propagation of inflammation. LPS-induced a significant increase in IL-1 β in primary mixed glia at mRNA and protein level, compared with control-treated mixed glia (** $p < 0.01$; *** $p < 0.001$; ANOVA; A, $F_{(3,29)} = 66.83$ and B, $F_{(3,20)} = 12.75$, Figure 3.3 A and B). Pre-treatment with FGL significantly attenuated the LPS-induced increase in mRNA expression and supernatant concentration (⁺ $p < 0.05$; ⁺⁺⁺ $p < 0.001$; ANOVA). The data also show that mixed glia exposed to LPS displayed a significant increase in the supernatant concentration of IL-6, compared with control-treated glia (** $p < 0.001$; ANOVA; $F_{(3,37)} = 35.92$, Figure 3.4). The LPS-induced increase in IL-6 was attenuated by pre-treatment in the presence of FGL (⁺ $p < 0.05$; ANOVA).

Figure 3.5 shows data from experiments that were conducted in isolated microglial cultures. LPS stimulated an increase in IL-1 β mRNA expression and supernatant concentration in these cells, compared with control-treated microglia (* $p < 0.05$; *** $p < 0.001$; ANOVA; A, $F_{(3,14)} = 7.44$ and B, $F_{(3,11)} = 13.39$). Pre-treatment of isolated microglia with FGL significantly attenuated the LPS-induced increase in IL-1 β release, but not mRNA expression, compared with microglia exposed to LPS alone (⁺ $p < 0.05$; ANOVA, Figure 3.5 A).

FGL was designed to mimic the interaction of NCAM with FGFR-1 and previous studies have found that specifically antagonising the tyrosine kinase domain of FGFR-1 using SU5402 can abrogate the action of this peptide (Cambon *et al.*, 2004; Neiiendam *et al.*, 2004). In Figure 3.6, LPS-induced an increase in mRNA expression and supernatant concentration of IL-1 β (* $p < 0.05$; ** $p < 0.01$; ANOVA; A, $F_{(4,13)} = 13.81$ and B, $F_{(6,27)} = 16.41$) and this was attenuated by FGL (⁺ $p < 0.05$; ANOVA). Exposure of mixed glia to SU5402, for 30 minutes prior to FGL, dose-dependently blocked the ability of FGL to attenuate the LPS-induced increase in IL-1 β mRNA expression and protein concentration. SU5402 (25 μ M) abrogated the FGL-induced attenuation of the LPS-stimulated increase in IL-1 β mRNA expression, to levels not significantly different to mixed glia exposed to LPS alone (FGL/LPS-treated glia compared with SU5402/FGL/LPS-treated glia; §§ $p < 0.01$; ANOVA, Figure 3.6 A). A higher dose of

SU5402 (50 μ M) was required to abrogate FGL-induced attenuation of the LPS-stimulated increase in IL-1 β release, to levels not significantly different from mixed glia exposed to LPS alone (FGL/LPS-treated glia compared with SU5402/FGL/LPS-treated glia, $^{\S\S}p < 0.01$; ANOVA, Figure 3.6 B).

3.3.2 Investigating the action of FGL on A β_{25-35} -stimulated primary glia

A β peptide is the primary component of A β plaques found in the brain of AD patients. In the following experiments a core fragment of the A β peptide, spanning the amino acid sequence 25 to 35 (A β_{25-35}), was used. It has been inferred that microglia in the brains of AD patients display enhanced expression of cell surface proteins, indicative of their activation state and secrete greater amounts of pro-inflammatory cytokines (Town *et al.*, 2001; Allan & Pinteaux, 2003). In the current study primary mixed glial cultures were treated with increasing concentrations of A β_{25-35} (1 μ M-50 μ M) for 24 hours. A β_{25-35} induced an increase in IL-1 β mRNA expression in mixed glial cultures, in a concentration-dependant manner, compared with control treated mixed glia ($^*p < 0.05$, $^{**}p < 0.01$; ANOVA; $F_{(3,16)} = 3.81$, Figure 3.7 A). A higher concentration of A β_{25-35} (50 μ M) was required to induced a significant increase in the supernatant concentration of IL-1 β in mixed glia, compared with control-treated glia (control compared with A β_{25-35} 50 μ M; $^*p < 0.05$; Student's *t*-test, Figure 3.8 B). Another A β dose curve illustrates A β_{25-35} induced a significant increase in MHC II mRNA expression, compared with control-treated glia ($^{***}p < 0.001$; ANOVA; $F_{(5,23)} = 12.50$, Figure 3.8). Interestingly, this increase was not found in mixed glial cultures stimulated with LPS (non-significant compared with control-treated glia; Figure 3.8).

A β_{25-35} stimulated a significant increase in CD40 mRNA expression in mixed glial cultures, compared with control-treated glia ($^*p < 0.05$; ANOVA; $F_{(3,11)} = 5.43$, Figure 3.8 A). The increase in CD40 mRNA expression was not modulated by pre-treatment with FGL (non-significant versus A β_{25-35} -treated glia; ANOVA). However, FGL attenuated the A β_{25-35} -induced increase in IL-1 β mRNA, compared with glia exposed to A β_{25-35} alone ($^+p < 0.05$; ANOVA).

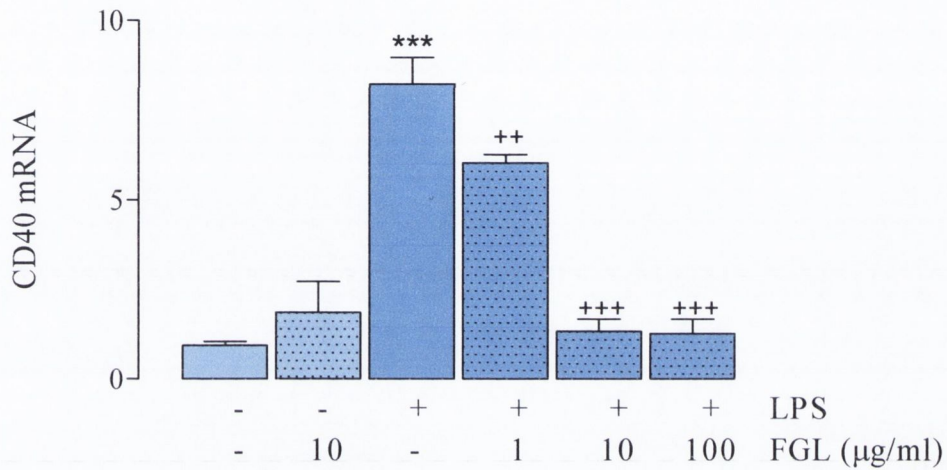


Figure 3.1. FGL significantly attenuated the LPS-induced increase in CD40 mRNA expression in cultured mixed glia.

LPS (1µg/ml; 24 hours) induced a significant increase in CD40 mRNA expression in cortical mixed glia (** $p < 0.001$; ANOVA; $F_{(5,29)} = 6.76$). Pre-treatment with FGL (1-100µg/ml) significantly attenuated the LPS-induced increase (** $p < 0.01$; +++ $p < 0.001$; ANOVA). Values are presented as means (\pm SEM; $n=6$) expressed as a ratio to β -actin mRNA and standardised to a control sample.

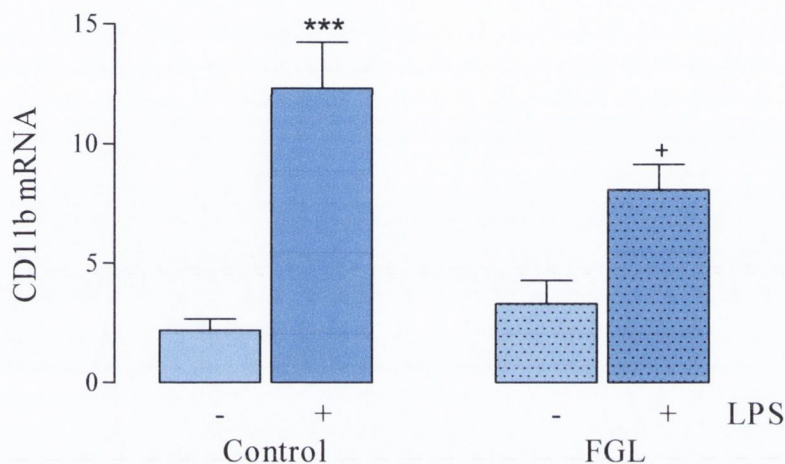


Figure 3.2. FGL attenuated the LPS-induced increase in CD11b mRNA expression in cultured mixed glia.

LPS (1µg/ml; 24 hours) induced a significant increase in CD11b mRNA expression in mixed glia, compared with control-treated glia (** $p < 0.001$; ANOVA; $F_{(3,28)} = 14.61$). Pre-treatment with FGL (10µg/ml) significantly attenuated the LPS-induced increase in CD11b mRNA ($^+p < 0.05$; ANOVA). Values are present as means (\pm SEM; $n=6$) expressed as a ratio to β -actin mRNA and standardised to a control sample.

18. 1987-1988

The following table shows the results of the survey conducted in 1987-1988. The data is presented in a tabular format, with columns representing different categories and rows representing specific data points. The table is organized into several sections, each corresponding to a different aspect of the survey. The first section deals with the general characteristics of the respondents, including their age, gender, and education level. The second section focuses on the respondents' views on various social and economic issues. The third section discusses the respondents' attitudes towards different political parties and candidates. The fourth section examines the respondents' perceptions of the current government and its policies. The fifth section explores the respondents' opinions on the role of the media and the judiciary. The sixth section addresses the respondents' concerns about the environment and natural resources. The seventh section discusses the respondents' views on the role of the state in the economy. The eighth section examines the respondents' attitudes towards different ethnic and religious groups. The ninth section discusses the respondents' perceptions of the current state of the country and its future prospects. The tenth section addresses the respondents' opinions on the role of the military and the police. The eleventh section examines the respondents' views on the role of the education system. The twelfth section discusses the respondents' attitudes towards different forms of entertainment and leisure activities. The thirteenth section addresses the respondents' perceptions of the current state of the country and its future prospects. The fourteenth section examines the respondents' views on the role of the state in the economy. The fifteenth section discusses the respondents' attitudes towards different ethnic and religious groups. The sixteenth section addresses the respondents' perceptions of the current state of the country and its future prospects. The seventeenth section examines the respondents' views on the role of the military and the police. The eighteenth section discusses the respondents' attitudes towards different forms of entertainment and leisure activities.

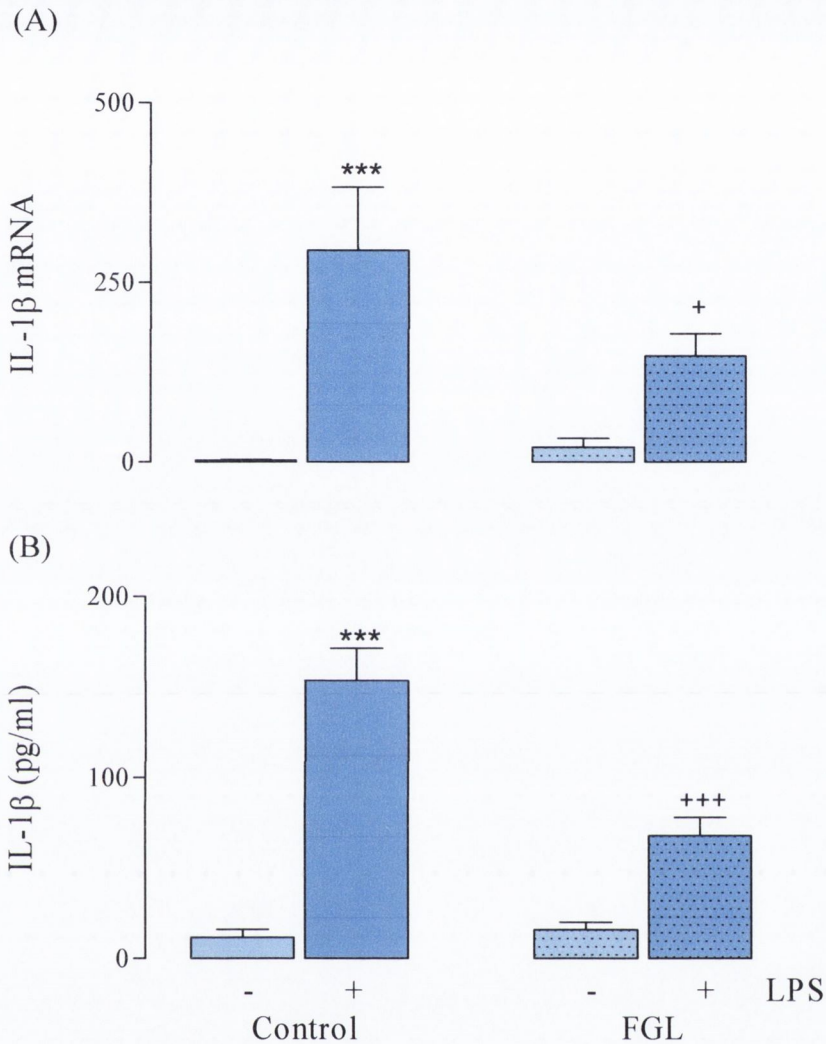


Figure 3.3. FGL significantly attenuated the LPS-induced increase in IL-1β mRNA expression and release in mixed glial cultures.

LPS (1μg/ml; 24 hours) significantly increased IL-1β mRNA expression (A) and release (B) in mixed glial cultures (* $p < 0.01$; *** $p < 0.001$; ANOVA; A, $F_{(3,29)} = 66.83$ and B, $F_{(3,20)} = 12.75$). Pre-treatment with FGL (10μg/ml) significantly attenuated the LPS-induced increase (+ $p < 0.05$; +++ $p < 0.001$; ANOVA). Values for Q-PCR are presented as means (\pm SEM; $n = 7$) expressed as a ratio to β -actin mRNA and standardised to a control sample. Values for cytokine release are presented as means (\pm SEM; $n = 6$) and expressed as pg IL-1β/ml.

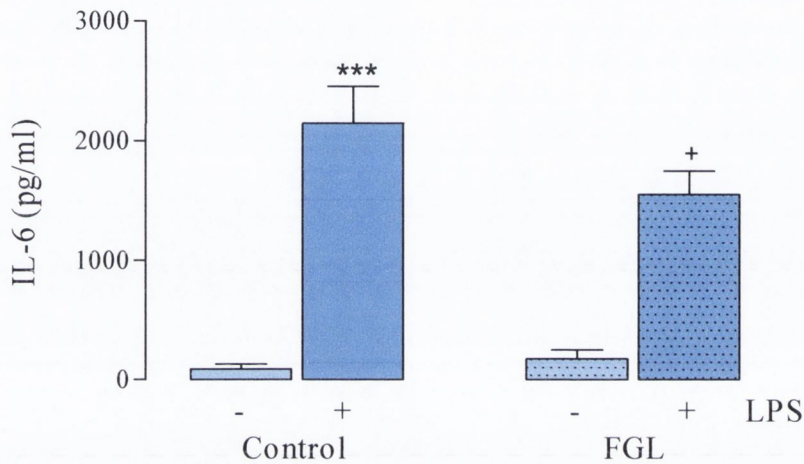


Figure 3.4. FGL significantly attenuated the LPS-stimulated increase in IL-6 concentration in cultured mixed glia.

IL-6 release was significantly increased in mixed glial cultures exposed to LPS (1 μ g/ml; 24 hours; *** p <0.001; ANOVA; $F_{(3,37)}=35.92$). Pre-treatment with FGL significantly attenuated this effect (+ p <0.05; ANOVA). Values are presented as means (\pm SEM; $n=6$) and expressed as pg IL-6/ml.

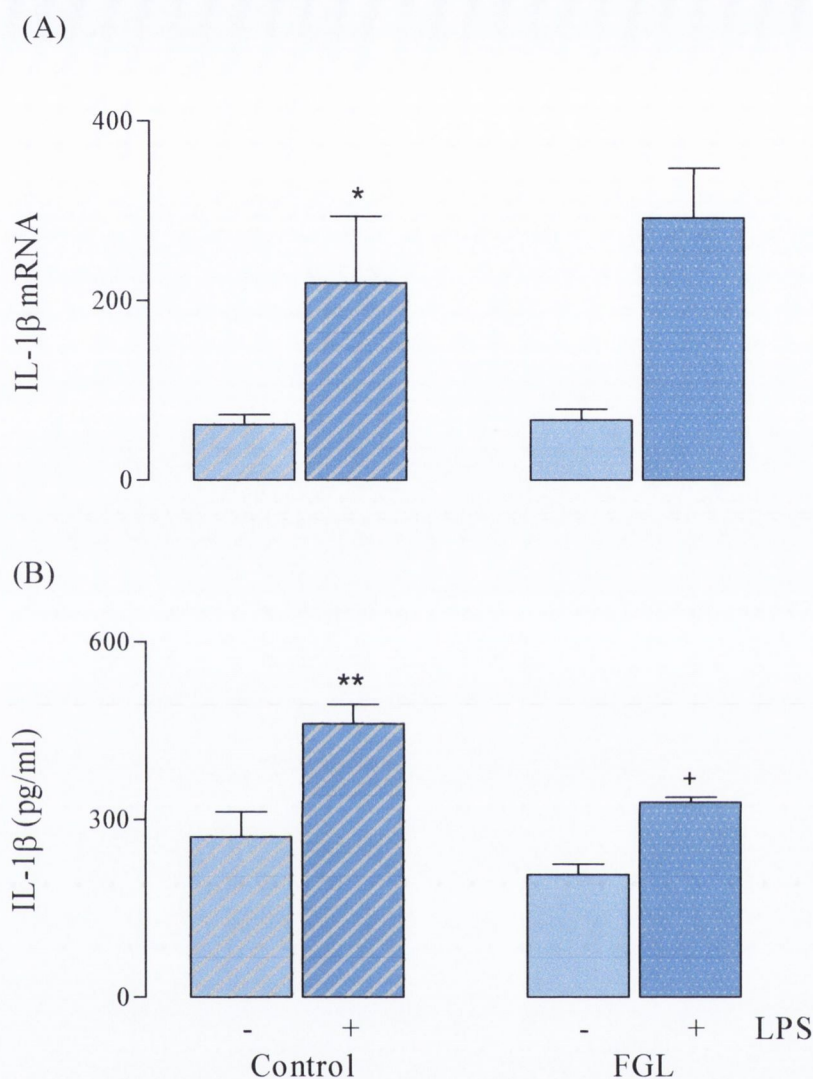


Figure 3.5. FGL significantly attenuated the LPS-induced increase in IL-1 β release, but not mRNA expression, in isolated microglial cultures.

LPS (1 μ g/ml; 24 hours) significantly increased IL-1 β mRNA expression (A) and release (B) in isolated microglial cultures (* p <0.05; ** p <0.01; ANOVA; A, $F_{(3,14)}=7.44$ and B, $F_{(3,11)}=13.39$). Pre-treatment with FGL (10 μ g/ml) significantly attenuated the LPS-induced increase in IL-1 β release (+ p <0.05; ANOVA), but not mRNA expression. Values for Q-PCR are presented as means (\pm SEM; $n=7$) expressed as a ratio to β -actin mRNA and standardised to a control sample. Values for cytokine release are presented as means (\pm SEM; $n=6$) and expressed as pg IL-1 β /ml.

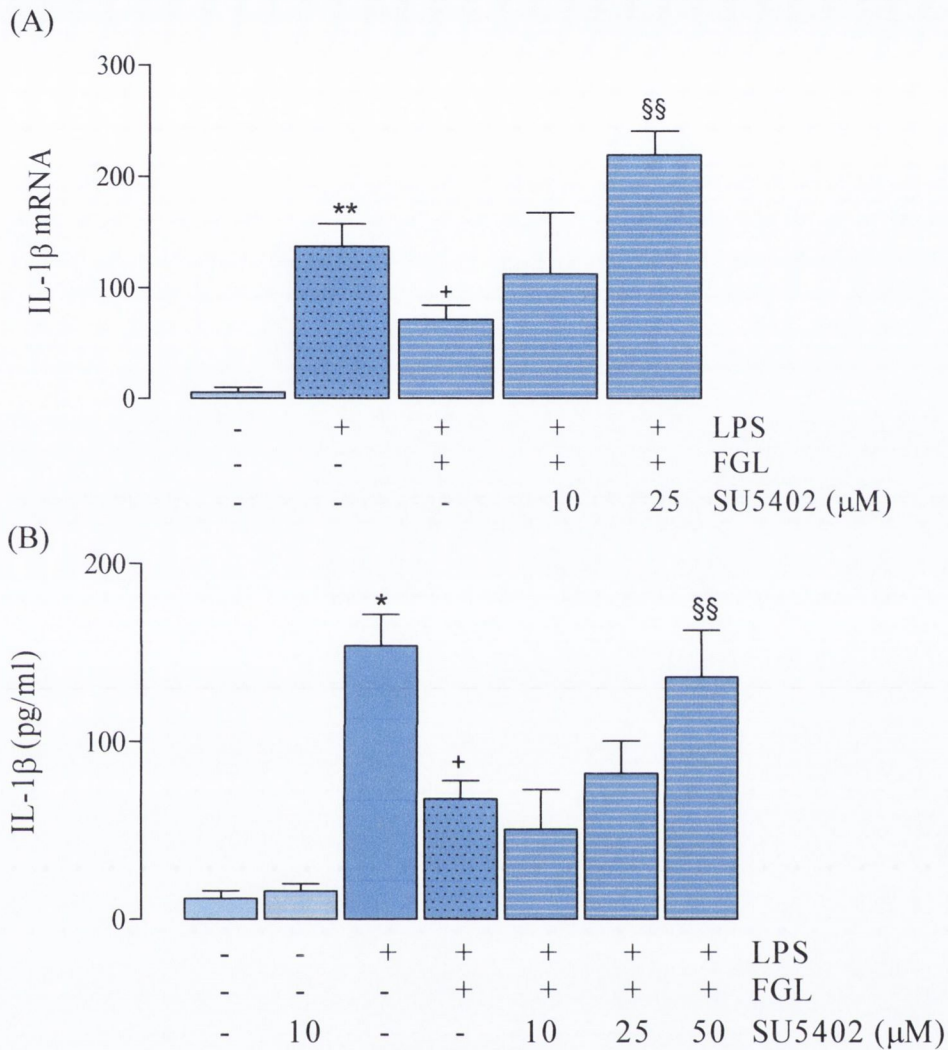


Figure 3.6. SU5402 blocked the ability of FGL to attenuate the LPS-induced increase in IL-1β mRNA expression and release in mixed glia.

LPS (1μg/ml; 24 hours) significantly increased IL-1β mRNA expression (A) and release (B) in mixed glial cultures (* $p < 0.05$; ** $p < 0.01$; ANOVA; A, $F_{(4,13)} = 13.81$ and B, $F_{(6,27)} = 16.41$), this release was attenuated by pre-treatment with FGL (10μg/ml; + $p < 0.05$; ANOVA; A and B). Pre-treatment with SU5402 (30 minutes) blocked the ability of FGL to attenuate the LPS-stimulated increase in IL-1β mRNA and release (FGL/LPS treated glia compared with SU5402/FGL/LPS treated glia; §§ $p < 0.01$; ANOVA). Values for Q-PCR are presented as means (\pm SEM; $n = 4$) expressed as a ratio to β -actin mRNA and standardised to a control sample. Values for cytokine release are presented as means (\pm SEM; $n = 6$) and expressed as pg IL-1β/ml.

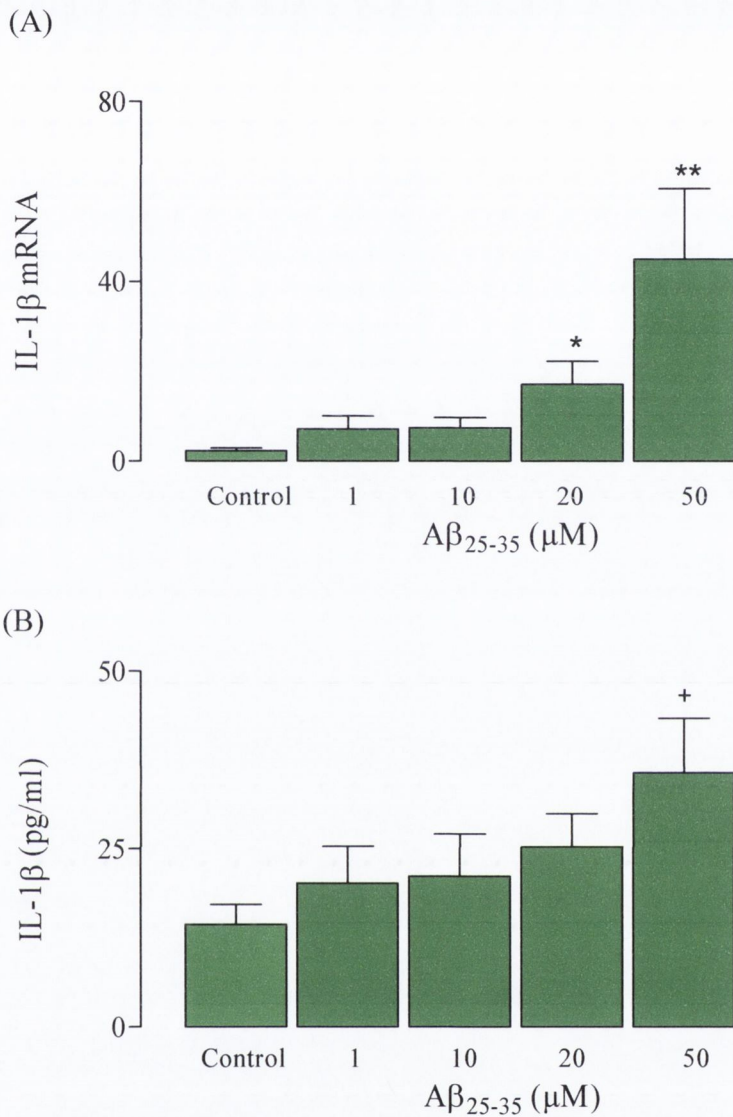


Figure 3.7. Aβ increased IL-1β mRNA expression and release in cultured mixed glia.

Aβ₂₅₋₃₅ induced an increase in IL-1β mRNA expression (A) and release (B) in mixed glia (*p<0.05; **p<0.001; ANOVA; $F_{(3,16)}=3.81$; +p<0.05; Student's *t*-test). Values for Q-PCR are presented as means (±SEM; n=5) expressed as a ratio to β-actin mRNA and standardised to a control sample. Values for cytokine release are presented as means (±SEM; n=5) and expressed as pg IL-1β/ml.

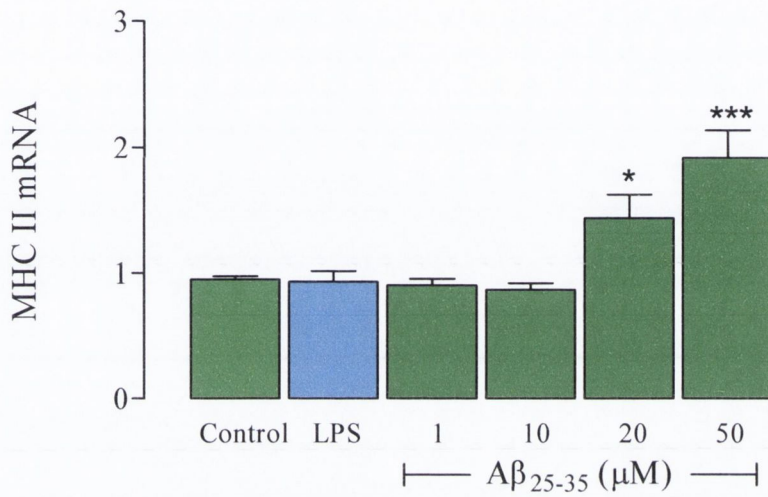
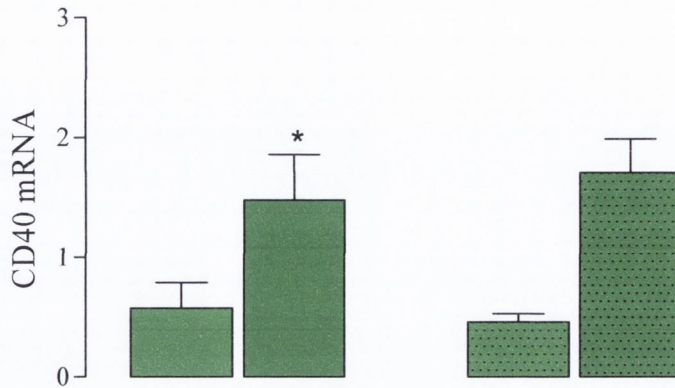


Figure 3.8. Aβ increased MHC II mRNA expression in cultured mixed glia.

Aβ₂₅₋₃₅ (24 hours) dose dependently increased MHC II mRNA expression in mixed glial cells, compared with control treated glia (*p<0.05; ***p<0.001; ANOVA; $F_{(5,23)}=12.50$). LPS (1μg/ml) failed to increase MHC II expression in cultured mixed glia. Values are presented as means (±SEM; n=5) expressed as a ratio to β-actin mRNA and standardised to a control sample.

(A)



(B)

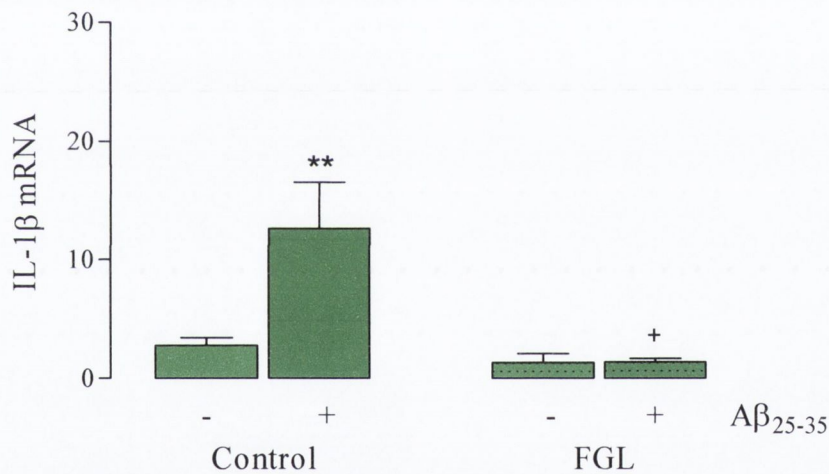


Figure 3.9. FGL attenuated the A β -stimulated increase in IL-1 β , but not CD40, mRNA expression in cultured mixed glia.

A β_{25-35} (20 μ M; 24 hours) significantly increased CD40 (A) and IL-1 β (B) mRNA expression in cultured mixed glial cells (* p <0.05; ** p <0.01; ANOVA; A, $F_{(3,11)}=5.43$ and B, $F_{(3,23)}=35.42$). Pre-treatment with FGL (10 μ g/ml) did not alter the A β -stimulated increase in CD40 mRNA expression, but it attenuated the A β -stimulated increase in IL-1 β mRNA expression (+ p <0.05; ANOVA). Values are presented as means (\pm SEM; $n=4$) expressed as a ratio to β -actin mRNA and standardised to a control sample.

3.4 Discussion

The first objective of this study was to examine the ability of FGL to modulate LPS-induced changes in cell surface markers of activation and pro-inflammatory cytokine expression in mixed glial and isolated microglial cultures. FGL attenuated the LPS-induced increase in CD40, CD11b and IL-1 β mRNA expression and decreased release of IL-6 and IL-1 β in mixed glial cultures. FGL also attenuated the LPS-stimulated increase in IL-1 β release from isolated microglial cultures. Secondly, the dependence of FGL on FGFR-1 activation, to modulate the LPS-induced changes, was assessed using SU5402, which inhibits the tyrosine kinase activity of FGFR-1. Incubating mixed glial cells in the presence of this inhibitor abrogated the anti-inflammatory action of FGL on the LPS-induced increase in IL-1 β mRNA expression and protein concentration. Finally, the inflammatory profile induced by A β ₂₅₋₃₅, and the proclivity of FGL to modulate this was examined. Mixed glial cells exposed to A β ₂₅₋₃₅ displayed increased expression of MHC II, CD40 and IL-1 β at an mRNA level, as well as increased supernatant concentration of IL-1 β . Incubation with FGL attenuated the A β ₂₅₋₃₅-induced increase in IL-1 β mRNA expression, suggesting an anti-inflammatory role for FGL.

LPS is a component of the outer membrane of Gram-negative bacteria and is one of the most frequently used inflammatory stimuli employed to investigate signalling cascades and pharmacological interventions *in vitro*. In this study, LPS significantly increased expression of the cell surface proteins CD11b and CD40 in mixed glial cultures. CD11b is constitutively expressed at low levels on microglia and plays a pivotal part in the migration and adhesion of these cells, allowing them to interact with and interpret their environment (Solovjov *et al.*, 2005). Microglial hypertrophy has been correlated with an increase in CD11b expression (Klementiev *et al.*, 2007). Here the increase in CD11b expression was attenuated by FGL, which suggests exposure to this peptide inhibits LPS-induced microglial activation. Roy and colleagues (2008) have also reported that LPS can up-regulate CD11b mRNA in primary microglial cultures and in a BV-2 microglial cell line, while exposing microglia to IL-1 β or A β ₁₋₄₂ had a similar stimulatory effect on expression of this integrin *in vitro*. It is emphasised that microglial activation is a hallmark of many neurodegenerative conditions and the level of CD11b expression correlates with the severity of microglial activation, therefore understanding how to manipulate its expression could be beneficial in developing therapeutic

agents (Roy *et al.*, 2006). FGL intracisternally prevented an A β_{25-35} -stimulated increase in CD11b and associated cognitive decline and this is in agreement with some aspects of the current study (Klementiev *et al.*, 2007). The current study demonstrates that the action exerted by FGL *in vitro* may have further clinical applications.

Once activated, glial cells interact and communicate with other cells via expression of cell surface proteins and release of small signalling molecules, which include cytokines. In the current study the LPS-induced increase in CD40 mRNA was dose-dependently attenuated by pre-treatment with FGL. The membrane protein CD40 plays a key role in propagating an inflammatory response primarily through interacting with its cognate ligand, CD40L (Benveniste *et al.*, 2004). It is well established that activated microglia express CD40 and there are reports of its expression on astrocytes *in vitro* (Abdel-Haq *et al.*, 1999; Benveniste *et al.*, 2004). CD40L displays transient expression and is primarily recorded on T cells, however, astrocytes and endothelial cells also have the capacity to express it (Schonbeck & Libby, 2001). An LPS-induced increase in CD40 expression in mixed glial cultures has been reported previously and additionally, it has been shown that LPS, IL-1 β and IL-6 can increase CD40 expression on isolated primary microglia and astrocytes (Abdel-Haq *et al.*, 1999; Watson *et al.*, 2010). Here FGL decreased the LPS-induced up-regulation of CD40 mRNA and this finding is consistent with others which have demonstrated the ability of FGL to attenuate interferon- γ (IFN γ)-induced CD40 expression in primary mixed glia (Downer *et al.*, 2009). IFN γ , like LPS, potently activates immune cells and enhances pro-inflammatory cytokine release, however, unlike LPS, IFN γ primarily acts on specific IFN receptors that induce activation of the JAK-STAT pathway (Murphy *et al.*, 2010).

Work from this laboratory has shown that FGL can enhance IL-4 expression in primary glial cultures and it was suggested this anti-inflammatory cytokine plays a critical part in FGL-induced immune modulation *in vitro* and *in vivo* (Downer *et al.*, 2008). Consistently, IL-4 potently inhibits CD40 expression on IFN γ -activated microglia by interfering with CD40 gene transcription (Nguyen & Benveniste, 2000). The mechanism underlying this effect has been examined and it was shown that IL-4 phosphorylates STAT-6, which binds to part of the CD40 promoter sequence thus preventing STAT-1 α from binding, resulting in down-regulation of transcription. It is plausible that IL-4 induced by FGL may modulate LPS-

stimulated CD40 transcription in a similar manner. FGFR-1 dependent IL-4 release is not restricted to the CNS and has been demonstrated in embryonic stem cells (Magnusson *et al.*, 2007). FGFR-1 deficient stem cells fail to release IL-4, resulting in impaired angiogenesis and hematopoiesis of helper T cells and mast cells (Sherman *et al.*, 2001). Although Magnusson (2007) focused on the role of FGFR-1 in the embryo, it is plausible that the FGFR-1 activation plays an integral role in IL-4 release through-out life. Taken with data from the current study, FGL, or a similar FGFR-1 stimulating drug, could exert an anti-inflammatory action in the periphery promoting immune cells with a STAT6-dependent IL-4 producing phenotype (Sherman *et al.*, 2001).

Cytokines play a critical role in the initiation and propagation of an inflammatory response. In the current study LPS induced an increase in mRNA expression and release of IL-1 β and IL-6 in mixed glia, these changes were attenuated by FGL. It is proposed that FGL acts via ligation of FGFR-1 and expression of this receptor it was confirmed by Q-PCR in isolated microglia and astrocytes (unpublished observation). This indicates that FGL can act on both cells in a mixed glial culture and it has previously been shown to attenuated cytokine release from purified astrocytes, stimulated with LPS (Downer *et al.*, 2008). In the current study isolated microglia were examined. FGL inhibited an LPS-induced increase in IL-1 β release, but failed to down-regulate mRNA expression. The explanation for this is not known, but it is possible that FGL can directly interfere with the release of IL-1 β . IL-1 β is produced as an inactive cytosolic precursor protein called proIL-1 β , which must be cleaved to its mature form by caspase-1 before being liberated (Martinon *et al.*, 2002). Assembly of a multiprotein complex known as the inflammasome promotes caspase-1 activity, leading to proteolytic cleavage and subsequent release of IL-1 β . By hindering assembly of the inflammasome, FGL could modulate IL-1 β release without effecting transcription of the protein.

Work in this laboratory has demonstrated the ability of LPS to up-regulate pro-inflammatory cytokines in mixed glial cultures and a variety of different pharmacological agents have been shown to attenuate the LPS-stimulated inflammatory response (Loane *et al.*, 2007; Clarke *et al.*, 2008; Costelloe *et al.*, 2008; Downer *et al.*, 2008). Novel anti-inflammatory actions for rosiglitazone, a drug used to enhance insulin sensitivity in diabetic patients, and atorvastatin, a cholesterol lowering drug, which was independent of their insulin or lipid modulating activity

were highlighted. The evidence suggested that their anti-inflammatory action was mediated by IL-4. This provides an interesting parallel with FGL; these agents up-regulate IL-4 expression *in vitro* and *in vivo* (Loane *et al.*, 2007; Clarke *et al.*, 2008; Downer *et al.*, 2008).

Another possible mechanism for the regulation of cytokine production is via the immune-suppressing membrane glycoprotein, CD200. A study investigating the action of FGL on age-related inflammatory changes found that the peptide reversed an age-related decline in hippocampal CD200 expression (Downer *et al.*, 2008). The same study reported that primary neurons incubating in the presence of FGL displayed increased CD200 expression, compared with control-treated neurons. In the current study the possibility exists that FGL exerted its action on microglial markers in mixed glial preparation because of an interaction with astrocytes which express CD200; this is shown in Chapter 4. In this case FACS was used to show expression of CD200 on a CD11b-negative population in mixed glial cultures. In addition, a study examining post-mortem tissue of MS patients reported CD200 expression on activated astrocytes (Koning *et al.*, 2009). Therefore, it is possible that in addition to increasing IL-4, FGL may modulate pro-inflammatory cytokines by means of up-regulating CD200 expression on astrocytes, within a mixed glial preparation

It is interesting that isolated microglia exposed to LPS responded differently to mixed glia exposed to the same stimuli. Whereas the effect of FGL on the LPS-induced increase in IL-1 β was marked in mixed glia, attenuating release by 226%, it was less profound in pure microglia, reducing the LPS-induced change by 140%. However, it should be pointed out that mean IL-1 β concentration in supernatant of un-stimulated mixed glia was 11.72pg/ml compared with 270.38pg/ml in pure microglial cultures. The data suggests that isolated microglia are in an activated state, which has previously been observed by other researchers (Floden & Combs, 2007). Floden and colleagues (2007) suggest that the microglial phenotype may be altered immediately after removal from a mixed glial culture and report that isolated microglia initially display an amoeboid phenotype. During an inflammatory challenge an active microglial phenotype is associated with assembly of the inflammasome and subsequent release of IL-1 β (Guarda & So, 2010). It is possible that the 23-fold increase in supernatant concentration of IL-1 β in isolated microglial cultures, compared with mixed glia, is a result of increased assemblage of the inflammasome's component proteins, enhancing caspase-1

activity resulting in maturation and release of IL-1 β . The shift in activation state in isolated microglia may further implicate an immunomodulatory role for astrocytes within a mixed glial preparation.

It has been established that FGL exerts an anti-inflammatory action *in vitro*, and the following set of experiment were designed to investigate if this was dependent on FGL induced FGFR-1 activation. SU5402 specifically inhibits the catalytic domain of FGFR-1 by blocking its tyrosine kinase activity (Mohammadi *et al.*, 1997). Here SU5402 blocked the ability of FGL to attenuate LPS-induced IL-1 β expression in primary mixed glia, indicating that the action of FGL was mediated by an interaction with FGFR-1. Other research groups investigating the action of FGL *in vitro* have reported an attenuation of its activity in the presence of SU5402 (Cambon *et al.*, 2004; Neiiendam *et al.*, 2004; Skibo *et al.*, 2005). Collectively it was found that SU5402 blocks an FGL-related enhancement in neurite outgrowth and pre-synaptic function as well as preventing the neuroprotective effects of FGL in neuronal cultures subjected to oxygen/glucose deprivation, a low KCl environment, A β ₂₅₋₃₅ or 6-OHDA. Furthermore, it has been shown that inhibiting FGFR-1 activation in macrophage cells in the periphery can be detrimental, as it suppresses FGF-related wound healing, thus emphasising a role for FGFR-1 in immune modulation (Numata *et al.*, 2006). The laboratory that developed FGL has shown that NCAM-induced ERK phosphorylation depends on FGFR-1 activation, which was demonstrated using neuronal cultures exposed to an NCAM-mimetic and incubated in the presence or absence of SU5402 (Ditlevsen *et al.*, 2008).

Although FGL-induced signalling is not specifically investigated in this thesis, previous work in this laboratory indicates FGL enhances ERK activation and stimulates signaling downstream of AKT (Downer *et al.*, 2008; Downer *et al.*, 2009). Fellow researchers focusing on assessing the consequence of FGF-stimulated FGFR-1 activation in cultured glia, have confirmed that SU5402 can inhibit ERK activation in isolated microglia, as well as ERK and AKT phosphorylation in cultured astrocytes (Ito *et al.*, 2007; Niidome *et al.*, 2009). Similarly, ERK- and AKT-mediated signaling has been associated with FGL-induced neurite outgrowth and neuroprotection (Neiiendam *et al.*, 2004; Downer *et al.*, 2008; Downer *et al.*, 2009). Thus, ERK signaling plays a critical role in FGL-dependent immune modulation, and inhibiting ERK activation prevents an FGL-induced increase in IL-4 concentration in cultured mixed glia and attenuates an FGL-stimulated increase in neuronal CD200 expression *in vitro* (Downer *et*

al., 2008; Downer *et al.*, 2009). Therefore, hindering FGFR-1 activation by SU5402 may prevent its ability to alter an LPS-induced increase in IL-1 β due to decreased ERK phosphorylation, thus leading to attenuation in IL-4 and CD200 expression *in vitro*.

Many neurodegenerative diseases are associated with neuroinflammation; one of the most prominent being is AD. Post-mortem analysis of brain tissue from AD patients reveals an abundance of A β -containing plaques, which some studies have co-localised with activated immune cells (Tan *et al.*, 1999). To replicate some aspects of this disease various forms of the A β peptide are injected into the brains of rodents. Although this is not a model for AD, and lacks many other aspects of its pathology, the A β peptide alone can induce an inflammatory response within the brain, which is believed to be instrumental in the cognitive decline associated with neurodegeneration. Mounting evidence suggests that chronic microglial activation in response to A β deposition can contribute to AD pathogenesis by promoting further plaque formation (Tan *et al.*, 1999; Townsend *et al.*, 2005). High levels of CD40 have been implicated in the pathogenesis of AD and exogenous A β has also been shown to up-regulate CD40 expression in isolated microglia (Tan *et al.*, 1999). In the current study A β_{25-35} increased CD40 and IL-1 β mRNA expression as well as supernatant concentration of IL-1 β . Klementiev (2007) found that injecting rodents with A β_{25-35} (icv) induced cognitive impairment and enhanced microgliosis as measured by CD11b immunoreactivity. The study reported that administration of FGL intracisternally attenuated an A β -related cognitive decline and CD11b expression. Here pre-treatment with FGL attenuated only the A β -stimulated increase in IL-1 β expression, but not CD40. This is an interesting finding as the current study has shown the proclivity of FGL to attenuate an LPS-induced increase in IL- β , in mixed glial cultures, and it is proposed that FGL induces a down-regulation in A β -stimulated IL-1 β in a similar fashion. However, FGL failed to alter CD40 mRNA expression induced by A β , despite significantly decreasing LPS-stimulated CD40. The disparity between these results could be due to the different inflammatory states induced by A β compared with LPS. Microglia and astrocytes can express MHC II, a surface molecule that binds antigen peptides for T cell presentation (Collawn & Benveniste, 1999; Neumann, 2001; De Keyser *et al.*, 2010). In the current study, LPS was not found to stimulate an increase in MHC II mRNA expression in mixed glial cultures, although other inflammatory markers were increased. In contrast A β increased MHC II mRNA in mixed glial cultures, which has also been shown with IFN γ , thus suggesting these inflammatory stimuli induce distinctive inflammatory profiles to LPS *in vitro*

(Downer *et al.*, 2009). Consistent with previous studies, LPS did not enhance MHC II expression in isolated microglia, while others investigating the action of LPS on astrocytes found higher concentration were required to stimulate an increase in MHC II surface expression (Morga *et al.*, 1999; Esen & Kielian, 2007; Vidyadaran *et al.*, 2009). Therefore, the LPS treatments protocol used in the current study induced a pro-inflammatory profile in the absence of increased MHC II expression, which corroborates what has been shown previously.

Expression of MHC II is indicative of antigen presentation and communication between cells. MHC II is associated with an up-regulation in co-stimulatory molecules, for example CD40, which enhances cell-cell interactions required to propagate an immune response (Collawn & Benveniste, 1999). Townsend and colleagues (2005) found that A β -induced CD40 on glial cells is associated with adaptive activation of microglia, which also display enhanced MHC II expression. Therefore, the proclivity of FGL to attenuate CD40 mRNA expression in mixed glia stimulated with LPS, but not A β , may be due to discrete interactions between MHC II positive glia, resulting in differential induction and expression of co-stimulatory molecule CD40.

The current study found that FGL exerted a distinct modulatory action on LPS- and A β -stimulated glia. It is well documented that LPS exerts its action chiefly through interacting with TLR4, which recognises it as a microbial pathogen (Medzhitov & Janeway, 1998). Upon ligation, TLR4 initiates a biochemical cascade of events, both dependent and independent of the adaptor protein MyD88, leading to translocation of NF κ B to the nucleus and up-regulation in NF κ B responsive genes including those for pro-inflammatory cytokines and cell adhesion molecules (Kopp & Medzhitov, 1999). FGL, potentially acting through ERK, attenuated expression of the co-stimulatory molecule CD40 and pro-inflammatory cytokines IL-1 β and IL-6 by interfering with NF κ B-related signalling. It is also suggested that exposure to FGL shifted the phenotype of the mixed glial cells, in favour of a more anti-inflammatory state, releasing IL-4 and expressing greater amounts of CD200.

The mechanisms by which A β peptides induce activation of glial cells is more elusive. Recent evidence has implicated TLR2 in A β -induced microglial activation and it has been shown that blocking this receptor suppresses A β -related pro-inflammatory cytokine production and

integrin expression *in vitro* (Jana *et al.*, 2008). However, much of the literature focuses on receptor for advanced glycation end-products (RAGE), a multiligand receptor expressed on neurons and glia that can act as a cell surface binding site for A β . Binding of A β to RAGE has been shown to phosphorylate various MAP kinases that are associated with synaptic dysfunction and an enhanced inflammatory profile, while also being implicated in NF κ B activation and related cytokine production (Du Yan *et al.*, 1997; Origlia *et al.*, 2009). Inflammatory signalling pathways triggered by A β continue to reveal novel and complex components with much opportunity for cross-talk. The characterisation of these biochemical cascades and cell specific interactions are required before mechanisms to manipulate them can be fully understood. FGL was initially developed as a drug to target diseases like AD, which are associated with cognitive decline. The current study demonstrates that FGL acts as an anti-inflammatory agent, which could be beneficial as enhanced neuroinflammation is associated with the pathogenesis of AD, as well as ischemic insults. While on a functional level, others have demonstrated its ability to acutely enhance synaptic integrity and cognitive function. However, further work is required to fully elucidate the neuroprotective action of FGL and its potential therapeutic application during chronic disease.

Chapter 4. Results

4.1 Introduction

The non-inflammatory state does not arise passively, but depends on the presence of soluble mediators and various cell-cell interactions. One repressor molecule involved in cell:cell interaction is CD200. It is a membrane-bound glycoprotein found on neurons and endothelial cells within the CNS and interaction of CD200 with its structurally-similar receptor, which is expressed on microglia, can maintain these cells in a quiescent state (Hoek *et al.*, 2000). Microglia of CD200-deficient mice spontaneously exhibit many features of activation, including a less ramified morphology and increased CD11b and CD45 expression. These mice display increased symptomatology in the experimentally-induced autoimmune diseases EAE and EAU (Hoek *et al.*, 2000; Copland *et al.*, 2007). Conversely, enhancing CD200 expression by genetic manipulation or administering a CD200 receptor agonist can be beneficial in restoring homeostasis after an inflammatory insult. Up-regulating CD200 by expression of a CD200 transgene promotes allograft acceptance, while administering a CD200 agonist has been shown to prevent bystander tissue damage in the lungs of mice inoculated with influenza virus, further implicating its role in immune tolerance (Snelgrove *et al.*, 2008; Gorczynski *et al.*, 2009).

IL-4 is an anti-inflammatory cytokine that acts in a negative feedback fashion on immune stimulation, in an effort to restore homeostasis. It is predominantly produced by a subset of helper T cells, Th 2 cells, which powerfully suppress IFN γ producing T cells (Seder, 1994). Low levels of IL-4 have been detected in the CNS and it is suggested that astrocytes are the primary source (Hulshof *et al.*, 2002). Work by Lyons and colleagues suggest that the anti-inflammatory action of IL-4 is in part due to its proclivity to increase neuronal CD200 expression (Lyons *et al.*, 2007; Lyons *et al.*, 2009b). This group report that incubating primary hippocampal neurons in the presence of IL-4 increased CD200 expression, while primary neurons from IL-4 deficient mice display a significantly less CD200. Furthermore, *in vivo*, ICV administration of IL-4 enhances neuronal CD200 in the hippocampus.

Lyons and colleagues have also reported that the A β -induced increase in markers of microglial activation is accompanied by a decrease in CD200 expression in hippocampus (Lyons *et al.*, 2007). Interestingly, an immunohistochemical examination of AD brains found a significant decrease in hippocampal CD200 expression (Walker *et al.*, 2009). While a decrease in CD200 expression on reactive astrocytes proximal to MS lesions has been reported (Koning *et al.*, 2009). Finally, Downer and colleagues describe a decrease in CD200 expression in the aged brain and this is reversed by FGL administered subcutaneously over a three week period (Downer *et al.*, 2008).

The objectives of the following set of experiments was to investigate some aspects of the profile of primary mixed glia prepared from CD200^{-/-} compared with wildtype mice, to assess the proclivity of FGL to attenuate LPS-induced changes in mixed glia prepared from CD200^{-/-} compared with wildtype mice and to examine astrocytic expression of CD200 *in vitro*, with the possibility of modulating microglial activation.

4.2 Methods

Mixed glial cell, isolated astrocytes and isolated microglia were prepared from neonatal wildtype or CD200^{-/-} C57BL/6 mice, and cultured for 14 days before treatment (see section 2.1 for details). In the case of FGL incubation, cells were exposed to the peptide for 24 hours before being incubated in the presence or absence of LPS (1µg/ml) for a further 24 hours (see section 2.1). An astrocytic membrane fraction was obtained by a serial centrifugation protocol (see section 2.1.6). Supernatant cytokine concentration was determined by ELISA and mRNA expression of surface proteins was assessed by Q-PCR (see section 2.3 and 2.4). Western immunoblotting was used to examine CD200 and GFAP expression (see section 2.5). Data are expressed as means ± SEM. ANOVA and Student's *t*-test were performed to determine whether significant differences existed between treatment groups and Newman-Keuls post-hoc tests were applied where appropriate.

4.3 Results

4.3.1 Mixed glia prepared from wildtype mice have an activated phenotype compared with glia from CD200^{-/-} mice.

Engagement of the widely-distributed membrane glycoprotein CD200 with its receptor, which is primarily located on cells of the myeloid lineage, can restrain myeloid cell activation and induce immune tolerance (Snelgrove *et al.*, 2008). It has previously been reported that microglia in CD200^{-/-} mice are phenotypically distinct from their wildtype counterparts. As adults, microglia in the brain and spinal cord express greater levels of CD11b and display a more amoeboid morphology (Hoek *et al.*, 2000). The aim of the following set of experiments was to investigate differences, if any, between mixed glia prepared from wildtype and CD200^{-/-} mice and to see if mixed glia from CD200^{-/-} mice respond differently to LPS and FGL.

Mixed glia prepared from CD200^{-/-} mice have significantly higher mRNA expression of CD11b and the lysosomal-associated membrane protein CD68, compared with mixed glia prepared from wildtype mice (***p*<0.001; Student's *t*-test, Figure 4.1). LPS induced a significant increase in CD40, ICAM-1 and CD11b mRNA expression in mixed glia prepared from wildtype and CD200^{-/-} mice (***p*<0.01; ****p*<0.001; ANOVA; A, $F_{(7,32)}=7.91$; B, $F_{(7,36)}=31.2$ and C, $F_{(7,34)}=60.95$, Figure 4.2) however, the LPS-induced increase was exaggerated in mixed glia prepared from CD200^{-/-} mice (§*p*<0.05; §§*p*<0.01; ANOVA, Figure 4.2 A, B and C). Pre-treatment with FGL attenuated the LPS-induced increase in CD40, ICAM-1 and CD11b mRNA expression in mixed glia prepared from wildtype, but not CD200^{-/-}, mice (†*p*<0.01; ††*p*<0.001; ANOVA, Figure 4.2 A, B and C).

LPS stimulated a significant increase in mRNA expression and supernatant concentration of IL-1β in mixed glia prepared from wildtype mice (***p*<0.001; ANOVA; A, $F_{(7,25)}=83.24$ and B, $F_{(7,35)}=7.77$, Figure 4.3) and this LPS-induced increase was exaggerated in mixed glia prepared from CD200^{-/-} mice (§§§*p*<0.001; ANOVA). LPS also stimulated an increase in TNF-α mRNA and supernatant concentration in mixed glia from wildtype mice (***p*<0.01; ****p*<0.001; ANOVA; A, $F_{(7,34)}=54.05$ and B, $F_{(3,12)}=73$, Figure 4.4), which was further enhanced in mixed glia cultured from CD200^{-/-} mice (§§§*p*<0.001; ANOVA). In a similar

fashion, LPS stimulated an increase in IL-6 mRNA and supernatant concentration in mixed glia from wildtype mice, compared with control treated mixed glia (^{***}p<0.001; ANOVA; A, $F_{(7,27)}=30.51$ and B, $F_{(7,34)}=1877$, Figure 4.5), which is further enhanced in mixed glia cultured from CD200^{-/-} mice (^{§§§}p<0.001; ANOVA). Pre-treatment with FGL attenuated the LPS-induced increase in mRNA expression and supernatant concentration of IL-1 β , TNF- α and IL-6 in mixed glia prepared from wildtype, but not CD200^{-/-}, mice (⁺⁺p<0.01, ⁺⁺⁺p<0.001; ANOVA, Figures 4.3-4.5).

4.3.2 CD200 is expressed on astrocytes

Much of the literature regarding CD200 in the CNS has focused on neuronal CD200 expression (Hoek *et al.*, 2000; Downer *et al.*, 2008). Using FACS analysis the present data demonstrate CD200 expression on CD11b-negative cells (Figure 4.6). Astrocytes do not express CD11b and since they are the most numerous cells in a mixed glial preparation, these data suggest that astrocytes express CD200 (Cowley *et al.*, 2010). To confirm these findings, purified astrocytes were prepared and assessed for CD200 using Western immunoblotting. The data verify the presence of CD200 on astrocytes and this expression is significantly up-regulated in astrocytes exposed to FGL (^{*}p<0.05; Student's *t*-test, Figure 4.7).

In the following set of experiments, isolated microglia prepared from wildtype mice were incubated in the presence or absence of a preparation of astrocytic membranes, prior to LPS exposure. The astrocytic membrane fraction was prepared by centrifugation of isolated astrocytes in a series of enzymatic buffers (see section 2.1.6 for details). A sample immunoblot shows expression of CD200 in the membrane, but not cytosolic, fraction while GFAP is present in the cytosolic fraction, with minimal expression in the membrane extract (Figure 4.8).

LPS induced a significant increase in IL-1 β mRNA expression in primary isolated microglia (^{***}p<0.001; ANOVA; $F_{(4,17)}=16.01$, Figure 4.9). Pre-incubation of microglia with an aliquot (20ng) of the membrane preparation obtained after incubating astrocytes in the presence of FGL, attenuated the LPS-induced increase in IL-1 β mRNA expression (LPS alone versus LPS/Astrocytic membrane; ⁺⁺⁺p<0.001; ANOVA, Figure 4.9). LPS also significantly up-

regulated mRNA expression and supernatant concentration of TNF- α and IL-6 in isolated microglia (** $p < 0.001$; ANOVA; A, $F_{(7,35)} = 7.77$ and B, $F_{(3,14)} = 18.27$, Figure 4.10 A, $F_{(3,21)} = 5.63$ and B, $F_{(3,17)} = 6.68$, Figure 4.11) and pre-incubation of microglia with an aliquot (20ng) of the membrane preparation obtained after incubating astrocytes in the presence of FGL, attenuated the LPS-induced increase in TNF- α and IL-6 mRNA expression and supernatant concentration (LPS alone versus LPS/Astrocytic membrane; $^+ p < 0.05$; $^{++} p < 0.01$; $^{+++} p < 0.001$; ANOVA, Figure 4.10 and 4.11).

An LDH assay was used to assess the effect of exposure to LPS or incubation in the presence of an astrocytic membrane fraction on viability of isolated microglial cultures. The data show that viability was not affected by any treatment (Figure 4.12).

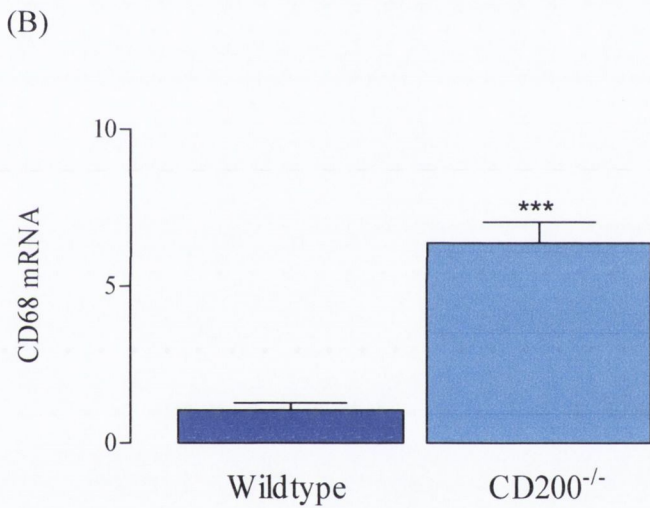
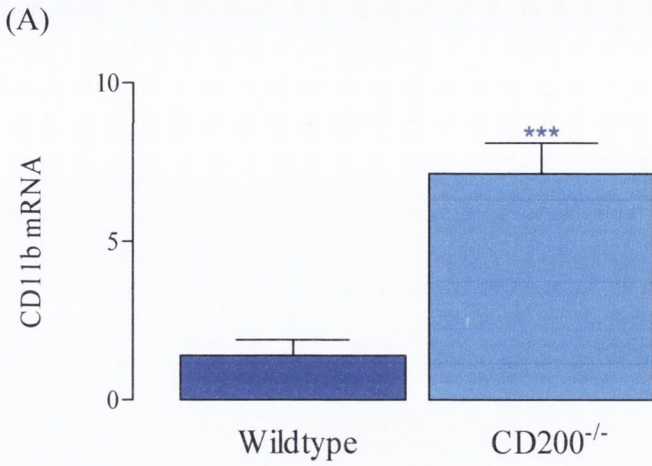


Figure 4.1. CD11b and CD68 mRNA expression was enhanced in mixed glia prepared from CD200^{-/-}, compared with wildtype, mice.

Expression of CD11b (A) and CD68 (B) mRNA was enhanced in untreated mixed glia prepared from CD200^{-/-}, compared with wildtype, mice (** $p < 0.001$; Student's *t*-test). Values are present as means (\pm SEM; $n=6$) expressed as a ratio to β -actin mRNA and standardised to a control sample.

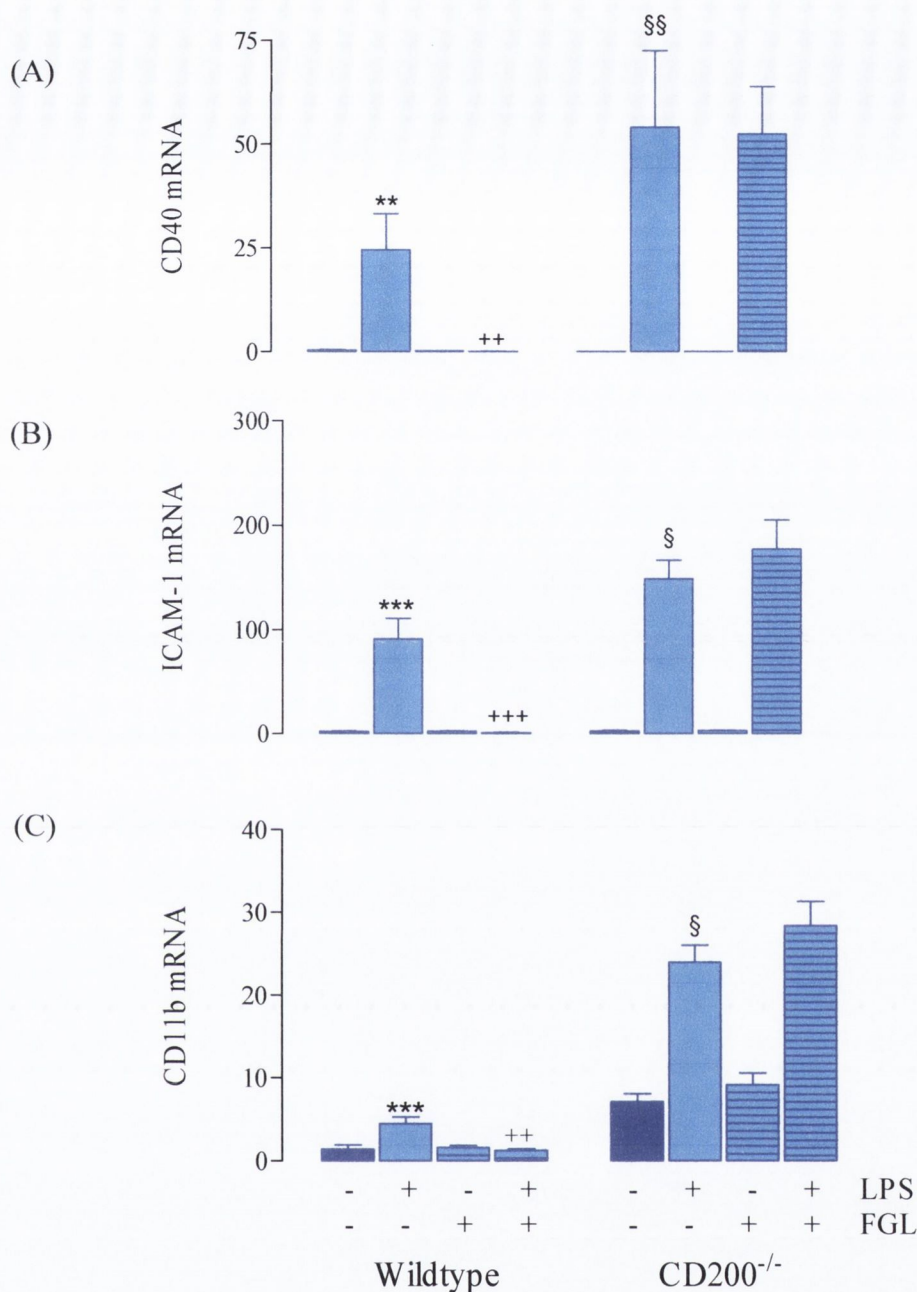


Figure 4.2. FGL attenuated the LPS-induced increase in CD40, ICAM-1 and CD11b mRNA in glia prepared from wildtype but not CD200^{-/-} mice.

LPS (1µg/ml; 24 hours) induced a significant increase in mRNA expression of CD40 (A), ICAM-I (B) and CD11b (C) in mixed glia cultured from wildtype and CD200^{-/-} mice (***p*<0.001; ANOVA; A, $F_{(7,32)}=7.91$, B, $F_{(7,36)}=31.2$ and C, $F_{(7,34)}=60.95$;) and these responses were enhanced in glia from CD200^{-/-} mice (§*p*<0.05; §§ *p*<0.01; ANOVA). Pre-treatment with FGL (10µg/ml) attenuated the LPS-induced changes in glia from wildtype, but not CD200^{-/-}, mice (+++*p*<0.001; ANOVA). Values are present as means (±SEM; n=6) expressed as a ratio to β-actin mRNA and standardised to a control sample.

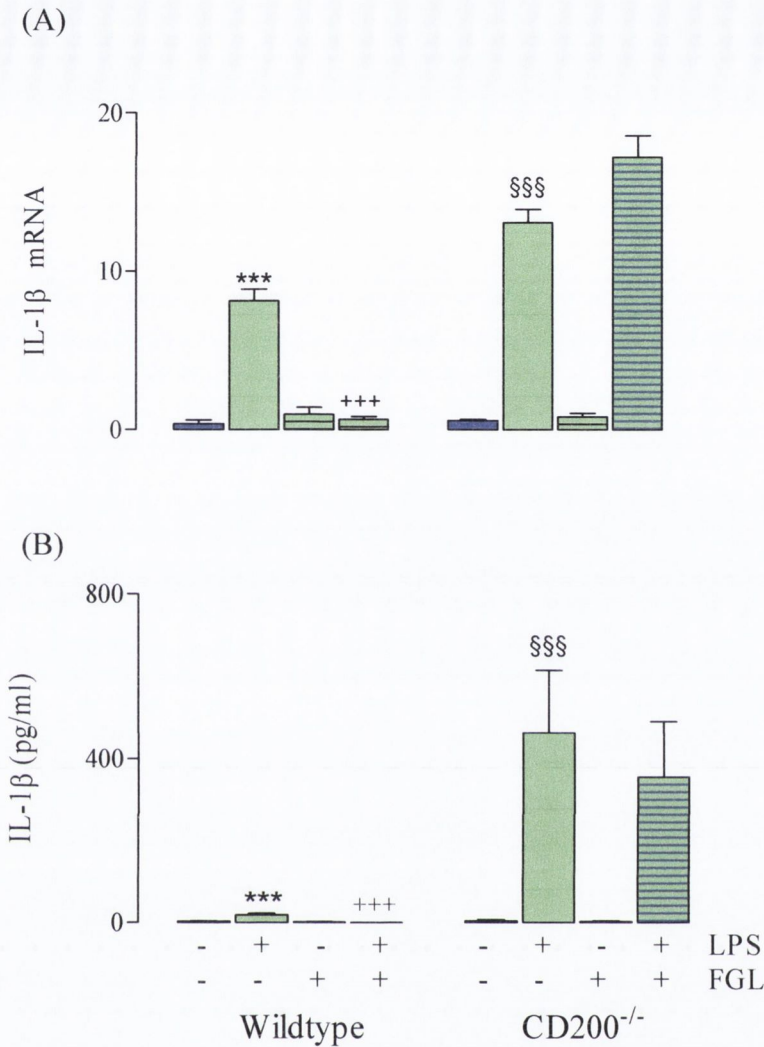


Figure 4.3. FGL attenuated the LPS-induced increase in IL-1 β mRNA and release in glia prepared from wildtype but not CD200^{-/-} mice.

LPS (1 μ g/ml; 24 hours) induced a significant increase in IL-1 β mRNA expression (A) and release (B) in mixed glia cultured from wildtype and CD200^{-/-} mice, (** p <0.001; ANOVA; A, $F_{(7,25)}=83.24$ and B, $F_{(7,35)}=7.77$). Pre-treatment with FGL (10 μ g/ml) attenuated the increase in IL-1 β expression in glia from wildtype, but not CD200^{-/-}, mice (+++ p <0.001; ANOVA). The response to LPS was markedly enhanced in glia cultured from CD200^{-/-}, compared with cells prepared from wildtype, mice (SSS p <0.001; ANOVA). Values for Q-PCR are presented as means (\pm SEM; $n=6$) expressed as a ratio to β -actin mRNA and standardised to a control sample. Values for cytokine release are presented as means (\pm SEM; $n=6$) and expressed as pg of IL-1 β /ml.

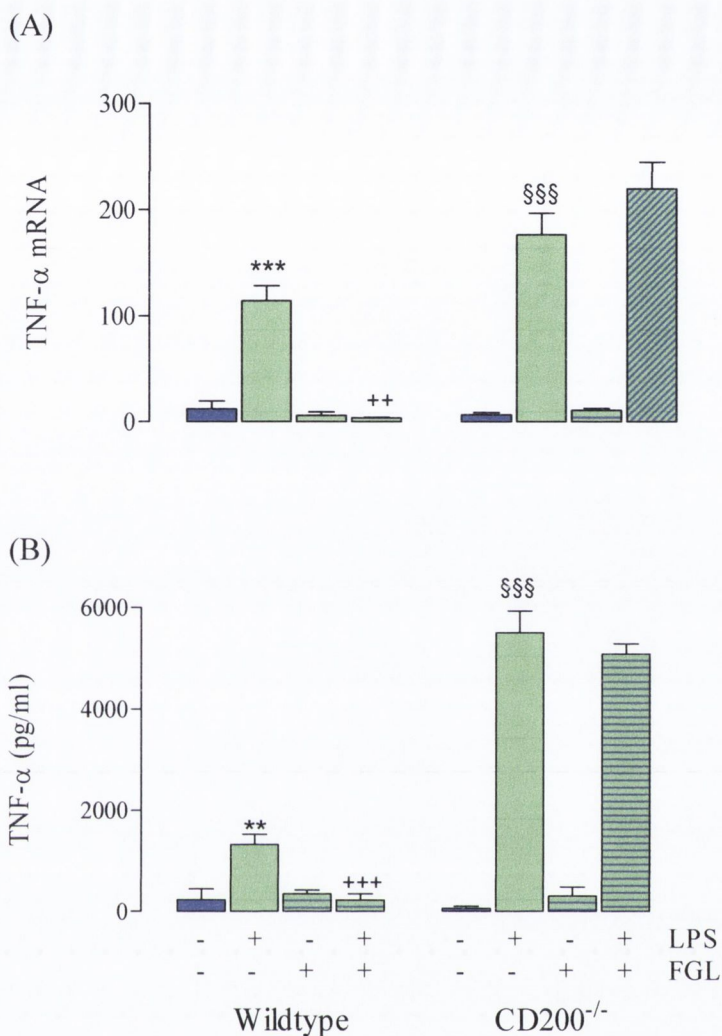


Figure 4.4. FGL attenuated the LPS-induced increase in TNF- α mRNA and release in glia prepared from wildtype but not CD200^{-/-} mice.

LPS (1 μ g/ml; 24 hours) induced a significant increase in TNF- α mRNA expression (A) and release (B) in mixed glia cultured from wildtype and CD200^{-/-} mice, (** p <0.01; *** p <0.001; ANOVA; A, $F_{(7,34)}=54.05$ and B, $F_{(3,12)}=73$). Pre-treatment with FGL (10 μ g/ml) attenuated the increase in TNF- α expression in glia from wildtype, but not CD200^{-/-}, mice (** p <0.01; +++ p <0.001; ANOVA). The response to LPS was markedly enhanced in glia cultured from CD200^{-/-}, compared with cells prepared from wildtype, animals (SSS p <0.001; ANOVA). Values for Q-PCR are presented as means (\pm SEM; $n=6$) expressed as a ratio to β -actin mRNA and standardised to a control sample. Values for cytokine release are presented as means (\pm SEM; $n=6$) and expressed as pg of TNF- α /ml.

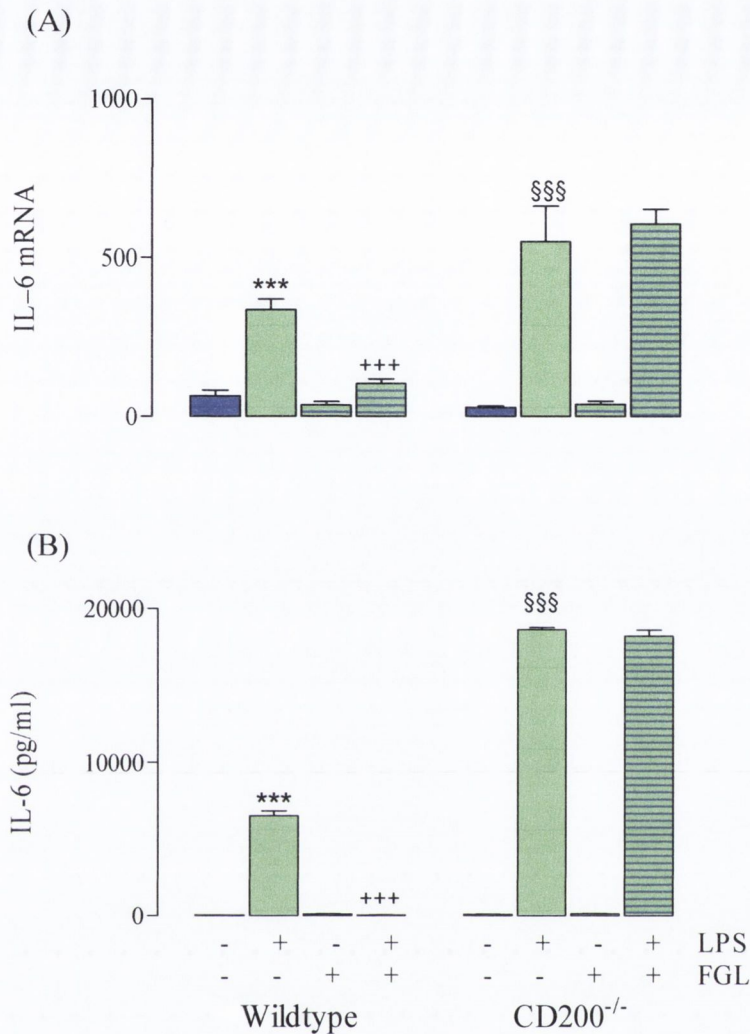


Figure 4.5. FGL attenuated the LPS-induced increase in IL-6 mRNA and release in glia prepared from wildtype but not CD200^{-/-} mice.

LPS (1 μ g/ml; 24 hours) induced a significant increase in IL-6 mRNA expression (A) and release (B) in mixed glia cultured from both mouse strains (** p <0.001; ANOVA; A, $F_{(7,27)}=30.51$ and B, $F_{(7,34)}=1877$). Pre-treatment with FGL (10 μ g/ml) attenuated the increase in IL-6 expression in glia from wildtype, but not CD200^{-/-}, mice (+++ p <0.001; ANOVA). The response to LPS was markedly enhanced in glia cultured from CD200^{-/-}, compared with cells prepared from wildtype, animals (SSS p <0.001; ANOVA). Values for Q-PCR are presented as means (\pm SEM; $n=6$) expressed as a ratio to β -actin mRNA and standardised to a control sample. Values for cytokine release are presented as means (\pm SEM; $n=6$) and expressed as pg of IL-6/ml.

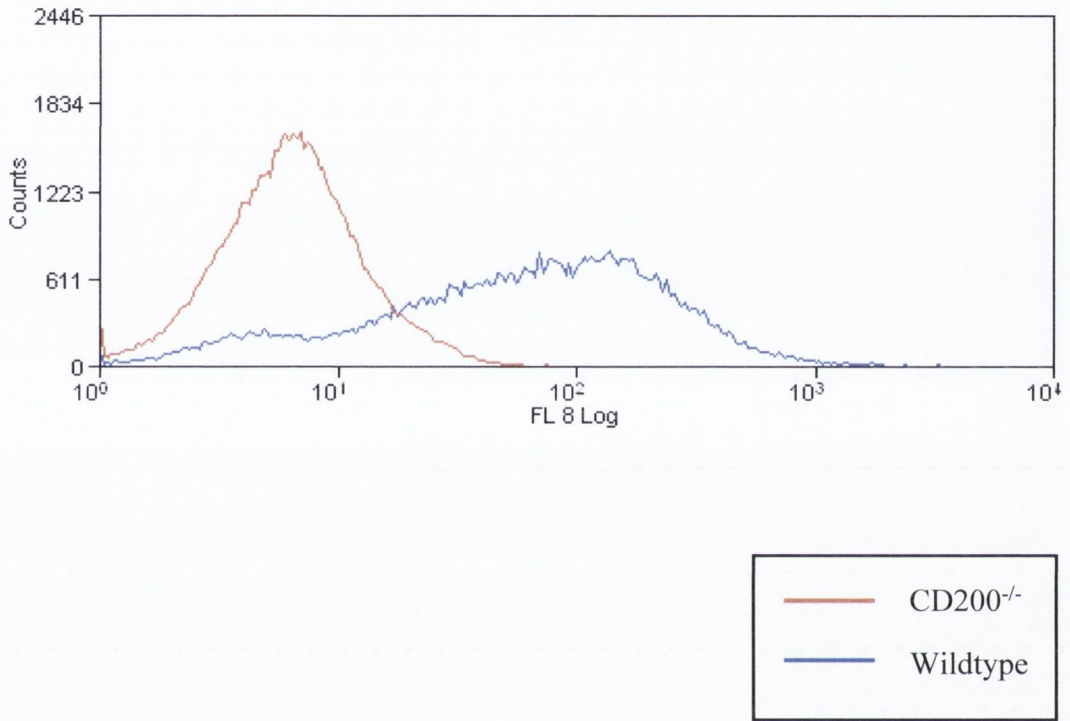


Figure 4.6. CD200 expression on CD11b-negative cells in a mixed glial prepared from wildtype mice.

Flow cytometric analysis indicate that CD200 was expressed on CD11b-negative cells in mixed glia cultured from wildtype mice (blue), but not the CD200^{-/-} strain (red).

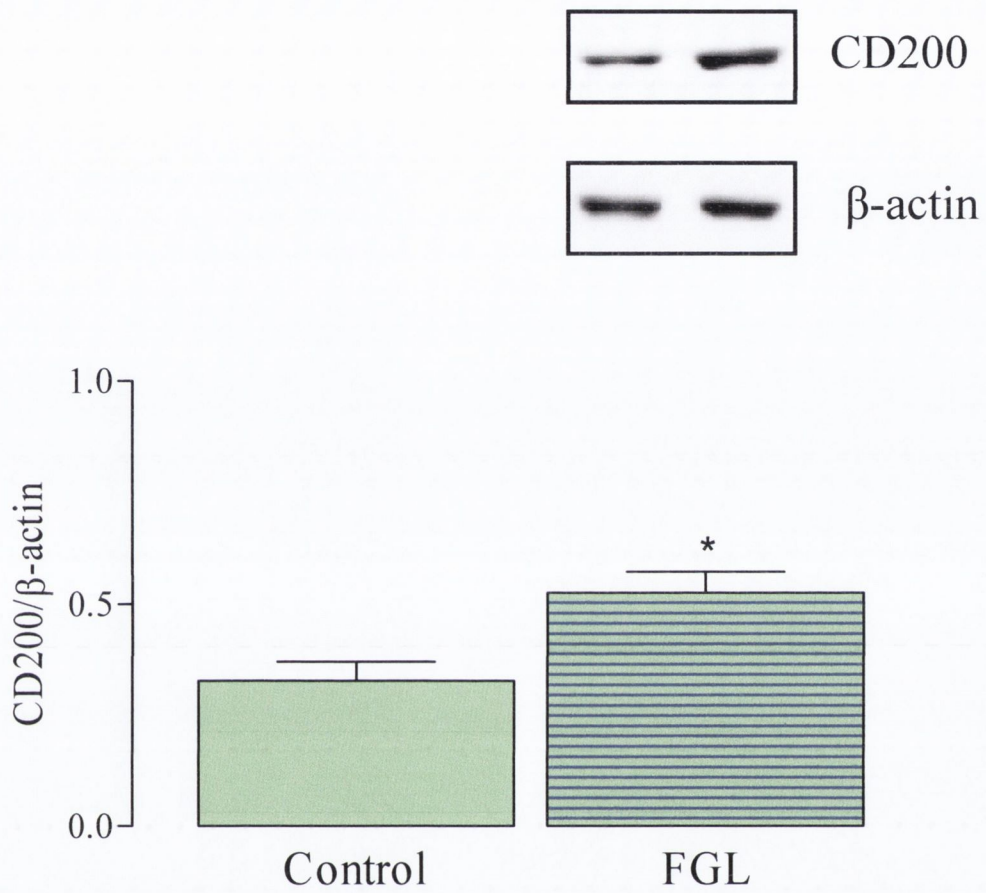


Figure 4.7. FGL enhanced CD200 expression in cultured astrocytes.

FGL (10μg/ml) induced a significant increase in CD200 protein concentration in isolated astrocytes prepared from wildtype mice (* $p < 0.05$; Student's *t*-test, densitometric units equalised to β-actin, $n=6$).

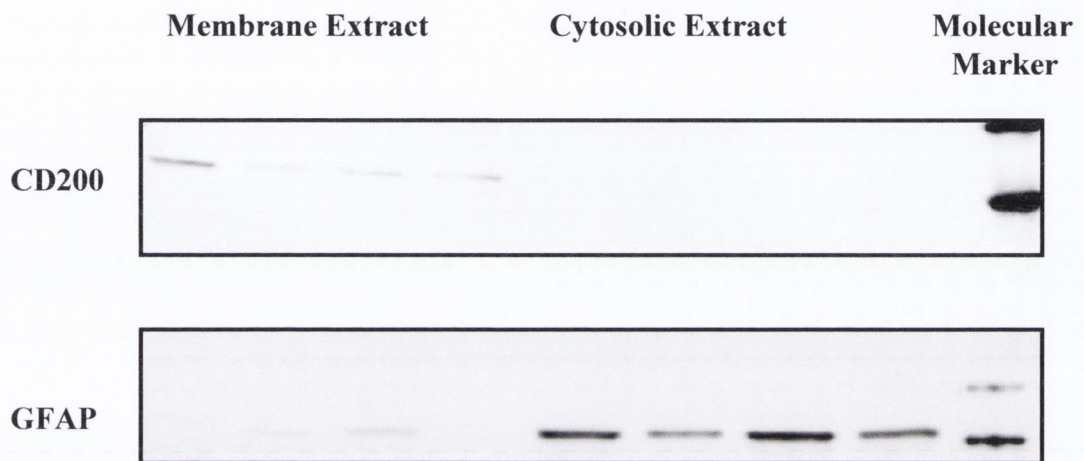


Figure 4.8. CD200 is expressed in an astrocytic membrane extract that contains minimal GFAP expression, compared with a cytosolic fraction.

Sample immunoblots show CD200 expression in a membrane fraction but not cytosolic fraction prepared from isolated astrocytes. GFAP is expressed in the cytosolic fraction, with minimal expression in the membrane extract, n=6.

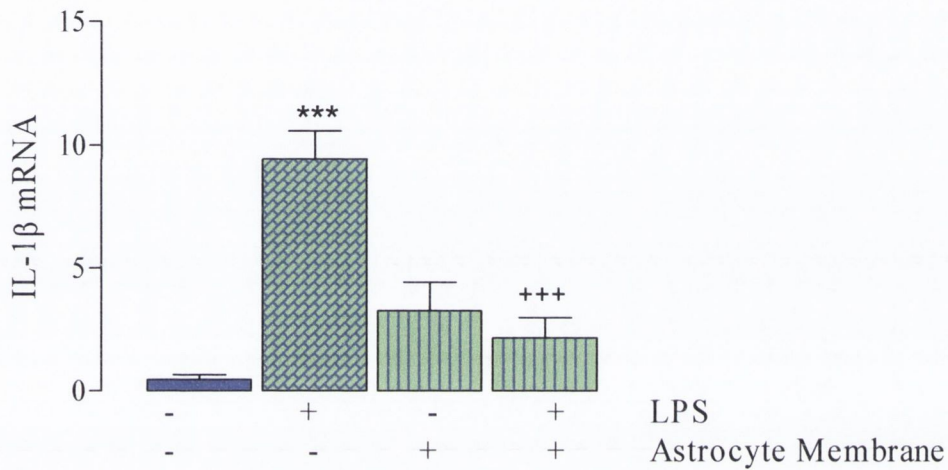


Figure 4.9. LPS induced an increase in IL-1 β mRNA expression in isolated microglia. Pre-incubation with an astrocytic membrane fraction attenuated the LPS-induced changes.

LPS (1 μ g/ml; 24 hours) induced a significant increase in IL-1 β mRNA expression in isolated microglia, (** p <0.01; *** p <0.001; ANOVA; $F_{(4,17)}=16.01$). Pre-treatment with an astrocytic membrane fraction attenuated the increase in IL-1 β mRNA expression in isolated microglia (+++ p <0.001; ANOVA). Values for Q-PCR are presented as means (\pm SEM; $n=6$) expressed as a ratio to β -actin mRNA and standardised to a control sample.

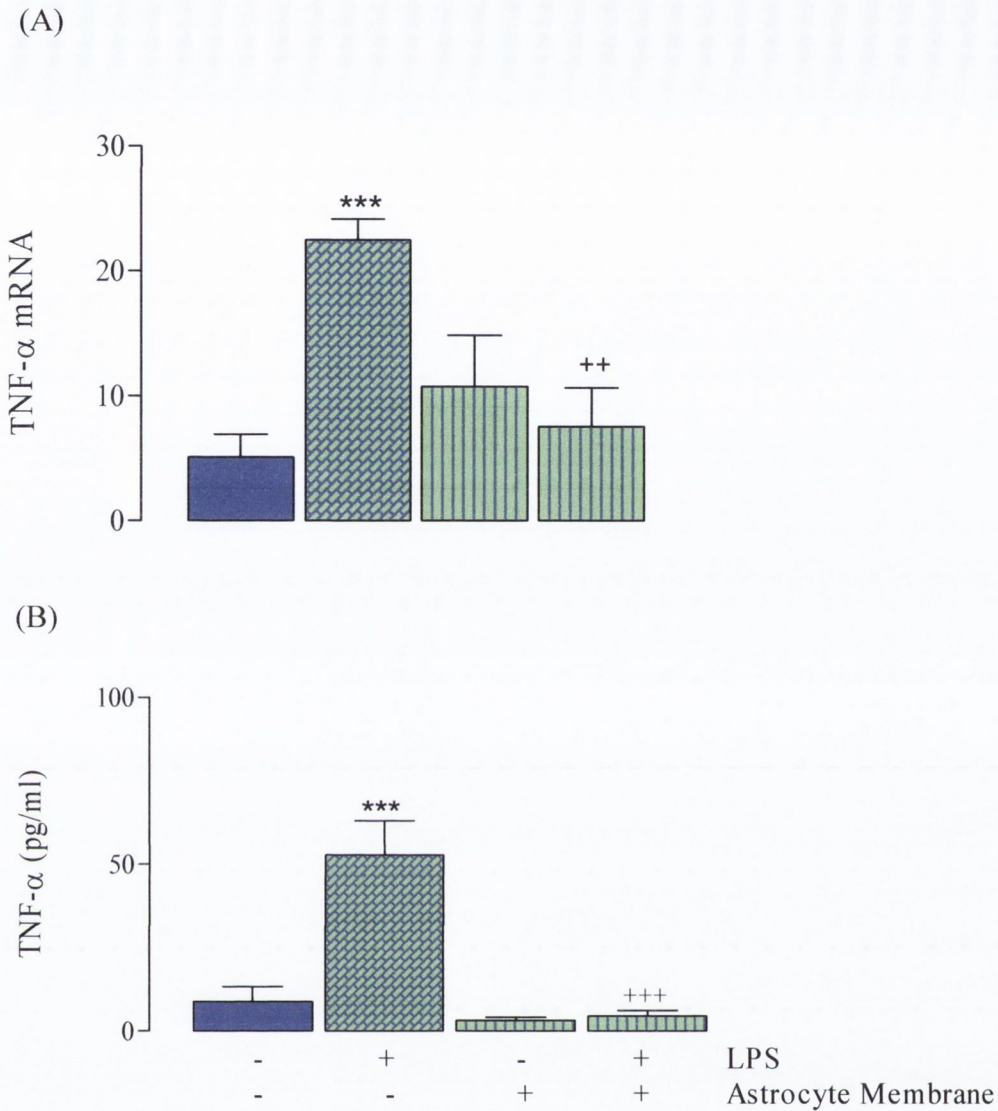


Figure 4.10. LPS induced an increase in TNF- α mRNA expression and release in isolated microglia. Pre-incubation with an astrocytic membrane fraction attenuated the LPS-induced changes.

LPS (1 μ g/ml; 24 hours) induced a significant increase in TNF- α mRNA expression (A) and release (B) in isolated microglia (** p <0.001; ANOVA; A, $F_{(7,35)}=7.77$ and B, $F_{(3,14)}=18.27$). Pre-treatment with an astrocytic membrane fraction attenuated the increase in TNF- α mRNA expression and release from isolated microglia (** p <0.01; +++ p <0.001; ANOVA). Values for Q-PCR are presented as means (\pm SEM; $n=6$) expressed as a ratio to β -actin mRNA and standardised to a control sample. Values for cytokine release are presented as means (\pm SEM; $n=6$) and expressed as pg TNF- α /ml.

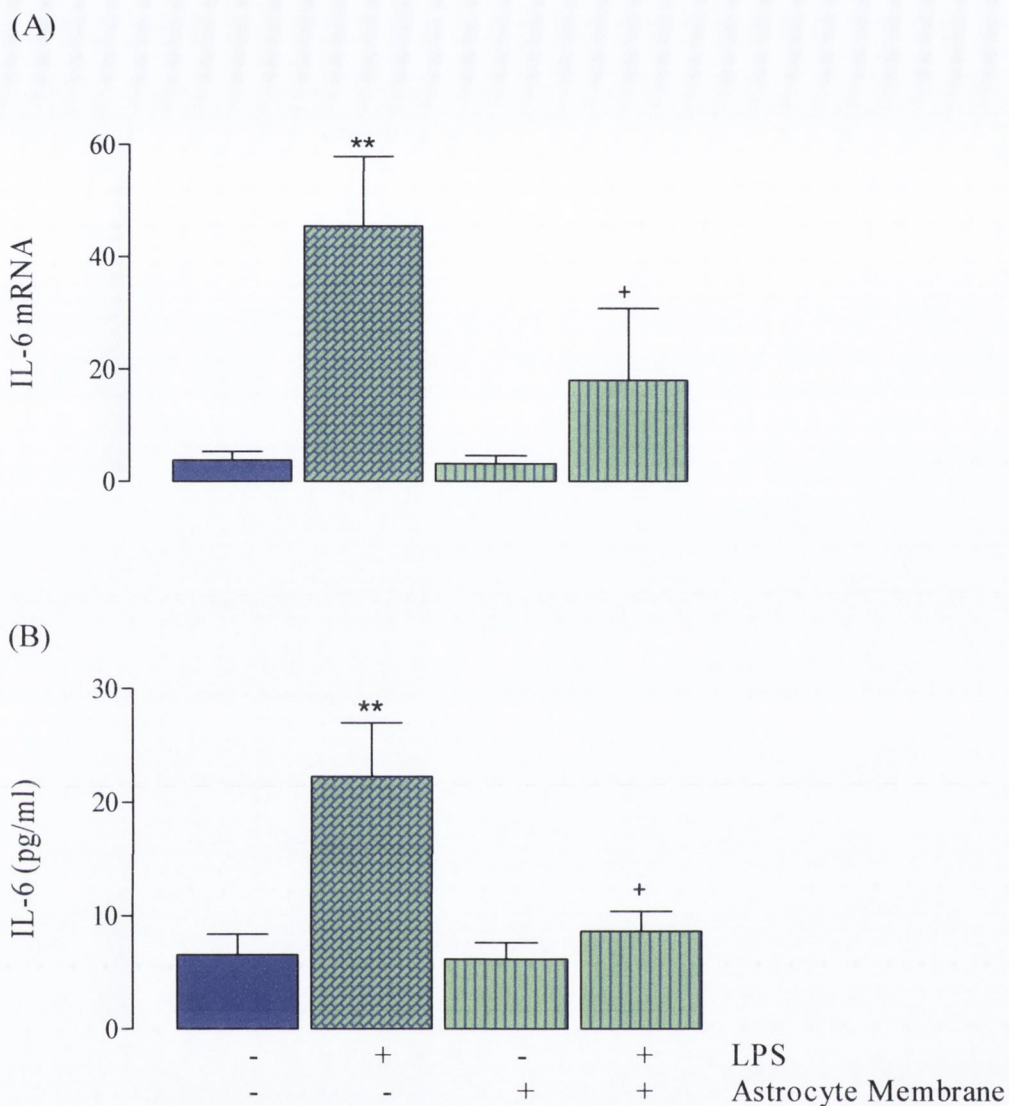


Figure 4.11. LPS induced an increase in IL-6 mRNA expression and release in isolated microglia. Pre-incubation with an astrocytic membrane fraction attenuated the LPS-induced changes.

LPS (1 μ g/ml; 24 hours) induced a significant increase in IL-6 mRNA expression (A) and release (B) in isolated microglia, (** p <0.01; ANOVA; A, $F_{(3,21)}=5.63$ and B, $F_{(3,17)}=6.68$). Pre-treatment with an astrocytic membrane fraction attenuated the increase in IL-6 mRNA expression and release from isolated microglia (+ p <0.05; ANOVA). Values for Q-PCR are presented as means (\pm SEM; $n=6$) expressed as a ratio to β -actin mRNA and standardised to a control sample. Values for cytokine release are presented as means (\pm SEM; $n=6$) and expressed as pg IL-6/ml.

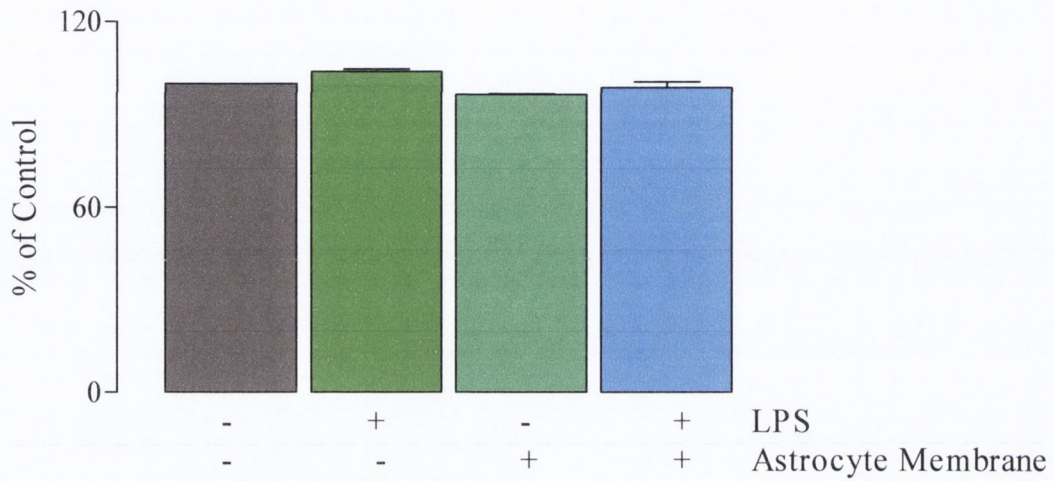


Figure 4.12. An LDH assay confirmed that exposure to LPS or an astrocytic membrane fraction did not compromise cell viability.

Cell viability was not altered in isolated microglia exposed to LPS (1 μ g/ml; 24 hours) or an astrocytic membrane fraction, quantified by the concentration of lactate dehydrogenase in control cells compared with treated cells. Values are presented as means (\pm SEM; n=6) and expressed as concentration of lactate dehydrogenase in treated cells as a percentage of that found in control treated glia.

4.4 Discussion

The first objective of this set of experiments was to examine the effects of LPS in mixed glial cultures prepared from CD200^{-/-}, compared with glia from wildtype mice. Secondly, the proclivity of FGL to modulated LPS-induced changes was assessed and the possibility of CD200 expression on glia evaluated.

Glia prepared from CD200^{-/-} mice display enhanced levels of CD11b and CD68 in the absence of an exogenous inflammatory stimulus. CD11b is a cell membrane protein constitutively expressed on microglia, it plays a role in migration and cell-cell or cell-substratum adhesion, and an increase in its expression is indicative of heightened microglial activation (Solovjov *et al.*, 2005; Roy *et al.*, 2006). In addition to antigen presentation, microglia are the primary effector cells of phagocytosis in the CNS. The current study found a greater CD68 expression on glia prepared from CD200^{-/-} mice, which is indicative of increased phagocytic activity (Cho *et al.*, 2006). CD68 is a heavily-glycosylated lysosomal membrane protein, with a high rate of cycling between the cell surface membrane and intracellular pools. It is hypothesised that CD68 maintains lysosomal membrane integrity during phagocytosis as its robust structure may protect the membrane from destructive lysosomal hydrolases (Kurushima *et al.*, 2000). Here an increase in CD68 mRNA expression was observed in unstimulated mixed glia prepared from CD200^{-/-} mice, compared with glia from their wildtype counterparts. Cho and colleagues (2006) reported that CD68 was co-localised with MHC II, signifying that activated microglia, at least those positive for MHC II, are phagocytic. This study also found ramified microglia that stained positive for CD68 and had phagocytic capability in the absence of MHC II, thus these two markers do not necessarily go hand-in-hand. It is proposed that the morphological phenotype of an active microglia is multifactorial, depending on its location within the brain and the pathology or integrity of that tissue. As the current study examined CD11b and CD68 at an mRNA level, immunocytochemical analysis is required to assess co-localisation of CD68 and CD11b on glia to further elucidate the activation state of these cells.

CD200^{-/-} mice appear to develop normally and their life-span is comparable to their wildtype littermates (Hoek *et al.*, 2000). Examination of tissue from CD200^{-/-} mice revealed the population of CD11b-positive cells was almost doubled in the spleen of CD200-deficient

mice, suggestive of an increase in macrophage and granulocyte population, and these cells also displayed markers indicative of inflammation. In addition to enlarged lymph nodes, Hoek reported that the macrophage population in lymph tissue was expanded and appear more activated in CD200^{-/-} mice. Finally, analysis of the CNS revealed that microglia with shorter processes and increased levels of MHC II, CD11b and CD45, which tended to form aggregates particularly in the spinal cord. These observations, in adult mice, advocate a critical role for CD200 in maintaining myeloid cells in a passive, quiescent state. While the data from the current study, reveals a critical role for CD200 in restraining immune cell activity in a mixed glial population *in vitro*.

Other markers of glial cell activation, namely CD40 and ICAM-1, were examined at mRNA level in mixed glia prepared from CD200^{-/-} and wildtype mice. Unlike CD11b or CD68, mRNA expression of these membrane proteins was very low in the absence of an inflammatory stimulus, in both strains. Exposure to LPS induced an increase in CD40 and ICAM-1 expression in glia from wildtype mice and this was greater in glia prepared from CD200^{-/-} mice; the same was true for CD11b mRNA, implying that glia from these animals are more responsive to LPS *in vitro*. ICAM-1 is a heavily glycosylated, membrane protein with a high affinity to many binding proteins, including CD11b. ICAM-1 becomes up-regulated during an immune response and plays a critical role in the transmigration of leukocytes out of the vasculature (Zen *et al.*, 2004). CD40 is also associated with immune cell activation and cytokine release (Benveniste *et al.*, 2004). The enhanced reactivity of immune cells from CD200^{-/-} mice to an inflammatory challenge *in vitro* corroborates reports by other groups that investigated inflammatory insults *in vivo*. Studies examining the susceptibility of CD200^{-/-} mice to experimentally-induced allergic disease or viral infection revealed increased responsiveness to these inflammatory stimuli (Campbell *et al.*, 2000; Hoek *et al.*, 2000; Snelgrove *et al.*, 2008). The onset of EAE was dramatically accelerated in CD200^{-/-} mice, the increase in activated macrophages, determined by positive iNOS and CD68 staining, appeared earlier in the spinal cord in CD200^{-/-} mice and these cells remained markedly enhanced throughout the disease (Hoek *et al.*, 2000). Disease kinetics of EAU in CD200^{-/-} mice displayed a similar course to that of EAE, with an earlier onset and increased severity of symptoms (Copland *et al.*, 2007).

During an inflammatory response it is hypothesised that much bystander damage, of motor neurons in the case of EAE, cartilage in the case of CIA and lung tissue in the case of influenza, is associated with cytokine release from resident and infiltrating cells that perpetuate local immune activity (Campbell *et al.*, 1997; Snelgrove *et al.*, 2008). The current study found that LPS induced an increase in supernatant concentration and mRNA expression of the pro-inflammatory cytokines, IL-1 β , TNF- α and IL-6 in mixed glia prepared from wildtype mice, and this increase was exaggerated in mixed glia prepared from CD200^{-/-} animals. LPS is a potent inflammatory stimulus and previous work for this laboratory has demonstrated its ability to stimulate transcription and release of inflammatory mediators in mixed glial cultures (Lyons *et al.*, 2009b; Cowley *et al.*, 2010; Watson *et al.*, 2010). The study by Lyons and colleagues (2009) found that LPS induced a greater increase in pro-inflammatory cytokine concentration in mixed glial cultures prepared from IL-4^{-/-} mice compared with glia from wildtype animals, suggesting that, like glia from CD200^{-/-} mice, these cells are more susceptible to an inflammatory challenge. This study also demonstrated that IL-4-deficient animals were more vulnerable to systemically-administered LPS, revealed by an up-regulation of cortical and hippocampal IL-1 β concentration and sickness behaviour. The current study did not measure IL-4 concentration, however Lyons also demonstrated that IL-4^{-/-} animals have decreased CD200 expression, therefore it would be interesting to see if there is a concomitant decrease in IL-4 expression in the absence of CD200, which could further account for perturbed immune cell regulation.

The current study focused on examining glia prepared from CD200^{-/-} mice *in vitro*, while other research groups investigating the role of CD200 have examined its function *in vivo*. Data from this study suggests that in the absence of CD200 stimulated immune cells release greater amounts of destructive, pro-inflammatory cytokines. Similarly, Snelgrove (2008) found that TNF- α and IFN γ concentration was enhanced in the airways of CD200^{-/-} mice infected with influenza virus, which was detrimental to surrounding lung tissue. These data indicate that immune cells from CD200^{-/-} mice not only display enhanced expression of membrane proteins associated with inflammation, but also release a greater amount of the potentially-destructive signalling molecules during an inflammatory challenge *in vivo*. The current study highlights the enhanced vulnerability of mixed glia from CD200^{-/-} mice to an inflammatory insult *in vitro*,

and it is inferred that enhanced cytokine production *in vivo* could have a negative impact on neuronal function.

FGL attenuated the LPS-induced increase in cell surface markers of activation and cytokine production in mixed glia prepared from wildtype, but not CD200^{-/-}, mice. It is evident that the absence of the immunosuppressive CD200 ligand results in increases reactivity to LPS. Furthermore, the absence of CD200 precludes the anti-inflammatory action of FGL. In chapter 3, the immune-modulating action of FGL was considered and evidence indicating that the anti-inflammatory properties of this peptide, are in part, due to an up-regulation in CD200 expression. The absence of a response to FGL in LPS-stimulated mixed glial cultures prepared from CD200^{-/-} mice further substantiates the proposal that the action of FGL is CD200-mediated.

Work from this laboratory has revealed the expression of CD200 on neurons *in vitro* and identified that the immunomodulatory capability of neurons on glial cells in culture was CD200-dependent (Lyons *et al.*, 2007). This proclivity is shared by endothelial cells (unpublished observation). The current study demonstrated the presence of CD200 on CD11b-negative cells suggesting that CD200 is found on astrocytes using two techniques, FACS and immunoblotting. Significantly the data show that incubating astrocytes in the presence of FGL enhances expression. These findings suggest that FGL may exerts its anti-inflammatory action *in vivo* by enhancing astrocytic, as well as neuronal CD200 expression, thus revising the hypothesis put forward by Downer (2008).

Astrocytes can modulate microglial activity by enhancing or dampening their activation state through release of pro- or anti-inflammatory cytokines (Eng *et al.*, 2000). To investigate the modulatory action of astrocytes on microglial activity, an astrocytic membrane fraction was prepared on which the membrane bound protein CD200 is located. LPS-induced changes in purified microglia were attenuated by co-incubating cells in the presence of an astrocytic membrane preparation. This action mimicked the effect of neurons on glia and is proposed to be a consequence of CD200 ligand-receptor interaction. An LDH assay measured cell viability and verified that neither treatment compromised cell survival.

It is concluded that astrocytes can modulate microglia activity by means of soluble factors and also by cell:cell contact, in which the role of CD200 is pivotal. However, it is acknowledged that one of the primary limitations of this study is that similar experiments were not performed in the presence of a CD200 antibody. Therefore factors other than CD200 may play a role in the modulatory effect. Indeed, the chemokine fractalkine has been advocated in maintaining microglia in a quiescent state and, while primarily tethered to the neuronal membrane by an extensively glycosylated stem, it has also been co-localised to GFAP-positive cells (Lindia *et al.*, 2005; Cardona *et al.*, 2006; Lyons *et al.*, 2009a). Further research is required to establish the contribution of astrocytic CD200 on modulating microglial activity and how CD200 expression can be manipulated.

Chapter 5. Results

5.1 Introduction

Senescence is associated with cognitive decline that reflects deficits caused by impaired hippocampal function (McEntee *et al.*, 1991). Physiological studies investigating the effect of aging on hippocampus have led to a superior understanding of age-related cognitive deterioration and many have implicated an enhanced inflammatory profile with these functional deficits. Impaired hippocampal function is typified by attenuation in the maintenance of hippocampal LTP and by poor performance in the Morris water maze, a spatial memory task that aged rats take significantly longer to execute (Barnes, 1979; Gage *et al.*, 1989). Consistent with an enhanced inflammatory profile, Murray and colleagues (1998) reported that the age-related impairment in LTP, which was paralleled by increased hippocampal IL-1 β concentration. Moreover, *in vivo* and *in vitro* electrophysiological data have demonstrated that increasing concentrations of IL-1 β can negatively impact on LTP (Cunningham *et al.*, 1996; Murray & Lynch, 1998). Subsequent studies have suggested that the age-related increase in inflammatory activity may be a consequence of enhanced reactive oxygen species (ROS) production, particularly in the hippocampus, which is an early target for age-associated structural and physiological changes (O'Donnell *et al.*, 2000). Neuronal tissue is especially susceptible to oxidative stress due to its high oxygen consumption and modest antioxidant defences, which are even further diminished with age (Halliwell, 1992; O'Donnell *et al.*, 2000). Although stereological cell-counting have revealed no age-related loss in hippocampal neurons, numerous researchers have reported a decrease in axospinous synapses in the dentate gyrus and a change in hippocampal network connections with age (Geinisman *et al.*, 1992; Rapp & Gallagher, 1996).

Previous studies have shown that both antioxidants and anti-inflammatory agents can positively impact on the ability of aged animals to sustain LTP (O'Donnell *et al.*, 2000; Downer *et al.*, 2008). Downer and colleagues report that the NCAM-mimetic peptide FGL restores age-related impairment in LTP, due to its anti-inflammatory action. This study also demonstrated the proclivity of the peptide to reverse the age-induced up-regulation in

hippocampal IL-1 β concentration and markers of microglial activation, and emphasised the integral role of CD200 expression in FGL-induced modulation. A subsequent study by this team reported that FGL impacts on neuronal CD200 expression by up-regulating insulin like growth factor (IGF)-1 (Downer *et al.*, 2009). IGF-1 is a polypeptide hormone that induces proliferation and neurogenesis in the hippocampus. A decline in this hormone in the aged brain has been associated with impaired plasticity (Anderson *et al.*, 2002). IGF-1 is one of the most potent stimulators of the AKT/PI-3 kinase pathway, which is fundamental in cell survival, growth and proliferation. Administration of FGL reversed the age-related decline in hippocampal IGF-1 concentration and the associated decrease in AKT phosphorylation (Downer *et al.*, 2009). *In vitro* analysis revealed the role of AKT/PI-3 kinase activation and ERK pathways in FGL-induced CD200 expression on primary neurons. These findings are consistent with work carried out on melanoma cells, which observed that RAF, a molecule upstream of PI-3 kinase and ERK, to be central in mediating CD200 expression (Petermann *et al.*, 2007).

Work presented in this thesis has demonstrated that FGL can exert an anti-inflammatory action on glial cells *in vitro*, while others have shown its ability to reverse an age-associated pro-inflammatory phenotype in hippocampus and abrogate deficits in LTP (Downer *et al.*, 2008). An up-regulation in the immune-modulating protein CD200 has been implicated in the beneficial action of FGL *in vitro* and *in vivo*. Therefore, the first objective of this set of experiments was to establish whether a CD200 fusion protein (CD200Fc) can directly exert an anti-inflammatory action similar to that established by FGL-treated cells/animals. First, to investigate if CD200Fc had a modulatory effect on primary mixed glia, cells were incubated with the fusion protein prior to LPS exposure. Next as an enhanced inflammatory profile is associated with impairment in hippocampal synaptic plasticity, the second objective of this study was to assess the effect of LPS or ageing on LTP in the perforant path-granule cell synapses. It has been proposed that FGL reversed the age-related deficit in LTP by up-regulating CD200 expression, so to further investigate a role for CD200 in modulating LTP CD200Fc was given prior to LTP induction. The final objective was to examine and compare the inflammatory profile of hippocampal tissue from young and aged rats, to assess the modulatory effect of CD200Fc *in vivo*.

5.2 Methods

To investigate the action of CD200Fc *in vitro* mixed glia were prepared from neonatal rat or mice cortices and cultured for 14 days before treatment (see section 2.1 for details). In the case of CD200Fc incubation, cells were incubated in the fusion protein (2.5µg/ml) for 2 hours prior LPS exposure (1µg/ml; 24 hours; see section 2.1). Supernatant cytokine concentration was determined by ELISA and mRNA expression assessed by Q-PCR (see section 2.3 and 2.4). To investigate the action of CD200Fc on LPS-induced nitrate production supernatant concentration of nitrate was also assessed by Griess assay (see section 2.7).

The proclivity of CD200Fc to attenuate age- or LPS-induced pro-inflammatory profile in hippocampus was investigated. For *in vivo* experiments animals were housed in groups of four, maintained under veterinary supervision in an ambient temperature of 22°-23°C, under a 12-hour light-dark cycle. Food and water were available *ad libitum* and all animal experimentation was performed under a license granted by the Minister for Health and Children Ireland (see section 2.2).

Briefly, male Wistar rats were anaesthetised by intraperitoneal (ip) injection of urethane. Depth of anaesthesia was determined by absence of a pedal reflex. In the case of the study using an LPS challenge, young animals (3-4 month) were divided into 4 groups: control rats that received saline intrahippocampally (ih) and either saline or LPS ip, or rats which received CD200Fc ih and, again, either saline or LPS ip. In the case of the study that assessed the effect of age, animals (3-4 months and 22-24 months) were divided into control and CD200Fc-treated groups; saline or CD200Fc was injected ih (for details see section 2.2). Three hours after treatment, the ability of rats to sustain LTP in perforant path-granule cell synapses in response to tetanic stimulation of the perforant path was assessed (see section 2.2.3). Animals were sacrificed by decapitation and a sagittal slice from left hemisphere of each brain was placed onto a cork disk coated in OCT[®] compound for immunohistochemical analysis. With the remaining brain tissue, the cortices and hippocampi were dissected free; tissue for RNA analysis was placed in RNase-free tubes, while tissue for ELISA and Western immunoblotting was washed and stored in Krebs buffer containing CaCl₂ and DMSO (see section 2.2.4 for details). Tissue was flash frozen in liquid nitrogen and stored at -80°C.

Expression of GFAP, MHC II and iNOS were assessed at mRNA level using Q-PCR, in hippocampal tissue from young and aged animals (see section 2.4). Hippocampal tissue for Western immunoblotting and IGF-1 analysis was homogenised with a Polytron homogeniser and equalised using a Bradford Microassay (see section 2.2.5). Synaptophysin, CD200, pAKT and β -actin were assessed in hippocampus using Western immunoblotting and hippocampal IGF-1 concentration was determined by ELISA (see sections 2.3 and 2.5). Sagittal sections (10 μ m) from young and aged animals were cut from the left hemisphere of each brain using a cryostat. Immunohistochemical analysis of microglial activation (MHC II) and oxidative stress (8-OHdG) was assessed in the sections (see section 2.7).

Data are expressed as means \pm SEM. ANOVA or Student's *t*-test were performed to determine whether significant differences existed between treatment groups and Newman-Keuls post-hoc tests were applied as appropriate.

5.3 Results

5.3.1 *CD200Fc attenuated an LPS-induced increase in pro-inflammatory cytokines and Nitrate production in mixed glial cells.*

Previously in this thesis, the anti-inflammatory action of the NCAM-mimetic peptide FGL was demonstrated to attenuate markers of glial cell activation in LPS-stimulated mixed glia. It was suggested that FGL partly exerted this effect by up-regulating expression of the immune-modulating protein CD200, on primary astrocytes within the mixed glia culture. Furthermore, it was shown that mixed glia prepared from CD200^{-/-} mice displayed an enhanced inflammatory profile *in vitro* and FGL failed to exert an anti-inflammatory effect on these cells.

In the current set of experiment the action of an exogenous source of CD200 (CD200Fc) was investigated on LPS-stimulated mixed glia. Similar to FGL, pre-treatment with CD200Fc (2µg/ml; 2 hours) decreased the LPS-induced up-regulation in the pro-inflammatory cytokines IL-1β, IL-6 and TNF-α at an mRNA and protein level ([†]p<0.05, ⁺⁺p<0.01, ⁺⁺⁺p<0.001; ANOVA, Figure 5.1 A-E). In addition to attenuating cytokine production, CD200Fc decreased the LPS-stimulated increase in Nitrite concentration in primary mixed glia, measured by Griess assay (*p<0.05, [†]p<0.05; ANOVA; F_(4,14)=4.046, Figure 5.2). Nitrite is a stable, non-volatile breakdown product of the signalling molecule nitric oxide (NO), which is implicated in the perpetuation of an immune response (Brown 2007). The results indicate that LPS induced an increase in NO concentration in the supernatant of mixed glia (**p<0.01; ANOVA; F_(4,14)=4.046, Figure 5.2), while pre-incubation with CD200Fc at various doses attenuated the LPS-induced increase of NO ([†]p<0.05; ANOVA).

5.3.2 *CD200Fc rescues LPS- and aged-induced impairment in LTP*

LTP is a form of synaptic plasticity, whereby there is a long-lasting enhancement in signal transmission after brief high-frequency stimulation. LTP assesses the functional integrity of the hippocampus and a deficit in LTP suggests impaired synaptic function. LTP was induced

in perforant path-granule cell synapses in hippocampus of young rats, administration of LPS significantly impaired LTP as measured by the mean changes in EPSP slope in the last 10 minutes of recording ($^{***}p < 0.001$; ANOVA; $F_{(1,40)} = 113.2$, Figure 5.3 B). The mean changes in EPSP slope in the last 10 minutes of recording also revealed a significant deficit in LTP in hippocampus of aged compared with young rats ($^{***}p < 0.001$; ANOVA; $F_{(1,40)} = 850.9$, Figure 5.4 B). Intrahippocampal injection of CD200Fc rescued the LPS-induced impairment and reduced the age-induced depression of LTP (LPS alone versus LPS with CD200Fc; $^{+++}p < 0.001$; ANOVA; $F_{(1,40)} = 417.1$, Figure 5.3, Aged versus Aged with CD200Fc, $^{+++}p < 0.001$; ANOVA, $F_{(1,40)} = 452.8$, Figure 5.4).

5.3.3 Aged-related changes in hippocampus

Aging can be characterised by the progressive deterioration in biological function, however, the underlying causes for this almost inevitable decline have yet to be established. Synaptophysin is the most abundant synaptic vesicle protein and its expression is indicative of synaptic density (Valtorta *et al.*, 2004). The data indicated that synaptophysin expression was decreased in tissue prepared from hippocampus of aged, compared with young, rats ($^*p < 0.05$; Student's *t*-test, Figure 5.5). Western immunoblotting and densitometric data also show a significant decrease in CD200 expression in hippocampal tissue prepared from aged, compared with young, rats ($^*p < 0.05$; Student's *t*-test, Figure 5.6).

5.3.4 CD200Fc attenuated age-induced markers of glial activity in hippocampus

It is well documented that enhanced reactivity of microglia and astrocytes is one of the manifestations of the aging brain (Cotrina & Nedergaard, 2002; Lynch, 2008). The 'Molecular Inflammatory Process of Aging' proposed by Chung and colleagues (2006), suggests that dysregulation of reduction/oxidation activity during aging leads to enhanced oxidative stress, which is a major risk factor for an increased inflammatory profile.

There was an age-related increase in MHC II mRNA expression, a marker of microglial activation, in hippocampal tissue prepared from aged, compared with young, rats ($^*p < 0.05$;

ANOVA; $F_{(3,19)}=4.148$, Figure 5.7). The age-related increase was significantly attenuated in hippocampus of aged animals that received CD200Fc, compared with age-matched controls ($^+p<0.05$; ANOVA, Figure 5.7). Cryostat sections prepared from brain tissue of young and aged animals illustrated an age-related increase in MHC II immunoreactivity in hippocampus (Figure 5.8). Positive expression appears as brown DAB staining and the sections were counter-stained with DAPI, which appears blue. The representative micrographs of the dentate gyrus and fornix region of hippocampus show an age-related increase, which appears to be attenuated in aged animals that received CD200Fc. MHC II permits antigen presentation between microglia and T cells, however, expression and engagement of co-stimulatory molecules are required for T cell activation. CD40 is a co-stimulatory molecule found on microglia and it interacts with its cognate ligand on T cells. CD40L mRNA expression was also increased in hippocampal tissue prepared from aged, compared with, young, rats, (data not shown) while administration of CD200Fc significantly attenuated the age-related increase in hippocampal CD40L mRNA expression, compared with age-matched controls (data not shown).

Under certain circumstances astrocytes act as immune effector cells of the CNS, releasing cytokines and performing antigen presenting functions (Lieberman *et al.*, 1989; Collawn & Benveniste, 1999). Astrocytosis is associated with an up-regulation in the intermediate filament protein, GFAP. The data show an age-related increase in GFAP mRNA in hippocampus of aged, compared with young, rats ($^*p<0.05$; ANOVA; $F_{(3,18)}=4.277$, Figure 5.9). This increase was attenuated in hippocampus of aged animals that received CD200Fc ($^+p<0.05$; ANOVA).

Most brain pathologies are accompanied by neuroinflammation and an accompanying up-regulation in NO and superoxide, along with their derivatives reactive nitrogen and oxygen species (RNS, ROS). Astrocytes and microglia are the primary source of NO, due to increased iNOS expression. Like ROS, NO and its derivatives are toxic and can lead to disruption of neuronal function (Brown, 2007). There was an age-related increase in iNOS mRNA expression in tissue prepared from hippocampus of aged, compared with young, rats ($^*p<0.05$; ANOVA; $F_{(1,36)}=5.007$, Figure 5.10). Administration of CD200Fc failed to significantly modulate this increase in hippocampus of aged rats, compared with aged-matched control

animals (Figure 5.10; $p=0.07$). Oxidative damage was assessed by 8-OHdG staining and representative micrographs of immunoreactivity in cryostat sections from young and aged rats, which received CD200Fc or saline, are shown in Figure 5.11. Although the quality of the micrographs shown is inferior, they do indicate an increase in 8-OHdG immunoreactivity in the dentate gyrus region of hippocampus in tissue from aged, compared with young, rats. Representative micrographs also show an apparent decrease in 8-OHdG immunoreactivity in aged animals that received CD200Fc, compared with age control-treated animals. This staining protocol has since been optimised and micrographs suitable for publication display the same pattern demonstrated here.

5.3.5 CD200Fc increases AKT phosphorylation

IGF-1 is a polypeptide hormone that is important during development and has restricted distribution in the adult brain. It plays a role in inducing proliferation and neurogenesis in the hippocampus throughout life and decreasing levels of IGF-1 have been associated with impaired synaptic plasticity (Anderson *et al.*, 2002). IGF-1 stimulates the AKT/PI-3 kinase signalling cascade, which is fundamental in cell survival, growth and proliferation (Willaime-Morawek *et al.*, 2005; Zheng & Quirion, 2006). There was an overall CD200Fc-related increase in IGF-1 concentration in hippocampus of rats ($*p<0.05$; ANOVA; $F_{(1,16)}=7.496$, Figure 5.12). While Western immunoblotting revealed a decrease in pAKT in hippocampus of aged, compared with young, rats that was significantly reversed in aged animals that received CD200 ($*p<0.05$; $^+p<0.05$; ANOVA; $F_{(1,14)}=15.04$, Figure 5.13).

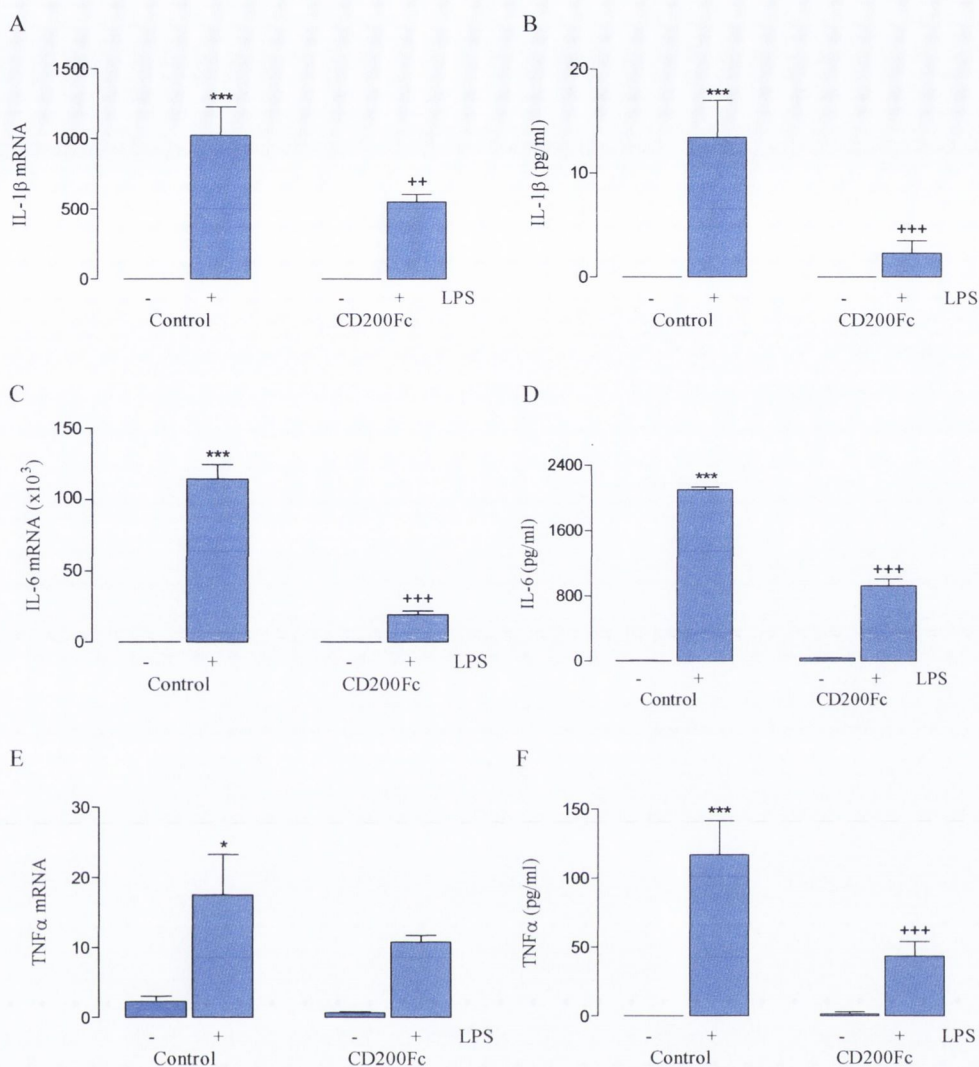


Figure 5.1. CD200Fc attenuated the LPS-induced increase in mRNA expression and release of pro-inflammatory cytokines in mouse primary glial cells.

LPS (1 μ g/ml; 24 hours) induced a significant increase in IL-1 β , IL-6 and TNF- α mRNA expression (A,C and E) and release (B, D and F) in mixed glia cultured from wildtype mice, (* p <0.05, *** p <0.001; ANOVA). Pre-treatment with CD200Fc (2.5 μ g/ml) attenuated the increase in pro-inflammatory cytokine expression in primary mixed glia (+ p <0.05, ++ p <0.01, +++ p <0.001; ANOVA). Values for Q-PCR are presented as means (\pm SEM; n =6) expressed as a ratio to β -actin mRNA and standardised to a control sample. Values for cytokine release are presented as means (\pm SEM; n =6) and expressed as pg of cytokine/ml.

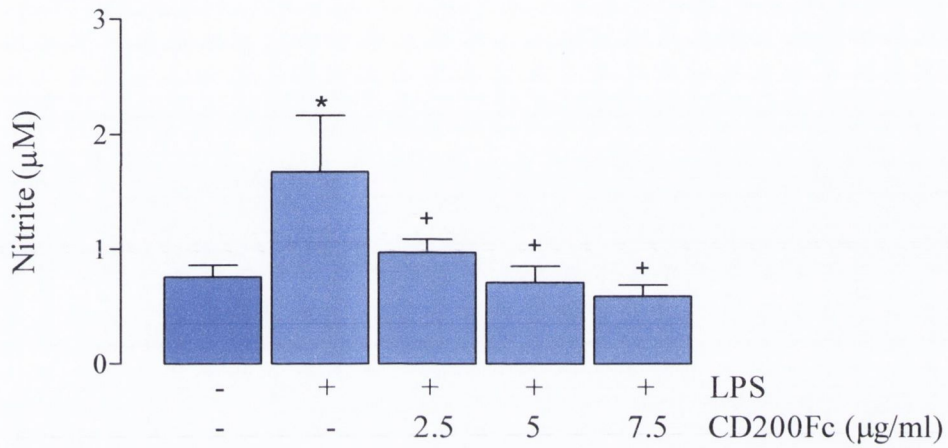


Figure 5.2. CD200Fc attenuated the LPS-induced increase in nitrite concentration in primary rat mixed glia.

LPS induced a significant increase in nitrite concentration in mixed glial cells prepared from neonatal rats (* $p < 0.05$; ANOVA; $F_{(4,14)}=4.046$). Pre-treatment with CD200Fc dose dependently attenuated this increase (+ $p < 0.05$; ANOVA). Values are presented as means (\pm SEM; $n=4$) and expressed as μ M Nitrate.

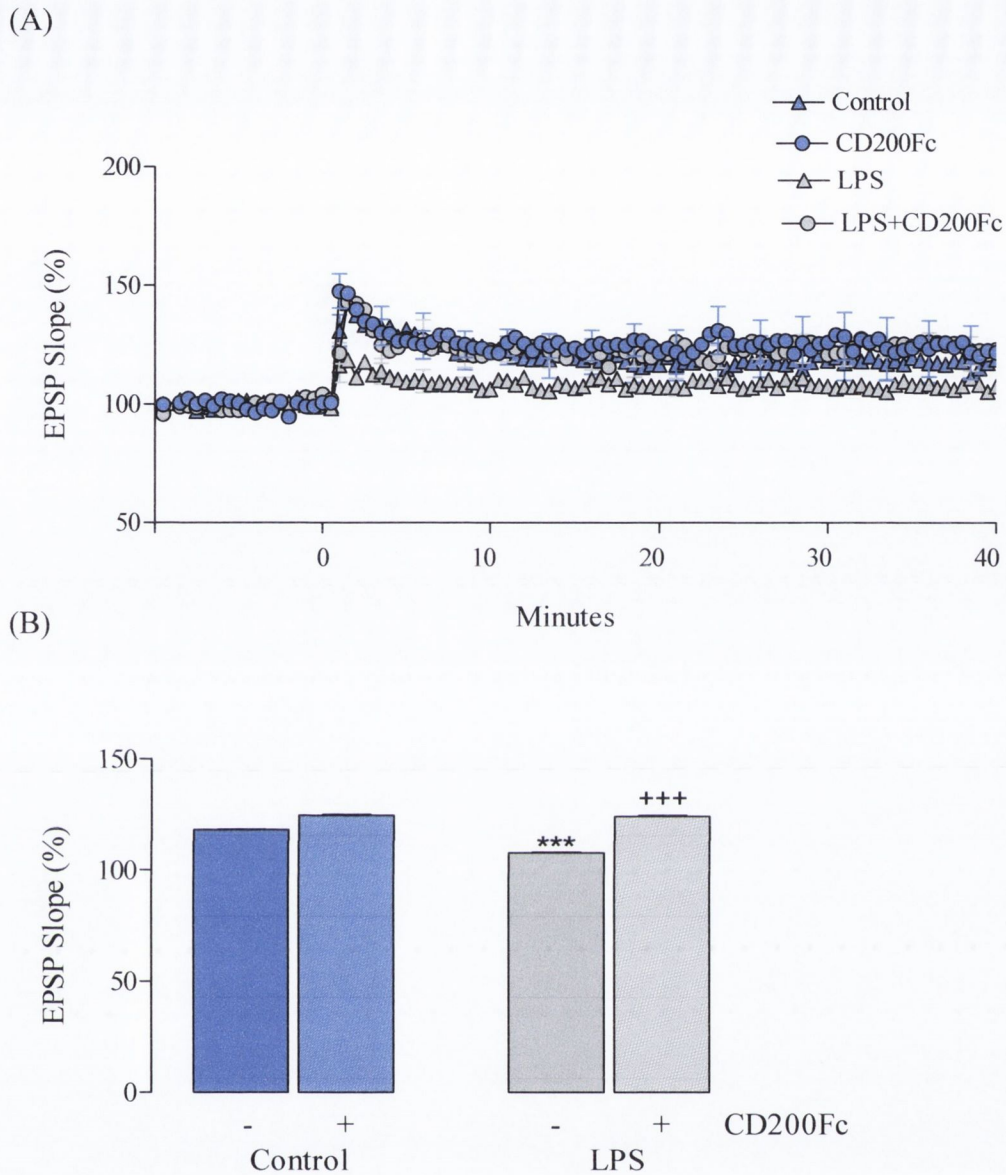


Figure 5.3. CD200Fc rescues LPS-induced impairment of LTP.

- (A) A high frequency train of stimuli to the perforant path induced an immediate and sustained increase in EPSP slope in control-treated rats, which was attenuated by ip injection of LPS ($100\mu\text{g}/\text{kg}$; $p < 0.001$; ANOVA). Intrahippocampal injection of CD200Fc ($10\mu\text{g}/5\ \mu\text{l}$ injection) reduced the LPS-induced depression of LTP ($p < 0.001$; ANOVA; $n = 6$).
- (B) The mean changes in EPSP slope in the last 10 minutes of the experiment revealed a significant LPS-induced decrease in the mean percentage change in the EPSP slope ($***p < 0.001$; ANOVA; $F_{(1,40)} = 113.2$), which was significantly attenuated in rats that received CD200Fc ($+++p < 0.001$; ANOVA; $F_{(1,40)} = 417.1$).

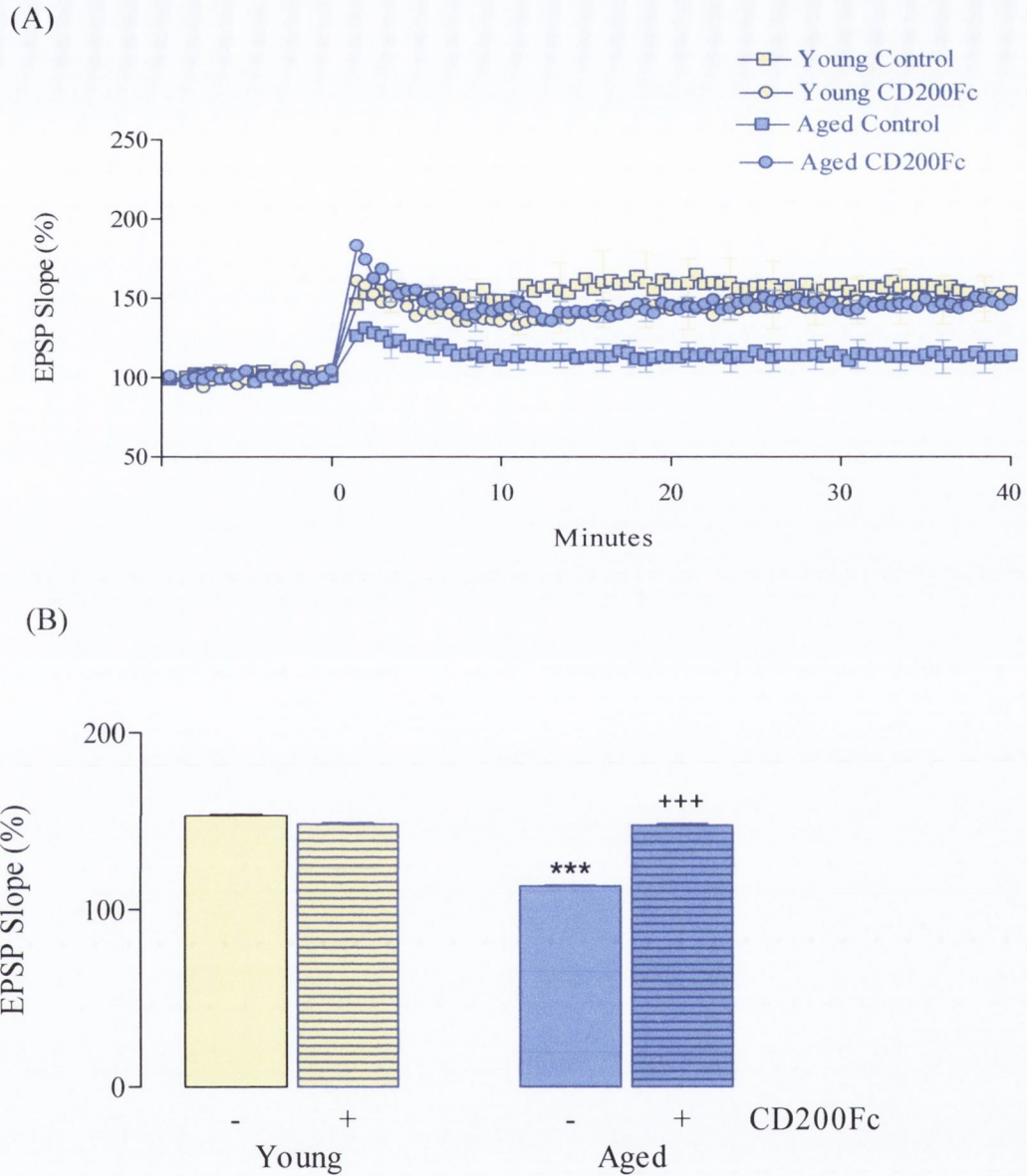


Figure 5.4. CD200Fc rescues the age-induced impairment of LTP.

- (A) A high frequency train of stimuli to the perforant path induced an immediate and sustained increase in EPSP slope in young control-treated rats that was attenuated in aged animals ($p < 0.001$; ANOVA;). Intrahippocampal injection of CD200Fc reduced the age-induced depression of LTP ($p < 0.001$; ANOVA; $n = 6$).
- (B) The mean percentage changes in EPSP slope in the last 10 minutes of the experiment revealed a significant age-induced decrease ($***p < 0.001$; ANOVA; $F_{(1,40)} = 850.9$), this was attenuated in rats which received CD200Fc ($+++p < 0.001$; ANOVA; $F_{(1,40)} = 452.8$).

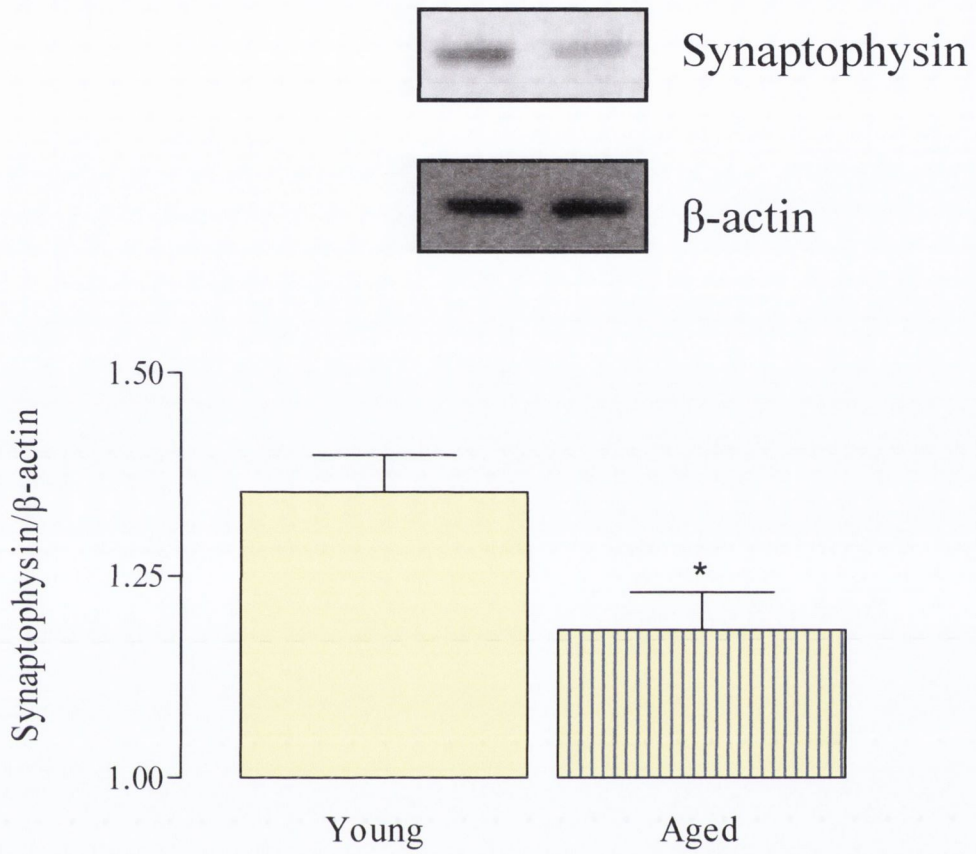


Figure 5.5. Synaptophysin expression decreases in hippocampus with age.

There was a significant decrease in synaptophysin expression in hippocampal tissue prepared from young, compared with aged, rats (* $p < 0.05$; Student's *t*-test, densitometric units equalised to β -actin, $n=6$).

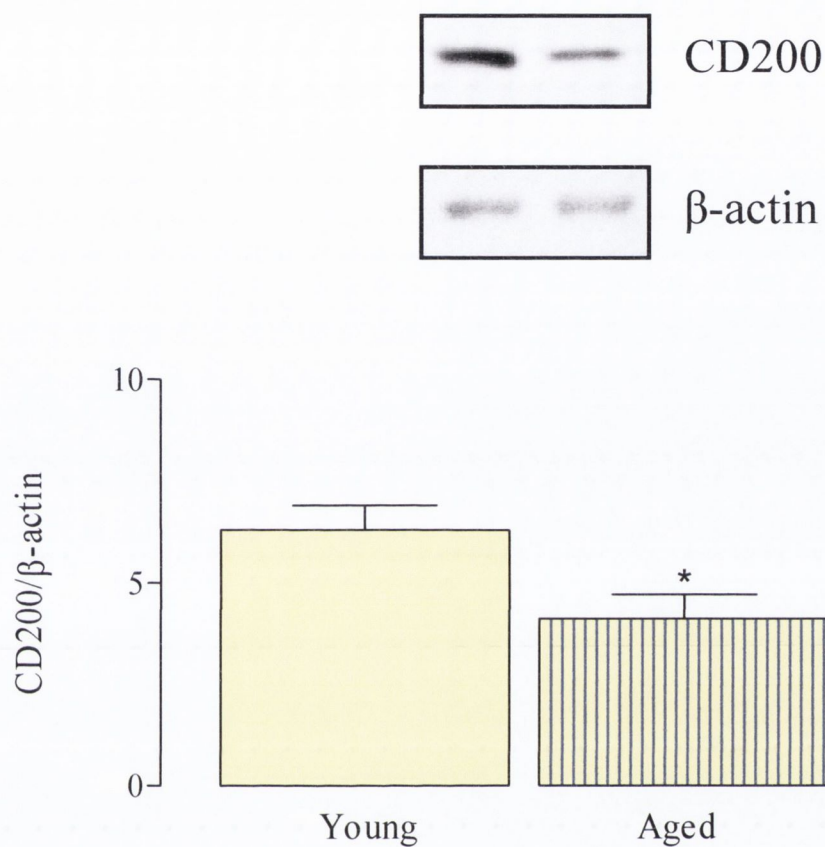


Figure 5.6 CD200 expression decreases in hippocampus with age.

There was a significant decrease in CD200 expression in hippocampal tissue prepared from young, compared with aged, rats (* $p < 0.05$; Student's *t*-test; densitometric units equalised to β -actin, $n=6$).

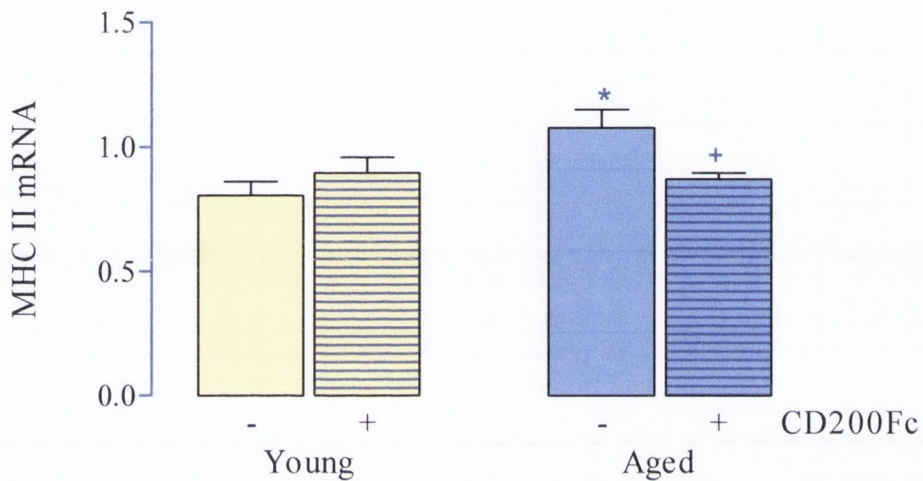


Figure 5.7. CD200Fc attenuated the age-induced increase in MHC II mRNA expression in hippocampus.

There was an age-related increase in MHC II mRNA expression in hippocampus of aged, compared with young, rats. (* $p < 0.05$; ANOVA; $F_{(3,19)} = 4.148$). Administration of CD200Fc significantly attenuated this increase († $p < 0.05$; ANOVA). Values are presented as means (\pm SEM; $n = 6$) expressed as a ratio to β -actin mRNA and standardised to a control sample.

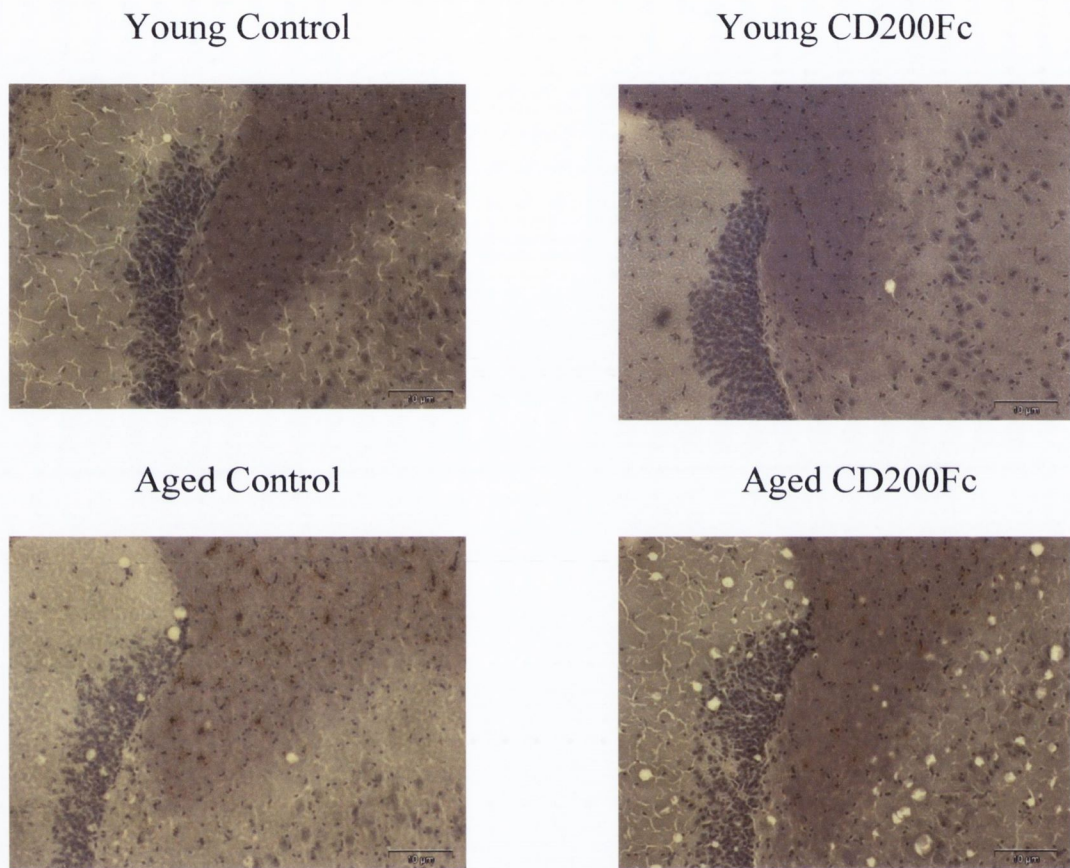


Figure 5.8. CD200Fc attenuated the age-related increase in hippocampal MHC II expression.

MHC II expression was assessed in cryostat sections from young and aged animals using immunohistochemistry. Increased MHC II-positive staining was observed in the dentate gyrus and fornix of aged, compared with young, rats and this appeared to be attenuated in aged animals that received CD200Fc.

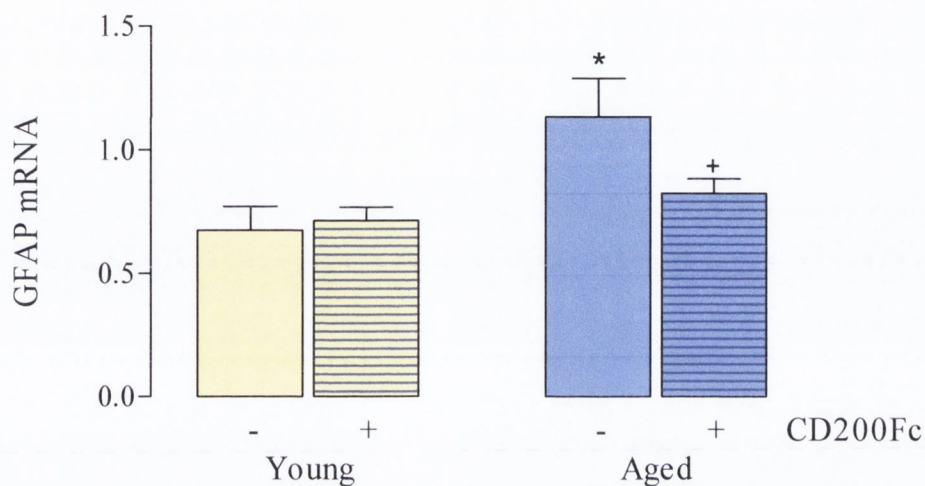


Figure 5.9. CD200Fc attenuated the age-induced increase in GFAP mRNA in hippocampus.

There was an age-related increase in GFAP mRNA expression in hippocampus of aged, compared with young, rats. (* $p < 0.05$; ANOVA; $F_{(3,18)} = 4.277$). Administration of CD200Fc significantly attenuated this increase (+ $p < 0.05$; ANOVA). Values are presented as means (\pm SEM; $n = 6$) expressed as a ratio to β -actin mRNA and standardised to a control sample.

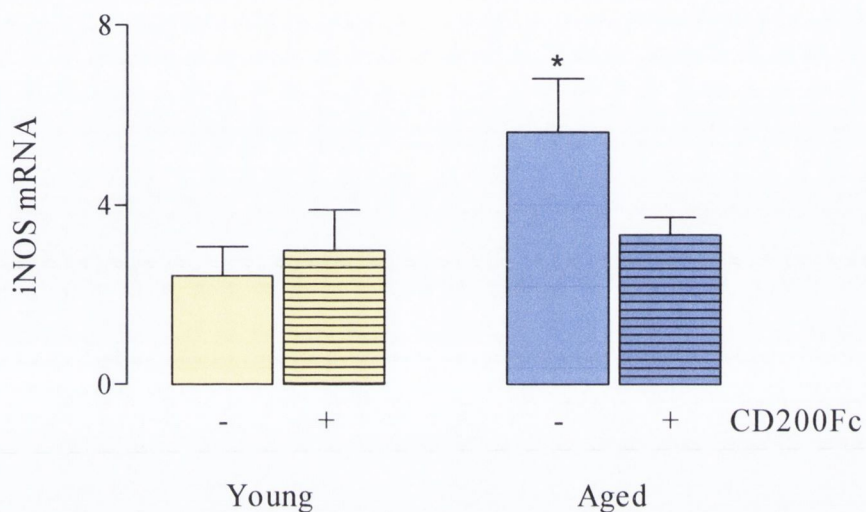


Figure 5.10. iNOS mRNA expression was increase in hippocampus with age.

There was an age-related increase in iNOS mRNA expression in hippocampus of aged, compared with young, rats. (* $p < 0.05$; ANOVA; $F_{(1,36)} = 5.007$). Administration of CD200Fc failed to significantly alter this increase (aged control versus aged CD200; $p = 0.07$). Values are presented as means (\pm SEM; $n = 6$) and expressed as a ratio to β -actin mRNA and standardised to a control sample.

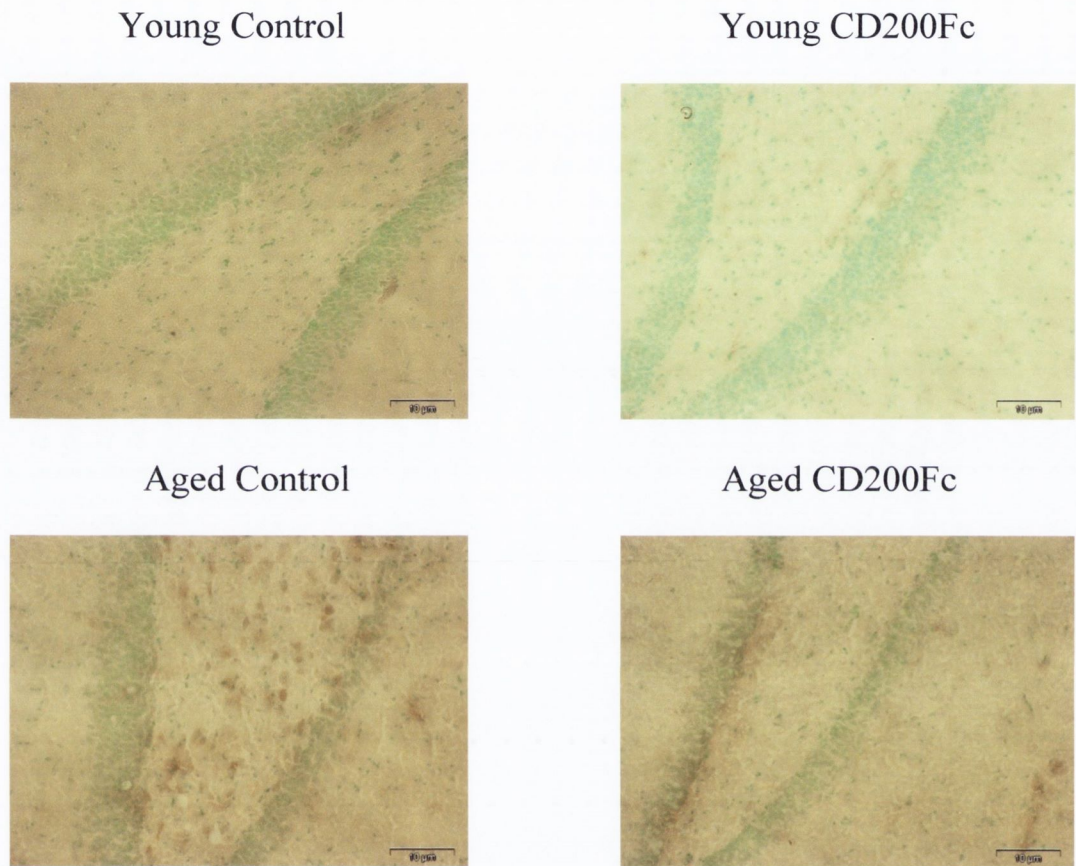


Figure 5.11. CD200Fc attenuated the age-related increase in hippocampal 8-OHdG expression.

8-OHdG expression was assessed in cryostat sections from young and aged animals using immunohistochemistry. Increased 8-OHdG-positive staining was observed in the dentate gyrus of aged, compared with young, rats and this appeared to be attenuated in aged animals that received CD200Fc.

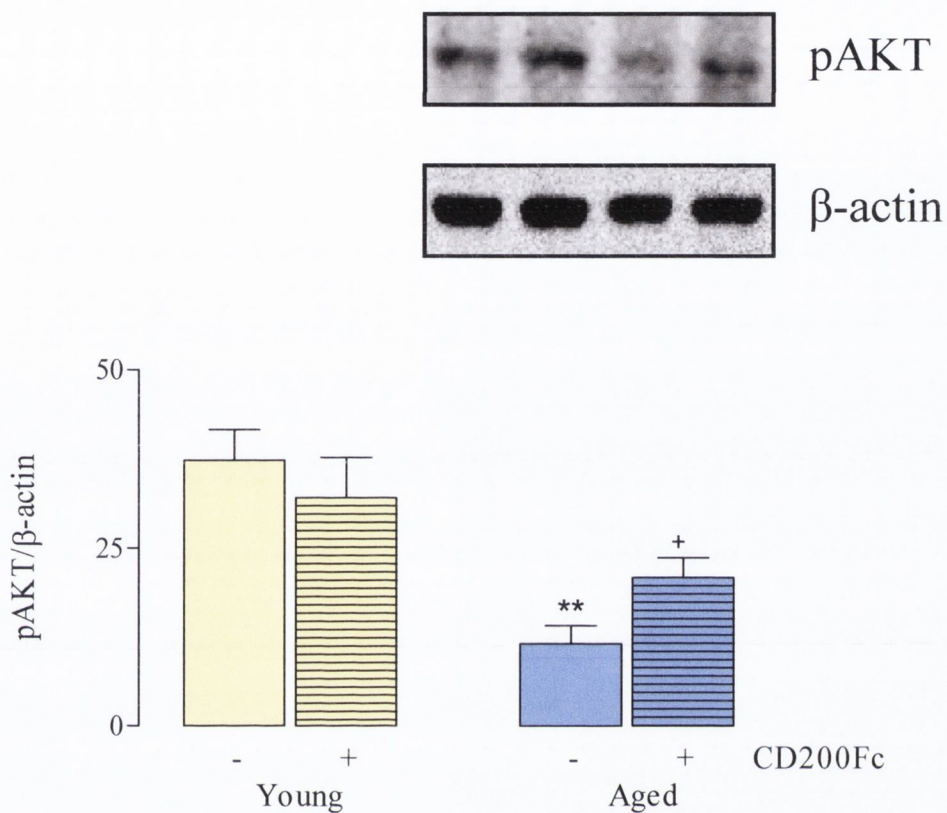


Figure 5.13. CD200Fc attenuated the age-related decrease in pAKT in hippocampus.

There was an age-related decrease in pAKT concentration in hippocampus of aged, compared with young, rats. (* $p < 0.001$; ANOVA; $F_{(1,14)} = 15.04$). Administration of CD200Fc significantly attenuated this increase (+ $p < 0.05$; ANOVA). Values are presented as means (\pm SEM; $n=6$) and expressed as a ratio to β -actin.

5.4 Discussion

The primary objective of the above experiments was to investigate the potential anti-inflammatory action of CD200Fc. *In vitro*, CD200Fc attenuated the LPS-induced increase in pro-inflammatory cytokines and NO production in primary mixed glia, while *in vivo*, the fusion protein reversed markers of microgliosis, astrogliosis and oxidative stress in hippocampus of aged animals.

An inflammatory phenotype within the CNS is associated with synaptic dysfunction and has been correlated with cognitive decline (Lynch 2008). Data from this laboratory have indicated that shifting the phenotype of microglia from a reactive to a quiescent state can have a beneficial outcome on the functional integrity of the hippocampus, determined by LTP (Lynch *et al.*, 2004). In the current study administration of CD200Fc directly into the hippocampus abrogated the LPS- and age-induced impairment in LTP recorded from perforant path-granule cell synapses. At a cellular level, CD200Fc attenuated the enhanced inflammatory profile observed in hippocampus of aged animals, down-regulating the age-related increase in MHC II and GFAP, in addition to reducing markers of oxidative stress. Finally, it was observed that CD200Fc enhanced IGF-1 concentration in hippocampus and reversed the age-related decrease in AKT phosphorylation.

Induction and maintenance of LTP is used as a correlate for synaptic plasticity within the hippocampus. Here peripheral administration of LPS induced impairment in LTP in the perforant path-granule cell synapses. LPS is a potent, prototypical endotoxin derived from the cell wall of Gram-negative bacteria and can rapidly stimulate an immune response. It is well documented that peripheral administration of LPS impairs neuronal function; its induction of sickness behaviour and ability to inhibit learning and memory are indicators of this (Dantzer *et al.*, 1998). The findings of the current study show that a peripheral LPS challenge impairs LTP in hippocampus, which has been reported previously (Vereker *et al.*, 2000). LPS activates TLR4, which induces a series of signalling events leading to an inflammatory response (O'Neill, 2002). Much of the literature does not reveal a direct role for LPS in impairing LTP, but suggests that an LPS-induced up-regulation in central IL-1 β is responsible for synaptic dysfunction (Kelly *et al.*, 2001). The presence of IL-1 β in the CNS after peripheral

administration of LPS has been found in many brain regions within 6 hours (Quan *et al.*, 1994). Quan (1994) demonstrated that the source of IL-1 β in the brain was not from the circulation but was secreted from brain cells after the peripheral inflammatory stimulus, which in turn can perpetuate an immune response within the CNS. It is widely accepted that IL-1 β , formally recognised simply as an endogenous pyrogen, can have a negative impact on brain function. In the current study it is proposed that the LPS-related impairment in the maintenance of LTP is due to an enhanced hippocampal pro-inflammatory profile, corroborating previous findings from this laboratory (Kelly *et al.*, 2001).

An age-related deficit in the maintenance of LTP was also observed. A common thread between LPS- and age-related cognitive dysfunction is an enhanced inflammatory profile in hippocampus, which is also believed to be a major component in the pathogenesis of neurodegenerative disease (Block & Hong, 2005). Similar to the LPS-induced deficit in LTP, IL-1 β is reported to play a key role in age-associated impairment. Consistent with the current study, others have shown an age-related deficit in synaptic plasticity described by an increase in LTP decay rate at the perforant path-granule cell synapse (Barnes, 1979; O'Donnell *et al.*, 2000). O'Donnell (2000) and colleagues reported that the age-related impairment in LTP was coupled with an increase in IL-1 β concentration in the dentate gyrus. The causative relationship between an enhanced inflammatory profile and a deficit in LTP has been substantiated by many research groups (Bach *et al.*, 1999; Kelly *et al.*, 2001). Direct administration of inflammatory mediators into hippocampus can inhibit LTP, while animals subjected to a stress protocol that induces an up-regulation in inflammatory markers in hippocampus are also unable to sustain LTP (Lynch, 1998; Murray & Lynch, 1998). In addition to pro-inflammatory cytokines, an age-related increase in ROS has been implicated as exerting a negative impact on neuronal function (O'Donnell *et al.*, 2000). In the current study CD200Fc attenuated the age-related increase in surface markers of microglial activation and oxidative stress in hippocampus. It is proposed that the age-induced impairment in LTP is associated with the increased inflammatory profile and an enhanced oxidative state.

Both the LPS- and age-related deficit in LTP was reversed by CD200Fc. CD200Fc is a chimeric protein consisting of the external region of the immuno-suppressive molecule CD200 linked to a murine IgG2a region. Previous studies have demonstrated the beneficial immune-

regulating action of this fusion protein during an inflammatory insult or tissue transplantation, however, its ability to modulate synaptic function has not been examined (Gorczynski *et al.*, 1999; Gorczynski *et al.*, 2001; Liu *et al.*, 2010). In a study by Gorczynski (2001) administration of bovine collagen emulsified in Freund's adjuvant induced arthritic symptomologies, but animals that received CD200Fc post-immunisation did not develop the autoimmune disease and presented with lower serum levels of TNF- α and IFN γ . Another research group demonstrated the proclivity of CD200Fc to reduce the severity of established collagen-induced arthritis at a clinical and histological level, while also decreasing expression of pro-inflammatory cytokines in the synovium (Simelyte *et al.*, 2008). These studies reveal the ability of CD200Fc to restrain immune activity and limit inflammation, thus preventing or decreasing collateral tissue damage. The present data indicate that CD200Fc is capable of attenuating the negative impact of ageing or LPS on synaptic function. A heightened inflammatory profile is correlated with a decrease in synaptic plasticity and a plethora of researchers have revealed CD200Fc to have immuno-suppressive properties, therefore it is suggested that CD200Fc maintains synaptic integrity through acting as an anti-inflammatory agent (Loane *et al.*, 2007; Lynch *et al.*, 2007).

Data from this laboratory have established that various agents with anti-inflammatory properties have a beneficial action on synaptic function. The anti-diabetic drug rosiglitazone and the NCAM-mimetic peptide FGL have been shown to exert an anti-inflammatory action *in vivo* by decreasing expression of markers of microglial activation, as well as reversing the age-related deficits in LTP (Loane *et al.*, 2007; Downer *et al.*, 2008). Both drugs also reversed the age-related decrease in the anti-inflammatory cytokine IL-4. The mechanism by which CD200Fc exerts its effect on LTP has yet to be elucidated; however, others have shown increased IL-4 production from splenocytes in animals that received CD200Fc intravenously. Therefore, it is possible that CD200Fc may up-regulate IL-4 production from glia cells, when administered centrally, thus modulating the inflammatory profile in the brain and restoring synaptic function.

Analysis of hippocampal tissue revealed an age-related decrease in the synaptic vesicle protein synaptophysin. Synaptophysin is an abundant synaptic protein and its ubiquitous expression contributes to its use as a marker of synaptic density (Eastwood *et al.*, 1995). The finding that

it was decreased in hippocampus with age is consistent with reports from other researchers, who found lower vesicle density and reduced synaptophysin content in hippocampus of aged rats (Davies *et al.*, 2003). The functional relevance of this protein in synaptic plasticity was highlighted by a study demonstrating that the ability of aged animals to synthesise synaptophysin following LTP was reduced. Interestingly, it has been shown in a human study that decreased synaptophysin expression correlated with cognitive decline in AD patients (Sze *et al.*, 1997; Ando *et al.*, 2002). Here the age-associated decrease in hippocampal synaptophysin expression may reflect a decline in neuronal connectivity, making synaptic transmission more vulnerable to inflammatory damage and contributing to the deficit in LTP.

Expression of CD200 was also found to be decreased in hippocampus of aged animals. CD200 is a membrane bound glycoprotein that can induce immuno-suppression following engagement with its cognate receptor, expressed on myeloid cells. It is believed that CD200, which is found on neurons, endothelial cells and astrocytes (see Figure 4.6 and 4.7) plays a critical role in maintaining microglia in a quiescent state (Hoek *et al.*, 2000). The down-regulation in hippocampal CD200 expression was paralleled by an increase in markers of inflammation and could be a factor in age-associated inflammatory changes that have been established by others (Griffin *et al.*, 2006; Gorczynski & Terzioglu, 2008). Here it is proposed that the decrease in CD200 perturbs homeostasis in the aged brain and removal of this immune-suppressive influence contributes to the shift in activation state of microglia.

Both MHC II mRNA and immunoreactivity were increased in hippocampus prepared from aged, compared with young, rats. MHC II is a marker of microglial activation and is required for the presentation of processed antigens to T cells (Carson & Sutcliffe, 1999). In contrast with other antigen presenting cells, microglia constitutively express MHC II at very low levels so an up-regulation in this molecule in the CNS is indicative of inflammatory activity (Wekerle *et al.*, 1986). MHC II can activate T cells when co-stimulatory molecules are expressed, resulting in an enhanced inflammatory response (Collawn & Benveniste, 1999). Simultaneous expression increases the avidity and duration of the APC-T cell coupling. Here the increase in MHC II was accompanied by a concurrent increase in CD40L mRNA expression in hippocampus of aged animals (data not shown). Together, these findings suggest enhanced immune activity in hippocampus with age, which is in agreement with data

previously reported by this and other laboratories (Lynch *et al.*, 2007; Richwine *et al.*, 2008; Cowley *et al.*, 2010). Interestingly, CD200Fc attenuated an age-related increases in MHC II and CD40L expression in hippocampus. Thus far, the action of CD200Fc has not been examined on age-related inflammatory changes. However, CD200Fc administered subcutaneously during the chronic stage of EAE reduced disease severity, demyelination and axonal damage and, consistent with the current study, there was a decrease in MHC II and NO expression in the CNS of these animals (Liu *et al.*, 2010).

In addition to CD200Fc modulating microglial activity, Liu (2010) reported that it attenuated astrocytic activity and decreased MHC II expression on this cell type. The current findings demonstrated that CD200Fc decreased the age-related increase in GFAP mRNA expression, also suggestive of a dampening of astrocytic activity. Much of the literature focuses of MHC II expression on microglia, although under certain circumstances astrocytes are capable of expressing this polymorphic molecule and partaking in antigen presentation (Collawn & Benveniste, 1999; Zeinstra *et al.*, 2000). Moreover, Chitnis (2007) reports that CD200R is not strictly restricted to cells of the myeloid lineage but can be found on astrocytes and this expression was increased after induction of EAE. With the current study in mind, it is possible CD200Fc attenuated MHC II mRNA expression through acting directly on astrocytes, as well as microglia, this is further validated by the finding that CD200Fc attenuated the age-related increase in GFAP.

The 'DNA damage theory of aging' proposes that the progressive and irreversible accumulation of DNA damage results in cellular senescence and cell dysfunction (Hamilton *et al.*, 2001). This hypothesis has gained acceptance due to the strong correlation between increasing age and enhanced levels of oxidative and nitrative damage, particularly in the CNS (Nguyen *et al.*, 1992; Wolf *et al.*, 2005). Here iNOS concentration was increased in hippocampus of aged rats and this was paralleled by an age-related increase in the oxidative stress marker 8-OHdG. Synthesis of iNOS by activated glial cells leads to the production of NO which, like ROS, acts as a free radical that is detrimental to host cells by interfering with and damaging DNA (Nguyen *et al.*, 1992). Many brain pathologies involving neuroinflammation are associated with an up-regulation in NO and ROS. O'Donnell (2000) proposed that the increase in inflammatory markers in hippocampus could be a consequence

of an age-related increase in oxidative stress and found an up-regulation in destructive ROS and a decrease in protective antioxidants in hippocampus with age, leading to functional alterations and pathological damage. The same laboratory reported the neuroprotective effect of polyunsaturated fatty acids in preventing age-related oxidative damage, measured by 8-OHdG staining, and neuronal function determined by LTP (Kelly *et al.*, 2010). Here the neuroprotective effect of CD200Fc was demonstrated. Acute administration of the fusion protein caused an apparent decrease in 8-OHdG immunoreactivity in hippocampus of aged rats. Furthermore, *in vitro* experiments revealed the proclivity of CD200Fc to attenuate an LPS-induced increase in nitrate concentration in mixed glial cultures. These results reveal a protective role for CD200Fc that is paralleled by its anti-inflammatory properties. The mechanism by which CD200Fc restores synaptic function has not been fully elucidated, however, the data presented here indicated that it might be due to its proclivity to attenuate microglial and astrocytic activity, in addition to regulating nitrate and oxidative stress.

One possible mechanism by which CD200Fc might exert a neuroprotective effects is by increasing IGF-1 and AKT phosphorylation in the hippocampus. IGF-1 is a potent activator of AKT. Here the phosphorylated form of AKT was decreased in hippocampal tissue prepared from aged rats; however, an age-related decrease in IGF-1 did not reach statistical significance. IGF-1 is a polypeptide hormone that stimulates the proliferation of a variety of cell types and it believed to play a critical function in stimulating neurogenesis of progenitor cells in the dentate gyrus of the adult brain (Anderson *et al.*, 2002). It acts on the AKT/PI-3 kinase signalling cascade, which is associated with proliferation, cell survival and is required for maintenance of LTP. Furthermore, down-regulation in this pathway has previously been observed with age (Kelly & Lynch, 2000; Anderson *et al.*, 2002; Ramsey *et al.*, 2004; Maher *et al.*, 2006; Downer *et al.*, 2009). A deficiency in IGF-1 leads to disrupted LTP, while administration of IGF-1 can reverse age-related behavioural and synaptic deficits (Ramsey *et al.*, 2004; Trejo *et al.*, 2007). Moreover, it has been shown to have neuroprotective properties against quinolinate-induced excitotoxicity and IFN γ -induced inflammation (Escartin *et al.*, 2004; Maher *et al.*, 2006; Downer *et al.*, 2009). Its role in attenuating collateral damage during an acute inflammatory episode or chronic inflammation, for example during neurodegenerative disease, has yet to be revealed. However, levels of IGF-1 are consistently low in the CNS of AD patients and administration of the hormone can benefit cognitive

function (Ramsey *et al.*, 2004). Here administration of CD200Fc increased hippocampal IGF-1 concentration, thus it is proposed that CD200Fc can maintaining homeostasis in hippocampus of aged rats and enhance neuronal function by increasing IGF-1 related signalling.

In conclusion, the acute administration of CD200Fc had the ability to attenuate LPS- and age-related deficits in synaptic plasticity. CD200Fc down-regulated markers associated with inflammatory activity and oxidative damage in primary glial cells, in addition to hippocampus of aged rats, which might contribute to the reversal of impaired synaptic function. Finally, the data revealed CD200Fc to increase hippocampal concentration of the neuroprotective hormone IGF-1 and its related signalling, which is likely to play a critical role in sustaining the integrity of neuronal circuits in this area.

Chapter 6. Conclusion

Microgliosis has been implicated as an underlying factor in a variety of neurodegenerative diseases (Block & Hong 2005). It is hypothesised that chronic inflammation is a critical mechanism in the progressive nature of neurodegeneration, although the triggers of various disorders may differ. Traditionally microglia were considered the resident immune cells of the CNS, however, it is now known that astrocytes also have immune effector capabilities and can adapt to changes in their microenvironment. The primary objective of this thesis was to investigate the action of novel anti-inflammatory compounds that regulate glial cell activation and synaptic function, and therefore may be beneficial in diseases associated with cognitive decline.

FGL, a neural cell adhesion molecule-mimetic peptide, was the first compound examined. The data show FGL exerted an anti-inflammatory action on primary glial cells that were previously exposed to either LPS or A β . A β is a peptide associated with the pathogenesis of Alzheimer's disease (AD), and like LPS, can recruit and activate microglia resulting in production of a barrage of neurotoxic inflammatory mediators (Pike *et al.*, 1995). The inflammatory stimuli induced an increase in cell surface markers of activation and pro-inflammatory cytokine release from primary mixed glia, which contain both microglia and astrocytes. Incubating glia in the presence of FGL attenuated markers of activation and this attenuation was paralleled by an up-regulation in the immunosuppressive surface protein CD200. It was suggested that the proclivity of FGL to act as an anti-inflammatory agent was partially dependent on enhancing CD200 expression *in vitro*. Interestingly, FGL failed to exert an anti-inflammatory action on glial cells prepared from CD200-deficient mice, thus reinforcing the proposal that the anti-inflammatory action of FGL is CD200 dependent.

The second compound investigated was a CD200 fusion protein (CD200Fc), which is a chimera consisting of the CD200 ligand ectodomain bound to a murine immunoglobulin subunit. Incubating LPS-stimulated mixed glia in the presence of CD200Fc abrogated markers of glial cell activation, similar to the down-regulation exerted by FGL. Finally, the anti-inflammatory effect of CD200Fc in the CNS was established and its ability to enhance synaptic function in the hippocampus revealed. These findings highlight a novel mechanism

by which enhancing CD200-related signalling, via exposing cells to FGL or CD200Fc, can impact on glial cell activation and subsequently synaptic integrity.

It has previously been reported that engagement of CD200 with its cognate receptor (CD200R) can maintain immune cells in a quiescent state. Furthermore, activation of CD200R has been identified as a potential therapeutic target in diseases associated with inflammation. Up-regulating CD200-related signalling by administration of a CD200R agonist or through use of transgenes has been beneficial in preventing inflammatory lung disease, enhancing allograft acceptance and reducing severity of autoimmune disorders, but whether these changes apply to the brain have yet to be systematically explored (Hoek *et al.*, 2000; Simelyte *et al.*, 2008; Snelgrove *et al.*, 2008; Gorczynski *et al.*, 2009).

This thesis investigated the dependence of FGL on CD200 expression in primary mixed glial cells. It has been established that these preparations contain approximately 30% microglia and 70% astrocytes, however cells previously shown to express the ligand, specifically neurons and endothelial cells are not present (Downer *et al.*, 2008, Cowly *et al.*, 2010). Therefore, the possibility that astrocytes express CD200 was considered. The data confirmed expression of CD200 on astrocytes *in vitro*. Thus far, most of the literature has focused on CD200 expressed on neurons and endothelial cells, which engage with CD200R on microglia and consequently maintain them in a quiescent state. However, this thesis puts forward the concept that astrocytes may also regulate microglial reactivity through CD200-related signalling. The heightened state of activation found in isolated microglial cultures and mixed glia prepared from CD200^{-/-} mice could partly be explained by the absence of an inhibitory signal from astrocytes. Astrocytes are one of the most abundant cells in the CNS, thus manipulating CD200 expression on this cell population could give great scope to modulate the activation state of microglia.

Inflammatory changes are thought to contribute to an age-related decline in cognitive function and play a critical role in the pathogenesis of neurodegenerative diseases (Town *et al.*, 2001; Griffin *et al.*, 2006). Here, CD200Fc was revealed to abrogate an LPS-induced impairment in the maintenance of long-term potentiation (LTP). Long-term potentiation of synaptic transmission in the hippocampus is the foremost experimental correlate for investigating the

synaptic basis of learning and memory (Bliss & Collingridge 1993). A peripheral LPS challenge can propagate an immune response within the brain and initiate production of pro-inflammatory cytokines by resident cells (Quan *et al.*, 1994). These findings indicate that CD200Fc has the ability to restore synaptic function through acting as an anti-inflammatory agent within the brain. Furthermore, CD200Fc reversed the age-related impairment in LTP and the age-associated increase in markers of inflammation in hippocampal tissue. Evidence from the literature suggests that hippocampus of aged rats display an enhanced inflammatory profile and this contributes to a decrease in synaptic plasticity (Lynch, 2010).

There was an age-induced increase in hippocampal expression of MHC II, which is suggestive of enhanced microglial activation, while the age-related up-regulation in GFAP is indicative of astrogliosis. Interestingly, a concomitant decrease in hippocampal CD200 expression was found, which potentially contributed to the enhanced microglial and astrogliosis detected in the aged brain. Researchers from this laboratory have described an enhanced inflammatory profile in CD200^{-/-} mice, typified by increased MHC II immunoreactivity. Also, there were distinct differences in MRI imaging from the CNS of CD200-deficient mice compared with wildtype animals, however, the functional consequences of this have yet to be established (unpublished observation). Furthermore, Hoek (2000) described a significant shift in the phenotype of microglia in the absence of CD200. Microglia in CD200^{-/-} mice display an amoeboid morphology with increased CD11b, MHC II and CD45 expression, indicative of myeloid cells in a tonically active state. Here there was also a shift in microglial cell activation state in hippocampus of aged animals, which was paralleled by a decrease in CD200 expression. It is proposed that a decrease in CD200-related inhibitory signalling distorts equilibrium and promotes a pro-inflammatory state. MHC II, CD40L and GFAP were attenuated in aged rats that received CD200Fc, thus further substantiating the critical role of CD200 in maintaining immune cell homeostasis and its potential application in restoring balance during acute and chronic inflammatory insults.

Immune cell activation is intertwined with oxidative and nitrative stress, while increased iNOS production is characteristic of activated microglia. The brain is particularly susceptible to oxidative damage due to low levels of endogenous anti-oxidants that further decline with age (Wolf *et al.*, 2005). Similar to neuroinflammatory changes, oxidative stress has been

correlated with impaired synaptic function (O'Donnell *et al.*, 2000; Kelly *et al.*, 2010). The current study found an increase in markers of oxidative and nitrative stress with age, which were attenuated in animals that received CD200Fc. The action of this fusion protein on LPS-induced nitrate production was also examined *in vitro* and was shown to abrogate nitrate production in stimulated mixed glial cells. The focus of this thesis was to investigate the modulatory action of CD200Fc on synaptic plasticity and markers of microglial activation. Others have reported the proclivity of CD200R agonists to decrease cytokine production and NO expression in peripheral macrophages, induced by various inflammatory insults however; the effect of CD200Fc in the hippocampus has not been explored (Hoek *et al.*, 2000; Copland *et al.*, 2007; Snelgrove *et al.*, 2008). Combined, these findings indicate a role for CD200 in controlling and restricting injurious immune cell activation, both in the CNS and the periphery. Manipulating the interplay between CD200 and its receptor can silence glial cell activation and promote synaptic plasticity.

If CD200 can restrain immune activity, then the absence of CD200 throughout the body would lead to myeloid cells with an activated, pro-inflammatory phenotype. Glia prepared from CD200^{-/-} animals displayed enhanced expression of CD11b and CD68, which signifies a heightened state of activation, even in the absence of an inflammatory stimulus. Furthermore, the LPS-induced increase in pro-inflammatory cytokine production and surface markers of activation was exaggerated in mixed glia cultured from CD200^{-/-} mice. These findings demonstrate that in the absence of CD200 glia are more vulnerable to an inflammatory challenge, which could be detrimental *in vivo*, thus resulting in delayed resolution of inflammation and instigating collateral tissue damage. From the evidence provided it is postulated that the declining levels of CD200 associated with senescence could render the CNS more vulnerable to a pathological challenge and accelerate degeneration. This corroborates other research groups that have reported CD200 deficient mice to be more susceptible to experimentally-induced autoimmune diseases, displaying a rapid onset of symptoms and increased severity of disease progression at a clinical and histological level (Hoek *et al.*, 2000; Copland *et al.*, 2007).

The NCAM-mimetic peptide FGL was shown to up-regulate CD200 expression in purified astrocytic cultures *in vitro*, which is consistent with previous reports noting its ability to

enhance neuronal CD200 expression (Downer *et al.*, 2008). Downer and colleagues (2008) demonstrated that chronic treatment with FGL restored an age-related deficit in LTP, which was accompanied by an FGL-induced increase in hippocampal CD200 expression and consequent decrease in markers of microgliosis. The effect of FGL on LTP was analogous to the reversal of synaptic impairment following acute administration of CD200Fc. As discussed previously, *in vitro* data reveal the proclivity of FGL to act as an anti-inflammatory agent and it is proposed that it exerts this action partly through up-regulating CD200 expression on astrocytes. The effect of FGL was abrogated in glia prepared from CD200^{-/-} animals, thus indicating the dependence of FGL on CD200 expression. Furthermore, the ability of an astrocytic membrane preparation to decrease LPS-induced cytokine production from isolated microglia was demonstrated, corroborating the hypothesis that interaction between the cell membranes of astrocytes and microglia plays a critical role in modulating an inflammatory response. One of the primary outcomes of this thesis was the suggestion that astrocytes modulate microglial activity through CD200 receptor-ligand engagement. The current evidence indicates that the FGL-induced enhancement of synaptic function and decrease in microgliosis, reported by Downer (2008), is not restricted to increased CD200 expression on neurons, but also on astrocytes; one of the most abundant cell type in the CNS (Wang & Bordey, 2008). It would be interesting to investigate the modulatory action of astrocytes on stimulated microglial cells in the presence of a CD200 antibody, as this would give a clearer indication as to what extent the immunosuppressive action of astrocytes rely upon CD200 signalling.

Another central finding of this thesis was that CD200Fc reversed an age-related and LPS-induced impairment in synaptic plasticity. Furthermore, unpublished data from this laboratory demonstrates the proclivity of CD200Fc to attenuate an A β -induced deficit in LTP (data not shown). The mechanisms involved in CD200Fc-induced restoration of synaptic integrity have yet to be delineated; however, the evidence indicates that inducing and sustaining LTP is intertwined with maintaining glia in a quiescent state. Thus, understanding the protective and pathogenic inflammatory pathways involved may be advantageous in comprehending the association between immune cell activation state and cognitive function. Here it is suggested that CD200Fc reduces markers of oxidative stress and enhances signalling downstream of

AKT, both of which are associated with promoting cell survival and are required for maintenance of LTP (Kelly & Lynch 2000; O'Donnell *et al.*, 2000).

Epidemiological studies have revealed non-steroidal anti-inflammatory drugs (NSAIDs) to be beneficial in both; decreasing the probability of developing a neurodegenerative disease and significantly increasing the age of onset (Walker *et al.*, 2009; Wilkinson *et al.*, 2010). Evidence that NSAIDs can reduce age-associated cognitive decline adds gravitas to a principal finding of this thesis; the anti-inflammatory agent CD200Fc reversed markers of glial cell activation and an age-related deficit in LTP, which is considered a cellular correlate for learning and memory. AD is an irreversible progressive neurodegenerative disorder that is diagnosed post-mortem by the presence of A β plaques. Its pathogenesis is correlated with an enhanced inflammatory profile, and senescence is a primary risk factor for developing the disease (Town *et al.*, 2001). A recent study identified lower levels of CD200 expression in AD pathological brain regions compared with tissue from aged-matched non-demented patients (Walker *et al.*, 2008). This finding is consistent with the documented increase in microglial activation in brain regions associated with AD and further validates investigating CD200/CD200R interaction to maintain immune-cell homeostasis and prevent a pretured inflammatory profile.

In spite of promising indications from longitudinal studies and animal models, the beneficial effect of NSAIDs has not been reproduced in clinical trials (Sastre & Gentleman, 2010). The failure of such trials has been attributed to various factors; from timing of drug administration, NSAIDs may not be effective once symptoms are evident, to concentration and penetration of the blood-brain barrier, which may be compromised as the disease progresses (Sastre & Gentleman 2010). NSAIDs have a diverse array of molecular targets, therefore, for a drug to be neuro-protective it would ideally target a processes implicated in the pathogenesis of the disease in question. Although many signalling pathways associated with neurodegeneration have not been sufficiently delineated, microglial cell activation is a common denominator among these diseases (Block & Hong 2005). Evidence from this thesis indicates the therapeutic potential of enhancing CD200/CD200R signalling, yet the method used to deliver CD200Fc, an intrahippocampal infusion, would not be feasible clinically. FGL was highlighted as a novel mechanism to up-regulate CD200 expression; however, as FGL is a

peptide it can not be taken orally, and would rely on intravenous or intranasal administration. Therefore, further studies should focus on less invasive methods of manipulating endogenous CD200 expression or enhancing CD200-related signalling to further elucidate strategies that are clinically applicable.

Chapter 7. Bibliography

- Abdel-Haq N, Hao HN & Lyman WD. (1999). Cytokine regulation of CD40 expression in fetal human astrocyte cultures. *J Neuroimmunol* **101**, 7-14.
- Adams JP & Sweatt JD. (2002). Molecular psychology: roles for the ERK MAP kinase cascade in memory. *Annu Rev Pharmacol Toxicol* **42**, 135-163.
- Alessi DR, Cuenda A, Cohen P, Dudley DT & Saltiel AR. (1995). PD 098059 is a specific inhibitor of the activation of mitogen-activated protein kinase kinase in vitro and in vivo. *J Biol Chem* **270**, 27489-27494.
- Allan SM. (2005). Pragmatic target discovery from novel gene to functionally defined drug target: the interleukin-1 story. *Methods Mol Med* **104**, 333-346.
- Allan SM & Pinteaux E. (2003). The interleukin-1 system: an attractive and viable therapeutic target in neurodegenerative disease. *Curr Drug Targets CNS Neurol Disord* **2**, 293-302.
- Allan SM, Tyrrell PJ & Rothwell NJ. (2005). Interleukin-1 and neuronal injury. *Nat Rev Immunol* **5**, 629-640.
- Aloisi F. (1999). The role of microglia and astrocytes in CNS immune surveillance and immunopathology. *Adv Exp Med Biol* **468**, 123-133.
- Aloisi F. (2001). Immune function of microglia. *Glia* **36**, 165-179.
- Anderson MF, Aberg MA, Nilsson M & Eriksson PS. (2002). Insulin-like growth factor-I and neurogenesis in the adult mammalian brain. *Brain Res Dev Brain Res* **134**, 115-122.
- Ando S, Tanaka Y, Toyoda nee Ono Y, Kon K & Kawashima S. (2002). Turnover of synaptic membranes: age-related changes and modulation by dietary restriction. *J Neurosci Res* **70**, 290-297.
- Angelo MF, Aviles-Reyes RX, Villarreal A, Barker P, Reines AG & Ramos AJ. (2009). p75(NTR) Expression is induced in isolated neurons of the penumbra after ischemia by cortical devascularization. *J Neurosci Res*. **87**, 1892-903.
- Arnett HA, Mason J, Marino M, Suzuki K, Matsushima GK & Ting JP. (2001). TNF alpha promotes proliferation of oligodendrocyte progenitors and remyelination. *Nat Neurosci* **4**, 1116-1122.
- Atkins AR, Chung J, Deechongkit S, Little EB, Edelman GM, Wright PE, Cunningham BA & Dyson HJ. (2001). Solution structure of the third immunoglobulin domain of the neural cell adhesion molecule N-CAM: can solution studies define the mechanism of homophilic binding? *J Mol Biol* **311**, 161-172.

- Bach ME, Barad M, Son H, Zhuo M, Lu YF, Shih R, Mansuy I, Hawkins RD & Kandel ER. (1999). Age-related defects in spatial memory are correlated with defects in the late phase of hippocampal long-term potentiation in vitro and are attenuated by drugs that enhance the cAMP signaling pathway. *Proc Natl Acad Sci U S A* **96**, 5280-5285.
- Ban E, Milon G, Prudhomme N, Fillion G & Haour F. (1991). Receptors for interleukin-1 (alpha and beta) in mouse brain: mapping and neuronal localization in hippocampus. *Neuroscience* **43**, 21-30.
- Barclay AN & Ward HA. (1982). Purification and chemical characterisation of membrane glycoproteins from rat thymocytes and brain, recognised by monoclonal antibody MRC OX 2. *Eur J Biochem* **129**, 447-458.
- Barnes CA. (1979). Memory deficits associated with senescence: a neurophysiological and behavioral study in the rat. *J Comp Physiol Psychol* **93**, 74-104.
- Bazan JF. (1990). Haemopoietic receptors and helical cytokines. *Immunol Today* **11**, 350-354.
- Becher B, Prat A & Antel JP. (2000). Brain-immune connection: immuno-regulatory properties of CNS-resident cells. *Glia* **29**, 293-304.
- Becker CG, Artola A, Gerardy-Schahn R, Becker T, Welzl H & Schachner M. (1996). The polysialic acid modification of the neural cell adhesion molecule is involved in spatial learning and hippocampal long-term potentiation. *J Neurosci Res* **45**, 143-152.
- Benveniste EN, Nguyen VT & Wesemann DR. (2004). Molecular regulation of CD40 gene expression in macrophages and microglia. *Brain Behav Immun* **18**, 7-12.
- Bliss TV & Collingridge GL. (1993). A synaptic model of memory: long-term potentiation in the hippocampus. *Nature* **361**, 31-39.
- Block ML & Hong JS. (2005). Microglia and inflammation-mediated neurodegeneration: multiple triggers with a common mechanism. *Prog Neurobiol* **76**, 77-98.
- Brenner T, Yamin A, Abramsky O & Gallily R. (1993). Stimulation of tumor necrosis factor-alpha production by mycoplasmas and inhibition by dexamethasone in cultured astrocytes. *Brain Res* **608**, 273-279.
- Brown GC. (2007). Mechanisms of inflammatory neurodegeneration: iNOS and NADPH oxidase. *Biochem Soc Trans* **35**, 1119-1121.
- Bushong EA, Martone ME, Jones YZ & Ellisman MH. (2002). Protoplasmic astrocytes in CA1 stratum radiatum occupy separate anatomical domains. *J Neurosci* **22**, 183-192.
- Cambon K, Hansen SM, Venero C, Herrero AI, Skibo G, Berezin V, Bock E & Sandi C. (2004). A synthetic neural cell adhesion molecule mimetic peptide promotes synaptogenesis, enhances presynaptic function, and facilitates memory consolidation. *J Neurosci* **24**, 4197-4204.

- Campbell IK, Bendele A, Smith DA & Hamilton JA. (1997). Granulocyte-macrophage colony stimulating factor exacerbates collagen induced arthritis in mice. *Ann Rheum Dis* **56**, 364-368.
- Campbell IK, Hamilton JA & Wicks IP. (2000). Collagen-induced arthritis in C57BL/6 (H-2b) mice: new insights into an important disease model of rheumatoid arthritis. *Eur J Immunol* **30**, 1568-1575.
- Campbell IL, Abraham CR, Masliah E, Kemper P, Inglis JD, Oldstone MB & Mucke L. (1993). Neurologic disease induced in transgenic mice by cerebral overexpression of interleukin 6. *Proc Natl Acad Sci U S A* **90**, 10061-10065.
- Cardona AE, Pioro EP, Sasse ME, Kostenko V, Cardona SM, Dijkstra IM, Huang D, Kidd G, Dombrowski S, Dutta R, Lee JC, Cook DN, Jung S, Lira SA, Littman DR & Ransohoff RM. (2006). Control of microglial neurotoxicity by the fractalkine receptor. *Nat Neurosci* **9**, 917-924.
- Carson MJ & Sutcliffe JG. (1999). Balancing function vs. self defense: the CNS as an active regulator of immune responses. *J Neurosci Res* **55**, 1-8.
- Chaplin DD & Fu Y. (1998). Cytokine regulation of secondary lymphoid organ development. *Curr Opin Immunol* **10**, 289-297.
- Chitnis T, Imitola J, Wang Y, Elyaman W, Chawla P, Sharuk M, Raddassi K, Bronson RT & Khoury SJ. (2007). Elevated neuronal expression of CD200 protects Wlds mice from inflammation-mediated neurodegeneration. *Am J Pathol* **170**, 1695-1712.
- Cho BP, Song DY, Sugama S, Shin DH, Shimizu Y, Kim SS, Kim YS & Joh TH. (2006). Pathological dynamics of activated microglia following medial forebrain bundle transection. *Glia* **53**, 92-102.
- Chrousos GP. (1995). The hypothalamic-pituitary-adrenal axis and immune-mediated inflammation. *N Engl J Med* **332**, 1351-62.
- Clark MJ, Gagnon J, Williams AF & Barclay AN. (1985). MRC OX-2 antigen: a lymphoid/neuronal membrane glycoprotein with a structure like a single immunoglobulin light chain. *EMBO J* **4**, 113-118.
- Clarke RM, Lyons A, O'Connell F, Deighan BF, Barry CE, Anyakoha NG, Nicolaou A & Lynch MA. (2008). A pivotal role for interleukin-4 in atorvastatin-associated neuroprotection in rat brain. *J Biol Chem* **283**, 1808-1817.
- Coan EJ & Collingridge GL. (1987). Characterization of an N-methyl-D-aspartate receptor component of synaptic transmission in rat hippocampal slices. *Neuroscience* **22**, 1-8.
- Collawn JF & Benveniste EN. (1999). Regulation of MHC class II expression in the central nervous system. *Microbes Infect* **1**, 893-902.

- Copland DA, Calder CJ, Raveney BJ, Nicholson LB, Phillips J, Cherwinski H, Jenmalm M, Sedgwick JD & Dick AD. (2007). Monoclonal antibody-mediated CD200 receptor signaling suppresses macrophage activation and tissue damage in experimental autoimmune uveoretinitis. *Am J Pathol* **171**, 580-588.
- Costelloe C, Watson M, Murphy A, McQuillan K, Loscher C, Armstrong ME, Garlanda C, Mantovani A, O'Neill LA, Mills KH & Lynch MA. (2008). IL-1F5 mediates anti-inflammatory activity in the brain through induction of IL-4 following interaction with SIGIRR/TIR8. *J Neurochem* **105**, 1960-1969.
- Cotrina ML & Nedergaard M. (2002). Astrocytes in the aging brain. *J Neurosci Res* **67**, 1-10.
- Cowley TR, O'Sullivan J, Blau C, Deighan BF, Jones R, Kerskens C, Richardson JC, Virley D, Upton N & Lynch MA. (2010). Rosiglitazone attenuates the age-related changes in astrocytosis and the deficit in LTP. *Neurobiol Aging*. [Epub ahead of print].
- Cuenda A, Rouse J, Doza YN, Meier R, Cohen P, Gallagher TF, Young PR & Lee JC. (1995). SB 203580 is a specific inhibitor of a MAP kinase homologue which is stimulated by cellular stresses and interleukin-1. *FEBS Lett* **364**, 229-233.
- Cunningham AJ, Murray CA, O'Neill LA, Lynch MA & O'Connor JJ. (1996). Interleukin-1 beta (IL-1 beta) and tumour necrosis factor (TNF) inhibit long-term potentiation in the rat dentate gyrus in vitro. *Neurosci Lett* **203**, 17-20.
- Cunningham C, Wilcockson DC, Champion S, Lunnon K, Perry VH. (2005). Central and systemic endotoxin challenges exacerbate the local inflammatory response and increase neuronal death during chronic neurodegeneration. *J Neurosci* **25**, 9275-9284.
- Dantzer R, Bluthé RM, Gheusi G, Cremona S, Laye S, Parnet P & Kelley KW. (1998). Molecular basis of sickness behavior. *Ann N Y Acad Sci* **856**, 132-138.
- Davalos D, Grutzendler J, Yang G, Kim JV, Zuo Y, Jung S, Littman DR, Dustin ML & Gan WB. (2005). ATP mediates rapid microglial response to local brain injury in vivo. *Nat Neurosci* **8**, 752-758.
- Davey FR, Cordell JL, Erber WN, Pulford KA, Gatter KC & Mason DY. (1988). Monoclonal antibody (Y1/82A) with specificity towards peripheral blood monocytes and tissue macrophages. *J Clin Pathol* **41**, 753-758.
- Davies CA, Loddick SA, Toulmond S, Stroemer RP, Hunt J & Rothwell NJ. (1999). The progression and topographic distribution of interleukin-1 beta expression after permanent middle cerebral artery occlusion in the rat. *J Cereb Blood Flow Metab* **19**, 87-98.
- Davies HA, Kelly A, Dhanrajan TM, Lynch MA, Rodriguez JJ & Stewart MG. (2003). Synaptophysin immunogold labelling of synapses decreases in dentate gyrus of the hippocampus of aged rats. *Brain Res* **986**, 191-195.

- Davis S, Vanhoutte P, Pages C, Caboche J & Laroche S. (2000). The MAPK/ERK cascade targets both Elk-1 and cAMP response element-binding protein to control long-term potentiation-dependent gene expression in the dentate gyrus in vivo. *J Neurosci* **20**, 4563-4572.
- De Keyser J, Laureys G, Demol F, Wilczak N, Mostert J & Clinckers R. (2010). Astrocytes as potential targets to suppress inflammatory demyelinating lesions in multiple sclerosis. *Neurochem Int* **57**, 446-50.
- de Toledo-Morrell L & Morrell F. (1985). Electrophysiological markers of aging and memory loss in rats. *Ann N Y Acad Sci* **444**, 296-311.
- Declercq W, Denecker G, Fiers W & Vandenameele P. (1998). Cooperation of both TNF receptors in inducing apoptosis: involvement of the TNF receptor-associated factor binding domain of the TNF receptor 75. *J Immunol* **161**, 390-399.
- Dinarello CA. (1996). Biologic basis for interleukin-1 in disease. *Blood* **87**, 2095-2147.
- Ditlevsen DK, Owczarek S, Berezin V & Bock E. (2008). Relative role of upstream regulators of Akt, ERK and CREB in NCAM- and FGF2-mediated signalling. *Neurochem Int* **53**, 137-147.
- Doherty P, Fruns M, Seaton P, Dickson G, Barton CH, Sears TA & Walsh FS. (1990). A threshold effect of the major isoforms of NCAM on neurite outgrowth. *Nature* **343**, 464-466.
- Downer EJ, Cowley TR, Cox F, Maher FO, Berezin V, Bock E & Lynch MA. (2009). A synthetic NCAM-derived mimetic peptide, FGL, exerts anti-inflammatory properties via IGF-1 and interferon-gamma modulation. *J Neurochem* **109**, 1516-1525.
- Downer EJ, Cowley TR, Lyons A, Mills KH, Berezin V, Bock E & Lynch MA. (2008). A novel anti-inflammatory role of NCAM-derived mimetic peptide, FGL. *Neurobiol Aging* **31**, 118-28.
- Du Yan S, Zhu H, Fu J, Yan SF, Roher A, Tourtellotte WW, Rajavashisth T, Chen X, Godman GC, Stern D & Schmidt AM. (1997). Amyloid-beta peptide-receptor for advanced glycation endproduct interaction elicits neuronal expression of macrophage-colony stimulating factor: a proinflammatory pathway in Alzheimer disease. *Proc Natl Acad Sci U S A* **94**, 5296-5301.
- Durieu-Trautmann O, Chaverot N, Cazaubon S, Strosberg AD & Couraud PO. (1994). Intercellular adhesion molecule 1 activation induces tyrosine phosphorylation of the cytoskeleton-associated protein cortactin in brain microvessel endothelial cells. *J Biol Chem* **269**, 12536-12540.
- Eastwood SL, Burnet PW & Harrison PJ. (1995). Altered synaptophysin expression as a marker of synaptic pathology in schizophrenia. *Neuroscience* **66**, 309-319.

- El Maarouf A & Rutishauser U. (2003). Removal of polysialic acid induces aberrant pathways, synaptic vesicle distribution, and terminal arborization of retinotectal axons. *J Comp Neurol* **460**, 203-211.
- Elkabes S, DiCicco-Bloom EM & Black IB. (1996). Brain microglia/macrophages express neurotrophins that selectively regulate microglial proliferation and function. *J Neurosci* **16**, 2508-2521.
- Eng LF, Ghirnikar RS & Lee YL. (2000). Glial fibrillary acidic protein: GFAP-thirty-one years (1969-2000). *Neurochem Res* **25**, 1439-1451.
- Eng LF, Vanderhaeghen JJ, Bignami A & Gerstl B. (1971). An acidic protein isolated from fibrous astrocytes. *Brain Res* **28**, 351-354.
- Errington ML, Lynch MA & Bliss TV. (1987). Long-term potentiation in the dentate gyrus: induction and increased glutamate release are blocked by D(-)aminophosphonovalerate. *Neuroscience* **20**, 279-284.
- Escartin C, Boyer F, Bemelmans AP, Hantraye P & Brouillet E. (2004). Insulin growth factor-1 protects against excitotoxicity in the rat striatum. *Neuroreport* **15**, 2251-2254.
- Esen N & Kielian T. (2007). Effects of low dose GM-CSF on microglial inflammatory profiles to diverse pathogen-associated molecular patterns (PAMPs). *J Neuroinflammation* **4**, 10.
- Feghali CA & Wright TM. (1997). Cytokines in acute and chronic inflammation. *Front Biosci* **2**, d12-26.
- Feuer R. (2007). Tickling the CD200 receptor: A remedy for those irritating macrophages. *Am J Pathol* **171**, 396-398.
- Floden AM & Combs CK. (2007). Microglia repetitively isolated from in vitro mixed glial cultures retain their initial phenotype. *J Neurosci Methods* **164**, 218-224.
- Fogal B & Hewett SJ. (2008). Interleukin-1beta: a bridge between inflammation and excitotoxicity? *J Neurochem* **106**, 1-23.
- Ford-Perriss M, Abud H & Murphy M. (2001). Fibroblast growth factors in the developing central nervous system. *Clin Exp Pharmacol Physiol* **28**, 493-503.
- Fox GB, Kennedy N & Regan CM. (1995). Polysialylated neural cell adhesion molecule expression by neurons and astroglial processes in the rat dentate gyrus declines dramatically with increasing age. *Int J Dev Neurosci* **13**, 663-672.
- Fukunaga K & Miyamoto E. (1998). Role of MAP kinase in neurons. *Mol Neurobiol* **16**, 79-95.

- Gage FH, Dunnett SB & Bjorklund A. (1989). Age-related impairments in spatial memory are independent of those in sensorimotor skills. *Neurobiol Aging* **10**, 347-352.
- Geinisman Y, deToledo-Morrell L, Morrell F, Persina IS & Rossi M. (1992). Age-related loss of axospinous synapses formed by two afferent systems in the rat dentate gyrus as revealed by the unbiased stereological dissector technique. *Hippocampus* **2**, 437-444.
- George CR. (2006). From Fahrenheit to cytokines: fever, inflammation and the kidney. *J Nephrol* **19 Suppl 10**, S88-97.
- Giese KP, Fedorov NB, Filipkowski RK & Silva AJ. (1998). Autophosphorylation at Thr286 of the alpha calcium-calmodulin kinase II in LTP and learning. *Science* **279**, 870-873.
- Giulian D, Baker TJ, Shih LC & Lachman LB. (1986). Interleukin 1 of the central nervous system is produced by ameboid microglia. *J Exp Med* **164**, 594-604.
- Gooney M, Shaw K, Kelly A, O'Mara SM & Lynch MA. (2002). Long-term potentiation and spatial learning are associated with increased phosphorylation of TrkB and extracellular signal-regulated kinase (ERK) in the dentate gyrus: evidence for a role for brain-derived neurotrophic factor. *Behav Neurosci* **116**, 455-463.
- Gorczyński RM, Bransom J, Cattral M, Huang X, Lei J, Xiaorong L, Min WP, Wan Y & Gauldie J. (2000). Synergy in induction of increased renal allograft survival after portal vein infusion of dendritic cells transduced to express TGFbeta and IL-10, along with administration of CHO cells expressing the regulatory molecule OX-2. *Clin Immunol* **95**, 182-189.
- Gorczyński RM, Cattral MS, Chen Z, Hu J, Lei J, Min WP, Yu G & Ni J. (1999). An immunoadhesin incorporating the molecule OX-2 is a potent immunosuppressant that prolongs allo- and xenograft survival. *J Immunol* **163**, 1654-1660.
- Gorczyński RM, Chen Z, He W, Khatri I, Sun Y, Yu K & Boudakov I. (2009). Expression of a CD200 transgene is necessary for induction but not maintenance of tolerance to cardiac and skin allografts. *J Immunol* **183**, 1560-1568.
- Gorczyński RM, Chen Z, Yu K & Hu J. (2001). CD200 immunoadhesin suppresses collagen-induced arthritis in mice. *Clin Immunol* **101**, 328-334.
- Gorczyński RM & Terzioglu E. (2008). Aging and the immune system. *Int Urol Nephrol* **40**, 1117-1125.
- Gosselin D & Rivest S. (2007). Role of IL-1 and TNF in the brain: twenty years of progress on a Dr. Jekyll/Mr. Hyde duality of the innate immune system. *Brain Behav Immun* **21**, 281-289.
- Griffin R, Nally R, Nolan Y, McCartney Y, Linden J & Lynch MA. (2006). The age-related attenuation in long-term potentiation is associated with microglial activation. *J Neurochem* **99**, 1263-1272.

- Gruol DL & Nelson TE. (1997). Physiological and pathological roles of interleukin-6 in the central nervous system. *Mol Neurobiol* **15**, 307-339.
- Guarda G & So A. (2010). Regulation of inflammasome activity. *Immunology* **130**, 329-336.
- Halliwell B. (1992). Reactive oxygen species and the central nervous system. *J Neurochem* **59**, 1609-1623.
- Hamilton ML, Van Remmen H, Drake JA, Yang H, Guo ZM, Kewitt K, Walter CA & Richardson A. (2001). Does oxidative damage to DNA increase with age? *Proc Natl Acad Sci U S A* **98**, 10469-10474.
- Hanisch UK & Kettenmann H. (2007). Microglia: active sensor and versatile effector cells in the normal and pathologic brain. *Nat Neurosci* **10**, 1387-1394.
- Harnett MM. (2004). CD40: a growing cytoplasmic tale. *Sci STKE* **2004**, pe25.
- Hatherley D & Barclay AN. (2004). The CD200 and CD200 receptor cell surface proteins interact through their N-terminal immunoglobulin-like domains. *Eur J Immunol* **34**, 1688-1694.
- Hebert AE & Dash PK. (2002). Extracellular signal-regulated kinase activity in the entorhinal cortex is necessary for long-term spatial memory. *Learn Mem* **9**, 156-166.
- Heinrich PC, Graeve L, Rose-John S, Schneider-Mergener J, Dittrich E, Erren A, Gerhartz C, Hemann U, Luticken C, Wegenka U & et al. (1995). Membrane-bound and soluble interleukin-6 receptor: studies on structure, regulation of expression, and signal transduction. *Ann N Y Acad Sci* **762**, 222-236; discussion 236-227.
- Hesseltger J & Horuk R. (1999). Chemokine and chemokine receptor expression in the central nervous system. *J Neurovirol* **5**, 13-26.
- Hoek RM, Ruuls SR, Murphy CA, Wright GJ, Goddard R, Zurawski SM, Blom B, Homola ME, Streit WJ, Brown MH, Barclay AN & Sedgwick JD. (2000). Down-regulation of the macrophage lineage through interaction with OX2 (CD200). *Science* **290**, 1768-1771.
- Holness CL & Simmons DL. (1993). Molecular cloning of CD68, a human macrophage marker related to lysosomal glycoproteins. *Blood* **81**, 1607-1613.
- Huang C & Springer TA. (1995). A binding interface on the I domain of lymphocyte function-associated antigen-1 (LFA-1) required for specific interaction with intercellular adhesion molecule 1 (ICAM-1). *J Biol Chem* **270**, 19008-19016.
- Huang YY & Kandel ER. (1994). Recruitment of long-lasting and protein kinase A-dependent long-term potentiation in the CA1 region of hippocampus requires repeated tetanization. *Learn Mem* **1**, 74-82.

- Hulshof S, Montagne L, De Groot CJ & Van Der Valk P. (2002). Cellular localization and expression patterns of interleukin-10, interleukin-4, and their receptors in multiple sclerosis lesions. *Glia* **38**, 24-35.
- Ito J, Nagayasu Y, Okumura-Noji K, Lu R, Nishida T, Miura Y, Asai K, Kheirollah A, Nakaya S & Yokoyama S. (2007). Mechanism for FGF-1 to regulate biogenesis of apoE-HDL in astrocytes. *J Lipid Res* **48**, 2020-2027.
- Jacque CM, Jorgensen OS & Bock E. (1974). Quantitative studies on the brain specific antigens S-100, GFA, 14-3-2, D1, D2, D3 and C1 in Quaking mouse. *FEBS Lett* **49**, 264-266.
- Jana M, Palencia CA & Pahan K. (2008). Fibrillar amyloid-beta peptides activate microglia via TLR2: implications for Alzheimer's disease. *J Immunol* **181**, 7254-7262.
- Jensen PH, Soroka V, Thomsen NK, Raets I, Berezin V, Bock E & Poulsen FM. (1999). Structure and interactions of NCAM modules 1 and 2, basic elements in neural cell adhesion. *Nat Struct Biol* **6**, 486-493.
- Johnson CP, Fujimoto I, Rutishauser U & Leckband DE. (2005). Direct evidence that neural cell adhesion molecule (NCAM) polysialylation increases intermembrane repulsion and abrogates adhesion. *J Biol Chem* **280**, 137-145.
- Johnson DE & Williams LT. (1993). Structural and functional diversity in the FGF receptor multigene family. *Adv Cancer Res* **60**, 1-41.
- Karwoski CJ, Lu HK & Newman EA. (1989). Spatial buffering of light-evoked potassium increases by retinal Muller (glial) cells. *Science* **244**, 578-580.
- Kelly A, Lynch A, Vereker E, Nolan Y, Queenan P, Whittaker E, O'Neill LA & Lynch MA. (2001). The anti-inflammatory cytokine, interleukin (IL)-10, blocks the inhibitory effect of IL-1 beta on long term potentiation. A role for JNK. *J Biol Chem* **276**, 45564-45572.
- Kelly A & Lynch MA. (2000). Long-term potentiation in dentate gyrus of the rat is inhibited by the phosphoinositide 3-kinase inhibitor, wortmannin. *Neuropharmacology* **39**, 643-651.
- Kelly L, Grehan B, Chiesa AD, O'Mara SM, Downer E, Sahyoun G, Massey KA, Nicolaou A & Lynch MA. (2010). The polyunsaturated fatty acids, EPA and DPA exert a protective effect in the hippocampus of the aged rat. *Neurobiol Aging* [Epub ahead of print].
- Kharitonov A, Chen Z, Sures I, Wang H, Schilling J & Ullrich A. (1997). A family of proteins that inhibit signalling through tyrosine kinase receptors. *Nature* **386**, 181-186.

- Kiselyov VV, Skladchikova G, Hinsby AM, Jensen PH, Kulahin N, Soroka V, Pedersen N, Tsetlin V, Poulsen FM, Berezin V & Bock E. (2003). Structural basis for a direct interaction between FGFR1 and NCAM and evidence for a regulatory role of ATP. *Structure* **11**, 691-701.
- Kiselyov VV, Soroka V, Berezin V & Bock E. (2005). Structural biology of NCAM homophilic binding and activation of FGFR. *J Neurochem* **94**, 1169-1179.
- Klementiev B, Novikova T, Novitskaya V, Walmod PS, Dmytriyeva O, Pakkenberg B, Berezin V & Bock E. (2007). A neural cell adhesion molecule-derived peptide reduces neuropathological signs and cognitive impairment induced by Abeta25-35. *Neuroscience* **145**, 209-224.
- Koning N, Swaab DF, Hoek RM & Huitinga I. (2009). Distribution of the immune inhibitory molecules CD200 and CD200R in the normal central nervous system and multiple sclerosis lesions suggests neuron-glia and glia-glia interactions. *J Neuropathol Exp Neurol* **68**, 159-167.
- Konsman JP, Vignes S, Mackerlova L, Bristow A & Blomqvist A. (2004). Rat brain vascular distribution of interleukin-1 type-1 receptor immunoreactivity: relationship to patterns of inducible cyclooxygenase expression by peripheral inflammatory stimuli. *J Comp Neurol* **472**, 113-129.
- Kopp EB & Medzhitov R. (1999). The Toll-receptor family and control of innate immunity. *Curr Opin Immunol* **11**, 13-18.
- Kreutzberg GW. (1996). Microglia: a sensor for pathological events in the CNS. *Trends Neurosci* **19**, 312-318.
- Kurushima H, Ramprasad M, Kondratenko N, Foster DM, Quehenberger O & Steinberg D. (2000). Surface expression and rapid internalization of macroscialin (mouse CD68) on elicited mouse peritoneal macrophages. *J Leukoc Biol* **67**, 104-108.
- Lee SJ & Benveniste EN. (1999). Adhesion molecule expression and regulation on cells of the central nervous system. *J Neuroimmunol* **98**, 77-88.
- Lee SJ, Drabik K, Van Wagoner NJ, Lee S, Choi C, Dong Y & Benveniste EN. (2000). ICAM-1-induced expression of proinflammatory cytokines in astrocytes: involvement of extracellular signal-regulated kinase and p38 mitogen-activated protein kinase pathways. *J Immunol* **165**, 4658-4666.
- Levy WB & Steward O. (1979). Synapses as associative memory elements in the hippocampal formation. *Brain Res* **175**, 233-245.
- Lieberman AP, Pitha PM, Shin HS & Shin ML. (1989). Production of tumor necrosis factor and other cytokines by astrocytes stimulated with lipopolysaccharide or a neurotropic virus. *Proc Natl Acad Sci USA* **86**, 6348-6352.

- Lindia JA, McGowan E, Jochnowitz N & Abbadie C. (2005). Induction of CX3CL1 expression in astrocytes and CX3CR1 in microglia in the spinal cord of a rat model of neuropathic pain. *J Pain* **6**, 434-438.
- Liu Y, Bando Y, Vargas-Lowy D, Elyaman W, Khoury SJ, Huang T, Reif K & Chitnis T. (2010). CD200R1 agonist attenuates mechanisms of chronic disease in a murine model of multiple sclerosis. *J Neurosci* **30**, 2025-2038.
- Loane DJ, Deighan BF, Clarke RM, Griffin RJ, Lynch AM & Lynch MA. (2009). Interleukin-4 mediates the neuroprotective effects of rosiglitazone in the aged brain. *Neurobiol Aging* **30**, 920-31.
- Lobner D & Ali C. (2002). Mechanisms of bFGF and NT-4 potentiation of necrotic neuronal death. *Brain Res* **954**, 42-50.
- Loddick SA, Turnbull AV & Rothwell NJ. (1998). Cerebral interleukin-6 is neuroprotective during permanent focal cerebral ischemia in the rat. *J Cereb Blood Flow Metab* **18**, 176-179.
- Lynch AM, Loane DJ, Minogue AM, Clarke RM, Kilroy D, Nally RE, Roche OJ, O'Connell F & Lynch MA. (2007). Eicosapentaenoic acid confers neuroprotection in the amyloid-beta challenged aged hippocampus. *Neurobiol Aging* **28**, 845-855.
- Lynch G, Larson J, Kelso S, Barrionuevo G & Schottler F. (1983). Intracellular injections of EGTA block induction of hippocampal long-term potentiation. *Nature* **305**, 719-721.
- Lynch GS, Dunwiddie T & Gribkoff V. (1977). Heterosynaptic depression: a postsynaptic correlate of long-term potentiation. *Nature* **266**, 737-739.
- Lynch MA. (1998). Age-related impairment in long-term potentiation in hippocampus: a role for the cytokine, interleukin-1 beta? *Prog Neurobiol* **56**, 571-589.
- Lynch MA. (2004). Long-term potentiation and memory. *Physiol Rev* **84**, 87-136.
- Lynch MA. (2008). The risky business of ageing. *Brain Behav Immun* **22**, 299-300.
- Lynch MA. (2010). Age-related neuroinflammatory changes negatively impact on neuronal function. *Front Aging Neurosci* **1**, 6.
- Lyons A, Downer EJ, Crotty S, Nolan YM, Mills KH & Lynch MA. (2007). CD200 ligand receptor interaction modulates microglial activation in vivo and in vitro: a role for IL-4. *J Neurosci* **27**, 8309-8313.
- Lyons A, Lynch AM, Downer EJ, Hanley R, O'Sullivan JB, Smith A & Lynch MA. (2009a). Fractalkine-induced activation of the phosphatidylinositol-3 kinase pathway attenuates microglial activation in vivo and in vitro. *J Neurochem* **110**, 1547-1556.

- Lyons A, McQuillan K, Deighan BF, O'Reilly JA, Downer EJ, Murphy AC, Watson M, Piazza A, O'Connell F, Griffin R, Mills KH & Lynch MA. (2009b). Decreased neuronal CD200 expression in IL-4-deficient mice results in increased neuroinflammation in response to lipopolysaccharide. *Brain Behav Immun* **23**, 1020-1027.
- Magnusson PU, Dimberg A, Mellberg S, Lukinius A, Claesson-Welsh L. (2007). FGFR-1 regulates angiogenesis through cytokines interleukin-4 and pleiotrophin. *Blood* **110**, 4214-22.
- Maher FO, Clarke RM, Kelly A, Nally RE & Lynch MA. (2006). Interaction between interferon gamma and insulin-like growth factor-1 in hippocampus impacts on the ability of rats to sustain long-term potentiation. *J Neurochem* **96**, 1560-1571.
- Maier SF & Watkins LR. (1995). Intracerebroventricular interleukin-1 receptor antagonist blocks the enhancement of fear conditioning and interference with escape produced by inescapable shock. *Brain Res* **695**, 279-282.
- Majumdar A, Cruz D, Asamoah N, Buxbaum A, Sohar I, Lobel P & Maxfield FR. (2007). Activation of microglia acidifies lysosomes and leads to degradation of Alzheimer amyloid fibrils. *Mol Biol Cell* **18**, 1490-1496.
- Markram K, Gerardy-Schahn R & Sandi C. (2007). Selective learning and memory impairments in mice deficient for polysialylated NCAM in adulthood. *Neuroscience* **144**, 788-796.
- Martin KC, Michael D, Rose JC, Barad M, Casadio A, Zhu H & Kandel ER. (1997). MAP kinase translocates into the nucleus of the presynaptic cell and is required for long-term facilitation in Aplysia. *Neuron* **18**, 899-912.
- Martinon F, Burns K & Tschopp J. (2002). The inflammasome: a molecular platform triggering activation of inflammatory caspases and processing of proIL-beta. *Mol Cell* **10**, 417-426.
- McEntee WJ, Crook TH, Jenkyn LR, Petrie W, Larrabee GJ & Coffey DJ. (1991). Treatment of age-associated memory impairment with guanfacine. *Psychopharmacol Bull* **27**, 41-46.
- McGahon B, Clements MP & Lynch MA. (1997). The ability of aged rats to sustain long-term potentiation is restored when the age-related decrease in membrane arachidonic acid concentration is reversed. *Neuroscience* **81**, 9-16.
- McGahon B, Maguire C, Kelly A & Lynch MA. (1999). Activation of p42 mitogen-activated protein kinase by arachidonic acid and trans-1-amino-cyclopentyl-1,3-dicarboxylate impacts on long-term potentiation in the dentate gyrus in the rat: analysis of age-related changes. *Neuroscience* **90**, 1167-1175.

- McGeer PL & McGeer EG. (1996). Anti-inflammatory drugs in the fight against Alzheimer's disease. *Ann N.Y. Acad Sci.* **777**, 213-220.
- McLay RN, Freeman SM, Harlan RE, Kastin AJ & Zadina JE. (1999). Tests used to assess the cognitive abilities of aged rats: their relation to each other and to hippocampal morphology and neurotrophin expression. *Gerontology* **45**, 143-155.
- Medzhitov R & Janeway CA, Jr. (1998). Innate immune recognition and control of adaptive immune responses. *Semin Immunol* **10**, 351-353.
- Merino JJ, Cordero MI & Sandi C. (2000). Regulation of hippocampal cell adhesion molecules NCAM and L1 by contextual fear conditioning is dependent upon time and stressor intensity. *Eur J Neurosci* **12**, 3283-3290.
- Merrill DA, Chiba AA & Tuszynski MH. (2001). Conservation of neuronal number and size in the entorhinal cortex of behaviorally characterized aged rats. *J Comp Neurol* **438**, 445-456.
- Merrill JE & Benveniste EN. (1996). Cytokines in inflammatory brain lesions: helpful and harmful. *Trends Neurosci* **19**, 331-338.
- Mihirshahi R, Barclay AN & Brown MH. (2009). Essential roles for Dok2 and RasGAP in CD200 receptor-mediated regulation of human myeloid cells. *J Immunol* **183**, 4879-4886.
- Mohammadi M, McMahon G, Sun L, Tang C, Hirth P, Yeh BK, Hubbard SR & Schlessinger J. (1997). Structures of the tyrosine kinase domain of fibroblast growth factor receptor in complex with inhibitors. *Science* **276**, 955-960.
- Morand EF & Leech M. (2001). Hypothalamic-pituitary-adrenal axis regulation of inflammation in rheumatoid arthritis. *Immunol Cell Biol* **79**, 395-399.
- Morga E, Faber C & Heuschling P. (1999). Regional heterogeneity of the astroglial immunoreactive phenotype: effect of lipopolysaccharide. *J Neurosci Res* **57**, 941-952.
- Morris RG, Anderson E, Lynch GS & Baudry M. (1986). Selective impairment of learning and blockade of long-term potentiation by an N-methyl-D-aspartate receptor antagonist, AP5. *Nature* **319**, 774-776.
- Morris RG, Garrud P, Rawlins JN & O'Keefe J. (1982). Place navigation impaired in rats with hippocampal lesions. *Nature* **297**, 681-683.
- Murakami M, Hibi M, Nakagawa N, Nakagawa T, Yasukawa K, Yamanishi K, Taga T & Kishimoto T. (1993). IL-6-induced homodimerization of gp130 and associated activation of a tyrosine kinase. *Science* **260**, 1808-1810.

- Murphy AC, Lalor SJ, Lynch MA & Mills KH. (2010). Infiltration of Th1 and Th17 cells and activation of microglia in the CNS during the course of experimental autoimmune encephalomyelitis. *Brain Behav Immun* **24**, 641-651.
- Murray CA & Lynch MA. (1998). Evidence that increased hippocampal expression of the cytokine interleukin-1 beta is a common trigger for age- and stress-induced impairments in long-term potentiation. *J Neurosci* **18**, 2974-2981.
- Napoli I & Neumann H. (2010). Protective effects of microglia in multiple sclerosis. *Exp Neurol* **225**, 24-8.
- Nathan C. (2002). Points of control in inflammation. *Nature* **420**, 846-852.
- Neiendam JL, Kohler LB, Christensen C, Li S, Pedersen MV, Ditlevsen DK, Kornum MK, Kiselyov VV, Berezin V & Bock E. (2004). An NCAM-derived FGF-receptor agonist, the FGL-peptide, induces neurite outgrowth and neuronal survival in primary rat neurons. *J Neurochem* **91**, 920-935.
- Nelson RW, Bates PA & Rutishauser U. (1995). Protein determinants for specific polysialylation of the neural cell adhesion molecule. *J Biol Chem* **270**, 17171-17179.
- Neumann H. (2001). Control of glial immune function by neurons. *Glia* **36**, 191-199.
- Nguyen T, Brunson D, Crespi CL, Penman BW, Wishnok JS & Tannenbaum SR. (1992). DNA damage and mutation in human cells exposed to nitric oxide in vitro. *Proc Natl Acad Sci U S A* **89**, 3030-3034.
- Nguyen VT & Benveniste EN. (2000). IL-4-activated STAT-6 inhibits IFN-gamma-induced CD40 gene expression in macrophages/microglia. *J Immunol* **165**, 6235-6243.
- Nichols NR. (1999). Glial responses to steroids as markers of brain aging. *J Neurobiol* **40**, 585-601.
- Niidome T, Nonaka H, Akaike A, Kihara T & Sugimoto H. (2009). Basic fibroblast growth factor promotes the generation of microtubule-associated protein 2-positive cells from microglia. *Biochem Biophys Res Commun* **390**, 1018-1022.
- Numata Y, Terui T, Okuyama R, Hirasawa N, Sugiura Y, Miyoshi I, Watanabe T, Kuramasu A, Tagami H & Ohtsu H. (2006). The accelerating effect of histamine on the cutaneous wound-healing process through the action of basic fibroblast growth factor. *J Invest Dermatol* **126**, 1403-1409.
- O'Donnell E, Vereker E & Lynch MA. (2000). Age-related impairment in LTP is accompanied by enhanced activity of stress-activated protein kinases: analysis of underlying mechanisms. *Eur J Neurosci* **12**, 345-352.
- O'Neill LA. (2002). Toll-like receptor signal transduction and the tailoring of innate immunity: a role for Mal? *Trends Immunol* **23**, 296-300.

- O'Neill LA & Greene C. (1998). Signal transduction pathways activated by the IL-1 receptor family: ancient signaling machinery in mammals, insects, and plants. *J Leukoc Biol* **63**, 650-657.
- Olsen M, Krog L, Edvardsen K, Skovgaard LT & Bock E. (1993). Intact transmembrane isoforms of the neural cell adhesion molecule are released from the plasma membrane. *Biochem J* **295** (Pt 3), 833-840.
- Olson JK & Miller SD. (2004). Microglia initiate central nervous system innate and adaptive immune responses through multiple TLRs. *J Immunol* **173**, 3916-3924.
- Ono J, Harada K, Hasegawa T, Sakurai K, Kodaka R, Tanabe Y, Tanaka J, Igarashi T, Nagai T & Okada S. (1994). Central nervous system abnormalities in chromosome deletion at 11q23. *Clin Genet* **45**, 325-329.
- Origlia N, Arancio O, Domenici L & Yan SS. (2009). MAPK, beta-amyloid and synaptic dysfunction: the role of RAGE. *Expert Rev Neurother* **9**, 1635-1645.
- Ornitz DM & Itoh N. (2001). Fibroblast growth factors. *Genome Biol* **2**, REVIEWS3005.
- Ornitz DM, Xu J, Colvin JS, McEwen DG, MacArthur CA, Coulier F, Gao G & Goldfarb M. (1996). Receptor specificity of the fibroblast growth factor family. *J Biol Chem* **271**, 15292-15297.
- Owens GC, Edelman GM & Cunningham BA. (1987). Organization of the neural cell adhesion molecule (N-CAM) gene: alternative exon usage as the basis for different membrane-associated domains. *Proc Natl Acad Sci U S A* **84**, 294-298.
- Pasti L, Volterra A, Pozzan T & Carmignoto G. (1997). Intracellular calcium oscillations in astrocytes: a highly plastic, bidirectional form of communication between neurons and astrocytes in situ. *J Neurosci* **17**, 7817-7830.
- Petermann KB, Rozenberg GI, Zedek D, Groben P, McKinnon K, Buehler C, Kim WY, Shields JM, Penland S, Bear JE, Thomas NE, Serody JS & Sharpless NE. (2007). CD200 is induced by ERK and is a potential therapeutic target in melanoma. *J Clin Invest* **117**, 3922-3929.
- Pike CJ, Walencewicz-Wasserman AJ, Kosmoski J, Cribbs DH, Glabe CG & Cotman CW. (1995). Structure-activity analyses of beta-amyloid peptides: contributions of the beta 25-35 region to aggregation and neurotoxicity. *J Neurochem* **64**, 253-265.
- Poitry-Yamate CL, Poitry S & Tsacopoulos M. (1995). Lactate released by Muller glial cells is metabolized by photoreceptors from mammalian retina. *J Neurosci* **15**, 5179-5191.
- Preston S, Wright GJ, Starr K, Barclay AN & Brown MH. (1997). The leukocyte/neuron cell surface antigen OX2 binds to a ligand on macrophages. *Eur J Immunol* **27**, 1911-1918.

- Pugh CR, Kumagawa K, Fleshner M, Watkins LR, Maier SF & Rudy JW. (1998). Selective effects of peripheral lipopolysaccharide administration on contextual and auditory-cue fear conditioning. *Brain Behav Immun* **12**, 212-229.
- Qin H, Wilson CA, Lee SJ, Zhao X & Benveniste EN. (2005). LPS induces CD40 gene expression through the activation of NF-kappaB and STAT-1alpha in macrophages and microglia. *Blood* **106**, 3114-3122.
- Quan N, Sundar SK & Weiss JM. (1994). Induction of interleukin-1 in various brain regions after peripheral and central injections of lipopolysaccharide. *J Neuroimmunol* **49**, 125-134.
- Ramsey MM, Weiner JL, Moore TP, Carter CS & Sonntag WE. (2004). Growth hormone treatment attenuates age-related changes in hippocampal short-term plasticity and spatial learning. *Neuroscience* **129**, 119-127.
- Rapp PR & Gallagher M. (1996). Preserved neuron number in the hippocampus of aged rats with spatial learning deficits. *Proc Natl Acad Sci U S A* **93**, 9926-9930.
- Regan CM & Fox GB. (1995). Polysialylation as a regulator of neural plasticity in rodent learning and aging. *Neurochem Res* **20**, 593-598.
- Ren L, Lubrich B, Biber K & Gebicke-Haerter PJ. (1999). Differential expression of inflammatory mediators in rat microglia cultured from different brain regions. *Brain Res Mol Brain Res* **65**, 198-205.
- Richwine AF, Parkin AO, Buchanan JB, Chen J, Markham JA, Juraska JM & Johnson RW. (2008). Architectural changes to CA1 pyramidal neurons in adult and aged mice after peripheral immune stimulation. *Psychoneuroendocrinology* **33**, 1369-1377.
- Risau W & Wolburg H. (1990). Development of the blood-brain barrier. *Trends Neurosci* **13**, 174-178.
- Ronn LC, Bock E, Linnemann D & Jahnsen H. (1995). NCAM-antibodies modulate induction of long-term potentiation in rat hippocampal CA1. *Brain Res* **677**, 145-151.
- Rothwell NJ. (1991). Functions and mechanisms of interleukin 1 in the brain. *Trends Pharmacol Sci* **12**, 430-436.
- Roy A, Fung YK, Liu X & Pahan K. (2006). Up-regulation of microglial CD11b expression by nitric oxide. *J Biol Chem* **281**, 14971-14980.
- Roy A, Jana A, Yatish K, Freidt MB, Fung YK, Martinson JA & Pahan K. (2008). Reactive oxygen species up-regulate CD11b in microglia via nitric oxide: Implications for neurodegenerative diseases. *Free Radic Biol Med* **45**, 686-699.
- Sandi C. (2004). Stress, cognitive impairment and cell adhesion molecules. *Nat Rev Neurosci* **5**, 917-930.

- Sastre M & Gentleman SM. (2010). NSAIDs: how they work and their prospects as therapeutics in Alzheimer's disease. *Front Aging Neurosci* **18**, 2-20.
- Schipper HM. (1996). Astrocytes, brain aging, and neurodegeneration. *Neurobiol Aging* **17**, 467-480.
- Schneider H, Pitossi F, Balschun D, Wagner A, del Rey A & Besedovsky HO. (1998). A neuromodulatory role of interleukin-1beta in the hippocampus. *Proc Natl Acad Sci USA* **95**, 7778-7783.
- Schonbeck U & Libby P. (2001). The CD40/CD154 receptor/ligand dyad. *Cell Mol Life Sci* **58**, 4-43.
- Scoville WB & Milner B. (1957). Loss of recent memory after bilateral hippocampal lesions. *J Neurol Neurosurg Psychiatry* **20**, 11-21.
- Seder RA. (1994). Acquisition of lymphokine-producing phenotype by CD4+ T cells. *J Allergy Clin Immunol* **94**, 1195-1202.
- Seki T & Arai Y. (1991). The persistent expression of a highly polysialylated NCAM in the dentate gyrus of the adult rat. *Neurosci Res* **12**, 503-513.
- Seki T & Rutishauser U. (1998). Removal of polysialic acid-neural cell adhesion molecule induces aberrant mossy fiber innervation and ectopic synaptogenesis in the hippocampus. *J Neurosci* **18**, 3757-3766.
- Selcher JC, Atkins CM, Trzaskos JM, Paylor R & Sweatt JD. (1999). A necessity for MAP kinase activation in mammalian spatial learning. *Learn Mem* **6**, 478-490.
- Sherman MA. (2001). The role of STAT6 in mast cell IL-4 production. *Immunol Rev* **179**, 48-56.
- Shohami E, Bass R, Wallach D, Yamin A & Gallily R. (1996). Inhibition of tumor necrosis factor alpha (TNFalpha) activity in rat brain is associated with cerebroprotection after closed head injury. *J Cereb Blood Flow Metab* **16**, 378-384.
- Simelyte E, Criado G, Essex D, Uger RA, Feldmann M & Williams RO. (2008). CD200-Fc, a novel antiarthritic biologic agent that targets proinflammatory cytokine expression in the joints of mice with collagen-induced arthritis. *Arthritis Rheum* **58**, 1038-1043.
- Sims JE, Gayle MA, Slack JL, Alderson MR, Bird TA, Giri JG, Colotta F, Re F, Mantovani A, Shanebeck K & et al. (1993). Interleukin 1 signaling occurs exclusively via the type I receptor. *Proc Natl Acad Sci U S A* **90**, 6155-6159.
- Skibo GG, Lushnikova IV, Voronin KY, Dmitrieva O, Novikova T, Klementiev B, Vaudano E, Berezin VA & Bock E. (2005). A synthetic NCAM-derived peptide, FGL, protects hippocampal neurons from ischemic insult both in vitro and in vivo. *Eur J Neurosci* **22**, 1589-1596.

- Skladchikova G, Ronn LC, Berezin V & Bock E. (1999). Extracellular adenosine triphosphate affects neural cell adhesion molecule (NCAM)-mediated cell adhesion and neurite outgrowth. *J Neurosci Res* **57**, 207-218.
- Snelgrove RJ, Goulding J, Didierlaurent AM, Lyonga D, Vekaria S, Edwards L, Gwyer E, Sedgwick JD, Barclay AN & Hussell T. (2008). A critical function for CD200 in lung immune homeostasis and the severity of influenza infection. *Nat Immunol* **9**, 1074-1083.
- Sobel RA, Mitchell ME & Fondren G. (1990). Intercellular adhesion molecule-1 (ICAM-1) in cellular immune reactions in the human central nervous system. *Am J Pathol* **136**, 1309-1316.
- Solovjov DA, Pluskota E & Plow EF. (2005). Distinct roles for the alpha and beta subunits in the functions of integrin alphaMbeta2. *J Biol Chem* **280**, 1336-1345.
- Soroka V, Kolkova K, Kastrup JS, Diederichs K, Breed J, Kiselyov VV, Poulsen FM, Larsen IK, Welte W, Berezin V, Bock E & Kasper C. (2003). Structure and interactions of NCAM Ig1-2-3 suggest a novel zipper mechanism for homophilic adhesion. *Structure* **11**, 1291-1301.
- Soulet D & Rivest S. (2008). Microglia. *Curr Biol* **18**, R506-508.
- Spriggs DR, Sherman ML, Frei E, 3rd & Kufe DW. (1987). Clinical studies with tumour necrosis factor. *Ciba Found Symp* **131**, 206-227.
- Sze CI, Troncoso JC, Kawas C, Mouton P, Price DL & Martin LJ. (1997). Loss of the presynaptic vesicle protein synaptophysin in hippocampus correlates with cognitive decline in Alzheimer disease. *J Neuropathol Exp Neurol* **56**, 933-944.
- Taga T & Kishimoto T. (1997). Gp130 and the interleukin-6 family of cytokines. *Annu Rev Immunol* **15**, 797-819.
- Takao T, Tracey DE, Mitchell WM & De Souza EB. (1990). Interleukin-1 receptors in mouse brain: characterization and neuronal localization. *Endocrinology* **127**, 3070-3078.
- Tan J, Hua Q, Gao J & Fan ZX. (2008). Clinical implications of elevated serum interleukin-6, soluble CD40 ligand, metalloproteinase-9, and tissue inhibitor of metalloproteinase-1 in patients with acute ST-segment elevation myocardial infarction. *Clin Cardiol* **31**, 413-418.
- Tan J, Town T, Paris D, Mori T, Suo Z, Crawford F, Mattson MP, Flavell RA & Mullan M. (1999). Microglial activation resulting from CD40-CD40L interaction after beta-amyloid stimulation. *Science* **286**, 2352-2355.
- The MHC sequencing consortium (1999). Complete sequence and gene map of a human major histocompatibility complex. *Nature* **401**, 921-923.

- Thiery JP. (2003). Cell adhesion in development: a complex signaling network. *Curr Opin Genet Dev* **13**, 365-371.
- Thiery JP, Brackenbury R, Rutishauser U & Edelman GM. (1977). Adhesion among neural cells of the chick embryo. II. Purification and characterization of a cell adhesion molecule from neural retina. *J Biol Chem* **252**, 6841-6845.
- Thornberry NA, Bull HG, Calaycay JR, Chapman KT, Howard AD, Kostura MJ, Miller DK, Molineaux SM, Weidner JR, Aunins J & et al. (1992). A novel heterodimeric cysteine protease is required for interleukin-1 beta processing in monocytes. *Nature* **356**, 768-774.
- Tobinick E, Gross H, Weinberger A & Cohen H. (2006). TNF-alpha modulation for treatment of Alzheimer's disease: a 6-month pilot study. *MedGenMed* **8**, 25.
- Town T, Tan J & Mullan M. (2001). CD40 signaling and Alzheimer's disease pathogenesis. *Neurochem Int* **39**, 371-380.
- Townsend KP, Town T, Mori T, Lue LF, Shytle D, Sanberg PR, Morgan D, Fernandez F, Flavell RA & Tan J. (2005). CD40 signaling regulates innate and adaptive activation of microglia in response to amyloid beta-peptide. *Eur J Immunol* **35**, 901-910.
- Trejo JL, Piriz J, Llorens-Martin MV, Fernandez AM, Bolos M, LeRoith D, Nunez A & Torres-Aleman I. (2007). Central actions of liver-derived insulin-like growth factor I underlying its pro-cognitive effects. *Mol Psychiatry* **12**, 1118-1128.
- Valtorta F, Pennuto M, Bonanomi D & Benfenati F. (2004). Synaptophysin: leading actor or walk-on role in synaptic vesicle exocytosis? *Bioessays* **26**, 445-453.
- Van Wagoner NJ & Benveniste EN. (1999). Interleukin-6 expression and regulation in astrocytes. *J Neuroimmunol* **100**, 124-139.
- Van Wagoner NJ, Oh JW, Repovic P & Benveniste EN. (1999). Interleukin-6 (IL-6) production by astrocytes: autocrine regulation by IL-6 and the soluble IL-6 receptor. *J Neurosci* **19**, 5236-5244.
- Vereker E, Campbell V, Roche E, McEntee E & Lynch MA. (2000). Lipopolysaccharide inhibits long term potentiation in the rat dentate gyrus by activating caspase-1. *J Biol Chem* **275**, 26252-26258.
- Vereker E, O'Donnell E, Lynch A, Kelly A, Nolan Y & Lynch MA. (2001). Evidence that interleukin-1beta and reactive oxygen species production play a pivotal role in stress-induced impairment of LTP in the rat dentate gyrus. *Eur J Neurosci* **14**, 1809-1819.
- Vidyadaran S, Ooi YY, Subramaiam H, Badiei A, Abdullah M, Ramasamy R & Seow HF. (2009). Effects of macrophage colony-stimulating factor on microglial responses to lipopolysaccharide and beta amyloid. *Cell Immunol* **259**, 105-110.

- Walker DG, Dalsing-Hernandez JE, Campbell NA & Lue LF. (2009). Decreased expression of CD200 and CD200 receptor in Alzheimer's disease: a potential mechanism leading to chronic inflammation. *Exp Neurol* **215**, 5-19.
- Wang DD & Bordey A. (2008). The astrocyte odyssey. *Prog Neurobiol* **86**, 342-367.
- Watson MB, Costello DA, Carney DG, McQuillan K & Lynch MA. (2010). SIGIRR modulates the inflammatory response in the brain. *Brain Behav Immun* **24**, 985-995.
- Webb AC, Collins KL, Auron PE, Eddy RL, Nakai H, Byers MG, Haley LL, Henry WM & Shows TB. (1986). Interleukin-1 gene (IL1) assigned to long arm of human chromosome 2. *Lymphokine Res* **5**, 77-85.
- Wekerle H, Schwab M, Linington C & Meyermann R. (1986). Antigen presentation in the peripheral nervous system: Schwann cells present endogenous myelin autoantigens to lymphocytes. *Eur J Immunol* **16**, 1551-1557.
- Wilkinson BL, Cramer PE, Varvel NH, Reed-Geaghan E, Jiang Q, Szabo A, Herrup K, Lamb BT & Landreth GE. (2010). Ibuprofen attenuates oxidative damage through NOX2 inhibition in Alzheimer's disease. *Neurobiol Aging* [Epub ahead of print].
- Willaime-Morawek S, Arbez N, Mariani J & Brugg B. (2005). IGF-I protects cortical neurons against ceramide-induced apoptosis via activation of the PI-3K/Akt and ERK pathways; is this protection independent of CREB and Bcl-2? *Brain Res Mol Brain Res* **142**, 97-106.
- Williams EJ, Walsh FS & Doherty P. (1994). The production of arachidonic acid can account for calcium channel activation in the second messenger pathway underlying neurite outgrowth stimulated by NCAM, N-cadherin, and L1. *J Neurochem* **62**, 1231-1234.
- Wolf FI, Fasanella S, Tedesco B, Cavallini G, Donati A, Bergamini E & Cittadini A. (2005). Peripheral lymphocyte 8-OHdG levels correlate with age-associated increase of tissue oxidative DNA damage in Sprague-Dawley rats. Protective effects of caloric restriction. *Exp Gerontol* **40**, 181-188.
- Wright GJ, Puklavec MJ, Willis AC, Hoek RM, Sedgwick JD, Brown MH & Barclay AN. (2000). Lymphoid/neuronal cell surface OX2 glycoprotein recognizes a novel receptor on macrophages implicated in the control of their function. *Immunity* **13**, 233-242.
- Yamamoto T, Ochalski A, Hertzberg EL & Nagy JI. (1990). On the organization of astrocytic gap junctions in rat brain as suggested by LM and EM immunohistochemistry of connexin43 expression. *J Comp Neurol* **302**, 853-883.
- Yan HQ, Banos MA, Herregodts P, Hooghe R & Hooghe-Peters EL. (1992). Expression of interleukin (IL)-1 beta, IL-6 and their respective receptors in the normal rat brain and after injury. *Eur J Immunol* **22**, 2963-2971.

- Zeinstra E, Wilczak N, Streefland C & De Keyser J. (2000). Astrocytes in chronic active multiple sclerosis plaques express MHC class II molecules. *Neuroreport* **11**, 89-91.
- Zen K, Utech M, Liu Y, Soto I, Nusrat A & Parkos CA. (2004). Association of BAP31 with CD11b/CD18. Potential role in intracellular trafficking of CD11b/CD18 in neutrophils. *J Biol Chem* **279**, 44924-44930.
- Zerlin M, Levison SW & Goldman JE. (1995). Early patterns of migration, morphogenesis, and intermediate filament expression of subventricular zone cells in the postnatal rat forebrain. *J Neurosci* **15**, 7238-7249.
- Zhang S & Phillips JH. (2006). Identification of tyrosine residues crucial for CD200R-mediated inhibition of mast cell activation. *J Leukoc Biol* **79**, 363-368.
- Zheng WH & Quirion R. (2006). Insulin-like growth factor-1 (IGF-1) induces the activation/phosphorylation of Akt kinase and cAMP response element-binding protein (CREB) by activating different signaling pathways in PC12 cells. *BMC Neurosci* **7**, 51.
- Zonta M, Angulo MC, Gobbo S, Rosengarten B, Hossmann KA, Pozzan T & Carmignoto G. (2003). Neuron-to-astrocyte signaling is central to the dynamic control of brain microcirculation. *Nat Neurosci* **6**, 43-50.

Appendix: Mean Data

Chapter 3

RQ	Rat Mixed Glial Cells					
	Control	FGL 10 μ g/ml	LPS1 μ g/ml			
				FGL 1 μ g/ml	FGL 10 μ g/ml	FGL 100 μ g/ml
CD40 mRNA	0.94 \pm 0.11	1.04 \pm 0.25	8.24 \pm 0.74	6.04 \pm 0.23	1.34 \pm 0.35	1.2745 \pm 0.41

Table I. Raw data from dose response curve, LPS and FGL-treated rat mixed glia. Values are expressed as means \pm SEM.

Variable Units	Rat Mixed Glial Cells			
	Control	LPS1 μ g/ml	FGL10 μ g/ml	FGL+LPS
CD11b mRNA (RQ)	2.20 \pm 0.46	12.33 \pm 1.91	3.31 \pm 0.97	8.08 \pm 1.07
IL-1 β mRNA (RQ)	2.71 \pm 0.82	294.48 \pm 88.21	21.25 \pm 11.82	148 \pm 30.71
IL-1 β (pg/ml)	11.72 \pm 4.25	153.80 \pm 17.86	15.85 \pm 4.27	67.82 \pm 10.29
IL-6 (pg/ml)	91.20 \pm 51.97	2147.35 \pm 310.89	176.48 \pm 81.56	1554.01 \pm 195.68

Table II. Raw data from LPS and FGL-treated rat mixed glia. Values are expressed as means \pm SEM.

Variable Units	Rat Mixed Glial Cells						
	Control	LPS	FGL+LPS	SU5402			
				10 μ g/ml	10 μ g/ml FGL+LPS	25 μ g/ml FGL+LPS	50 μ g/ml FGL+LPS
IL-1 β mRNA (RQ)	5.62 \pm 4.40	136.91 \pm 20.35	71.0 \pm 13.0	N/A	112.21 \pm 45.14	218.98 \pm 17.73	N/A
IL-1 β (pg/ml)	11.72 \pm 4.25	153.79 \pm 17.86	67.82 \pm 10.29	15.85 \pm 4.27	50.74 \pm 15.73	82.09 \pm 12.99	136.33 \pm 21.57

Table III. Raw data from LPS, FGL and SU5402-treated rat mixed glia. Values are expressed as means \pm SEM.

Variable Units	Isolated Microglia			
	Control	LPS1 μ g/ml	FGL10 μ g/ml	FGL+LPS
IL-1 β mRNA (RQ)	0.62 \pm 0.10	1.90 \pm 0.59	0.67 \pm 0.11	3.37 \pm 0.57
IL-1 β (pg/ml)	270.38 \pm 41.9	461.63 \pm 33.29	207.16 \pm 17.69	328.69 \pm 8.99
IL-1 β mRNA (RQ)	Isolated Astrocytes			
	0.76 \pm 0.080	356.52 \pm 13.19	0.59 \pm 0.08	289.78 \pm 11.91

Table IV. Raw data from LPS and FGL-treated isolated microglia and astrocytes. Values are expressed as means \pm SEM.

Variable Units	Rat Mixed Glial Cells					
	Control	LPS	A β_{25-35}			
			1Mm	10 μ M	20 μ M	50 μ M
MHC II mRNA (RQ)	0.95 \pm 0.02	0.93 \pm 0.08	0.91 \pm 0.05	0.87 \pm 0.05	1.44 \pm 0.15	1.92 \pm 0.20
IL-1 β mRNA (RQ)	Control		7.16 \pm 2.93	7.42 \pm 2.33	17.13 \pm 5.094	44.99 \pm 15.74
	2.34 \pm 0.61					
IL-1 β (pg/ml)	14.42 \pm 2.55		20.23 \pm 4.71	21.20 \pm 5.41	25.28 \pm 4.29	35.72 \pm 7.04

Table V. Raw data from LPS and A β -treated rat mixed glial cells. Values are expressed as means \pm SEM.

RQ	Rat Mixed Glial Cells			
	Control	A β_{25-35} 20 μ M	FGL10 μ g/ml	FGL+ A β_{25-35}
CD40 mRNA	0.58 \pm 0.18	1.48 \pm 0.38	0.46 \pm 0.07	1.71 \pm 0.28
IL-1 β mRNA	2.75 \pm 0.66	12.65 \pm 3.88	1.32 \pm 0.76	1.39 \pm 0.31

Table VI. Raw data from A β and FGL-treated rat mixed glia cells. Values are expressed as means \pm SEM.

Chapter 4

RQ	Mouse Mixed Glial Cells	
	Wildtype	CD200 ^{-/-}
CD11b mRNA	1.40±0.50	7.14±0.88
CD68 mRNA	1.05±0.24	6.39±0.60

Table VII. Raw data from mixed glia prepared from wildtype and CD200^{-/-} mice. Values are expressed as means ± SEM.

Variable Units	Mouse Mixed Glial Cells							
	Wildtype				CD200 ^{-/-}			
	Control	LPS	FGL	FGL+ LPS	Control	LPS	FGL	FGL+ LPS
CD40 mRNA (RQ)	0.28	24.48	0.16	0.06	0.04	54.0	0.02	52.32
	± 0.18	± 8.69	± 0.01	± 0.02	± 0.01	± 18.51	± 0.004	± 11.37
ICAM-1 mRNA (RQ)	2.12	91.06	2.27	1.09	2.73	148.38	2.78	177.21
	± 0.48	± 19.75	± 0.50	± 0.41	± 0.47	± 18.18	± 0.34	± 27.56
CD11b mRNA (RQ)	1.40	4.51	1.57	1.24	7.14	23.99	9.16	28.38
	± 0.50	± 0.76	± 0.25	± 0.16	± 0.96	± 2.07	± 1.27	± 2.94
IL-1β mRNA (RQ)	0.37	8.13	0.97	0.66	0.59	13.08	0.82	17.21
	± 0.20	± 0.68	± 0.32	± 0.13	± 0.066	± 0.75	± 0.21	± 1.25
IL-1β (pg/ml)	3.47	18.66	1.86	0.48	4.17	464.31	2.24	355.61
	± 1.04	± 4.07	± 0.98	± 0.20	± 3.13	± 151.40	± 2.24	± 124.04
TNF-α mRNA (RQ)	12.24	113.98	6.36	3.77	6.93	176.21	11.04	219.64
	± 7.62	± 14.18	± 3.18	± 0.71	± 2.02	± 15.67	± 1.75	± 23.08
TNF-α (pg/ml)	94.63	1322.5	355.4	231.20	57.15	5507.4	309.70	5092.43
	± 63.37	± 184.85	± 70.09	± 112.57	± 37.53	± 429.94	± 176.45	± 179.88
IL-6 mRNA (RQ)	65.65	336.94	36.69	83.59	22.11	551.38	39.78	606.96
	± 14.97	± 32.91	± 10.77	± 21.68	± 6.44	± 98.98	± 8.98	± 37.47
IL-6 (pg/ml)	42.16	6526.1	100.54	51.73	90.66	18642	113.89	18231.9
	± 5.92	± 312.87	± 20.47	± 11.50	± 13.91	± 136.79	± 17.28	± 352.79

Table VIII. Raw data from LPS and FGL-treated mixed glia prepared from wildtype and CD200^{-/-} mice. Values are expressed as means ± SEM.

Arbitrary Units	Isolated Astrocytes	
	Control	FGL
CD200	0.33±0.04	0.53±0.04

Table IX. Raw data from purified mouse astrocytes exposed to FGL. Values are expressed as means ± SEM.

Variable Units	Isolated Microglia			
	Control	LPS	Astrocytic Membrane	Membrane+ LPS
IL-1 β mRNA (RQ)	0.46±0.20	9.43±1.14	3.27±1.03	2.16±0.83
TNF- α mRNA (RQ)	5.09±1.83	22.48±1.68	10.75±3.548	11.09±3.40
TNF- α (pg/ml)	8.81±4.55	52.78±10.44	3.21±0.88	4.52±1.63
IL-6 mRNA (RQ)	3.76±1.66	45.46±12.44	3.13±1.45	18.04±12.76
IL-6 (pg/ml)	6.53±1.85	22.26±4.75	6.16±1.43	8.63±1.78
LDH Assay (% of Control)	100±0	103.94±0.80	96.47±0.26	98.69±1.96

Table X. Raw data of purified mouse microglia exposed to LPS and astrocytic membrane fraction. Values are expressed as means ± SEM.

Chapter 5

% EPSP Slope (Last 10 minutes)	LTP			
	Young Control	Young CD200Fc	Young LPS	Young CD200Fc+LPS
	118.07±0.25	124.45±0.49	107.51±0.28	124.08±0.42
	Young Control	Young CD200Fc	Aged Control	Aged CD200Fc
	153.17±0.90	148.24±0.67	113.49±0.35	147.73±0.72

Table XI. Raw data of LTP in perforant path-granule cell synapses. Values are expressed as means ± SEM.

Arbitrary Units	Hippocampal Tissue	
	Young	Aged
Synaptophysin	1.35±0.05	1.18±0.05
CD200	6.30±0.61	4.12±0.60

Table XII. Raw data from young and aged hippocampus. Values are expressed as means ± SEM.

Variable Units	Hippocampal Tissue			
	Young Control	Young CD200Fc	Aged Control	Aged CD200Fc
GFAP mRNA (RQ)	0.68±0.095	0.718±0.05	1.14±0.15	0.83±0.06
MHC II mRNA (RQ)	0.81±0.06	0.90±0.06	1.08±0.07	0.87±0.03
CD40 mRNA (RQ)	0.68±0.145	0.92±0.17	1.47±0.30	0.50±0.12
iNOS mRNA (RQ)	2.44±0.64	2.99±0.91	5.63±1.19	3.34±0.39
IGF-1 (pg/ml)	135.24±23.30	190.46±33.16	82.27±15.90	162.28±23.33
pARK (Arbitrary Units)	37.34±4.31	32.12±5.65	11.58±2.55	20.96±3.03

Table XIII. Raw data from hippocampus of young and aged rats that received CD200Fc. Values are expressed as means ± SEM.

Variable Units	Rat Mixed Glial Cells					
	Control	LPS	CD200Fc (µg/ml) + LPS			
			2.5	5	7.5	5+LY294002
Nitrite (µM)	0.76 ± 0.10	1.40 ± 0.44	0.97 ± 0.12	0.71 ± 0.14	0.59 ± 0.10	0.76 ± 0.05

Table XIV. Raw data of rat mixed glia treated with LPS and CD200Fc. Values are expressed as means ± SEM.

A synthetic NCAM-derived mimetic peptide, FGL, exerts anti-inflammatory properties via IGF-1 and interferon- γ modulation

Eric J. Downer,^{*,1} Thelma R. Cowley,^{*} Fionnuala Cox,^{*} Francis O. Maher,^{*} Vladimir Berezin,[†] Elisabeth Bock[†] and Marina A. Lynch^{*}

^{*}Trinity College Institute for Neuroscience, Physiology Department, Trinity College, Dublin, Ireland

[†]Protein Laboratory, Institute of Neuroscience and Pharmacology, School of Medicine, University of Copenhagen, Copenhagen, Denmark

Abstract

Microglial cell activity increases in the rat hippocampus during normal brain aging. The neural cell adhesion molecule (NCAM)-derived mimetic peptide, FG loop (FGL), acts as an anti-inflammatory agent in the hippocampus of the aged rat, promoting CD200 ligand expression while attenuating glial cell activation and subsequent pro-inflammatory cytokine production. The aim of the current study was to determine if FGL corrects the age-related imbalance in hippocampal levels of insulin-like growth factor-1 (IGF-1) and pro-inflammatory interferon- γ (IFN γ), and subsequently attenuates the glial reactivity associated with aging. Administration of FGL reversed the age-related decline in IGF-1 in hippocampus, while abrogating the age-related increase in IFN γ . FGL robustly promotes IGF-1 release from primary neurons and IGF-1 is

pivotal in FGL induction of neuronal Akt phosphorylation and subsequent CD200 ligand expression *in vitro*. In addition, FGL abrogates both age- and IFN γ -induced increases in markers of glial cell activation, including major histocompatibility complex class II (MHCII) and CD40. Finally, the proclivity of FGL to attenuate IFN γ -induced glial cell activation *in vitro* is IGF-1-dependent. Overall, these findings suggest that FGL, by correcting the age-related imbalance in hippocampal levels of IGF-1 and IFN γ , attenuates glial cell activation associated with aging. These findings also highlight a novel mechanism by which FGL can impact on neuronal CD200 ligand expression and subsequently on glial cell activation status.

Keywords: age, CD200, insulin-like growth factor-1, interferon- γ , microglia, neural cell adhesion molecule.

J. Neurochem. (2009) **109**, 1516–1525.

Brain glial cells, including microglia and astrocytes, become reactive during normal brain aging, an event associated with cytokine imbalance (Kim and Joh 2006), blunting of neuronal expression of CD200 ligand (Lyons *et al.* 2007b; Downer *et al.* 2008) and synaptic dysfunction (Wang *et al.* 2004; Griffin *et al.* 2006). The activity of microglia is regulated by maintaining a balance between inhibitory and activating signals. Interferon- γ (IFN γ), a type II pro-inflammatory cytokine, is one of the most potent microglial cell activators, inducing the expression of CD40 via signal transducer and activator of transcription (STAT)-1 α on activated microglia (Benveniste *et al.* 2004). However, recent evidence also highlights the fact that interaction between microglia and neurons regulates the activation status of microglia, with the neuronal membrane glycoprotein CD200 providing a key inhibitory signal (Hoek *et al.* 2000; Lyons *et al.* 2007b). CD200, which is widely expressed on endothelial cells, dendritic cells and neurons (Preston *et al.* 1997; Matsumoto *et al.* 2007), interacts with its structurally

similar receptor (CD200R), the expression of which is restricted to cells of the myeloid lineage, including microglia (Barclay *et al.* 2002).

The neural cell adhesion molecule (NCAM) is a membrane-associated glycoprotein expressed abundantly on

Received November 17, 2008; revised manuscript received March 25, 2009; accepted March 25, 2009.

Address correspondence and reprints requests to Eric J. Downer, Trinity College Institute for Neuroscience, Physiology Department, Trinity College, Dublin 2, Ireland. E-mail: Eric.Downer@nuim.ie

¹The present address of Eric J. Downer is the Institute of Immunology, Department of Biology, National University of Ireland, Maynooth, County Kildare, Ireland.

Abbreviations used: A β , β -amyloid; ERK, extracellular signal-regulated kinase; FGFR, fibroblast growth factor receptor; IFN γ , interferon- γ ; IGF-1, insulin-like growth factor-1; IL-4, interleukin-4; LPS, lipopolysaccharide; LTP, long-term potentiation; MAPK, mitogen-activated protein kinase; MHCII, major histocompatibility complex II; NCAM, neural cell adhesion molecule; PI-3 kinase, phosphatidylinositol-3 kinase; STAT, signal transducer and activator of transcription.

neurons and glial cells where it engages in cell-cell interactions (Welzl and Stork 2003). NCAM is pivotal in synaptogenesis (Cremer *et al.* 1997), neuroprotection (Skibo *et al.* 2005), plasticity and learning (Sandi *et al.* 2003). Furthermore, NCAM modulates many intracellular signaling events by heterophilic interaction with the fibroblast growth factor receptor (FGFR) (Kiselyov *et al.* 2003), resulting in activation of protein kinase C (Kolkova *et al.* 2000), phosphatidylinositol-3 kinase (PI-3 kinase) (Ditlevsen *et al.* 2003; Neiiendam *et al.* 2004) and extracellular signal-regulated kinase (ERK) (Neiiendam *et al.* 2004) signaling events. A peptide mimicking the heterophilic interaction between NCAM and FGFR1 has been developed (Berezin and Bock 2004). This peptide, identified as FG loop (FGL), is derived from the second fibronectin type III module of NCAM. *In vitro*, FGL acts as a neuroprotectant (Skibo *et al.* 2005) in addition to promoting neurite outgrowth (Neiiendam *et al.* 2004), enhancing pre-synaptic function (Cambon *et al.* 2004; Skibo *et al.* 2005) and acting as an anti-inflammatory peptide (Downer *et al.* 2008). *In vivo*, neuroprotective (Skibo *et al.* 2005; Klementiev *et al.* 2007) and memory enhancing properties of FGL have been demonstrated (Cambon *et al.* 2004; Downer *et al.* 2008).

Our laboratory has demonstrated that FGL can regulate cytokine levels in glial cells, promoting the production of the anti-inflammatory cytokine interleukin-4 (IL-4), which acts on neurons to maintain CD200 ligand expression (Downer *et al.* 2008). By regulating CD200 expression at the neuronal membrane, FGL maintains the CD200-CD200R interaction between neurons and glia, and subsequently attenuates glial cell activation. Furthermore, we (Downer *et al.* 2008) and others (Petermann *et al.* 2007) have demonstrated the role of the ERK pathway in regulating CD200 expression in primary neurons and melanoma cell lines, respectively. It is noteworthy that there are declining levels of the polypeptide hormone, insulin-like growth factor-1 (IGF-1), in the normal aging brain (Anderson *et al.* 2002), and this decline mirrors the expression profile of CD200 (Downer *et al.* 2008). IGF-1, in addition to being a key inhibitor of IFN γ -induced microglial activation (Maher *et al.* 2006), is a stimulator of the ERK and PI-3 kinase/Akt pathway in neurons (Willaime-Morawek *et al.* 2005; Zheng and Quirion 2006).

We set out to delineate the mechanism by which FGL modulates the neuroinflammatory changes in the hippocampus of the aged rat, to further identify the molecular signaling mechanism by which FGL regulates glial cell activation *in vitro* and to determine the role of IGF-1, Akt and ERK signaling in the modulation of CD200. We demonstrate a novel mechanism by which FGL regulates neuronal CD200 ligand expression, by promoting neuronal production of IGF-1, which in turn enhances CD200 ligand via PI 3-kinase/Akt and ERK signaling events. The data also show that FGL can ameliorate IFN γ -induced glial cell activation in an IGF-1-dependent manner. The evidence indicates that these changes

are consistent with the observation that FGL reversed the age-related changes in IGF-1 and IFN γ in the hippocampus.

Materials and methods

Animals and treatments

Male Wistar rats (Trinity College, Dublin, Ireland) aged 4 months (250–350 g) or 22 months (550–650 g) were housed under a 12 h light schedule with controlled ambient temperature (22–23°C) and maintained under veterinary supervision throughout the study. These experiments were performed under a license issued by the Department of Health (Ireland) and in accordance with the guidelines laid down by the local ethical committee. FGL (8 mg/kg) or vehicle (sterile water) was injected subcutaneously on alternate days for 3 weeks. The dose and route of administration was based on previous publications (Secher *et al.* 2006). The injected form (dimeric) of the peptide consists of two FGL monomers linked at the N-terminal. This dimeric form of FGL has been selected for clinical development (Anand *et al.* 2007). Rats were anesthetized 24 h following final FGL injection by intraperitoneal injection of urethane (1.5 g/kg), killed by cervical dislocation and hippocampal tissue frozen.

Preparation of primary cultures and treatments

Mixed glia were prepared from the cortices of 1-day-old Wistar rats (Trinity College, Dublin, Ireland), and plated on 6-well plates (160 $\mu\text{L}/\text{cm}^2$) at 0.25×10^6 cells/mL as previously described (Nolan *et al.* 2005). After 2 weeks, mixed glia were pre-treated with FGL (0.1–10 $\mu\text{g}/\text{mL}$) for 24 h and incubated in the presence or absence of IFN γ (10 ng/mL; 1 endotoxin unit/ μg ; Peprotech, London, UK) for 24 h. In a second experiment, mixed glia were exposed to an anti-IGF-1 antibody (10 $\mu\text{g}/\text{mL}$; Millipore, Cork, Ireland) for 30 min prior to FGL (10 $\mu\text{g}/\text{mL}$; 24 h) and subsequent IFN γ (10 ng/mL; 24 h) exposure.

Cultured neurons were prepared from the cortices of 1-day-old Wistar rats (BioResources Unit, Trinity College, Dublin) and plated on 24-well plates (30 $\mu\text{L}/\text{cm}^2$) at 0.25×10^6 cells/mL as previously described (Nolan *et al.* 2005). The purity of neuronal cultures was determined by visual counting of markers of astrocytes and microglia. Findings from eight independent experiments determined a neuronal purity of >95%. Neurons were treated with FGL (1–100 $\mu\text{g}/\text{mL}$), IGF-1 (100 ng/mL; R&D Systems, Abingdon, UK) or IL-4 (200 ng/mL; R&D Systems) for 24 h. In other experiments, neurons were pre-treated with the specific PI-3 kinase inhibitor LY 294002 (10 μM ; Calbiochem, Nottingham, UK), the FGFR inhibitor SU5402 (10 μM ; Calbiochem) or an anti-IGF-1 antibody (1–10 $\mu\text{g}/\text{mL}$; Millipore) for 30 min prior to FGL (100 $\mu\text{g}/\text{mL}$; 24 h) exposure. Finally, neurons were pre-treated with the mitogen-activated protein kinase (MAPK)/ERK kinase (MEK) inhibitor PD98059 (50 μM ; Merck Biosciences Ltd., Nottingham, UK) for 1 h prior to exposure to FGL (100 $\mu\text{g}/\text{mL}$; 24 h).

Analysis of IFN γ and IGF-1

IFN γ and IGF-1 were assessed in hippocampal homogenates and in samples of supernatant from neuronal cultures (for IGF-1) by enzyme-linked immunosorbent assay (R&D Systems) as previously described (Maher *et al.* 2006).

RNA isolation and cDNA synthesis

RNA was extracted from hippocampal tissue and cultured neurons/glia using a NucleoSpin® RNAII isolation kit (Macherey-Nagel Inc., Duren, Germany) and the concentration was determined using a UV/Vis spectrophotometer (Beckman Coulter Inc., Galway, Ireland). cDNA synthesis was performed on 1–2 µg RNA using a High Capacity cDNA RT Kit (Applied Biosystems, CA, USA) according to the manufacturer's instructions. Equal amounts of cDNA were used for RT-PCR amplification.

Real-time PCR

Real-time PCR primers were delivered as "Taqman® Gene Expression Assays" containing forward and reverse primers, and a FAM-labeled MGB Taqman probe for each gene (Applied Biosystems). Primers used were as follows: IGF-1, IFN γ , major histocompatibility complex II (MHCII) and CD40 (Taqman® Gene Expression Assay no. Rn00710306_m1, Rn00594078_m1, Rn01768597_m1 and Rn01423583_m1, respectively). A 1 in 4 dilution of cDNA was prepared and real-time PCR performed using Applied Biosystems 7300 Real-time PCR System. cDNA was mixed with qPCR™ Mastermix Plus (Applied Biosystems) and the respective gene assay in a 25 µL volume (10 µL of diluted cDNA, 12.5 µL Taqman® Universal PCR Mastermix, 1.25 µL target primer and 1.25 µL β -actin). Rat β -actin was used as an endogenous control and expression was conducted using a gene expression assay containing forward and reverse primers and a VIC-labeled MGB Taqman probe (#4352340E; Applied Biosystems). Samples were run in duplicate and 40 cycles were run as follows: 10 min at 95°C and for each cycle, 15 s at 95°C and 1 min at 60°C. Gene expression was calculated relative to the endogenous control and analysis was performed using the $2^{-\Delta\Delta CT}$ method. In all experiments no change in relative β -actin mRNA expression between treatment groups was observed.

Western immunoblotting

CD200 ligand and phosphorylated Akt were separated by SDS-PAGE as previously described (Lyons *et al.* 2007a). Protein expression was detected using goat polyclonal CD200 antibody (1 : 200; overnight at 4°C; Santa Cruz Biotechnology Inc., CA, USA) and rabbit monoclonal phospho-Akt (Ser473) antibody (1 : 1000; overnight at 4°C; Cell Signaling Technology, Wicklow, Ireland). Membranes were stripped (Re-blot Plus; Chemicon International Inc., CA, USA) and incubated with mouse monoclonal anti- β -actin antibody (1 : 10,000; overnight at 4°C, Sigma-Aldrich, Dublin, Ireland). Molecular weight markers were used to confirm molecular weight of bands. Data represent the ratio of density of the target protein to β -actin. No significant changes were observed in β -actin.

Statistical analysis

Data are expressed as means with standard errors (SE), and the results represent two or three independent experiments. Statistical comparisons of different treatments were performed by either Student's *t*-test for independent means (data in Fig. 2d), or a one-way or two-way analysis of variance (ANOVA) using a post hoc Student–Newman–Keuls test, as appropriate. Differences with a *P*-value < 0.05 were considered statistically significant.

Results

FGL reverses age-related changes in IGF-1 and IFN γ *in vivo*

Here we analyzed IGF-1 and IFN γ mRNA and protein expression in hippocampal tissue prepared from vehicle- and FGL-treated, young and aged, rats. Two-way ANOVA analysis revealed that treatment of aged animals with FGL reversed the age-related decline in IGF-1 mRNA (age \times FGL interaction: $F_{(1,22)} = 4.54$, $^+p < 0.05$; Fig. 1a) and protein expression (age \times FGL interaction: $F_{(1,23)} = 5.24$, $^+p < 0.05$; Fig. 1b). IGF-1 mRNA ($*p < 0.05$; Fig. 1a) and protein ($*p < 0.05$; Fig. 1b) expression were significantly decreased in hippocampal tissue prepared from aged, compared with young rats, as determined by post-hoc analysis. Furthermore, FGL treatment reversed the age-related decline in IGF-1 mRNA ($^+p < 0.05$; Fig. 1a) and protein ($^+p < 0.05$; Fig. 1b). Two-way ANOVA analysis also revealed that treatment of aged animals with FGL reversed the age-related increase in IFN γ mRNA (age \times FGL interaction: $F_{(1,19)} = 8.04$, $^+p < 0.05$; Fig. 1c) and protein expression (age \times FGL interaction: $F_{(1,12)} = 8.65$, $^{++}p < 0.01$; Fig. 1d); post-hoc analysis determined that IFN γ mRNA ($*p < 0.05$; Fig. 1c) and protein ($*p < 0.05$; Fig. 1d) expression were significantly increased in hippocampal tissue prepared from vehicle-treated aged, compared with vehicle-treated young, rats. This suggests that the age-associated changes in IGF-1 in hippocampus may be correlated with the hippocampal expression pattern of IFN γ ; indeed, a significant inverse correlation between the mRNA expression and protein levels of IGF-1 and IFN γ was observed in hippocampal tissue (data not shown).

FGL enhances neuronal IGF-1 *in vitro*

In primary cultures of neuronal cells we tested the effect of FGL on IGF-1 production. As demonstrated in Fig. 2a, FGL dose-dependently enhanced relative IGF-1 mRNA expression. One-way ANOVA analysis revealed that IGF-1 mRNA was significantly increased in neurons *in vitro* exposed to FGL at 100 µg/mL ($***p < 0.001$; Fig. 2a), while exposure of neurons to FGL at 1 and 10 µg/mL failed to enhance IGF-1 mRNA expression. This effect was time-dependent as shorter FGL incubations (1–6 h) failed to enhance IGF-1 mRNA expression (data not shown). Furthermore, the stimulatory effect of FGL on IGF-1 mRNA in neurons was FGFR-dependent, with one-way ANOVA analysis demonstrating that pre-exposure of cells to the FGFR inhibitor SU5402, prevented the FGL (100 µg/mL) induction of IGF-1 mRNA ($^+p < 0.05$; one-way ANOVA; Fig. 2b). Figure 2c demonstrates that FGL dose-dependently enhanced IGF-1 protein production from primary neurons *in vitro* with one-way ANOVA analysis demonstrating that FGL at 100 µg/mL significantly increased IGF-1 protein expression above control levels ($***p < 0.001$; Fig. 2c).

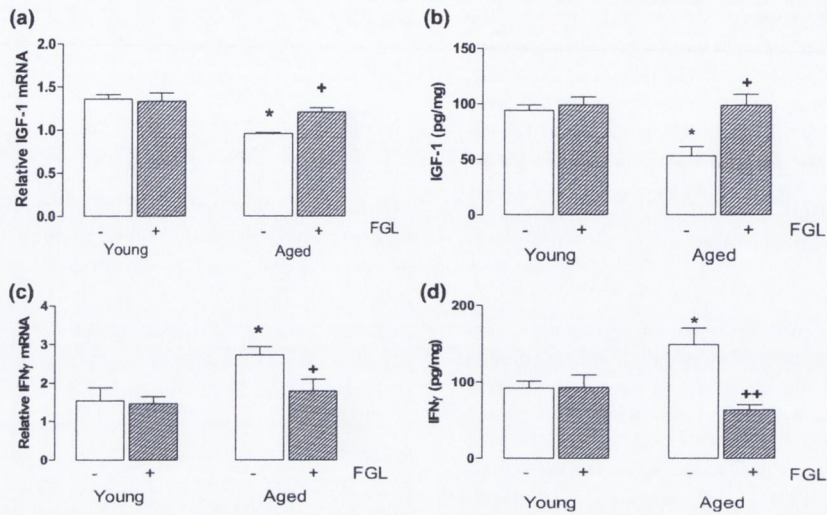


Fig. 1 FGL-reverses age-related changes in hippocampal levels of IGF-1 and IFN γ *in vivo*. Animals were injected subcutaneously with FGL (8 mg/kg) or vehicle (sterile water) on alternate days for 3 weeks. (a) IGF-1 relative mRNA and (b) protein expression were decreased in vehicle-treated aged rats. This was reversed in aged rats treated with FGL. Values are relative mRNA expression for PCR analysis and the concentration of IGF-1 in pg/mg protein for 6 animals per experimental

group from ELISA analysis. (c) Relative IFN γ mRNA expression and (d) protein concentration were increased in vehicle-treated aged rats. This was attenuated in aged rats treated with FGL. Values are relative mRNA expression from 5-6 animals per experimental group for PCR analysis and the concentration of IFN γ in pg/mg protein for 3 animals per group from ELISA analysis. All values are mean \pm SE.

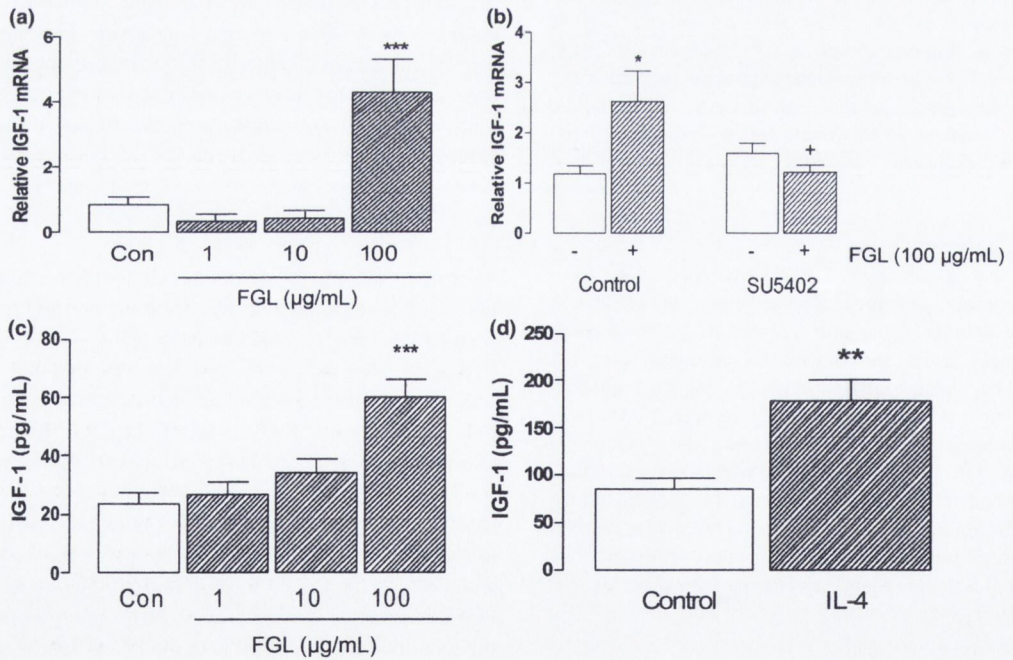


Fig. 2 FGL promotes neuronal production of IGF-1. (a) Relative IGF-1 mRNA expression was increased in cultured neurons *in vitro* by treatment with FGL (24 h) at 100 μ g/mL. Values are relative mRNA expression and are representative of two independent experiments. (b) Pre-treatment (30 min) of neurons with the FGFR inhibitor SU5402 (10 μ M) prevented FGL (100 μ g/mL; 24 h)-induced relative IGF-1 mRNA. Values are relative mRNA expression and are representative of two independent experiments. (c) Neuronal IGF-1 protein produc-

tion *in vitro* was increased following exposure to FGL (24 h) at 100 μ g/mL. Values are expressed as concentration of IGF-1 in pg/mL and are representative of two independent experiments. (d) Treatment of neurons with IL-4 (200 ng/mL) for 24 h enhanced production of IGF-1 from cultured neurons. Values are expressed as concentration of IGF-1 in pg/mL and are representative of two independent experiments. All values are mean \pm SE.

Previously we have demonstrated that FGL reverses the age- and lipopolysaccharide (LPS)-induced decline in anti-inflammatory IL-4 production in the hippocampus *in vivo* and glial cells *in vitro*, respectively (Downer *et al.* 2008). Here we demonstrate that IL-4, like FGL, promotes IGF-1 protein production from primary cortical neurons *in vitro* (Student's *t*-test; $**p < 0.01$; Fig. 2d). This experiment was also performed in primary hippocampal neurons, with a similar stimulatory effect of IL-4 observed (data not shown). Furthermore, a significant correlation between IL-4 and IGF-1 protein levels in hippocampus *in vivo* was determined (data not shown). This argues that FGL, in addition to directly promoting neuronal IGF-1 production, may induce IGF-1 release from neurons by regulating IL-4 release from glial cells.

FGL enhances phospho-Akt and CD200 ligand in neurons *in vitro* via IGF-1

To investigate the role of IGF-1 in FGL-induced neuronal signaling events related to glial cell activation, we employed the use of an anti-IGF-1 antibody to specifically inhibit IGF-1 activity. In support of previous evidence from primary cerebellar granule neurons (Neiendam *et al.* 2004), FGL (100 $\mu\text{g}/\text{mL}$) enhanced Akt phosphorylation in primary neurons *in vitro* ($**p < 0.01$; one-way ANOVA; Fig. 3a). This effect was also observed with shorter FGL incubation times (30 min–1 h; data not shown) and this event was most likely mediated via FGL induction of FGFR signaling. Interestingly, the ability of FGL to enhance phospho-Akt protein expression was abrogated by co-treatment with anti-IGF-1 antibody at 10 $\mu\text{g}/\text{mL}$ ($^{++}p < 0.01$; one-way ANOVA; Fig. 3a).

Previous evidence from our laboratory has indicated that CD200 ligand is pivotal in controlling microglial activation (Lyons *et al.* 2007b). Furthermore, we have recently reported that FGL reverses the age-related decline in CD200 mRNA and protein expression in hippocampus *in vivo*, an event contributing to the attenuation of neuroinflammatory changes associated with aging in the rat hippocampus (Downer *et al.* 2008). In support of this, data herein reveal that FGL (24 h; 100 $\mu\text{g}/\text{mL}$) enhanced CD200 ligand expression in primary neurons *in vitro* ($**p < 0.01$; one-way ANOVA; Fig. 3b); this was abrogated by co-treatment with anti-IGF-1 antibody at 10 $\mu\text{g}/\text{mL}$ ($^+p < 0.05$; one-way ANOVA; Fig. 3b). No age- or FGL-related changes in CD200R expression were observed (data not shown). These findings suggest that the proclivity of FGL to promote Akt phosphorylation and CD200 in cultured neurons *in vitro* is IGF-1-dependent.

FGL induces phospho-Akt *in vivo*: Akt and ERK signaling mediate FGL induction of CD200 ligand *in vitro*

To determine if FGL regulates Akt signaling events *in vivo* we analyzed phosphorylated Akt protein expression in hippocampal tissue prepared from vehicle- and FGL-treated,

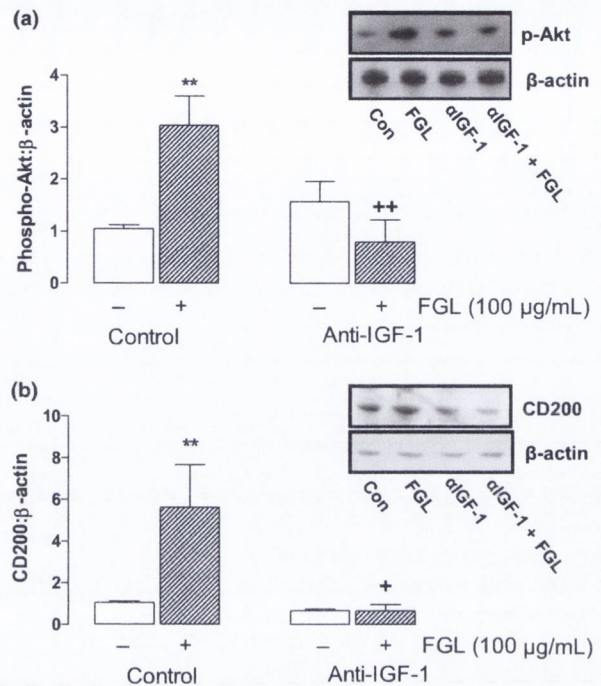


Fig. 3 FGL enhances protein expression of phospho-Akt and CD200 ligand in neurons via IGF-1. (a) Phospho-Akt and (b) CD200 protein expression were enhanced on neurons *in vitro* following exposure to FGL (24 h; 100 $\mu\text{g}/\text{mL}$). The ability of FGL to enhance neuronal (a) phospho-Akt and (b) CD200 protein expression was abrogated by pre-treatment with an anti-IGF-1 antibody (30 min; 10 $\mu\text{g}/\text{mL}$) prior to FGL exposure. Values are the ratio of density of the target protein to β -actin and are representative of three independent experiments. All values are mean \pm SE.

young and aged, rats. Previous evidence from our laboratory has demonstrated that the expression of phosphorylated Akt is decreased in the hippocampus with age (Maher *et al.* 2006). Consistent with this, the combined age \times FGL interaction by two-way ANOVA had a significant impact on Akt phosphorylation ($F_{(1,18)} = 6.15$, $*p < 0.05$; Fig. 4a), with post-hoc analysis revealing an FGL-induced increase in Akt phosphorylation in hippocampal tissue prepared from aged rats ($*p < 0.05$; Fig. 4a). To investigate the role of Akt in FGL-induced CD200 ligand expression in neurons *in vitro*, we employed the use of the PI-3 kinase inhibitor LY 294002. Data in Fig. 4b demonstrate that both FGL (24 h; 100 $\mu\text{g}/\text{mL}$), and recombinant IGF-1 (24 h; 100 ng/mL), enhanced CD200 ligand expression in neurons *in vitro* ($*p < 0.05$ in both cases; one-way ANOVA). However, the stimulatory effect of FGL and IGF-1 on CD200 was ameliorated by pre-exposure of neurons to LY 294002 ($^+p < 0.05$ in both cases), indicating that the effect of FGL on CD200 is dependent on neuronal PI-3 kinase/Akt signaling (Fig. 4b). Treatment with LY 294002 alone had no effect on basal neuronal expression of CD200.

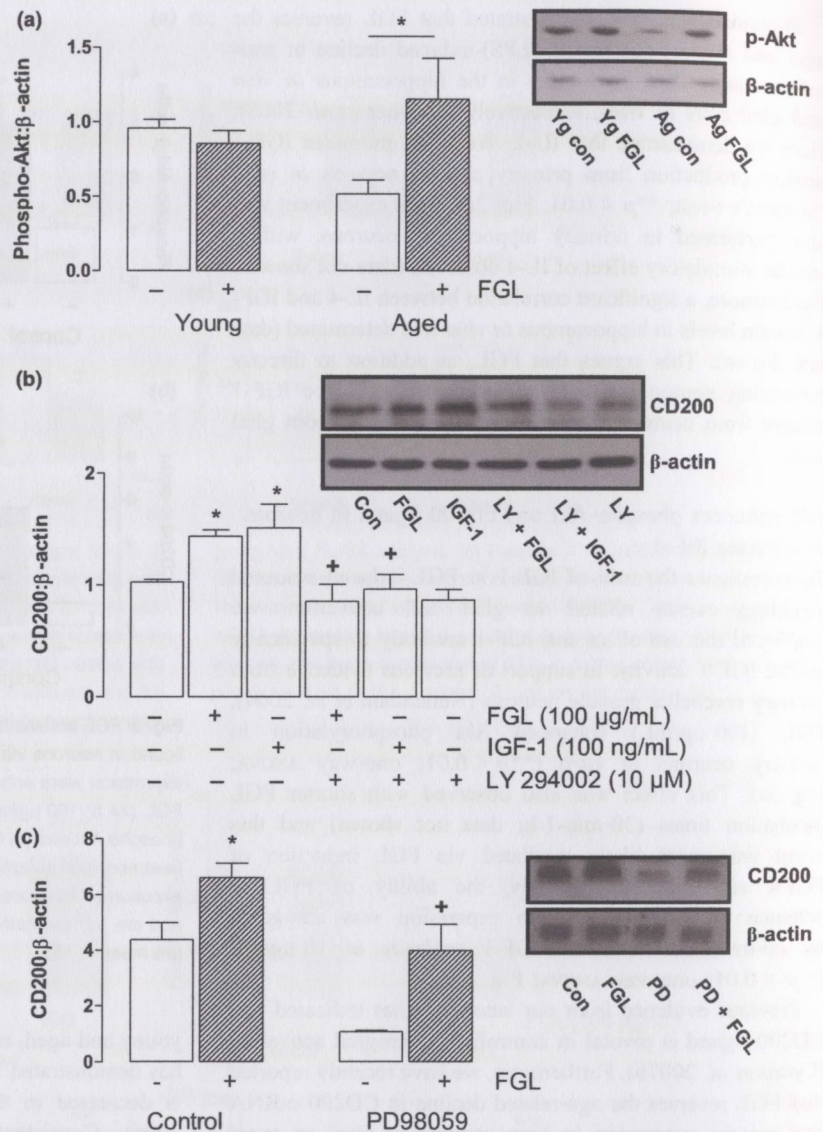


Fig. 4 FGL enhances protein expression of phospho-Akt *in vivo* while Akt and ERK mediate FGL induction of CD200 *in vitro*. (a) Phosphorylated Akt protein expression was decreased in vehicle-treated aged rats and this was reversed in aged rats treated with FGL. Values are the ratio of density of the target protein to β -actin from five animals per group. (b) CD200 ligand expression was enhanced following exposure of cultured neurons to FGL (24 h; 100 μ g/mL) and recombinant IGF-1 (24 h; 100 ng/mL). FGL and IGF-1 induction of CD200 was abated by pre-exposure (30 min) of neurons to PI-3 kinase inhibitor LY 294002 (10 μ M). LY 294002 alone (24 h; 10 μ M) had no effect on basal neuronal expression of CD200. Values are the ratio of density of the target protein to β -actin and are representative of three independent experiments. (c) FGL (24 h; 100 μ g/mL) induction of CD200 on cultured neurons is attenuated by pre-treatment (1 h) with the MEK inhibitor PD98059 (50 μ M). Values are the ratio of density of the target protein to β -actin and are representative of two independent experiments in which six replicates were evaluated on both occasions. All values are mean \pm SE.

IL-4 is a potent inducer of CD200 ligand on neurons, and this is mediated by ERK signaling (Downer *et al.* 2008). The present data demonstrate that FGL (100 μ g/mL; 24 h) induction of neuronal CD200 *in vitro*, in addition to being reliant on Akt signaling (Fig. 4b), is abated by pre-exposure of neurons to the MEK inhibitor, PD98059 ($^+p < 0.05$; one-way ANOVA; Fig. 4c). This indicates that the stimulatory effect of FGL on CD200 ligand is also dependent on ERK signaling events.

FGL attenuates age- and IFN γ -induced glial cell activation

Much evidence indicates neuroinflammatory changes are associated with an increase in cell surface markers of activated glial cells in the hippocampus of aged rats (Griffin *et al.* 2006; Loane *et al.* 2007). Indeed, we have recently published evidence that the protein expression of microglial

activation markers, including the co-stimulatory molecule CD86, and the intercellular cell adhesion molecule (ICAM-1), are enhanced in the hippocampus of aged animals; FGL attenuates the increase in these markers in parallel (Downer *et al.* 2008). In the present study, we focused on the expression of two glial surface molecules which are necessary for antigen presentation, CD40 and MHCII. The interaction of age \times FGL, as reported by two-way ANOVA had a significant impact on relative mRNA expression of MHCII ($F_{(1,21)} = 4.94$, $^+p < 0.05$; Fig. 5a) and CD40 ($F_{(1,20)} = 7.66$, $^{++}p < 0.01$; Fig. 5b). Post-hoc analysis demonstrated that MHCII and CD40 mRNA expression were both increased in hippocampal tissue obtained from vehicle-treated aged, compared with young, rats ($^*p < 0.05$ for MHCII; $p = 0.09$ for CD40). Furthermore, *post-hoc* analysis demonstrated that FGL significantly attenuated the age-

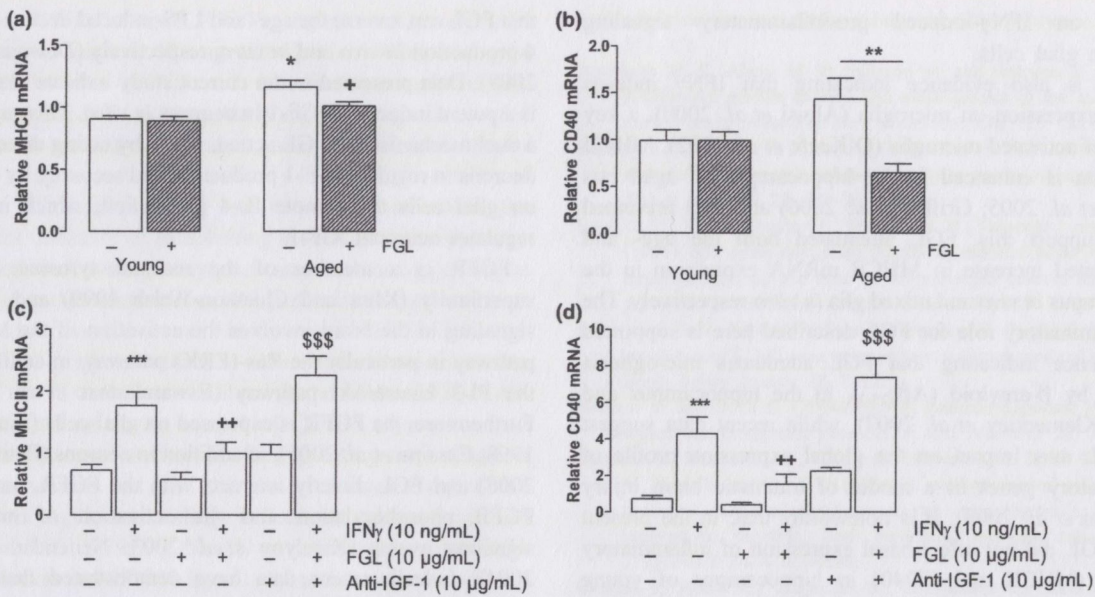


Fig. 5 FGL attenuates age- and IFN γ -induced glial cell activation; FGL attenuates IFN γ -induced effects via IGF-1. (a) MHCII mRNA and (b) CD40 mRNA expression were increased in vehicle-treated aged rats. These effects were attenuated in FGL-treated aged rats. Values are relative mRNA expression for five animals per experimental group. Exposure of mixed glial cells *in vitro* to IFN γ (24 h; 10 ng/mL) induced

related increase in MHCII ($^+p < 0.05$; Fig. 5a) and CD40 ($^{**}p < 0.01$; Fig. 5b) mRNA relative expression.

To further investigate the anti-inflammatory role of FGL we assessed the impact of FGL on IFN γ -induced glial cell activation in cultured mixed glial cells *in vitro*. Exposure of glial cells to IFN γ induced expression of both MHCII ($^{***}p < 0.001$; one-way ANOVA; Fig. 5c) and CD40 ($^{***}p < 0.01$; one-way ANOVA; Fig. 5d) mRNA expression. One-way ANOVA analysis revealed that pre-exposure to FGL (24 h) at 10 $\mu\text{g/mL}$ abrogated the IFN γ -induced MHCII mRNA ($^{++}p < 0.01$; Fig. 5c) and CD40 mRNA expression ($^{++}p < 0.01$; one-way ANOVA; Fig. 5d) in mixed glia. Similar attenuation of this IFN γ -induced effect was observed when FGL was used at 0.1 and 1 $\mu\text{g/mL}$ (data not shown). To address the role of IGF-1 in FGL-induced regulation of IFN γ -induced glial cell activation *in vitro*, mixed glia were treated with FGL prior (24 h; 10 $\mu\text{g/mL}$) to IFN γ exposure, in the presence of absence or an anti-IGF-1 antibody (10 $\mu\text{g/mL}$). Importantly, we demonstrate that addition of anti-IGF-1 antibody in the presence of FGL abrogated the effect of FGL ($^{$$$}p < 0.001$ for both MHCII and CD40; one-way ANOVA). These data highlight the pivotal role of IGF-1 in the ability of FGL to attenuate IFN γ -induced glial cell activation.

Discussion

We set out to assess the interaction between IGF-1 and IFN γ in the hippocampus of aged animals, to determine if this

a significant increase in (c) MHCII mRNA and (d) CD40 mRNA expression. This was attenuated by pre-treatment with FGL (24 h; 10 $\mu\text{g/mL}$) prior to IFN γ exposure. Addition of an anti-IGF-1 antibody (10 $\mu\text{g/mL}$) in the presence of FGL and IFN γ abrogated the effect of FGL. Values are relative mRNA expression and are representative of three independent experiments. All values are mean \pm SE.

interaction is modulated by the NCAM mimetic FGL, and subsequently to establish if this modulation is coupled to the control of glial cell activation. FGL, in addition to reversing the age-related decline in IGF-1 and increase in IFN γ in hippocampus *in vivo*, promoted neuronal production of IGF-1 *in vitro*. We provide evidence that FGL induction of IGF-1 is involved in attenuating glial cell activation and propose a dual mechanism of action of IGF-1: FGL-induced attenuation of IFN γ -induced glial cell activation and FGL-triggered induction of CD200.

IFN γ is a potent activator of microglia *in vitro* (Hashioka *et al.* 2007) and *in vivo* (Lynch *et al.* 2006) and its actions include inducing transactivation of multiple effector genes, including CD40 and inducible nitric-oxide synthase, via the Janus kinase/STAT-1 pathway (Benveniste *et al.* 2004). CD40 expression is implicated in many CNS disorders; indeed, CD40-positive microglia are observed in the CNS of animals in which experimental autoimmune encephalomyelitis was induced (Laman *et al.* 1998). Previous evidence from our laboratory has indicated that normal aging is associated with an increase in IFN γ (Clarke *et al.* 2008) and CD40 (Griffin *et al.* 2006) in the hippocampus, and the present data support these findings. FGL attenuated the age-related increase in hippocampal IFN γ and CD40, supporting the proposal that FGL acts as an anti-inflammatory agent. Furthermore, FGL attenuated IFN γ -induced CD40 expression in mixed glial cultures *in vitro*, indicating that FGL has the proclivity to impact

directly on IFN γ -induced pro-inflammatory signaling events in glial cells.

There is also evidence indicating that IFN γ induces MHCII expression on microglia (Aloisi *et al.* 2000), a key marker of activated microglia (O'Keefe *et al.* 2002). MHCII expression is enhanced in the hippocampus of aged rats (Moore *et al.* 2005; Griffin *et al.* 2006) and data presented herein support this. FGL attenuated both the age- and IFN γ -related increase in MHCII mRNA expression in the hippocampus *in vivo* and mixed glia *in vitro* respectively. The anti-inflammatory role for FGL described here is supported by evidence indicating that FGL attenuates microgliosis induced by β -amyloid (A β)₂₅₋₃₅ in the hippocampus and cortex (Klementiev *et al.* 2007), while recent data suggest that FGL may impact on the global expression profile of inflammatory genes in a model of traumatic brain injury (Pedersen *et al.* 2008). It is noteworthy that, in the present study, FGL did not affect basal expression of inflammatory markers (MHCII and CD40) in hippocampus of young animals, indicating that the biological effects of FGL *in vivo* are operative in response to inflammatory conditions, for example in the aged brain.

FGL enhances neuronal production of IGF-1 *in vitro*, in addition to reversing the age-related decline in IGF-1 in rat hippocampus. IGF-1 is a polypeptide hormone produced in the CNS and extraneural organs. In the CNS, IGF-1 expression is low compared with other organs and a progressive decline in IGF-1 is observed which may produce deleterious consequences on neuronal function in old age (Fernandez *et al.* 2007). IGF-1 plays a role in cell survival (Beck *et al.* 1995), growth (Russo *et al.* 2005), inflammation (Pons and Torres-Aleman 2000) and plasticity (Ahmadian *et al.* 2004) in the brain and evidence indicates that anti-inflammatory actions of IGF-1 exist. Indeed, enhanced astroglial reactivity has been demonstrated at inflammatory sites after brain injury following IGF-1 inhibition (Fernandez *et al.* 1997) and it is proposed that this is due to the ability of IGF-1 to inhibit tumor necrosis factor- α -induced pro-inflammatory signaling in astrocytes (Pons and Torres-Aleman 2000). These data support previous evidence indicating that IGF-1 can ameliorate glial reactivity specifically induced by IFN γ exposure, in both glial cells *in vitro* and in the rat hippocampus *in vivo* (Maher *et al.* 2006). Here we demonstrate that a correlation exists between IGF-1, IFN γ and markers of activated glial cells in the hippocampus of aged animals, and that FGL can correct the imbalance in these target molecules observed in the hippocampus of aged rats. Importantly, we report that the ability of FGL to attenuate IFN γ -induced glial cell activation *in vitro* is prevented following IGF-1 inhibition, indicating that FGL, acting via IGF-1, directly impacts on IFN γ -induced pro-inflammatory signaling in glia.

In addition to promoting IGF-1 release directly from neurons, our data indicate that FGL may control IGF-1 production via IL-4. This is based on our previous evidence

that FGL can reverse the age- and LPS-induced decline in IL-4 production *in vivo* and *in vitro*, respectively (Downer *et al.* 2008). Data presented in the current study indicate that IL-4 is a potent inducer of IGF-1 in neurons *in vitro*. This suggests a dual mechanism of FGL action, firstly by acting directly on neurons to regulate IGF-1 production and secondly by acting on glial cells to promote IL-4 production, which in turn regulates neuronal IGF-1.

FGFR is a member of the receptor tyrosine kinase superfamily (Klint and Claesson-Welsh 1999) and FGFR signaling in the brain involves the activation of the MAPK pathway in particular the Ras-(ERK) pathway, in addition to the PI-3 kinase/Akt pathway (Eswarakumar *et al.* 2005). Furthermore, the FGFR is expressed on glial cells (Liu *et al.* 1998; Cassina *et al.* 2005), in addition to neurons (Petri *et al.* 2008) and FGL directly interacts with the FGFR, inducing FGFR phosphorylation and the activation of multiple signaling events (Kiselyov *et al.* 2003; Neiiendam *et al.* 2004). Indeed, recent data have demonstrated that FGL attenuates LPS-induced microglial cell activation, and this is prevented by the FGFR inhibitor SU5402 (E.J. Downer, F. Cox and M.A. Lynch unpublished), while FGL induction of IGF-1 mRNA in neurons is also attenuated by SU5402. FGL robustly enhances ERK phosphorylation in cultured neurons (Neiiendam *et al.* 2004) and in the rat hippocampus *in vivo* (Downer *et al.* 2008). Data herein demonstrate that FGL induction of ERK signaling is central in regulating CD200 ligand expression. This is consistent with the findings of Petermann *et al.* (2007), which have shown that CD200 expression is controlled by ERK signaling events in melanoma cells. In addition to its effect on ERK described in the current study, we provide evidence that FGL induces Akt phosphorylation in cultured cortical neurons *in vitro*. This is consistent with the effect of FGL on cerebellar granule neurons, a signaling event associated with FGL-induced neurite outgrowth and survival (Neiiendam *et al.* 2004). Our findings further elaborate the role FGL-induced Akt signaling on neuronal function, indicating that Akt, in addition to ERK, is central in controlling FGL-induced CD200 ligand expression. FGL also reverses the age-related decline in phospho-Akt expression in the hippocampus *in vivo*, a significant finding considering the role of PI-3 kinase and Akt in the expression of long-term potentiation (LTP) (Kelly and Lynch 2000). Overall these data indicate that FGL induction of Akt and ERK signaling events in parallel, are central in controlling neuronal CD200 ligand expression.

It has been shown that basic fibroblast growth factor induces IGF-1 release from hypothalamic cell cultures of neurons and glia (Pons and Torres-Aleman 1992), highlighting the role of FGFR signaling in controlling IGF-1 production in the brain. In support of this, analysis of the effect of FGL on neuronal IGF-1 production demonstrated that FGL enhanced both IGF-1 mRNA and protein expression in cultured neurons, and reversed the age-related decline

in IGF-1 in hippocampus. IGF-1 is a potent activator of Akt signaling in neurons (Zheng and Quirion 2006) and glial cells (Strle *et al.* 2002) and our findings support this, indicating that FGL induces Akt phosphorylation in cultured neurons in an IGF-1-dependent manner. This was demonstrated using an anti-IGF-1 antibody to inhibit the activity of IGF-1. This antibody was not used *in vivo* due to the technical difficulty of establishing that intracerebroventricular injection of this antibody gains access to the hippocampus in sufficient concentrations. Of particular importance, we demonstrate that IGF-1 and Akt are central in FGL induction of CD200 ligand on neurons *in vitro*. As far as we are aware, this is the first evidence indicating the role of IGF-1/Akt signaling events in the control of CD200 expression, and represents a novel mechanism for regulating the interaction between neurons and glial cells, and subsequently glial cell activation. Again our findings indicate a dual mechanism of action of FGL; by acting directly on neurons to regulate IGF-1 production and CD200 ligand expression and secondly by acting on glial cells to promote IL-4 production which in turn regulates neuronal IGF-1.

Overall, our findings further elucidate the therapeutic potential of FGL, particularly in relation to age-associated neurodegenerative disorders. FGL rapidly reaches the plasma and CSF following subcutaneous administration to rats (Secher *et al.* 2006) while recent pre-clinical studies have also shown an absence of systemic toxicity following intranasal or parenteral administration to rats, dogs and monkeys (Anand *et al.* 2007). The findings presented here demonstrate that FGL, by correcting the age-related imbalance in hippocampal levels of IGF-1 and IFN γ , attenuates glial reactivity associated with aging. We highlight a novel mechanism by which FGL regulates neuronal CD200 ligand *in vitro* via IGF-1, Akt and ERK signaling and present evidence indicating that this is central in controlling glial cell activation status.

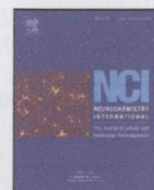
Acknowledgments

This work was supported by the EU-supported integrated project PROMEMORIA. FOM was supported on a grant provided by Science Foundation Ireland.

References

- Ahmadian G., Ju W., Liu L. *et al.* (2004) Tyrosine phosphorylation of GluR2 is required for insulin-stimulated AMPA receptor endocytosis and LTD. *EMBO J.* **23**, 1040–1050.
- Aloisi F., De Simone R., Columba-Cabezas S., Penna G. and Adorini L. (2000) Functional maturation of adult mouse resting microglia into an APC is promoted by granulocyte-macrophage colony-stimulating factor and interaction with Th1 cells. *J. Immunol.* **164**, 1705–1712.
- Anand R., Seiberling M., Kamtchoua T. and Pokorny R. (2007) Tolerability, safety and pharmacokinetics of the FGL peptide, a novel mimetic of neural cell adhesion molecule, following intranasal administration in healthy volunteers. *Clin. Pharmacokin.* **46**, 351–358.
- Anderson M. F., Aberg M. A., Nilsson M. and Eriksson P. S. (2002) Insulin-like growth factor-I and neurogenesis in the adult mammalian brain. *Brain Res. Dev. Brain Res.* **134**, 115–122.
- Barclay A. N., Wright G. J., Brooke G. and Brown M. H. (2002) CD200 and membrane protein interactions in the control of myeloid cells. *Trends Immunol.* **23**, 285–290.
- Beck K. D., Powell-Braxton L., Widmer H. R., Valverde J. and Hefti F. (1995) Igf1 gene disruption results in reduced brain size, CNS hypomyelination, and loss of hippocampal granule and striatal parvalbumin-containing neurons. *Neuron* **14**, 717–730.
- Benveniste E. N., Nguyen V. T. and Wesemann D. R. (2004) Molecular regulation of CD40 gene expression in macrophages and microglia. *Brain Behav. Immun.* **18**, 7–12.
- Berezin V. and Bock E. (2004) NCAM mimetic peptides: Pharmacological and therapeutic potential. *J. Mol. Neurosci.* **22**, 33–39.
- Cambon K., Hansen S. M., Venero C., Herrero A. I., Skibo G., Berezin V., Bock E. and Sandi C. (2004) A synthetic neural cell adhesion molecule mimetic peptide promotes synaptogenesis, enhances presynaptic function, and facilitates memory consolidation. *J. Neurosci.* **24**, 4197–4204.
- Cassina P., Pehar M., Vargas M. R., Castellanos R., Barbeito A. G., Estevez A. G., Thompson J. A., Beckman J. S. and Barbeito L. (2005) Astrocyte activation by fibroblast growth factor-1 and motor neuron apoptosis: implications for amyotrophic lateral sclerosis. *J. Neurochem.* **93**, 38–46.
- Clarke R. M., Lyons A., O'Connell F., Deighan B. F., Barry C. E., Anyakoha N. G., Nicolaou A. and Lynch M. A. (2008) A pivotal role for interleukin-4 in atorvastatin-associated neuroprotection in rat brain. *J. Biol. Chem.* **283**, 1808–1817.
- Cremer H., Chazal G., Goridis C. and Represa A. (1997) NCAM is essential for axonal growth and fasciculation in the hippocampus. *Mol. Cell. Neurosci.* **8**, 323–335.
- Ditlevsen D. K., Kohler L. B., Pedersen M. V., Risell M., Kolkova K., Meyer M., Berezin V. and Bock E. (2003) The role of phosphatidylinositol 3-kinase in neural cell adhesion molecule-mediated neuronal differentiation and survival. *J. Neurochem.* **84**, 546–556.
- Downer E. J., Cowley T. R., Lyons A., Mills K. H., Berezin V., Bock E. and Lynch M. A. (2008) A novel anti-inflammatory role of NCAM-derived mimetic peptide, FGL. *Neurobiol. Aging*, in press, doi:10.1016/j.neurobiolaging.2008.03.017.
- Eswarakumar V. P., Lax I. and Schlessinger J. (2005) Cellular signaling by fibroblast growth factor receptors. *Cytokine Growth Factor Rev.* **16**, 139–149.
- Fernandez A. M., Garcia-Estrada J., Garcia-Segura L. M. and Torres-Aleman I. (1997) Insulin-like growth factor I modulates c-Fos induction and astrocytosis in response to neurotoxic insult. *Neuroscience* **76**, 117–122.
- Fernandez S., Fernandez A. M., Lopez-Lopez C. and Torres-Aleman I. (2007) Emerging roles of insulin-like growth factor-I in the adult brain. *Growth Horm. IGF Res.* **17**, 89–95.
- Griffin R., Nally R., Nolan Y., McCartney Y., Linden J. and Lynch M. A. (2006) The age-related attenuation in long-term potentiation is associated with microglial activation. *J. Neurochem.* **99**, 1263–1272.
- Hashioka S., Han Y. H., Fujii S., Kato T., Monji A., Utsumi H., Sawada M., Nakanishi H. and Kanba S. (2007) Phosphatidylserine and phosphatidylcholine-containing liposomes inhibit amyloid beta and interferon-gamma-induced microglial activation. *Free Radic. Biol. Med.* **42**, 945–954.
- Hoek R. M., Ruuls S. R., Murphy C. A. *et al.* (2000) Down-regulation of the macrophage lineage through interaction with OX2 (CD200). *Science* **290**, 1768–1771.

- Kelly A. and Lynch M. A. (2000) Long-term potentiation in dentate gyrus of the rat is inhibited by the phosphoinositide 3-kinase inhibitor, wortmannin. *Neuropharmacology* **39**, 643–651.
- Kim Y. S. and Joh T. H. (2006) Microglia, major player in the brain inflammation: their roles in the pathogenesis of Parkinson's disease. *Exp. Mol. Med.* **38**, 333–347.
- Kiselyov V. V., Skladchikova G., Hinsby A. M. *et al.* (2003) Structural basis for a direct interaction between FGFR1 and NCAM and evidence for a regulatory role of ATP. *Structure* **11**, 691–701.
- Klementiev B., Novikova T., Novitskaya V., Walmod P. S., Dmytriyeva O., Pakkenberg B., Berezin V. and Bock E. (2007) A neural cell adhesion molecule-derived peptide reduces neuropathological signs and cognitive impairment induced by Abeta25-35. *Neuroscience* **145**, 209–224.
- Klint P. and Claesson-Welsh L. (1999) Signal transduction by fibroblast growth factor receptors. *Front. Biosci.* **4**, D165–D177.
- Kolkova K., Novitskaya V., Pedersen N., Berezin V. and Bock E. (2000) Neural cell adhesion molecule-stimulated neurite outgrowth depends on activation of protein kinase C and the Ras-mitogen-activated protein kinase pathway. *J. Neurosci.* **20**, 2238–2246.
- Laman J. D., De Boer M. and Hart B. A. (1998) CD40 in clinical inflammation: from multiple sclerosis to atherosclerosis. *Dev. Immunol.* **6**, 215–222.
- Liu X., Mashour G. A., Webster H. F. and Kurtz A. (1998) Basic FGF and FGF receptor 1 are expressed in microglia during experimental autoimmune encephalomyelitis: temporally distinct expression of midkine and pleiotrophin. *Glia* **24**, 390–397.
- Loane D. J., Deighan B. F., Clarke R. M., Griffin R. J., Lynch A. M. and Lynch M. A. (2007) Interleukin-4 mediates the neuroprotective effects of rosiglitazone in the aged brain. *Neurobiol. Aging*, in press, doi:10.1016/j.neurobiolaging.2007.09.001.
- Lynch A. M., Loane D. J., Minogue A. M., Clarke R. M., Kilroy D., Nally R. E., Roche O. J., O'Connell F. and Lynch M. A. (2006) Eicosapentaenoic acid confers neuroprotection in the amyloid-beta challenged aged hippocampus. *Neurobiol. Aging* **28**, 845–855.
- Lyons A., Griffin R. J., Costelloe C. E., Clarke R. M. and Lynch M. A. (2007a) IL-4 attenuates the neuroinflammation induced by amyloid-beta in vivo and in vitro. *J. Neurochem.* **101**, 771–781.
- Lyons A., Downer E. J., Crotty S., Nolan Y. M., Mills K. H. and Lynch M. A. (2007b) CD200 ligand receptor interaction modulates microglial activation in vivo and in vitro: a role for IL-4. *J. Neurosci.* **27**, 8309–8313.
- Maher F. O., Clarke R. M., Kelly A., Nally R. E. and Lynch M. A. (2006) Interaction between interferon gamma and insulin-like growth factor-1 in hippocampus impacts on the ability of rats to sustain long-term potentiation. *J. Neurochem.* **96**, 1560–1571.
- Matsumoto H., Kumon Y., Watanabe H., Ohnishi T., Takahashi H., Imai Y. and Tanaka J. (2007) Expression of CD200 by macrophage-like cells in ischemic core of rat brain after transient middle cerebral artery occlusion. *Neurosci. Lett.* **418**, 44–48.
- Moore M. E., Piazza A., McCartney Y. and Lynch M. A. (2005) Evidence that vitamin D3 reverses age-related inflammatory changes in the rat hippocampus. *Biochem. Soc. Trans.* **33**, 573–577.
- Neijendam J. L., Kohler L. B., Christensen C., Li S., Pedersen M. V., Ditlevsen D. K., Kornum M. K., Kiselyov V. V., Berezin V. and Bock E. (2004) An NCAM-derived FGF-receptor agonist, the FGL-peptide, induces neurite outgrowth and neuronal survival in primary rat neurons. *J. Neurochem.* **91**, 920–935.
- Nolan Y., Maher F. O., Martin D. S., Clarke R. M., Brady M. T., Bolton A. E., Mills K. H. and Lynch M. A. (2005) Role of interleukin-4 in regulation of age-related inflammatory changes in the hippocampus. *J. Biol. Chem.* **280**, 9354–9362.
- O'Keefe G. M., Nguyen V. T. and Benveniste E. N. (2002) Regulation and function of class II major histocompatibility complex, CD40, and B7 expression in macrophages and microglia: Implications in neurological diseases. *J. Neurovirol.* **8**, 496–512.
- Pedersen M. V., Helweg-Larsen R. B., Nielsen F. C., Berezin V., Bock E. and Penkowa M. (2008) The synthetic NCAM-derived peptide, FGL, modulates the transcriptional response to traumatic brain injury. *Neurosci. Lett.* **437**, 148–153.
- Petermann K. B., Rozenberg G. I., Zedek D. *et al.* (2007) CD200 is induced by ERK and is a potential therapeutic target in melanoma. *J. Clin. Invest.* **117**, 3922–3929.
- Petri S., Krampfl K., Kuhlemann K., Dengler R. and Grothe C. (2008) Preserved expression of fibroblast growth factor (FGF)-2 and FGF receptor 1 in brain and spinal cord of amyotrophic lateral sclerosis patients. *Histochem. Cell Biol.*, in press, doi:10.1007/s00418-008-0549-x.
- Pons S. and Torres-Aleman I. (1992) Basic fibroblast growth factor modulates insulin-like growth factor-I, its receptor, and its binding proteins in hypothalamic cell cultures. *Endocrinology* **131**, 2271–2278.
- Pons S. and Torres-Aleman I. (2000) Insulin-like growth factor-I stimulates dephosphorylation of ikappa B through the serine phosphatase calcineurin (protein phosphatase 2B). *J. Biol. Chem.* **275**, 38620–38625.
- Preston S., Wright G. J., Starr K., Barclay A. N. and Brown M. H. (1997) The leukocyte/neuron cell surface antigen OX2 binds to a ligand on macrophages. *Eur. J. Immunol.* **27**, 1911–1918.
- Russo V. C., Gluckman P. D., Feldman E. L. and Werther G. A. (2005) The insulin-like growth factor system and its pleiotropic functions in brain. *Endocr. Rev.* **26**, 916–943.
- Sandi C., Merino J. J., Cordero M. I., Kruyt N. D., Murphy K. J. and Regan C. M. (2003) Modulation of hippocampal NCAM polysialylation and spatial memory consolidation by fear conditioning. *Biol. Psychiatry* **54**, 599–607.
- Secher T., Novitskaia V., Berezin V., Bock E., Glenthøj B. and Klementiev B. (2006) A neural cell adhesion molecule-derived fibroblast growth factor receptor agonist, the FGL-peptide, promotes early postnatal sensorimotor development and enhances social memory retention. *Neuroscience* **141**, 1289–1299.
- Skibo G. G., Lushnikova I. V., Voronin K. Y., Dmitrieva O., Novikova T., Klementiev B., Vaudano E., Berezin V. A. and Bock E. (2005) A synthetic NCAM-derived peptide, FGL, protects hippocampal neurons from ischemic insult both in vitro and in vivo. *Eur. J. Neurosci.* **22**, 1589–1596.
- Strle K., Zhou J. H., Broussard S. R., Venters H. D., Johnson R. W., Freund G. G., Dantzer R. and Kelley K. W. (2002) IL-10 promotes survival of microglia without activating Akt. *J. Neuroimmunol.* **122**, 9–19.
- Wang Q., Rowan M. J. and Anwyl R. (2004) Beta-amyloid-mediated inhibition of NMDA receptor-dependent long-term potentiation induction involves activation of microglia and stimulation of inducible nitric oxide synthase and superoxide. *J. Neurosci.* **24**, 6049–6056.
- Welzl H. and Stork O. (2003) Cell adhesion molecules: key players in memory consolidation? *News Physiol. Sci.* **18**, 147–150.
- Willaime-Morawek S., Arbez N., Mariani J. and Brugg B. (2005) IGF-I protects cortical neurons against ceramide-induced apoptosis via activation of the PI-3K/Akt and ERK pathways; is this protection independent of CREB and Bcl-2? *Brain Res. Mol. Brain Res.* **142**, 97–106.
- Zheng W. H. and Quirion R. (2006) Insulin-like growth factor-1 (IGF-1) induces the activation/phosphorylation of Akt kinase and cAMP response element-binding protein (CREB) by activating different signaling pathways in PC12 cells. *BMC Neurosci.* **7**, 51.



The age- and amyloid- β -related increases in Nogo B contribute to microglial activation

Kevin J. Murphy, Anne-Marie Miller, R. Thelma, F. Cowley, F. Fionnuala Cox, Marina A. Lynch*

Trinity College Institute of Neuroscience and Physiology Department, Trinity College, Dublin 2, Ireland

ARTICLE INFO

Article history:

Received 2 October 2010

Accepted 10 November 2010

Available online 24 November 2010

Keywords:

Nogo
Hippocampus
Amyloid- β
Age
Neuroinflammation
Microglial activation
Synaptic deterioration
Caspase
Long term potentiation

ABSTRACT

The family of reticulons include three isoforms of the Nogo protein, Nogo A, Nogo B and Nogo C. Nogo A is expressed on neuronal tissue and its primary effect is widely acknowledged to be inhibition of neurite outgrowth. Although both Nogo B and Nogo C are also expressed in neuronal tissue, their roles in the CNS remain to be identified. In this study, we set out to assess whether expression of Nogo A or Nogo B was altered in tissue prepared from aged rats in which increased microglial activation is accompanied by decreased synaptic plasticity. The data indicate that Nogo B, but not Nogo A, was markedly increased in hippocampal tissue prepared from aged rats and that, at least *in vitro*, Nogo B increased several markers of microglial activation. In a striking parallel with the age-related changes, we demonstrate that intracerebroventricular delivery of amyloid- β ($A\beta$)₁₋₄₀ + $A\beta$ ₁₋₄₂ for 8 days was associated with a depression of long-term potentiation (LTP) and an increase in markers of microglial activation and Nogo B. In both models, evidence of cell stress was identified by increased activity of caspases 8 and 3 and importantly, incubation of cultured neurons in the presence of Nogo B increased activity of both enzymes. The data identify, for the first time, an effect of Nogo B in the brain and specifically show that its expression is increased in conditions where synaptic plasticity is compromised.

© 2010 Elsevier Ltd. All rights reserved.

1. Introduction

Several markers of microglial activation are increased in the brain of aged animals; these include cell surface markers like CD11b, CD40 and major histocompatibility complex class II (MHCII), while increased production of inflammatory cytokines has also been reported (see Clarke et al., 2008; Loane et al., 2009; Lynch, 2009). These changes are coupled with a deficit in synaptic plasticity, characterized by a decrease in the ability of animals to sustain long-term potentiation (LTP), and a convincing correlation between neuroinflammatory changes and inhibition of synaptic function (Clarke et al., 2008; Downer et al., 2010), and therefore cognitive function (Hein et al., 2009; Moore et al., 2009), has been described by several groups (see Lynch, 2010). Several of these inflammatory changes have also been identified in tissue prepared from animals treated with amyloid- β ($A\beta$) (Clarke et al., 2007; Lyons et al., 2007) and a deficit in synaptic function, both behavioural function and LTP, has been reported. When inflammatory changes are inhibited, for example by the anti-inflammatory cytokine IL-4, by the inhibitor of microglial activation

minocycline, or by the polyunsaturated fatty acid eicosapentaenoic acid, the deficits in synaptic function are ameliorated in both aged and $A\beta$ -treated (Lynch et al., 2007; Lyons et al., 2007; Minogue et al., 2007; Nolan et al., 2005) animals, suggesting a causal relationship between neuroinflammatory changes and loss of plasticity.

Under normal conditions, microglia are in a resting state because appropriate cell–cell interactions are maintained and concentrations of inflammatory cytokines like interferon- γ (IFN- γ), which leads to their activation, are low. This homeostatic arrangement is disrupted in the brain of aged and $A\beta$ -treated animals (see Lynch, 2010). However it is undoubtedly the case that other factors also play a role in modulating microglial activation; for example in ischaemic injury, traumatic brain injury and spinal cord injury numerous factors are released from infiltrating cells including matrix metalloproteinases, reactive oxygen and nitrogen species and heat shock proteins which may contribute to activation of both astrocytes and microglia (Beck et al., 2010; Kim and Suh, 2009) and consequently contribute to poor recovery. Interestingly minocycline improves functional outcome identifying the negative impact of microglial activation on recovery (Stirling et al., 2004) although it is widely recognized that endogenous inhibitory factors, including a family of myelin-associated glycoproteins generated from the *nogo/RTN-4* gene, play a major role in preventing axonal regeneration and therefore functional recovery (Kilic et al., 2010).

* Corresponding author at: Cellular Neuroscience Trinity College Institute of Neuroscience, Trinity College, Dublin 2, Ireland. Tel.: +353 1 8968531; fax: +353 1 8963183.

E-mail address: lynchma@tcd.ie (M.A. Lynch).

The family of reticulons include three isoforms of the Nogo protein, Nogo A, Nogo B and Nogo C. Nogo-A is mainly expressed on neuronal tissue, especially oligodendrocytes in the adult CNS (Chen et al., 2000; GrandPre et al., 2000; Prinjha et al., 2000), and both Nogo A and Nogo B are expressed on central and peripheral neurons (Huber et al., 2002; Josephson et al., 2001; Oertle et al., 2003a,b; Wang et al., 2002). Nogo-B and Nogo C are expressed in several peripheral tissues, with Nogo C particularly expressed on muscle (Josephson et al., 2001; Morris et al., 1999; Oertle et al., 2003a,b). With respect to the brain, protein and mRNA levels of all three isoforms have been detected in the spinal cord, and cerebral cortex, hippocampus and cerebellum brain regions (Chen et al., 2000; Huber et al., 2002; Yan et al., 2006).

A great deal of evidence has been accumulated highlighting the negative influence of Nogo A on functional outcome and repair in a variety of models of neurogenerative change (Freund et al., 2009; Kilic et al., 2010; Marklund et al., 2007). Fewer studies have investigated potential roles for Nogo B in the CNS. Here we report that Nogo B, but not Nogo A, was increased in hippocampal tissue prepared from aged rats and rats which received an intracerebroventricular infusion of A β for 8 days. This increase was coupled with evidence of microglial activation and increased caspase 3 activity. Significantly, we observed that Nogo B was capable of triggering microglial activation in a culture of mixed glial cells and that it potently increased caspase 3 activity in neuronal cultures. These findings highlight previously unidentified effects of Nogo B in the brain.

2. Materials and methods

2.1. Animals

Male Wistar rats (Bantham and Kingman, UK) aged 3 months (250–350 g) or 22 months (550–650 g) were housed under a 12 h light/dark schedule and at an ambient temperature of 22–23 °C. Rats were maintained in the BioResources Unit at Trinity College, Dublin, under veterinary supervision throughout the study and experiments were performed under a license issued by the Department of Health (Ireland) and in accordance with the guidelines laid down by the local ethical committee.

In one study, in which only young rats were used, rats were randomly assigned to a group which were treated with a cocktail of A β _{1–40} + A β _{1–42}, and a control group which received the reverse peptide, A β _{40–1} for a period of 8 days (Miller et al., 2009). Animals were anaesthetized with ketamine (75 mg/kg) and xylazine (10 mg/kg) and implanted with osmotic mini-pumps (model 2004, Alzet, USA). The pump was implanted subcutaneously in the mid-scapular region and was attached via polyvinylchloride tubing (Alzet, 0.69 mm diameter) to a chronic indwelling cannula (Alzet, Infusion Kit II), which was positioned stereotaxically in the ventricle (0.9 mm posterior to bregma, 1.3 lateral to the midline and 3.5 mm ventral to the dura). The cannula was affixed to the skull using cyanoacrylate gel and was secured in place by a smooth covering of dental cement (Stoelten, USA). Post-operative care included a subcutaneous injection of the analgesic Rimadil (5 mg/kg). The pumps delivered a cocktail of A β _{1–40} (26.9 μ M) and A β _{1–42} (36.9 μ M; aggregated for 24 h at 25 °C and 37 °C for 48 h; Biosource, Belgium) or control peptide A β _{40–1} (63.8 μ M) intracerebroventricularly at the rate of 0.25 μ l/h (\pm 0.05 μ l) for 8 days. Analysis of the A β preparation by the thioflavin T fluorescent assay and gel electrophoresis revealed the presence of low oligomeric species; the predominant form (36% of the total) was the 13.5 kDa species.

2.2. Analysis of LTP

LTP was assessed in young and aged animals and in animals which received A β _{1–40} + A β _{1–42} or control peptide. Rats were anaesthetized with urethane (1.5 mg/kg) and assessed for their ability to sustain LTP in perforant path-granule cell synapses as described previously (Nolan et al., 2005). Briefly, a bipolar stimulating electrode was positioned in the perforant path (4.4 mm lateral to lambda), a unipolar recording electrode was positioned in the dorsal cell body region of the dentate gyrus (2.5 mm lateral and 3.9 mm posterior to bregma) and test shocks were delivered to the perforant path at 30 s intervals for up to an hour allowing the response to stabilize. Recordings were made for 10 min before and 40 min after tetanic stimulation (3 trains of stimuli; 250 Hz for 200 ms; 30 s intertrain interval) and at the end of this time, rats were killed by decapitation, the brains were rapidly removed and the hippocampus and cortex were dissected free. Tissue was divided into one portion which was flash frozen and later used for PCR, and a second portion, which was cross-chopped (350 μ m \times 350 μ m) and stored at –80 °C in Krebs buffer (composition in mM: NaCl 136, KCl 2.54, KH₂PO₄ 1.18, MgSO₄·7H₂O 1.18, NaHCO₃ 16, glucose 10) with added CaCl₂ (1.13 mM) and 10% dimethyl sulphoxide (DMSO);

the latter portion was used for Western immunoblotting and for analysis of activities of caspases 8 and 3.

2.3. Preparation and treatment of primary glial and neuronal cultures

Mixed glial cultures and neuronal cultures were prepared from the cortices of 1 day old Wistar rats (Trinity College, Dublin, Ireland) as previously described (Loane et al., 2009). Briefly, cortical tissue was dissected free, cross-chopped and triturated in Dulbecco's Modified Eagle's Medium (DMEM, Invitrogen, UK) supplemented with 10% Fetal Bovine Serum (FBS). The cells were passed through a sterile mesh filter (40 μ m), centrifuged at 2000 \times g for 3 min and plated (2.5 \times 10⁵ cells/ml). To prepare neuronal cultures, tissue was cross-chopped and incubated in phosphate-buffered saline (PBS) with trypsin (0.25 μ g/ml, Sigma, UK) for 25 min at 37 °C, triturated in PBS containing soybean trypsin inhibitor (0.2 μ g/ml, Sigma, UK) and DNase (0.2 mg/ml, Sigma, UK) and gently passed through a sterile mesh filter (40 μ m). The suspension was centrifuged at 2000 \times g for 3 min at 20 °C, and the pellet was resuspended in warm NeuroBasal Media (NBM, Invitrogen, UK), supplemented with 10% FBS, penicillin (100 units/ml, Invitrogen, UK) and B27 (Gibco). After 48 h the neurons were treated with Ara-C (5 μ g/ml, Sigma) for 24 h.

Glia were treated after 12 days in culture with Nogo B (10 or 100 ng/ml) and, after 24 h, cells were harvested for analysis of MHCII mRNA and CD11b mRNA by PCR. Neurons were similarly treated with Nogo B after 7 days in culture and, in this case, cells were harvested for analysis of activities of caspases 8 and 3. In both cases, cells were maintained at 37 °C in a humidified atmosphere containing 5% CO₂:95% air and media was replaced every 3 days.

Neurons were also treated with A β _{1–40} (4.2 μ M) + A β _{1–42} (5.6 μ M) or control peptide (10 μ M) for 48 h and treated 24 h subsequently with the Nogo receptor (NgR) antagonist NEP1-40 (Alpha Diagnostic Intl. Inc., TX 78244, USA). The cells were harvested 24 h later and assessed for caspase 3 activation. Supernatants were assessed for LDH release as a measure of cytotoxicity (Promega, Southampton, UK).

2.4. Assessment of caspase activity

Activities of caspase 8 and caspase 3 were analyzed using a colorimetric method (Biomol, UK), in samples of cortical and hippocampal homogenate prepared from young and aged rats, and rats treated with A β _{1–40} + A β _{1–42} or control peptide. Enzyme activity was also assessed in harvested cortical neurons. Samples and standards (25 μ l) were added to assay buffer (25 μ l) in a 96 well plate and aliquots of substrates for caspases 8 and 3 (Ac-IEITD-p-nitroanilide; pNA and Ac-DEVD-pNA, respectively; 50 μ l; 200 μ M final concentration) were added to start the reaction. Absorbance was measured continuously from 0 to 20 min at 405 nm, values were calculated with respect to the pNA calibration standard (100 μ l) and enzyme activity was expressed as pmol/min/mg protein.

2.5. Real-time PCR analysis of MHCII and CD11b mRNA expression

Total RNA was extracted from snap-frozen hippocampal tissue and harvested mixed glial cells using a NucleoSpin[®] RNAII isolation kit (Macherey-Nagel Inc., Germany) as per manufacturer's instructions. Denaturing agarose gel electrophoresis was used to assess the RNA integrity. Total RNA concentrations were determined by spectrophotometry, samples were equalised and stored at –80 °C until required for cDNA synthesis. cDNA synthesis was performed on 1 μ g total RNA using a High Capacity cDNA RT kit (Applied Biosystems, Germany). Real-time PCR was performed using Taqman Gene Expression Assays (Applied Biosystems, Germany) which contain forward and reverse primers, and a FAM-labelled MGB Taqman probe for each gene of interest; the assay IDs for MHCII and CD11b were Rn01768597_m1 and Rn00709342_m1, respectively. Real-time PCR was conducted using an ABI Prism 7300 instrument (Applied Biosystems, Germany). A 20 μ l volume was added to each well (9 μ l of diluted cDNA, 1 μ l of primer and 10 μ l of Taqman[®] Universal PCR Master Mix). Samples were assayed in duplicate in one run (40 cycles), which consisted of 3 stages, 95 °C for 10 min, 95 °C for 15 s for each cycle (denaturation) and finally the transcription step at 60 °C for 1 min. β -Actin was used as endogenous control to normalize gene expression data, and β -actin expression was conducted using a gene expression assay containing forward and reverse primers (primer limited) and a VIC-labelled MGB Taqman probe from Applied Biosystems (Germany; Assay ID: 4352341E). Gene expression was calculated relative to the endogenous control samples and to the control sample giving an RQ value (2^{–DDCt}, where Ct is the threshold cycle).

2.6. Analysis of Nogo, ICAM, CD86 and synaptophysin by Western immunoblotting

Tissue was equalized for protein, aliquots (10 μ l) were loaded onto 10% NuPAGE[®] Novex Bis-Tris gels (Invitrogen, UK), and were separated by application of a constant voltage (170 V; 70 min) and transferred onto nitrocellulose strips (30 V; 65 min). Proteins were immunoblotted for 2 h at room temperature with antibodies (1:100 in milk for Nogo A (Abcam, UK) and B (Chemicon International, USA); 1:200 in Tris-buffered saline (TBS)–Tween containing 2% BSA for CD86 and (R&D Systems, USA) ICAM-1 (Santa Cruz Biotechnology Inc., USA) and 1:400 in 1% BSA for synaptophysin (Sigma–Aldrich, UK) respectively. Membranes were washed three times in TBS–Tween, incubated with the appropriate secondary antibody (1:1000),

stripped with 'Reblot' (1:10 dilution; Chemicon International, USA) and stained for actin expression to ensure equal loading of protein. Actin expression was assessed using a mouse monoclonal IgG₁ antibody (1:10,000 in TBS-Tween containing 0.1% BSA; Santa Cruz Biotechnology Inc., USA). Immunoreactive bands were detected using peroxidase-conjugated anti-mouse IgG (Sigma) and ECL (GE Healthcare, UK) chemiluminescence and were quantified using densitometry (Labworks, UVP Biolmaging Systems, UK).

2.7. Statistical analysis

Data were analyzed using either Student's *t*-test for independent means, or analysis of variance (ANOVA) followed by post hoc Student Newman-Keuls test to determine which conditions were significantly different from each other. Data are expressed as means \pm SEM.

3. Results

LTP in perforant path-granule cell synapses was markedly decreased in aged, compared with young, rats ($***p < 0.001$; ANOVA; Fig. 1a) as previously described (Loane et al., 2009); the mean percentage changes (\pm SEM) in population epsp slope in the last 10 min of the experiment were 130.3 ± 0.57 and 107.6 ± 0.56 in young and aged rats, respectively. Nogo A and Nogo B were assessed in hippocampal tissue prepared from young and aged rats and the data indicate that, while there was no change in Nogo A, Nogo B was significantly increased in tissue prepared from aged, compared with young, rats ($***p < 0.01$; student's *t*-test for independent means; Fig. 1b, c). These changes were accompanied by evidence of microglial activation; thus increases in MHCII mRNA and in CD11b mRNA were observed in hippocampal tissue prepared from aged, compared with young, rats ($*p < 0.05$; $***p < 0.001$; student's *t*-test for independent means; Fig. 2a, b). In addition, both CD86 and ICAM-1 were increased ($*p < 0.05$; student's *t*-test for independent means; Fig. 2c, d) which is a further indication of an age-related increase in microglial activation, and which supports previous evidence (Griffin et al., 2006).

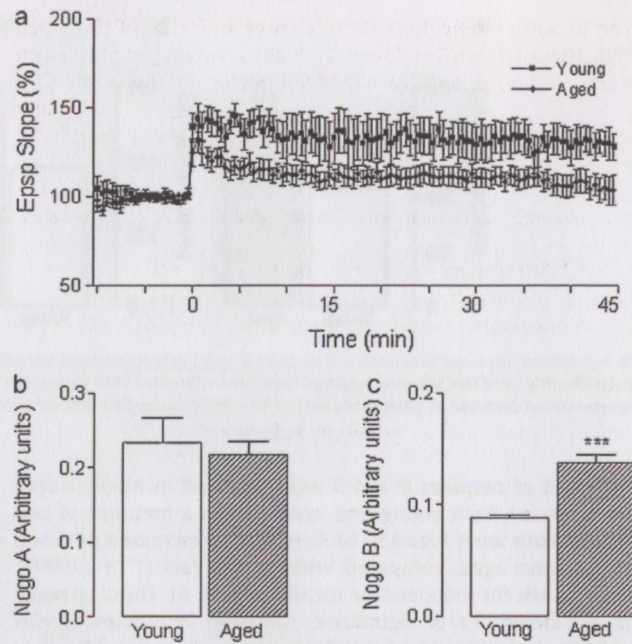


Fig. 1. The age-related decrease in LTP is accompanied by increased Nogo B in hippocampus. (a) LTP was significantly decreased in aged (22 months), compared with young (3 months), rats ($***p < 0.001$; $n = 8$). Nogo A (b) was unchanged but Nogo B (c) was significantly increased in hippocampal tissue prepared from aged, compared with young, rats ($***p < 0.001$; student's *t*-test for independent means). Data are expressed as means \pm SEM ($n = 6$).

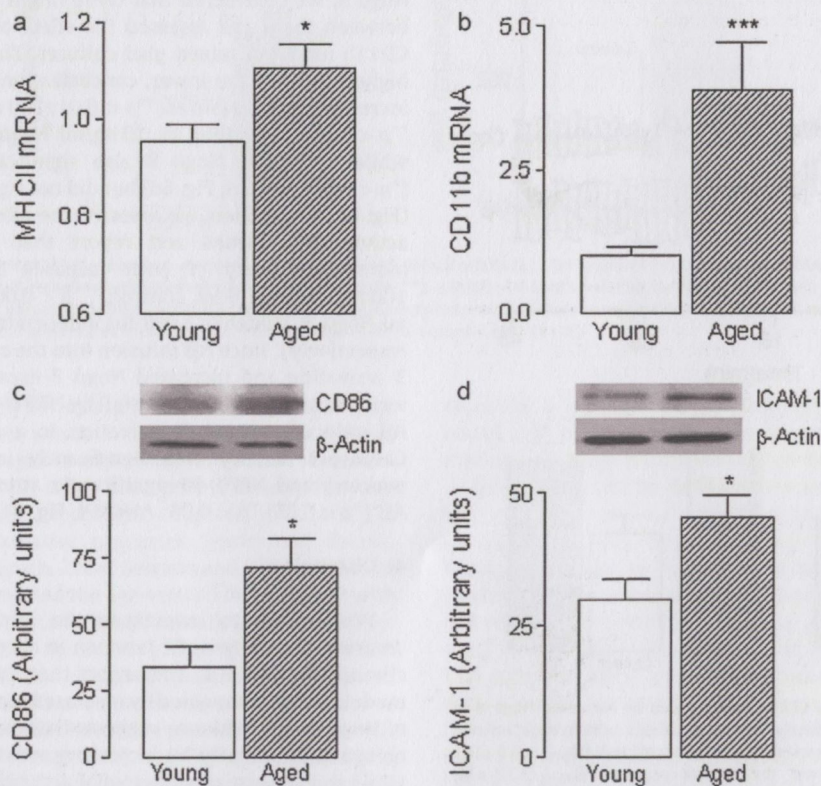


Fig. 2. Markers of microglial activation are increased in hippocampus of aged rats. MHCII mRNA (a) and CD11b mRNA (b) were significantly increased in hippocampal tissue prepared from aged, compared with young, rats ($*p < 0.05$, $***p < 0.001$; student's *t*-test for independent means) and these were accompanied by increases in CD86 (c) and ICAM-1 (d) ($*p < 0.05$; Student's *t*-test for independent means). Sample immunoblots for CD86 and ICAM-1 are shown. Data are expressed as means \pm SEM ($n = 8$).

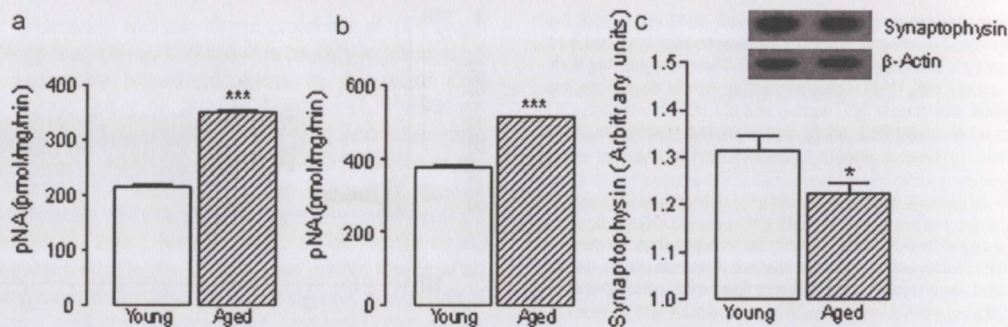


Fig. 3. Age-related increases in activities of caspases 8 and 3 in hippocampus are accompanied by a decrease in synaptophysin. Activities of caspase 8 (a) and caspase 3 (b) were significantly increased in tissue prepared from aged, compared with young, rats (*** $p < 0.001$; Student's t -test for independent means; $n = 6$) and this was accompanied by an age-related decrease in synaptophysin ((c) * $p < 0.05$; Student's t -test for independent means; $n = 8$).

Activities of caspases 8 and 3 were assessed in hippocampal tissue prepared from young and aged rats as a measure of cell stress and both were found to be significantly increased in tissue prepared from aged, compared with young, rats (*** $p < 0.001$; student's t -test for independent means; Fig. 3a, b). These changes were paralleled by a significant decrease in synaptophysin (* $p < 0.05$; student's t -test for independent means; Fig. 3c).

Having shown that the age-related deficit in LTP was coupled with increased expression of Nogo B and increased microglial activation, we investigated whether a similar coupling was observed in tissue prepared from A β -treated rats. Fig. 4 shows that chronic infusion of A β for 8 days led to a marked decrease in LTP; the mean percentage changes (\pm SEM) in population epsp slope in the last 10 min of the experiment were 114.8 ± 0.78 in rats treated with the control peptide A β_{40-1} and 87.0 ± 0.60 in rats treated with A $\beta_{1-42} + A\beta_{1-40}$. Analysis of tissue prepared from these rats revealed

that Nogo B was significantly increased (* $p < 0.05$; student's t -test for independent means; Fig. 4c), whereas Nogo A was similar in both cohorts of animals (Fig. 4b).

We next evaluated MHCII and CD11b mRNA as indicators of microglial activation and observed that both were significantly increased in hippocampal tissue prepared from rats which received A $\beta_{1-42} + A\beta_{1-40}$ compared with control (* $p < 0.05$; *** $p < 0.001$; student's t -test for independent means; Fig. 5a, b) and these changes were paralleled by an A β -induced increase in CD86 and ICAM-1 (* $p < 0.05$; *** $p < 0.001$; student's t -test for independent means; Fig. 5c, d). As in the case of aged animals, the increase in microglial activation was accompanied by increased activity of caspases 8 and 3 (*** $p < 0.001$; student's t -test for independent means; Fig. 5e, f).

Because the A β -induced and age-associated increases in markers of microglial activation were mirrored by an increase in Nogo B, we considered that there might be a causal relationship between them and assessed the effect of Nogo B on MHCII and CD11b mRNA in mixed glial cultures. The data indicate that the higher, but not the lower, concentration of Nogo B significantly increased both measures (** $p < 0.01$; 100 ng/ml Nogo B vs. control; ** $p < 0.01$; 100 ng/ml vs. 10 ng/ml Nogo B; ANOVA; Fig. 6a, b), while 100 ng/ml Nogo B also significantly increased ICAM-1 (* $p < 0.05$; ANOVA; Fig. 6d) but did not significantly increase CD86 (Fig. 6c). In addition, we assessed the effect of Nogo B on caspase activity in neurons and report that 100 ng/ml significantly increased activity of both caspases 8 and 3 (*** $p < 0.001$; 100 ng/ml Nogo B vs. control; *** $p < 0.001$; 100 ng/ml vs. 10 ng/ml Nogo B; student's t -test for independent means; Fig. 7a and b, respectively). Since A β infusion into the rat brain induced caspase 3 activation and increased Nogo B expression, we investigated whether antagonism of the NgR by NEP1-40 peptide could prevent A β -induced caspase 3 activation in a culture system (Fig. 8). Caspase-3 activity was significantly increased in A β -treated neurons, and NEP1-40 significantly attenuated the effect of the A β (* $p < 0.05$; * $p < 0.05$; ANOVA; Fig. 8).

4. Discussion

We set out to investigate the impact of Nogo B on the deterioration of synaptic function in aged rats and in rats treated chronically with A β , and report that the deficit in LTP in both models was accompanied by increased hippocampal concentration of Nogo B. The evidence suggests that Nogo B negatively impacts on synaptic integrity by increasing activities of caspases 8 and 3 while it also increases microglial activation.

First we showed that Nogo B was markedly increased in hippocampal tissue prepared from aged rats in which LTP in perforant path-granule cell synapses was decreased. The age-

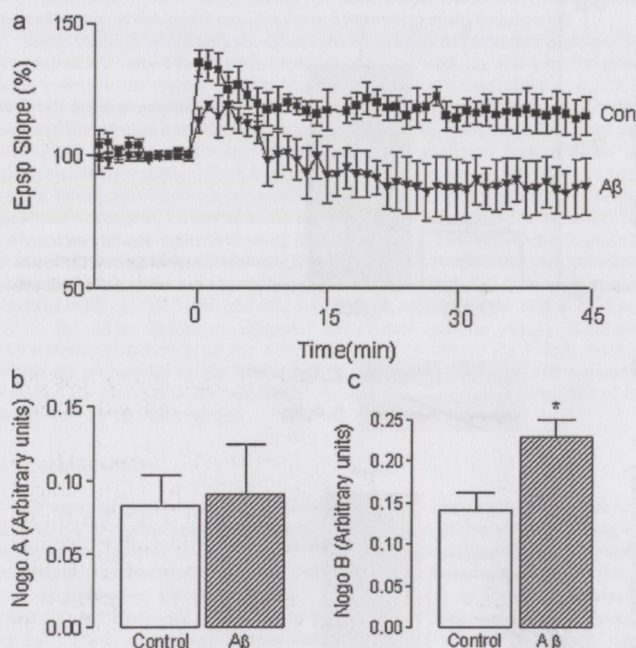


Fig. 4. The A β -induced decrease in LTP is accompanied by increased Nogo B in hippocampus. (a) LTP was significantly decreased in rats which were infused intracerebroventricularly for 8 days with A β_{1-40} (26.9 μ M) and A β_{1-42} (36.9 μ M), compared with rats which received the control peptide A β_{40-1} (63.8 μ M; *** $p < 0.001$; ANOVA; $n = 6$). Nogo A (b) was unchanged but Nogo B (c) was significantly increased in hippocampal tissue prepared from A β -treated, compared with control-treated, rats (* $p < 0.05$; student's t -test for independent means). Data are expressed as means \pm SEM ($n = 6$).

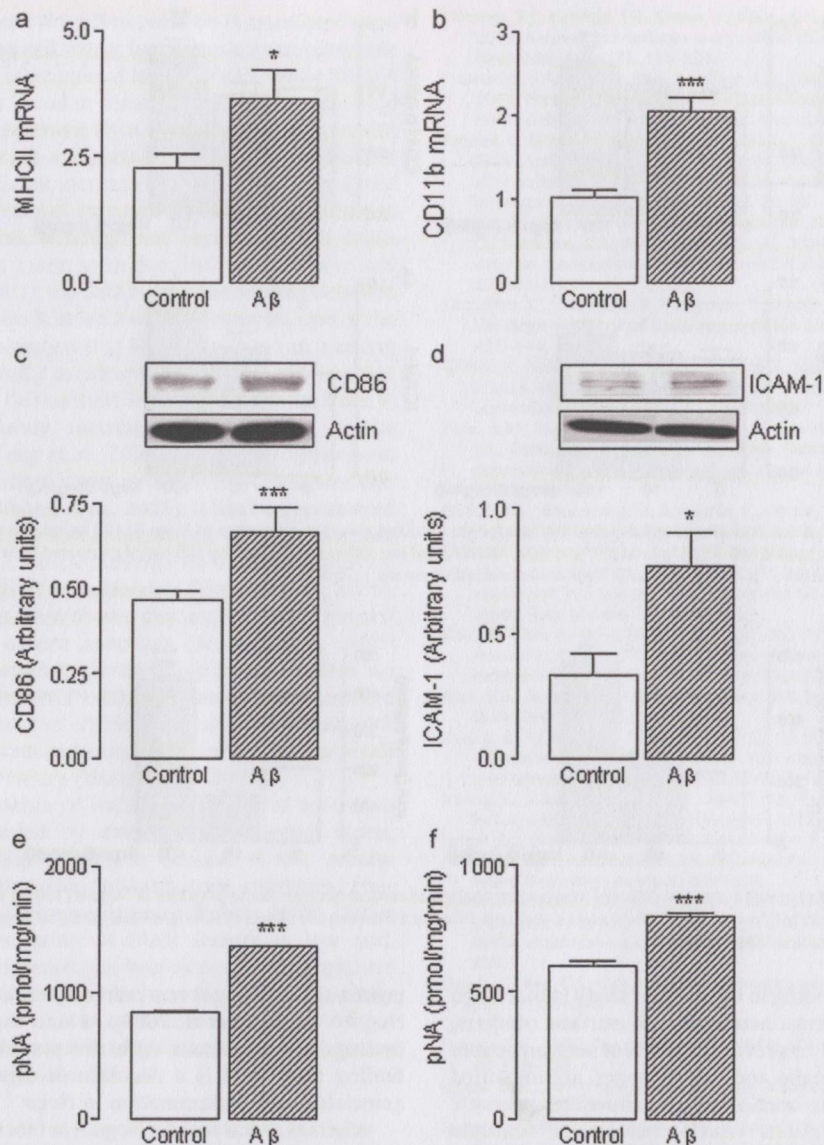


Fig. 5. A β induces changes in microglial activation and activities of caspases 8 and 3. MHCII mRNA (a), CD11b mRNA (b), CD86 (c) and ICAM-1 (d) were significantly increased in tissue prepared from A β -treated, compared with control-treated, rats (* $p < 0.05$; *** $p < 0.001$; student's *t*-test for independent means); sample immunoblots for CD86 and ICAM-1 are shown. Activities of caspase 8 (e) and caspase 3 (f) were also significantly increased in tissue prepared from A β -treated, compared with control-treated, rats (*** $p < 0.001$; Student's *t*-test for independent means; $n = 6$). Data are expressed as means \pm SEM ($n = 6$).

related deficit in LTP is well-documented and several authors have reviewed the many changes which contribute to the deficit; these include synaptic loss, changes in expression of specific receptors, alterations in signalling cascades and gene transcription and dysfunction in homeostatic mechanisms especially in terms of calcium handling and oxidative processes (Burke and Barnes, 2006; Lynch et al., 2006; Lynch, 2004; Serrano and Klann, 2004). In this laboratory, we have coupled the age-related deficit in LTP with evidence of microglial activation (Lynch, 2010), and the findings presented here support this, by showing that MHCII mRNA and CD11b mRNA are upregulated in hippocampus of aged, compared with young, rats. We have reported a similar age-related change in MHCII mRNA, though not in CD11b mRNA, previously (Lyons et al., 2009). CD86 and ICAM-1 are expressed on activated microglia and age-related increases in both markers are demonstrated here and elsewhere (Downer et al., 2010). Thus the increase in microglial activation is accompanied by increased Nogo B, but not Nogo A and, to our knowledge, there are no previous data which have

reported a similar change although, interestingly, a positive correlation between expression of genes associated with inflammation and Nogo B has been suggested (Yu et al., 2009).

We made a similar link between increased hippocampal Nogo B, increased microglial activation, and the deficit in LTP induced by A β . Once again, the change was specific to Nogo B, with no change observed in Nogo A, and no change in Nogo receptor (NgR) was observed (data not shown). Intracerebroventricular delivery of a cocktail of A $\beta_{1-40+1-42}$ for 8 days resulted in a marked decrease in the ability of rats to sustain LTP and, although LTP has not been evaluated previously using this delivery, delivery of A β for 28 days has a negative effect on spatial learning (Frautschy et al., 2001), inhibits LTP (Miller et al., 2009) and increases microglial activation (Frautschy et al., 2001; Piazza and Lynch, 2009). As in the case of aged animals the deficit in LTP is coupled with evidence of increased microglial activation and also increased Nogo B, strengthening the correlation between these 3 factors.

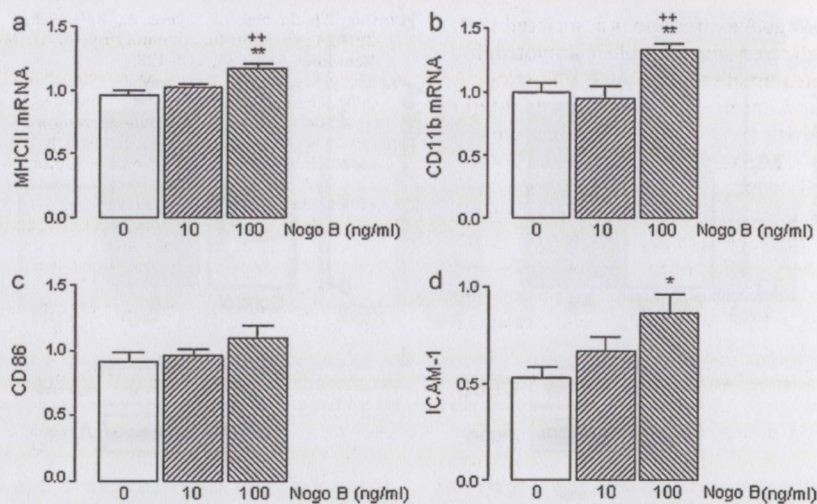


Fig. 6. Nogo B increases expression of markers of microglial activation. Incubation of mixed glia in the presence of Nogo B (100 ng/ml, but not 10 ng/ml) increased MHCII mRNA (a), CD11b mRNA (b), CD86 (c) and ICAM-1 ((d) * $p < 0.05$; ** $p < 0.01$; ANOVA) and the difference induced by 100 ng/ml compared with 10 ng/ml was significant in the case of MHCII mRNA and CD11b mRNA (** $p < 0.01$; ANOVA). Data are expressed as means \pm SEM ($n = 6$).

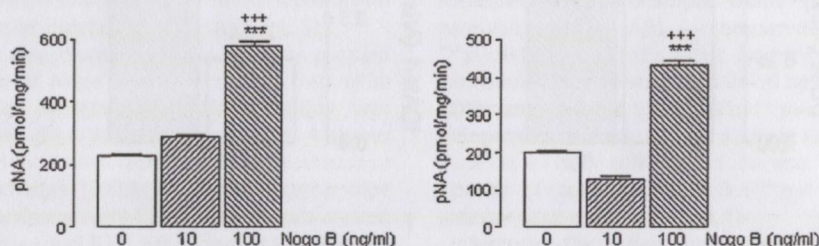


Fig. 7. Nogo B increases activities of caspases 8 and 3 in cultured neurons. Incubation of cortical neurons in the presence of Nogo B (100 ng/ml, but not 10 ng/ml) increased activity of caspase 8 (a) and caspase 3 (b; *** $p < 0.001$; ANOVA) and a significant difference between the effects of 100 ng/ml and 10 ng/ml Nogo B was observed (*** $p < 0.001$; ANOVA). Data are expressed as means \pm SEM ($n = 6$).

A significant and novel finding in the present study is that Nogo B activates microglia *in vitro*, increasing cell surface markers, MHCII and CD11b. There are no previous reports of such an action. However activation of microglia and macrophages, accompanied by upregulation of NgR, has been reported following traumatic brain injury and in the lesions which characterize multiple sclerosis (David et al., 2008). In an animal model of Alzheimer's disease the plaque-associated activated microglia (Simard et al., 2006) also seem to be associated with increased expression of NgR (Park et al., 2006). Interestingly, a role for Nogo B in recruitment of macrophages was implicated by *in vitro* analysis of the effect of Nogo B on chemotaxis and by the finding that infiltration of F4/80

positive macrophages was markedly reduced in ischaemic tissue in Nogo^{-/-} mice (Yu et al., 2009). At least in the broadest sense, these findings are consistent with the present observation, as is the finding that there is a decrease in expression of several genes associated with inflammation in Nogo^{-/-} mice (Yu et al., 2009).

Whereas a vital role for Nogo A in blocking neurite outgrowth is widely recognized (Yan et al., 2006), the function of Nogo B, particularly in the brain where expression has been reported (Acevedo et al., 2004; Chen et al., 2000; Huber et al., 2002; Yan et al., 2006), is almost unexplored. However the presence of the 3 Nogo transcripts in the hippocampus during development points to a physiological role (Meier et al., 2003) but the nature of the role, specifically in the context of Nogo B is currently unclear. Its marked expression in blood vessels, and in cultured endothelial cells and smooth muscle cells, has led to the proposal that it is an important factor in vascular remodelling and there is certainly evidence to support this (Acevedo et al., 2004). Data from a recent study demonstrated that recovery of blood flow following ischaemic injury to the hindlimb, and the associated angiogenesis and arteriogenesis, was reduced in Nogo^{-/-} mice (Yu et al., 2009). The evidence linked this poor recovery with a Nogo B-associated decrease in the recruitment of macrophages to the ischaemic tissue (Yu et al., 2009). In this context therefore, it was somewhat surprising that genetic deletion of Nogo A and B was associated with reduced recovery in 12-month-old rats following traumatic brain injury (Marklund et al., 2009). Nogo B, but particularly Nogo A, was increased in the hippocampus following deafferentation and, in the case of Nogo B, this upregulation persisted until axonal sprouting peaked at which time its expression returned to control levels (Meier et al., 2003).

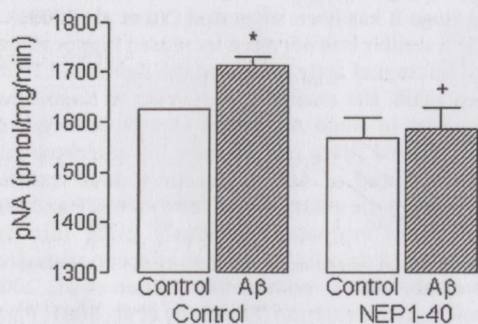


Fig. 8. NgR antagonist NEP1-40 rescued the A β -induced activation of caspase 3 in cultured neurons. A β significantly induced caspase 3 activation after 48 h in cultured neurons (* $p < 0.05$; ANOVA) and this was significantly attenuated by treatment with NEP1-40 (1 μ M; + $p < 0.05$; ANOVA).

It is known that increased Nogo A expression is associated with conditions characterized by cell stress, for example in amyotrophic lateral sclerosis (ALS) and in an animal model of ALS, while Nogo A autoantibodies have been found in serum and cerebrospinal fluid of patients with multiple sclerosis (Yan et al., 2006). Here we did not find any age-related or A β -associated change in Nogo A but the age-related and A β -associated increase in Nogo B was associated with increases in the activities of caspases 8 and 3. These enzymes are indicators of cell stress, although not necessarily cell death (Garnier et al., 2004) and taken with the findings of Meier and colleagues (Meier et al., 2003), the data suggest a coupling between tissue or cell stress and Nogo B, at least in hippocampus. One of the significant findings in this study is that Nogo B induced an increase in activities of caspases 8 and 3 in cultured neurons suggesting that it can trigger cell stress. In this context, it is interesting that Nogo B, like the other Nogo family members, is abundant in the endoplasmic reticulum (Teng et al., 2004) and its overexpression induces endoplasmic reticulum stress, which at least in some cases is linked with apoptosis (Kuang et al., 2006). It has been proposed that an apoptotic signal arises as a consequence of the interaction between Nogo B and Bcl-2 which prevents its translocation from the endoplasmic reticulum to mitochondria (Tagami et al., 2000). Consistent with this, it has been shown that expression of Nogo B in cancer cell lines can induce apoptosis (Kuang et al., 2005) although this has been disputed (Oertle et al., 2003a,b). Here we show that the NgR antagonist NEP1-40 attenuated the A β -induced increase in caspase 3 activation which is broadly consistent with the finding that NEP1-40 reduced caspase-3 activation as a result of focal cerebral ischemic injury (Wang et al., 2008).

Several factors are capable of inducing microglial activation which is often accompanied by evidence of neuronal stress, presumably as a consequence of the actions of the release neuromodulatory molecules, like inflammatory cytokines, chemokines, and oxidative and nitrogen species (Lynch, 2009). Under resting conditions concentration of these factors is low and, together with appropriate interactions between cells, microglia are maintained in a quiescent state. The findings of this study identify Nogo B as another factor which contributes to activation of microglia and highlights the need to establish the mechanisms by which its expression is modulated.

Acknowledgements

This work was funded by the Health Research Board Ireland and Science Foundation Ireland.

References

- Acevedo, L., Yu, J., Erdjument-Bromage, H., Miao, R.Q., Kim, J.E., Fulton, D., Tempst, P., Strittmatter, S.M., Sessa, W.C., 2004. A new role for Nogo as a regulator of vascular remodeling. *Nat. Med.* 10, 382–388.
- Beck, K.D., Nguyen, H.X., Galvan, M.D., Salazar, D.L., Woodruff, T.M., Anderson, A.J., 2010. Quantitative analysis of cellular inflammation after traumatic spinal cord injury: evidence for a multiphasic inflammatory response in the acute to chronic environment. *Brain*.
- Burke, S.N., Barnes, C.A., 2006. Neural plasticity in the ageing brain. *Nat. Rev. Neurosci.* 7, 30–40.
- Chen, M.S., Huber, A.B., van der Haar, M.E., Frank, M., Schnell, L., Spillmann, A.A., Christ, F., Schwab, M.E., 2000. Nogo-A is a myelin-associated neurite outgrowth inhibitor and an antigen for monoclonal antibody IN-1. *Nature* 403, 434–439.
- Clarke, R.M., Lyons, A., O'Connell, F., Deighan, B.F., Barry, C.E., Anyakoha, N.G., Nicolaou, A., Lynch, M.A., 2008. A pivotal role for interleukin-4 in atorvastatin-associated neuroprotection in rat brain. *J. Biol. Chem.* 283, 1808–1817.
- Clarke, R.M., O'Connell, F., Lyons, A., Lynch, M.A., 2007. The HMG-CoA reductase inhibitor, atorvastatin, attenuates the effects of acute administration of amyloid-beta-1-42 in the rat hippocampus in vivo. *Neuropharmacology* 52, 136–145.
- David, S., Fry, E.J., Lopez-Vales, R., 2008. Novel roles for Nogo receptor in inflammation and disease. *Trends Neurosci.* 31, 221–226.
- Downer, E.J., Cowley, T.R., Lyons, A., Mills, K.H., Berezin, V., Bock, E., Lynch, M.A., 2010. A novel anti-inflammatory role of NCAM-derived mimetic peptide, FGL. *Neurobiol. Aging* 31, 118–128.
- Frautschy, S.A., Hu, W., Kim, P., Miller, S.A., Chu, T., Harris-White, M.E., Cole, G.M., 2001. Phenolic anti-inflammatory antioxidant reversal of Abeta-induced cognitive deficits and neuropathology. *Neurobiol. Aging* 22, 993–1005.
- Freund, P., Schmidlin, E., Wannier, T., Bloch, J., Mir, A., Schwab, M.E., Rouiller, E.M., 2009. Anti-Nogo-A antibody treatment promotes recovery of manual dexterity after unilateral cervical lesion in adult primates—re-examination and extension of behavioral data. *Eur. J. Neurosci.* 29, 983–996.
- Garnier, P., Prigent-Tessier, A., Van Hoeck, M., Bertrand, N., Demougeot, C., Sordet, O., Swanson, R.A., Marie, C., Beley, A., 2004. Hypoxia induces caspase-9 and caspase-3 activation without neuronal death in gerbil brains. *Eur. J. Neurosci.* 20, 937–946.
- GrandPre, T., Nakamura, F., Vartanian, T., Strittmatter, S.M., 2000. Identification of the Nogo inhibitor of axon regeneration as a Reticulon protein. *Nature* 403, 439–444.
- Griffin, R., Nally, R., Nolan, Y., McCartney, Y., Linden, J., Lynch, M.A., 2006. The age-related attenuation in long-term potentiation is associated with microglial activation. *J. Neurochem.* 99, 1263–1272.
- Hein, A.M., Stasko, M.R., Matousek, S.B., Scott-McKean, J.J., Maier, S.F., Olschowka, J.A., Costa, A.C., O'Banion, M.K., 2009. Sustained hippocampal IL-1beta overexpression impairs contextual and spatial memory in transgenic mice. *Brain Behav. Immun.*
- Huber, A.B., Weinmann, O., Brosamle, C., Oertle, T., Schwab, M.E., 2002. Patterns of Nogo mRNA and protein expression in the developing and adult rat and after CNS lesions. *J. Neurosci.* 22, 3553–3567.
- Josephson, A., Widenfalk, J., Widmer, H.W., Olson, L., Spenger, C., 2001. Nogo mRNA expression in adult and fetal human and rat nervous tissue and in weight drop injury. *Exp. Neurol.* 169, 319–328.
- Kilic, E., Elali, A., Kilic, U., Guo, Z., Ugru, M., Uslu, U., Bassetti, C.L., Schwab, M.E., Hermann, D.M., 2010. Role of Nogo-A in neuronal survival in the reperfused ischemic brain. *J. Cereb. Blood Flow Metab.*
- Kim, H.S., Suh, Y.H., 2009. Minocycline and neurodegenerative diseases. *Behav. Brain Res.* 196, 168–179.
- Kuang, E., Wan, Q., Li, X., Xu, H., Liu, Q., Qi, Y., 2005. ER Ca²⁺ depletion triggers apoptotic signals for endoplasmic reticulum (ER) overload response induced by overexpressed reticulon 3 (RTN3/HAP). *J. Cell Physiol.* 204, 549–559.
- Kuang, E., Wan, Q., Li, X., Xu, H., Zou, T., Qi, Y., 2006. ER stress triggers apoptosis induced by Nogo-B/ASY overexpression. *Exp. Cell Res.* 312, 1983–1988.
- Loane, D.J., Deighan, B.F., Clarke, R.M., Griffin, R.J., Lynch, A.M., Lynch, M.A., 2009. Interleukin-4 mediates the neuroprotective effects of rosiglitazone in the aged brain. *Neurobiol. Aging* 30, 920–931.
- Lynch, A.M., Loane, D.J., Minogue, A.M., Clarke, R.M., Kilroy, D., Nally, R.E., Roche, O.J., O'Connell, F., Lynch, M.A., 2007. Eicosapentaenoic acid confers neuroprotection in the amyloid-beta challenged aged hippocampus. *Neurobiol. Aging* 28, 845–855.
- Lynch, G., Rex, C.S., Gall, C.M., 2006. Synaptic plasticity in early aging. *Ageing Res. Rev.* 5, 255–280.
- Lynch, M.A., 2004. Long-term potentiation and memory. *Physiol. Rev.* 84, 87–136.
- Lynch, M.A., 2009. The multifaceted profile of activated microglia. *Mol. Neurobiol.* 40, 139–156.
- Lynch, M.A., 2010. Age-related neuroinflammatory changes negatively impact on neuronal function. *Front Aging Neurosci.* 1, 6.
- Lyons, A., Griffin, R.J., Costelloe, C.E., Clarke, R.M., Lynch, M.A., 2007. IL-4 attenuates the neuroinflammation induced by amyloid-beta in vivo and in vitro. *J. Neurochem.* 101, 771–781.
- Lyons, A., Lynch, A.M., Downer, E.J., Hanley, R., O'Sullivan, J.B., Smith, A., Lynch, M.A., 2009. Fractalkine-induced activation of the phosphatidylinositol-3 kinase pathway attenuates microglial activation in vivo and in vitro. *J. Neurochem.* 110, 1547–1556.
- Marklund, N., Bareyre, F.M., Royo, N.C., Thompson, H.J., Mir, A.K., Grady, M.S., Schwab, M.E., McIntosh, T.K., 2007. Cognitive outcome following brain injury and treatment with an inhibitor of Nogo-A in association with an attenuated downregulation of hippocampal growth-associated protein-43 expression. *J. Neurosurg.* 107, 844–853.
- Marklund, N., Morales, D., Clausen, F., Hanell, A., Kiwanuka, O., Pitkanen, A., Gimbel, D.A., Philipson, O., Lannfelt, L., Hillered, L., Strittmatter, S.M., McIntosh, T.K., 2009. Functional outcome is impaired following traumatic brain injury in aging Nogo-A/B-deficient mice. *Neuroscience* 163, 540–551.
- Meier, S., Brauer, A.U., Heimrich, B., Schwab, M.E., Nitsch, R., Savaskan, N.E., 2003. Molecular analysis of Nogo expression in the hippocampus during development and following lesion and seizure. *FASEB J.* 17, 1153–1155.
- Miller, A.M., Piazza, A., Martin, D.S., Walsh, M., Mandel, A., Bolton, A.E., Lynch, M.A., 2009. The deficit in long-term potentiation induced by chronic administration of amyloid-beta is attenuated by treatment of rats with a novel phospholipid-based drug formulation, VP025. *Exp. Gerontol.* 44, 300–304.
- Minogue, A.M., Lynch, A.M., Loane, D.J., Herron, C.E., Lynch, M.A., 2007. Modulation of amyloid-beta-induced and age-associated changes in rat hippocampus by eicosapentaenoic acid. *J. Neurochem.* 103, 914–926.
- Moore, A.H., Wu, M., Shaftel, S.S., Graham, K.A., O'Banion, M.K., 2009. Sustained expression of interleukin-1beta in mouse hippocampus impairs spatial memory. *Neuroscience*.
- Morris, N.J., Ross, S.A., Neveu, J.M., Lane, W.S., Lienhard, G.E., 1999. Cloning and characterization of a 22 kDa protein from rat adipocytes: a new member of the reticulon family. *Biochim. Biophys. Acta* 1450, 68–76.

- Nolan, Y., Maher, F.O., Martin, D.S., Clarke, R.M., Brady, M.T., Bolton, A.E., Mills, K.H., Lynch, M.A., 2005. Role of interleukin-4 in regulation of age-related inflammatory changes in the hippocampus. *J. Biol. Chem.* 280, 9354–9362.
- Oertle, T., Huber, C., van der Putten, H., Schwab, M.E., 2003a. Genomic structure and functional characterisation of the promoters of human and mouse *nogo/rtn4*. *J. Mol. Biol.* 325, 299–323.
- Oertle, T., Merkler, D., Schwab, M.E., 2003b. Do cancer cells die because of Nogo-B? *Oncogene* 22, 1390–1399.
- Park, J.H., Gimbel, D.A., GrandPre, T., Lee, J.K., Kim, J.E., Li, W., Lee, D.H., Strittmatter, S.M., 2006. Alzheimer precursor protein interaction with the Nogo-66 receptor reduces amyloid-beta plaque deposition. *J. Neurosci.* 26, 1386–1395.
- Piazza, A., Lynch, M.A., 2009. Neuroinflammatory changes increase the impact of stressors on neuronal function. *Biochem. Soc. Trans.* 37, 303–307.
- Prinjha, R., Moore, S.E., Vinson, M., Blake, S., Morrow, R., Christie, G., Michalovich, D., Simmons, D.L., Walsh, F.S., 2000. Inhibitor of neurite outgrowth in humans. *Nature* 403, 383–384.
- Serrano, F., Klann, E., 2004. Reactive oxygen species and synaptic plasticity in the aging hippocampus. *Ageing Res. Rev.* 3, 431–443.
- Simard, A.R., Soulet, D., Gowing, G., Julien, J.P., Rivest, S., 2006. Bone marrow-derived microglia play a critical role in restricting senile plaque formation in Alzheimer's disease. *Neuron* 49, 489–502.
- Stirling, D.P., Khodarahmi, K., Liu, J., McPhail, L.T., McBride, C.B., Steeves, J.D., Ramer, M.S., Tetzlaff, W., 2004. Minocycline treatment reduces delayed oligodendrocyte death, attenuates axonal dieback, and improves functional outcome after spinal cord injury. *J. Neurosci.* 24, 2182–2190.
- Tagami, S., Eguchi, Y., Kinoshita, M., Takeda, M., Tsujimoto, Y., 2000. A novel protein, RTN-XS, interacts with both Bcl-XL and Bcl-2 on endoplasmic reticulum and reduces their anti-apoptotic activity. *Oncogene* 19, 5736–5746.
- Teng, F.Y., Ling, B.M., Tang, B.L., 2004. Inter- and intracellular interactions of Nogo: new findings and hypothesis. *J. Neurochem.* 89, 801–806.
- Wang, Q., Gou, X., Xiong, L., Jin, W., Chen, S., Hou, L., Xu, L., 2008. Trans-activator of transcription-mediated delivery of NEP1-40 protein into brain has a neuroprotective effect against focal cerebral ischemic injury via inhibition of neuronal apoptosis. *Anesthesiology* 108, 1071–1080.
- Wang, X., Chun, S.J., Treloar, H., Vartanian, T., Greer, C.A., Strittmatter, S.M., 2002. Localization of Nogo-A and Nogo-66 receptor proteins at sites of axon-myelin and synaptic contact. *J. Neurosci.* 22, 5505–5515.
- Yan, R., Shi, Q., Hu, X., Zhou, X., 2006. Reticulon proteins: emerging players in neurodegenerative diseases. *Cell Mol. Life Sci.* 63, 877–889.
- Yu, J., Fernandez-Hernando, C., Suarez, Y., Schleicher, M., Hao, Z., Wright, P.L., DiLorenzo, A., Kyriakides, T.R., Sessa, W.C., 2009. Reticulon 4B (Nogo-B) is necessary for macrophage infiltration and tissue repair. *Proc. Natl. Acad. Sci. U.S.A.* 106, 17511–17516.

Long-term potentiation is impaired in CD200-deficient mice: a role for Toll-like receptor activation.

**Derek A. Costello*, Anthony Lyons*, Tara Browne, Stephanie Denieffe, F. Fionnuala Cox
and Marina A. Lynch**

From Department of Physiology and Trinity College Institute of Neuroscience,
Trinity College, Dublin 2, Ireland.

Running title: Increased TLR enhances susceptibility in CD200^{-/-} mice

Correspondence should be addressed to Derek Costello, Department of Physiology, Trinity College Institute of Neuroscience, Trinity College, Dublin 2, Ireland

Email: derek.costello@tcd.ie

*These authors contributed equally to this work

ABSTRACT

The membrane glycoprotein CD200 is expressed on several cell types including neurons whereas expression of its receptor, CD200R, is restricted principally to cells of the myeloid lineage, including microglia. The interaction between CD200 and CD200R maintains microglia and macrophages in a quiescent state, therefore CD200-deficient mice express an inflammatory phenotype exhibiting increased macrophage or microglial activation in models of arthritis, encephalitis and uveoretinitis. Here, we report that lipopolysaccharide (LPS) and Pam₃CysSerLys₄ (Pam₃Csk₄) exerted more profound effects on release of the proinflammatory cytokines, interleukin (IL)-1 β , IL-6 and tumour necrosis factor (TNF)- α in glia prepared from CD200^{-/-}, compared with wildtype, mice. This effect is explained by the loss of CD200 on astrocytes which modulates microglial activation. Expression of Toll-like receptors (TLR)-4 and -2 was increased in glia prepared from CD200^{-/-} mice and the evidence indicates that microglial activation, assessed by the increased numbers of CD11b⁺ cells which stained positively for both MHCII and CD40, was enhanced in CD200^{-/-}, compared with wildtype, mice. These neuroinflammatory changes were associated with impaired long-term potentiation (LTP) in CA1 of hippocampal slices prepared from CD200^{-/-} mice. One possible explanation for this is the increase in TNF α in hippocampal tissue prepared from CD200^{-/-} mice, since TNF α application inhibited LTP in CA1. Significantly, LPS and Pam₃Csk₄, at concentrations which did not affect LTP in wildtype mice, inhibited LTP in slices prepared from CD200^{-/-} mice, likely due to the accompanying increase in TLR2 and TLR4. Thus the neuroinflammatory changes which result from CD200 deficiency have a negative impact on synaptic plasticity.

INTRODUCTION

CD200 is a type-1 membrane glycoprotein which has been identified as an immunosuppressive molecule, consistent with its expression on cells of the immune system including dendritic cells, T and B cells, endothelial and epithelial cells (1). Diverse immuno-

modulatory roles for CD200 have been reported; these include antigen-specific T cell responses, suppression of regulatory T cells (2), cytotoxic T cell-mediated tumour suppression (3), graft survival (4) and apoptosis-associated immune tolerance (5).

In the brain, CD200 is expressed on neurons (6) and oligodendrocytes (7) but not on microglia (8). A recent report has indicated that CD200 is expressed on reactive astrocytes in lesions from postmortem multiple sclerosis brains (7). Expression of CD200R is mainly restricted to cells of the myeloid lineage and therefore, in the brain, has been identified on microglia (6,7) but not on neurons (8). The complementary expression of ligand and receptor on neurons and microglia respectively suggests that their interaction may play a role in modulating microglial activation and recent evidence has supported this contention. The LPS-induced increases in expression of cell surface markers of microglial activation and inflammatory cytokine production were inhibited by addition of neurons and this attenuating effect of neurons was blocked by an anti-CD200 antibody (8). This finding suggests that interaction of CD200 with its receptor has the capacity to modulate microglial activation.

In CD200-deficient mice, increased microglial and/or macrophage activation has been described in several models of inflammation, for example facial nerve transection, experimental autoimmune encephalomyelitis (EAE), an animal model of arthritis (9) and experimental autoimmune uveoretinitis (10). Conversely, administration of a CD200 fusion protein ameliorates the inflammatory changes observed in collagen-induced arthritis (11,12), while the decrease in EAE-like symptoms in *Wld^s* mice has been attributed to increased expression of CD200 on spinal cord neurons (13).

Reduced expression of CD200 is coupled with increased microglial activation in hippocampus of aged and β -amyloid (A β)-treated rats (8,14), and synaptic plasticity, specifically long-term potentiation (LTP), is impaired when microglial activation is increased (15,16). Therefore we predicted that glia prepared from CD200-deficient mice would respond more profoundly to LPS and that this would be coupled with evidence of impaired LTP. The data show that LPS and

Pam₃Csk₄ exert a greater effect on glia prepared from CD200^{-/-} mice, presumably due to the observed increase in expression of TLR4 and TLR2 on these cells. In addition, LTP was markedly reduced at CA1 synapses of hippocampal slices prepared from CD200^{-/-}, compared with wildtype, mice. LPS and Pam₃Csk₄ further attenuated LTP in slices prepared from CD200^{-/-} mice. The data provide further evidence for an important immunomodulatory role for CD200, and couples the loss of CD200 with a deficit in synaptic function and with increased expression of TLR 2 and 4.

EXPERIMENTAL PROCEDURES

Animals

1 day-old and 2-6 month-old C57BL/6 or CD200^{-/-} mice were used for preparation of glial cultures or for preparation of hippocampal slices respectively. Tissue from 2-6 month-old mice was also used for analysis of expression of TLR2 and 4 and HMGB1. All experiments were performed under licence (Department of Health and Children, Ireland) and with ethical approval (BioResources, Trinity College, Dublin) in accordance with local guidelines. Animals were housed under controlled conditions (20-22°C, food and water *ad lib*) and maintained under veterinary supervision.

Preparation and treatment of primary glial cultures.

Mixed glial cultures were prepared from 1-day-old C57BL/6 mice or CD200^{-/-} mice as previously described (8). These cultures contained approximately 70% astrocytes and 30% microglia as assessed by expression of CD11b using FACS. We used mixed glia because CD200 is expressed on astrocytes, but not microglia. This means that knocking out CD200 will have no impact on microglia unless they are in culture with astrocytes and, in this case, the effect can be attributed to the loss of signaling through CD200R. In the context of this study, isolated microglia prepared from wildtype and CD200^{-/-} are essentially the same.

In one series of experiments, cells were harvested for flow cytometric analysis to evaluate expression of cell surface markers of microglial activation, GLAST to identify astrocytes, or for PCR to evaluate expression of TLRs 2 and 4. In a second series of experiments, cells were incubated in the presence or absence of LPS (100ng/ml;

Alexis Biochemical; US) or Pam₃Csk₄ (100ng/ml; InvivoGen, US) and, 24h later, supernatant was collected and assessed for concentration of IL-1 β , IL-6 and TNF α .

Purified astrocytes were prepared as described previously, using the shaking method to remove microglia (17), and membranes were isolated using a subcellular protein fractionation kit (Thermo Scientific, USA). Cells were incubated in trypsin-EDTA (1ml, 15 min, 37°C), centrifuged (500 x g, 5 min), washed with ice-cold PBS, resuspended in PBS and centrifuged (500 x g, 5 min). The pellet was re-suspended in ice-cold Cytoplasmic Extraction Buffer containing protease inhibitors (Thermo Scientific, USA), incubated (4°C, 10 min) and centrifuged (3,000 x g, 5 min); the supernatant provided the cytosolic fraction, while the pellet, which contained the membrane fraction, was resuspended in ice-cold Membrane Extraction Buffer containing protease inhibitors (Thermo Scientific, USA), incubated (4°C, 10 min) and centrifuged (3,000 x g, 5 min). The resultant supernatant provided the membrane fraction.

To prepare microglia, cells were initially seeded onto 25cm² flasks and, after 24 hours, media was replaced with cDMEM containing GM-CSF (20ng/ml) and M-CSF (5ng/ml). After 10-14 days in culture, non-adherent microglia were harvested by shaking (110rpm, 2 hours, room temperature), tapping and centrifuging (2000rpm, 5 min). The pellet was resuspended in cDMEM, the microglia were plated onto 24-well plates at a density of 1 x 10⁵ cells/ml and maintained at 37°C in a 5% CO₂ humidified atmosphere for up to 3 days prior to treatment.

Flow cytometry.

Glial cells were trypsinized (0.25% Trypsin-EDTA, Sigma, UK), washed 3 times in FACS buffer (2% FBS, 0.1% NaN₃ in PBS). Whole brain tissue was harvested and passed through a cell strainer (70 μ m) and centrifuged (170 x g, 10 min). The pellet was resuspended in PBS containing collagenase D (1mg/ml) and DNase I (200 μ g/ml), incubated at 37°C for 30 min and centrifuged (170 x g, 5 min). Pellets were resuspended in 1.088g/ml Percoll (9ml), overlaid with 1.122g/ml Percoll (5ml), and overlaid with 1.072g/ml and 1.030g/ml (9ml each) Percoll and PBS (9ml) and centrifuged

(1250 x g, 45 min). The mononuclear cells (between the 1.088:1.072 and 1.072:1.030) were centrifuged and the pellets were washed. All cells were blocked for 15 min at room temperature in FACS block (Mouse BD Fc Block (BD Pharmingen, UK); 1:500 in FACS buffer). Cells were incubated with PE-Cy7- or APC-rat anti-mouse CD11b (BD Biosciences, UK), FITC-rat anti-mouse CD40 (BD Biosciences, UK), PE-rat anti-mouse MHCII (BD Biosciences, UK), APC-rat anti-mouse CD200 (BD Biosciences, UK), PE-rat anti-mouse CD200R (Serotec, UK), FITC-rat anti-mouse TLR2 (Cambridge Biosciences, UK), FITC-rat anti-mouse TLR4 (Cambridge Biosciences, UK), PE-Cy7-anti-mouse CD45 (BD Biosciences, UK) and APC-rat anti-mouse GLAST (BD Biosciences, UK). Antibodies were diluted (1:400) in FACS buffer. Immunofluorescence analysis was performed on a DAKO Cyan ADP 7 colour flow cytometer (DAKO Cytomation, UK) with Summit v4.3 software.

Real-time PCR analysis of CD11b, CD40, TLR2 and TLR4.

Total RNA was extracted from snap-frozen hippocampal tissue and harvested mixed glial cells using a NucleoSpin® RNAII isolation kit (Macherey-Nagel Inc., Germany) and cDNA synthesis was performed on 1 µg total RNA using a High Capacity cDNA RT kit (Applied Biosystems, Germany); the protocols used were according to the manufacturer's instructions. Real-time PCR was performed as described previously (8) using an ABI Prism 7300 instrument (Applied Biosystems, Germany). The primers IDs were as follows CD11b: Mm01271265_m1, CD40: Mm00441895_m1, TLR2: Mm00442346_m1 and TLR4: Mm00445273_m1 (Applied Biosystems, Germany). Samples were assayed in duplicate and gene expression was calculated relative to the endogenous control samples (β -actin) to give an RQ value ($2^{-\Delta\Delta Ct}$, where CT is the threshold cycle).

Analysis of IL-1 β , IL-6 and TNF α .

The concentrations of IL-1 β , IL-6 and TNF α were analyzed in triplicate by ELISA in samples of supernatant obtained from *in vitro* experiments as previously described (8).

Analysis of CD200, GFAP, pI κ B α , IL-1 α , IL-1 β and TNF α by Western immunoblotting

Hippocampal lysate was assessed for expression of IL-1 α , IL-1 β and TNF α , glial cell lysate was evaluated for expression of pI κ B α , and membrane and cytosolic preparations obtained from purified astrocytes were evaluated for expression of CD200 and GFAP using standard Western immunoblotting methods (8,18). Primary antibodies directed against CD200 (anti-goat; 1:500; Santa Cruz Biotechnology, US), GFAP (anti-rabbit; 1:1000; Invitrogen, US), pI κ B α (ser32) (anti-rabbit; 1:1000; Cell Signaling, US), IL-1 α (anti-goat; 1:1000; R & D Systems, US), IL-1 β (anti-goat; 1:500; Santa Cruz Biotechnology, US) and TNF α (anti-rabbit; 1:500; Cell Signaling, US) were incubated overnight at 4°C. The secondary antibodies were conjugated to horseradish peroxidase (1:5000; Jackson ImmunoResearch, US) and after a 2 hour incubation step, membranes were washed and protein complexes visualised (Immobilon Western chemiluminescent substrate, Millipore, US). Membrane were stripped and probed for β -actin (to confirm equal loading) as previously described (8,18). Images were captured using the Fujifilm LAS-3000 imager, and densitometric analysis was used to quantify expression of the proteins. Values are presented as mean \pm SEM, normalised to β -actin.

Hippocampal slice preparation and LTP recording

Acute hippocampal slices (400µm) from C57BL/6 and CD200^{-/-} mice were prepared using a McIlwain tissue chopper as previously described (18), and maintained in oxygenated artificial cerebrospinal fluid (aCSF; composition in mM: 125 NaCl, 1.25 KCl, 2 CaCl₂, 1.5 MgCl₂, 1.25 KH₂PO₄, 25 NaHCO₃, and 10 D-glucose), at room temperature (21-23°C) in a holding chamber for a minimum of 1 hour before being transferred to a submersion recording chamber. Slices were continuously perfused (2-3ml/min) with oxygenated aCSF at room temperature (21-23°C). The Schaffer collateral-commissural pathway was stimulated at 0.033Hz (0.1ms duration; 30-50% of maximal EPSP amplitude) using a bipolar tungsten stimulation electrode (Advent Materials). Stable

field excitatory postsynaptic potentials (EPSPs) were recorded from the CA1 stratum radiatum using a monopolar glass recording electrode filled with aCSF. We assessed input-output response and paired pulse facilitation to evaluate neurotransmission at CA1 synapses, and found that there were no differences between slices obtained from wildtype and CD200^{-/-} mice. In addition there was no evidence of epileptiform activity in any slice. Stable baseline EPSPs were recorded for 20 min prior to application of theta-burst stimulation [TBS; 10 trains (4 pulses at 100 Hz) repeated at 5 Hz, (18)]. In some experiments, LPS (Alexis Biochemicals, Switzerland) or Pam₃Csk₄ (InvivoGen, US) was added to the perfusate (10 µg/ml x 20 min, or 20 µg/ml x 60 min) prior to TBS. In an additional set of experiments, slices were perfused with mouse recombinant TNFα (R & D Systems, UK; 3 ng/ml in 0.002% BSA) or vehicle alone (0.002% BSA), for 20 min prior to LTP induction. This concentration of TNFα is less than that previously demonstrated to impair LTP in hippocampal slices prepared from rat (19,20). Data were acquired using WinWCP v4.0.7 software (Dr J. Dempster, Strathclyde, UK). Evoked EPSPs were normalised to the slope recorded in the 5 min period prior to LTP induction. The level of LTP was evaluated as the mean % EPSP slope during the last 5 min of recording and data are presented as mean % EPSP slope ± SEM.

Hippocampal slices not used for electrophysiology were prepared for western immunoblot analysis of IL-1α, IL-1β and TNFα expression (described above). These slices were incubated as described for a minimum of 1 hour following the slicing procedure, plus a further incubation period equivalent to the duration of LTP recording.

Statistical analysis.

Data were analyzed using either Student's t-test for independent means, or analysis of variance (ANOVA) followed by post hoc Student Newman-Keuls test to determine which conditions were significantly different from each other. Data are expressed as means with standard errors.

RESULTS

Loss of CD200 has been associated with evidence of increased inflammatory changes in hippocampal tissue prepared from aged animals as well as LPS- and Aβ-treated animals and LPS (8,21). In this study, the effect of the TLR4 and TLR2 agonists, LPS and Pam₃Csk₄, were assessed on cytokine production in mixed glia prepared from wildtype and CD200^{-/-} mice. The data indicate that incubation of cells prepared from wildtype mice in the presence of LPS (100 ng/ml) increased release of the proinflammatory cytokines, IL-1β, IL-6 and TNFα and the effect was significant in the case of IL-6 and TNFα (**p < 0.001; ANOVA; Figure 1a-c). The effect of LPS was significantly greater in cells prepared from CD200^{-/-} mice (***p < 0.001; ANOVA; Figure 1). Incubation of mixed glia prepared from wildtype mice in the presence of Pam₃Csk₄ (100 ng/ml) also significantly increased release of inflammatory cytokines (**p < 0.01; ***p < 0.001; ANOVA; Figure 1d-f). The effect of Pam₃Csk₄ was greater in mixed glia prepared from CD200^{-/-} mice and this was statistically significant in the case of IL-6 and TNFα (***p < 0.001; wildtype vs CD200^{-/-}; ANOVA). Both LPS and Pam₃Csk₄ also increased mRNA expression of these inflammatory cytokines and the effect was greater in cells prepared from CD200^{-/-} mice (data not shown). These data indicate that tonic activation by CD200 modulates cytokine release from glia. Analysis of the effect of LPS on cytokine release prepared from purified microglia obtained from wildtype and CD200^{-/-} mice revealed no genotype-related change for IL-1β (99.64 ± 26.52 pg/ml vs 62.89 ± 6.47 pg/ml for wildtype and CD200^{-/-} cells respectively), IL-6 (3837 ± 171.8 vs 3875 ± 144.8) and TNFα (1559 ± 88.31 vs 1533 ± 204.5). This is consistent with the view that isolated microglia prepared from CD200^{-/-} mice are unaffected, whereas when cultured with astrocytes which are deficient in CD200, an activated phenotype is evident.

Using CD11b as a marker of microglia, we show that the number of CD11b⁺ MHCII⁺ cells and CD11b⁺ CD40⁺ cells was increased in a mixed glial population prepared from CD200^{-/-}, compared with wildtype, mice (Figure 2). These data suggest that CD200 contributes to maintenance of microglia (in a mixed glial preparation) in a quiescent state and therefore suggests that CD200 is expressed on astrocytes. To date, its expression

on astrocytes has been reported only on reactive astrocytes in lesions from postmortem brains of individuals with multiple sclerosis (7). Here, flow cytometry was used to evaluate CD200 expression on GLAST⁺ cells in a purified culture of astrocytes prepared from wildtype and CD200^{-/-} mice (Figure 3a,b). Whereas CD200 expression was evident on GLAST⁺ cells prepared from wildtype mice, expression was absent on GLAST⁺ cells prepared from CD200^{-/-} mice. To confirm astrocytic expression of CD200, purified astrocytes were used to prepare membrane and cytosolic fractions for analysis by Western immunoblotting. CD200 was evident in membrane, but not cytosolic, fractions (Figure 3c) whereas GFAP expression was, predictably, largely confined to the cytosolic fractions.

A possible explanation for the increase in responsiveness of cells from CD200^{-/-} mice to LPS and Pam₃Csk₄ is the significant increase in expression of both TLR2 and TLR4 mRNA in mixed glia prepared from CD200^{-/-}, compared with wildtype, mice (*p < 0.05; student's t-test for independent means; Figure 4a and d). Flow cytometric analysis demonstrated that cell surface expression of both receptors was increased on CD11b⁺ cells obtained from CD200^{-/-}, compared with wildtype, mice, but the increase was significant only in the case of TLR2 (**p < 0.01; student's t-test for independent means; Figure 4b,c,e,f). The significant increase in phosphorylated I κ B α in cells prepared from CD200^{-/-}, compared with wildtype, mice (*p < 0.05; student's t-test for independent means; Figure 4g) indicates that signalling through TLR is upregulated in cells prepared from CD200^{-/-} mice.

CD200 deficiency is accompanied by inflammatory changes (9,10) and, in the brain, microglial activation is coupled with decreased CD200 in brains of aged animals and also in LPS-treated and A β -treated animals (8,21). To investigate this correlation further, we evaluated expression of surface markers of microglial activation on cells prepared from CD200^{-/-} and wildtype mice using PCR and flow cytometry, and show that CD40 mRNA, although not CD11b mRNA, was significantly increased in tissue prepared from CD200^{-/-}, compared with wildtype, mice (*p < 0.05; student's t-test for independent means; Figure 5a,b). Analysis by flow cytometry indicated that there was no genotype-related

change in CD11b⁺ cells (Figure 5c) but the percentage of CD11b⁺ cells which were positive for MHCII and CD40 was significantly increased (*p < 0.05; ***p < 0.001; student's t-test for independent means; Figure 5d-g).

CD45 has been used as a means of discriminating between macrophages (which express high levels of CD45) and microglial (which express low levels of CD45 (22)). Flow cytometric analysis revealed that the numbers of CD11b⁺ CD45^{low} cells were significantly increased in hippocampus of CD200^{-/-}, compared with wildtype, mice (***p < 0.001; student's t-test for independent means; Figure 6a) and that CD200R expression (b), CD40 (c), TLR2 (d) and TLR4 (f) on these cells was greater in tissue prepared from CD200^{-/-}, compared with wildtype, mice. The numbers of macrophages in the brain (i.e. CD11b⁺ CD45^{high} cells) were negligible in CD200^{-/-} and wildtype mice. Analysis of expression of TLR in hippocampus revealed that both TLR2 and 4 were increased in CD200^{-/-}, compared with wildtype, mice (*p < 0.05; **p < 0.01; student's t-test for independent means; Figure 6e,g). These changes indicate that microglial activation occurs in brain tissue of CD200^{-/-} mice and therefore the changes *in vitro* are reflected *in vivo*, although the increase in expression of TLR2 mRNA in hippocampus is markedly greater than the change observed in cultured cells. Significantly, this was accompanied by a deficit in LTP in CA1 synapses where the response, 60 min following application of TBS, was markedly reduced in slices prepared from CD200^{-/-} mice (12 slices from 7 mice) compared with wildtype mice (15 slices from 11 mice; p < 0.001; unpaired Student's t-test; Figure 6h). Although a number of inflammatory cytokines released from activated microglia might exert this effect (17-21), here we show that whereas expression of IL-1 α and IL-1 β were similar in hippocampal tissue prepared from wildtype and CD200^{-/-} mice (Figure 7a,b), TNF α was increased (p < 0.05; student's t-test for independent means; Figure 7c). As previously demonstrated in hippocampal slices prepared from rats (19,20,23), application of TNF α (3 ng/ml) to mouse hippocampal slices significantly impaired LTP relative to vehicle controls (p < 0.05; unpaired Student's t-test; 3 slices from 2 mice; Figure 7d).

Since cells prepared from CD200^{-/-} mice showed increased susceptibility to LPS, we

predicted that concentrations of LPS which exerted no effect on LTP in wildtype mice may attenuate it in CD200^{-/-} mice. Application of LPS (20 µg/ml) to hippocampal slices from wildtype mice for 60 min prior to TBS inhibited LTP (5 slices from 5 mice) compared with controls (15 slices from 11 mice; $p < 0.001$; Figure 8a). In contrast, a lower concentration of LPS (10 µg/ml; 20 min pre-treatment) which exerted no effect on LTP in slices prepared from wildtype mice (7 slices from 6 mice; Figure 8b) significantly decreased LTP in slices from CD200^{-/-} mice (13 slices from 9 mice) relative to control (12 slices from 7 mice; $p < 0.05$; Figure 8c).

Like LPS, Pam₃Csk₄ exerted a greater effect on inflammatory markers in cells prepared from CD200^{-/-} mice, and therefore we predicted that its effect on LTP would be genotype-specific. Application of Pam₃Csk₄ (20 µg/ml) to hippocampal slices prepared from wildtype mice for 60 min prior to TBS inhibited LTP (3 slices from 3 mice) compared with untreated controls (15 slices from 11 mice; $p < 0.001$; Figure 9a). A lower concentration of Pam₃Csk₄ (10 µg/ml), applied for 20 min prior to TBS, did not affect LTP in slices prepared from wildtype mice (4 slices from 3 mice; Figure 9b), but significantly reduced LTP in slices prepared from CD200^{-/-} mice (6 slices from 5 mice) compared with control (12 slices from 7 mice; $p < 0.05$; Figure 9c).

DISCUSSION

The loss of CD200 has a significant impact on activation of microglia in response to inflammatory stimuli, probably because of increased expression of TLR4 and TLR2 *in vitro* and *in vivo*. Whereas LTP in Schaffer collateral-CA1 synapses was markedly impaired in slices prepared from CD200-deficient mice under control conditions, activation of TLR4 and TLR2, by LPS and Pam₃Csk₄ respectively, exerted a more profound effect on LTP in slices prepared from CD200^{-/-} mice. We propose that the increased expression of TLR4 and TLR2 provides a plausible explanation for the increased responsiveness of CD200^{-/-} mice to inflammatory stimuli.

LPS and Pam₃Csk₄ increased the release of proinflammatory cytokines, IL-1β, IL-6 and TNFα

from mixed glial cultures, confirming previously-described effects of TLR4 and TLR2 (21,24,25). Both agonists exerted a greater effect on release of proinflammatory cytokines in mixed glia prepared from CD200^{-/-} mice, compared with wildtype mice. Thus tonic activation of CD200 receptor by CD200 is required to modulate inflammatory cytokine production. This concurs with data indicating that the interaction of neurons and microglia by means of CD200 receptor engagement by CD200 decreased microglial activation and production of IL-1β (8). In the current study in which a mixed glial preparation was used, we propose that the modulating effect is a consequence of the interaction between microglia and astrocytes, which we demonstrate express CD200. It is known that CD200 is widely expressed on numerous cell types although, in the case of astrocytes, expression to date has been reported only on reactive astrocytes in lesions from postmortem brains of individuals with multiple sclerosis (7). An interesting possibility is that the relatively activated state of microglia in a purified microglial culture may be a consequence of the loss of the CD200-controlled modulating effect of astrocytes.

The present findings in glia mirror those observed in peritoneal macrophages; thus stimulation with LPS and peptidoglycan, and also poly I:C, increased release of TNFα and IL-6 to a greater extent in macrophages prepared from CD200^{-/-} mice compared with wildtype mice (26). Similarly alveolar macrophages prepared from CD200^{-/-} mice, when stimulated *ex vivo* with LPS or IFNγ, expressed more MHCII and released more inflammatory cytokines than macrophages from wildtype mice (27). It has been known for many years that astrocytes are capable of modulating microglial/macrophage function. They have been shown to modulate LPS-induced changes in inducible nitric oxide synthase and NO production (28,29) and expression of MHCII (30); effects which have been attributed to astrocytic release of soluble factors like transforming growth factor (TGF)β. The present findings uncover another mechanism by which astrocytes can modulate microglial activation.

Several studies have established that responses to insults which induce inflammatory changes are exacerbated in CD200^{-/-} mice. Thus the symptoms and inflammation associated with experimental

autoimmune encephalomyelitis, *Toxoplasma* encephalitis, experimental autoimmune uveoretinitis, collagen-induced arthritis and facial nerve transection and are more profound in CD200-deficient mice (9,10,31). In addition, the response to an influenza dose of haemagglutination was much more severe (inducing some fatalities) in CD200-deficient, compared with wildtype, mice (27). Although it has been shown that CD200R activation by a CD200Fc ameliorates the symptoms associated with these conditions, and although CD200R-mediated regulation of macrophages relies on the binding of dok2 to the PTB binding motif in the cytoplasmic region of CD200R and the subsequent recruitment and activation of RasGAP (32), the mechanism by which these changes lead to dampening the activation of macrophage/microglia remains to be fully explained. In this study we show that increased expression of both TLR4 and TLR2 was observed in glia prepared from CD200^{-/-} mice and this may, at least in part, provide an explanation for the susceptibility of CD200^{-/-} mice to inflammatory stimuli. Both TLR2 and TLR4 ultimately lead to activation of NFκB and, in this study, the increased receptor expression in glia prepared from CD200^{-/-} mice is coupled with increased expression of phosphorylated IκB, which is indicative of NFκB activation. These changes clearly provide one possible explanation for the increased responsiveness of these cells to LPS and Pam₃Csk₄ in the present study, and perhaps also in other models.

Loss of CD200 increases expression of markers of microglial activation in mixed glial cultures; CD200 deficiency was associated with enhanced expression of both CD40 and CD68 mRNA, although not CD11b mRNA. In parallel, flow cytometry revealed that these markers, and also MHCII, were increased on CD11b-positive cells prepared from CD200^{-/-} mice. Previous studies have highlighted the importance of the interaction between CD200 and CD200R in maintaining the quiescent state of microglia, and have revealed that the age-related and Aβ-induced increases in microglial activation are coupled with decreased CD200 expression on neurons (8,14,21). The present observations also concur with the findings that under resting conditions, spinal cord microglia adopt an inflammatory morphology expressing more CD11b (9) and the number of CD45⁺CD11b⁺

cells prepared from retina of CD200^{-/-} mice was increased (10).

In the past decade it has become clear that neuroinflammatory changes, coupled with increased microglial activation, negatively affect synaptic plasticity in aged, LPS-treated and Aβ-treated rats (15,33-35). These observations are corroborated in this study where we directly associate the loss of CD200 with microglial activation and a deficit in LTP. The evidence indicates that slices prepared from CD200^{-/-} mice do not display LTP to the same degree as slices prepared from wildtype mice. One possible explanation for this is that TNFα, which is increased in hippocampal tissue prepared from these mice, is released from activated microglia and inhibits LTP. We demonstrate that TNFα inhibits TBS-induced LTP in mouse Schaffer collateral-CA1 synapses, which concurs with previous evidence indicating that it exerts a similar effect on tetanus-induced LTP in rats, *in vitro* and *in vivo* (17,19,23).

In addition to the decrease in LTP observed in untreated slices prepared from CD200^{-/-} mice, the data indicate that a subthreshold concentration of LPS or Pam₃Csk₄, which exerts minimal effects on LTP in wildtype mice, markedly impairs LTP in slices prepared from CD200^{-/-} mice. These findings show for the first time that activation of TLR2 leads to inhibition of LTP and further emphasizes the protective effect of CD200-CD200R interaction such that a deficit in CD200 leads to increased susceptibility to inflammatory stimuli. At this point it is unclear whether the effects of LPS or Pam₃Csk₄ on LTP are secondary to changes in glia, or are a consequence of a direct effect on neuronal TLR4 and TLR2. In this regard it is important to note that while some groups have reported neuronal expression of most TLRs both *in vitro* and *in vivo* (36),(37), others have been unable to demonstrate expression of TLR2 on neurons (38). The implication of this finding for the present study is that the mechanism underlying the Pam₃Csk₄-induced depression in LTP may result from its ability to release IL-1β, IL-6 and TNFα from glia; each of these inflammatory cytokines has been shown to inhibit LTP (17,39,40).

While there is an accumulating body of evidence indicating that CD200 deficiency is associated with increased inflammatory changes in several tissues including the brain, the effect on

neuronal function is relatively unexplored. Here we report that activation of TLR4 and 2 exacerbates neuroinflammatory changes in the absence of CD200 and, importantly, demonstrate that CD200 deficiency also exerts a negative effect on LTP. A key factor underlying these changes is

increased expression of these receptors. The findings highlight the importance of CD200 as a potential therapeutic target in disorders which are characterised by neuroinflammatory changes, coupled with loss of synaptic function.

REFERENCES

1. Barclay, A. N. (1981) *Immunology* **44**, 727-736
2. Pallasch, C. P., Ulbrich, S., Brinker, R., Hallek, M., Uger, R. A., and Wendtner, C. M. (2009) *Leuk Res* **33**, 460-464
3. Siva, A., Xin, H., Qin, F., Oltean, D., Bowdish, K. S., and Kretz-Rommel, A. (2008) *Cancer Immunol Immunother* **57**, 987-996
4. Gorczynski, R. M., Yu, K., and Clark, D. (2000) *J Immunol* **165**, 4854-4860
5. Rosenblum, M. D., Olasz, E., Woodliff, J. E., Johnson, B. D., Konkol, M. C., Gerber, K. A., Orentas, R. J., Sandford, G., and Truitt, R. L. (2004) *Blood* **103**, 2691-2698
6. Barclay, A. N., Wright, G. J., Brooke, G., and Brown, M. H. (2002) *Trends Immunol* **23**, 285-290
7. Koning, N., Swaab, D. F., Hoek, R. M., and Huitinga, I. (2009) *J Neuropathol Exp Neurol* **68**, 159-167
8. Lyons, A., Downer, E. J., Crotty, S., Nolan, Y. M., Mills, K. H., and Lynch, M. A. (2007) *J Neurosci* **27**, 8309-8313
9. Hoek, R. M., Ruuls, S. R., Murphy, C. A., Wright, G. J., Goddard, R., Zurawski, S. M., Blom, B., Homola, M. E., Streit, W. J., Brown, M. H., Barclay, A. N., and Sedgwick, J. D. (2000) *Science* **290**, 1768-1771
10. Broderick, C., Hoek, R. M., Forrester, J. V., Liversidge, J., Sedgwick, J. D., and Dick, A. D. (2002) *Am J Pathol* **161**, 1669-1677
11. Gorczynski, R. M., Chen, Z., Yu, K., and Hu, J. (2001) *Clin Immunol* **101**, 328-334
12. Gorczynski, R. M., Chen, Z., Lee, L., Yu, K., and Hu, J. (2002) *Clin Immunol* **104**, 256-264
13. Chitnis, T., Imitola, J., Wang, Y., Elyaman, W., Chawla, P., Sharuk, M., Raddassi, K., Bronson, R. T., and Khoury, S. J. (2007) *Am J Pathol* **170**, 1695-1712
14. Downer, E. J., Cowley, T. R., Lyons, A., Mills, K. H., Berezin, V., Bock, E., and Lynch, M. A. *Neurobiol Aging* **31**, 118-128
15. Lynch, A. M., Loane, D. J., Minogue, A. M., Clarke, R. M., Kilroy, D., Nally, R. E., Roche, O. J., O'Connell, F., and Lynch, M. A. (2007) *Neurobiol Aging* **28**, 845-855
16. Nolan, Y., Maher, F. O., Martin, D. S., Clarke, R. M., Brady, M. T., Bolton, A. E., Mills, K. H., and Lynch, M. A. (2005) *J Biol Chem* **280**, 9354-9362
17. Cowley, T. R., O'Sullivan, J., Blau, C., Deighan, B. F., Jones, R., Kerskens, C., Richardson, J. C., Virley, D., Upton, N., and Lynch, M. A. *Neurobiol Aging*
18. Costello, D. A., Watson, M. B., Cowley, T. R., Murphy, N., Murphy Royal, C., Garlanda, C., and Lynch, M. A. (2011) *J Neurosci* **31**, 3871-3879
19. Butler, M. P., O'Connor, J. J., and Moynagh, P. N. (2004) *Neuroscience* **124**, 319-326
20. Cunningham, A. J., Murray, C. A., O'Neill, L. A., Lynch, M. A., and O'Connor, J. J. (1996) *Neurosci Lett* **203**, 17-20

21. Lyons, A., McQuillan, K., Deighan, B. F., O'Reilly, J. A., Downer, E. J., Murphy, A. C., Watson, M., Piazza, A., O'Connell, F., Griffin, R., Mills, K. H., and Lynch, M. A. (2009) *Brain Behav Immun*
22. Carson, M. J., Reilly, C. R., Sutcliffe, J. G., and Lo, D. (1998) *Glia* **22**, 72-85
23. Tancredi, V., D'Arcangelo, G., Grassi, F., Tarroni, P., Palmieri, G., Santoni, A., and Eusebi, F. (1992) *Neurosci Lett* **146**, 176-178
24. Lin, H. Y., Tang, C. H., Chen, J. H., Chuang, J. Y., Huang, S. M., Tan, T. W., Lai, C. H., and Lu, D. Y. (2010) *J Cell Physiol*
25. Lotz, M., Ebert, S., Esselmann, H., Iliev, A. I., Prinz, M., Wiazewicz, N., Wiltfang, J., Gerber, J., and Nau, R. (2005) *J Neurochem* **94**, 289-298
26. Mukhopadhyay, S., Pluddemann, A., Hoe, J. C., Williams, K. J., Varin, A., Makepeace, K., Akin, M. L., Bowdish, D. M., Smale, S. T., Barclay, A. N., and Gordon, S. *Cell Host Microbe* **8**, 236-247
27. Snelgrove, R. J., Goulding, J., Didierlaurent, A. M., Lyonga, D., Vekaria, S., Edwards, L., Gwyer, E., Sedgwick, J. D., Barclay, A. N., and Hussell, T. (2008) *Nat Immunol* **9**, 1074-1083
28. Vincent, V. A., Tilders, F. J., and Van Dam, A. M. (1997) *Glia* **19**, 190-198
29. Vincent, V. A., Van Dam, A. M., Persoons, J. H., Schotanus, K., Steinbusch, H. W., Schoffemeer, A. N., and Berkenbosch, F. (1996) *Glia* **17**, 94-102
30. Hailer, N. P., Heppner, F. L., Haas, D., and Nitsch, R. (1998) *Brain Pathol* **8**, 459-474
31. Deckert, M., Sedgwick, J. D., Fischer, E., and Schluter, D. (2006) *Acta Neuropathol (Berl)* **111**, 548-558
32. Mirshahi, R., Barclay, A. N., and Brown, M. H. (2009) *J Immunol* **183**, 4879-4886
33. Hauss-Wegrzyniak, B., Lynch, M. A., Vraniak, P. D., and Wenk, G. L. (2002) *Exp Neurol* **176**, 336-341
34. Rosi, S., Vazdarjanova, A., Ramirez-Amaya, V., Worley, P. F., Barnes, C. A., and Wenk, G. L. (2006) *Neuroscience* **142**, 1303-1315
35. Griffin, R., Nally, R., Nolan, Y., McCartney, Y., Linden, J., and Lynch, M. A. (2006) *J Neurochem* **99**, 1263-1272
36. Tang, S. C., Arumugam, T. V., Xu, X., Cheng, A., Mughal, M. R., Jo, D. G., Lathia, J. D., Siler, D. A., Chigurupati, S., Ouyang, X., Magnus, T., Camandola, S., and Mattson, M. P. (2007) *Proc Natl Acad Sci U S A* **104**, 13798-13803
37. Mishra, B. B., Mishra, P. K., and Teale, J. M. (2006) *J Neuroimmunol* **181**, 46-56
38. Lehnardt, S., Henneke, P., Lien, E., Kasper, D. L., Volpe, J. J., Bechmann, I., Nitsch, R., Weber, J. R., Golenbock, D. T., and Vartanian, T. (2006) *J Immunol* **177**, 583-592
39. Tancredi, V., D'Antuono, M., Cafe, C., Giovedi, S., Bue, M. C., D'Arcangelo, G., Onofri, F., and Benfenati, F. (2000) *J Neurochem* **75**, 634-643
40. Murray, C. A., and Lynch, M. A. (1998) *J Neurosci* **18**, 2974-2981

FIGURE LEGENDS

Figure 1. TLR2- and TLR4-induced increases in inflammatory cytokines are enhanced in glia prepared from CD200^{-/-} mice.

Incubation of mixed glia prepared from wildtype mice in the presence of LPS (100 ng/ml; a-c) or Pam₃Csk₄ (Pam; 100 ng/ml; d-f) increased supernatant concentrations of IL-1 β , IL-6 and TNF α (a-c; ***p < 0.001;

ANOVA; $n=6-8$) and the effect of LPS and Pam₃Csk₄ was significantly greater in cells prepared from CD200^{-/-} mice (⁺⁺⁺ $p < 0.001$; ANOVA; $n = 4$).

Figure 2. MHCII⁺ CD11b⁺ and CD40⁺ CD11b⁺ cells are increased in glia prepared from CD200^{-/-} mice. The mean percentage CD11b⁺ cells which also stained positively for MHCII⁺ (top panels) and CD40 (lower panels). Data is presented as target proteins versus side scatter (SSC). Right hand panels illustrate representative overlays.

Figure 3. CD200 is expressed on astrocytes. CD200 expression was observed on GLAST⁺ cells from purified astrocytic cultures obtained from wildtype (a) but not CD200^{-/-} (b) mice. CD200 was observed in membrane, but not cytosolic, fractions prepared from purified astrocytes obtained from wildtype mice. GFAP expression was observed in the cytosolic fraction (c).

Figure 4. Expression of TLR2 and TLR4 is increased in glia prepared from CD200^{-/-} mice. TLR4 mRNA (a) and TLR2 mRNA (d) and the number of CD11b⁺ cells which stained positively for TLR4 (b,c) and TLR2 (e,f) were increased in glia prepared from CD200^{-/-}, compared with wildtype, mice ($*p < 0.05$; student's t-test for independent means; $n = 5$). (g) A sample immunoblot and mean data from densitometric analysis reveal that phosphorylated I κ B α is increased in cells prepared from CD200^{-/-}, compared with wildtype, mice ($*p < 0.05$; student's t-test for independent means; $n = 4-6$).

Figure 5. Markers of microglial activation are increased in cells prepared from CD200^{-/-} mice. (a,b) Expression of CD40 mRNA, but not CD11b mRNA, was significantly greater in mixed glia prepared from CD200^{-/-}, compared with wildtype, mice ($*p < 0.05$; student's t-test for independent means; $n=4-5$). (c-f) Flow cytometric analysis revealed that the percentage of CD11b⁺ cells was similar in wildtype and CD200^{-/-} (c) but the percentage of CD11b⁺ cells which also stained positively for CD40 (d,e) and MHCII (f,g) was significantly greater in mixed glia obtained from CD200^{-/-}, compared with wildtype, mice ($*p < 0.05$; $***p < 0.001$; student's t-test for independent means; $n=4-8$).

Figure 6. The increase in hippocampal expression of TLR2 and TLR4 in CD200^{-/-} mice is coupled with a deficit in LTP.

(a) Greater numbers of CD11b⁺CD45^{low} cells were found in hippocampus of CD200^{-/-}, compared with wildtype, mice ($***p < 0.001$; student's t-test for independent means) and expression of CD200R expression (b) and CD40 (c) was greater in tissue prepared from CD200^{-/-}, compared with wildtype, mice. TLR2 (d) and TLR4 (f) expression on CD11b⁺CD45^{low} cells was greater in tissue prepared from CD200^{-/-}, compared with wildtype, mice, while TLR2 mRNA (e) and TLR4 mRNA (g) expression were significantly increased in hippocampal tissue prepared from CD200^{-/-}, compared with wildtype, mice ($*p < 0.05$; $**p < 0.01$; student's t-test for independent means; $n = 5$). (h) Theta-burst stimulation (TBS; arrow) induced LTP in CA1 synapses of hippocampal slices prepared from wildtype mice (15 slices from 11 mice). LTP, measured as mean % EPSP slope in the last 5 min of the experiment, was significantly reduced in slices prepared from CD200^{-/-} mice relative to wildtype mice ($p < 0.001$; 12 slices from 7 mice). Sample recordings immediately before, and 60 min following TBS are shown for wildtype and CD200^{-/-} mice (scale bars: 1mV/20ms).

Figure 7. Increased hippocampal expression of TNF α in CD200^{-/-} mice may underlie the associated deficit in LTP.

IL-1 α and IL-1 β were similar in tissue prepared from wildtype and CD200^{-/-} mice (a,b) but TNF α was significantly increased ($p < 0.05$; student's t-test for independent means; c) as revealed by sample immunoblots and analysis of densitometric data. Application of TNF α (3 ng/ml) to hippocampal slices significantly impaired LTP relative to vehicle controls ($p < 0.05$; unpaired Student's t-test; 3 slices from 2 mice; d). Sample EPSP traces immediately prior to, and 60 min following TBS are presented (scale bars: 1mV/20ms).

Figure 8. LTP is attenuated by LPS in CD200^{-/-} mice

(a) Perfusion of LPS (20 $\mu\text{g}/\text{ml}$) for 60 min prior to TBS (arrow) decreased LTP in slices prepared from wildtype mice (5 slices from 5 mice) and the mean % EPSP slope in the last 5 min of the experiment was significantly decreased compared with control slices ($p < 0.0001$; 15 slices from 11 mice). (b and c) LTP in slices prepared from wildtype mice was unaffected by perfusion of 10 $\mu\text{g}/\text{ml}$ LPS for 20 min prior to TBS (b; 7 slices from 6 mice relative to control 15 slices from 11 mice), but LTP was attenuated in slices from CD200^{-/-} mice (c; $p < 0.05$; 13 slices from 9 mice relative to control 12 slices from 7 mice). Sample EPSP traces immediately prior to, and 60 min following TBS are presented (scale bars: 1mV/20ms).

Figure 9. LTP is attenuated by Pam₃Csk₄ in CD200^{-/-} mice

(a) Perfusion of Pam₃Csk₄ (20 $\mu\text{g}/\text{ml}$) for 60 min prior to TBS (arrow) decreased LTP in slices prepared from wildtype mice (3 slices from 3 mice) and the mean % EPSP slope in the last 5 min of the experiment was significantly decreased compared with control slices (15 slices from 11 mice; $p < 0.001$). (b and c) LTP in slices prepared from wildtype mice was unaffected by perfusion of 10 $\mu\text{g}/\text{ml}$ Pam₃Csk₄ for 20 min prior to TBS (b; 4 slices from 3 mice relative to control 15 slices from 11 mice). However, LTP was attenuated in slices from CD200^{-/-} mice following treatment with 10 $\mu\text{g}/\text{ml}$ Pam₃Csk₄ (c; 6 slices from 5 mice relative to control 12 slices from 7 mice; $p < 0.05$). Sample EPSP traces immediately prior to, and 60 min following TBS are presented (scale bars: 1mV/20ms).

Acknowledgements: This work was funded by Science Foundation Ireland and The Health Research Board, Ireland. The authors wish to thank Dr Jonathon D. Sedgwick for the gift of CD200^{-/-} mice.

FIGURE 1

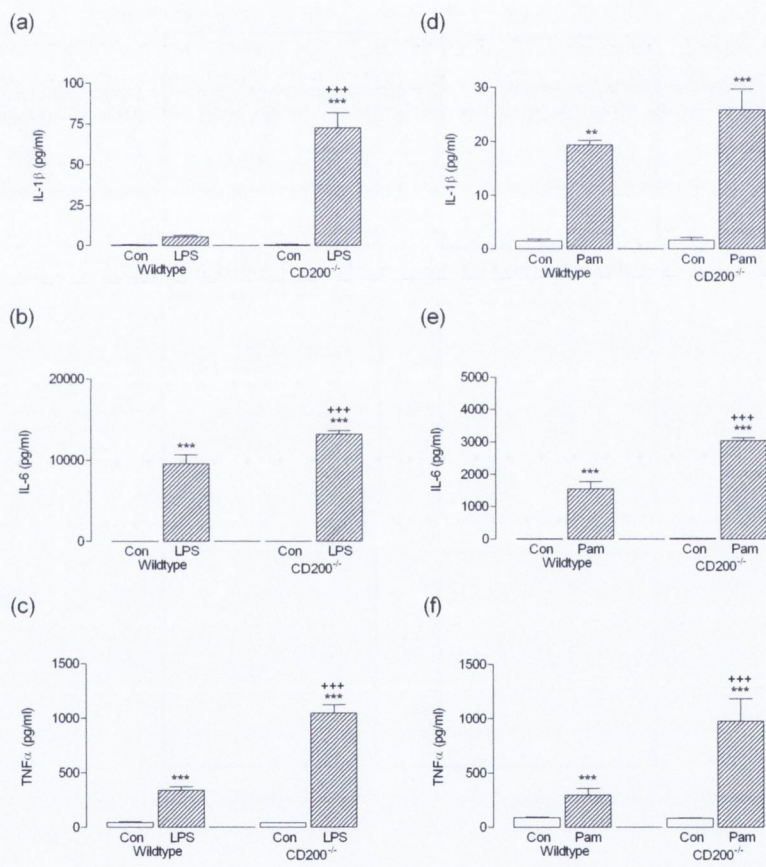


FIGURE 2

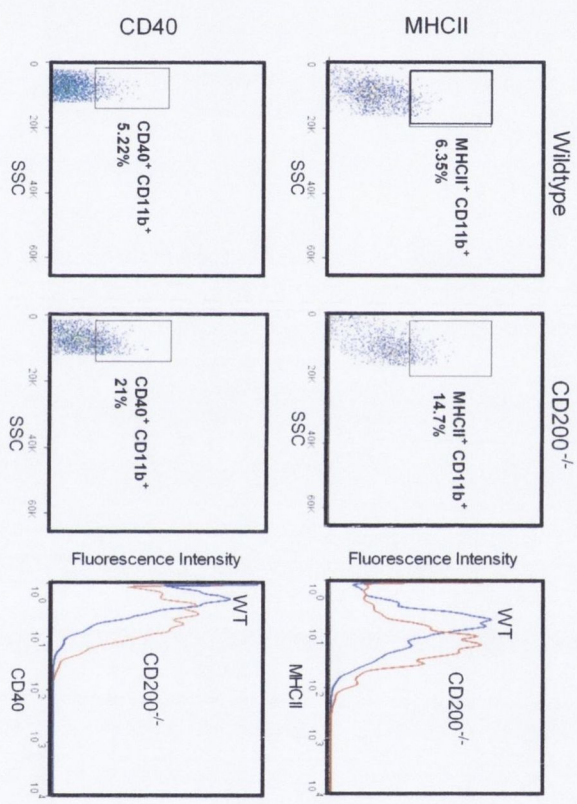
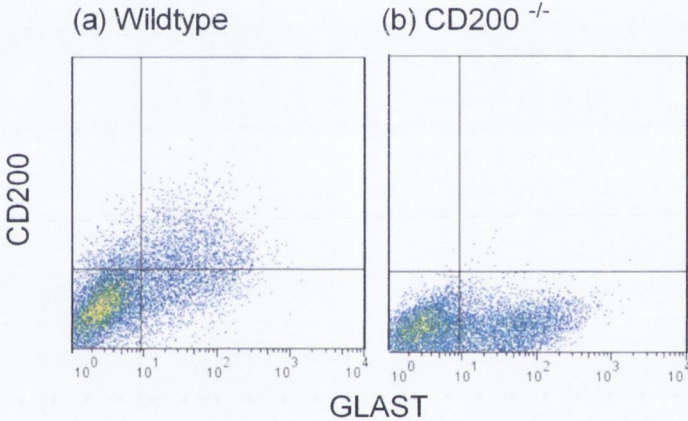


FIGURE 3



(c) Cultured astrocytes

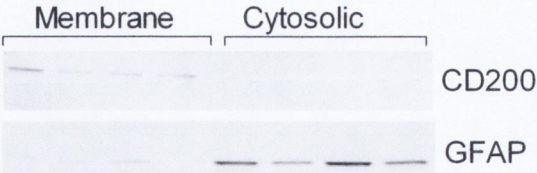


FIGURE 4

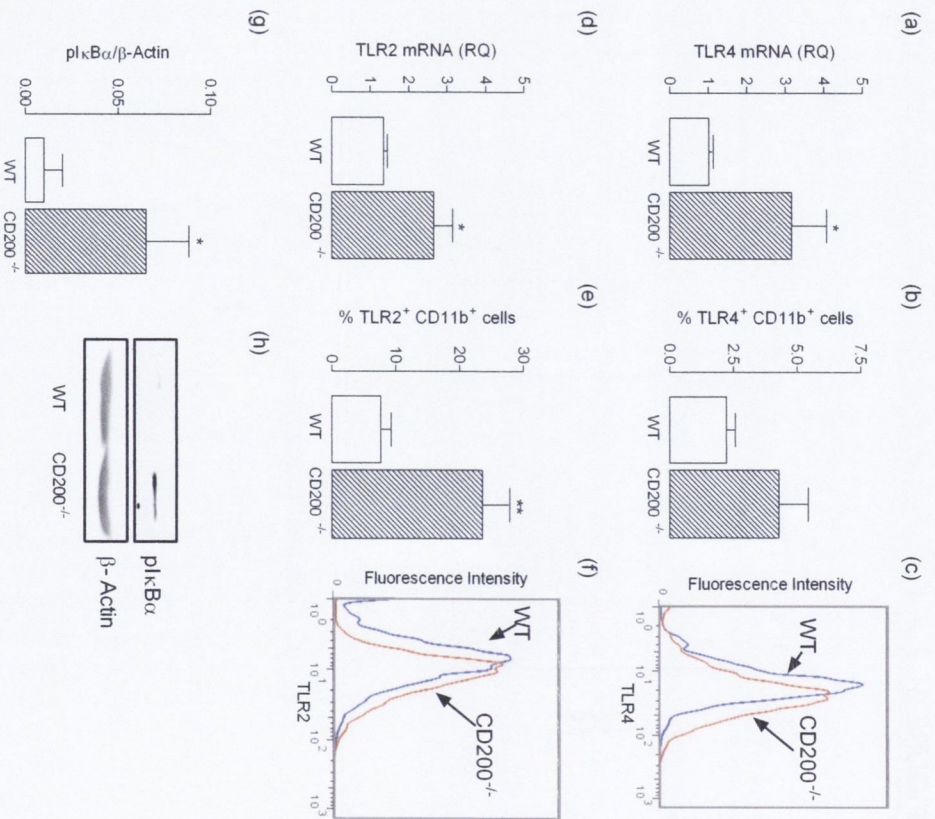


FIGURE 5

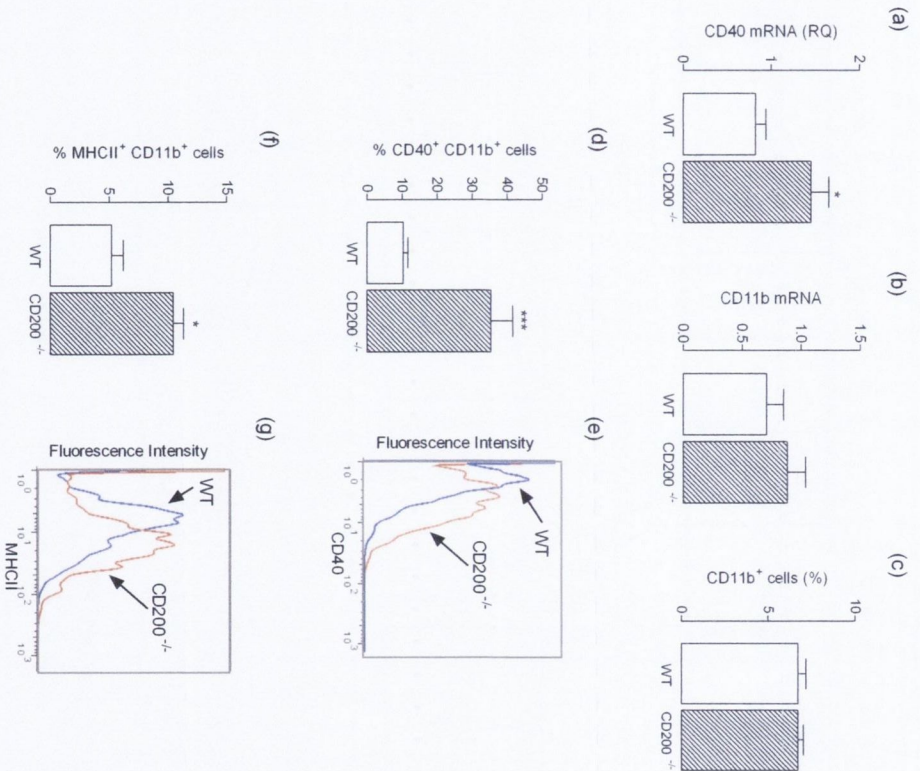


FIGURE 6

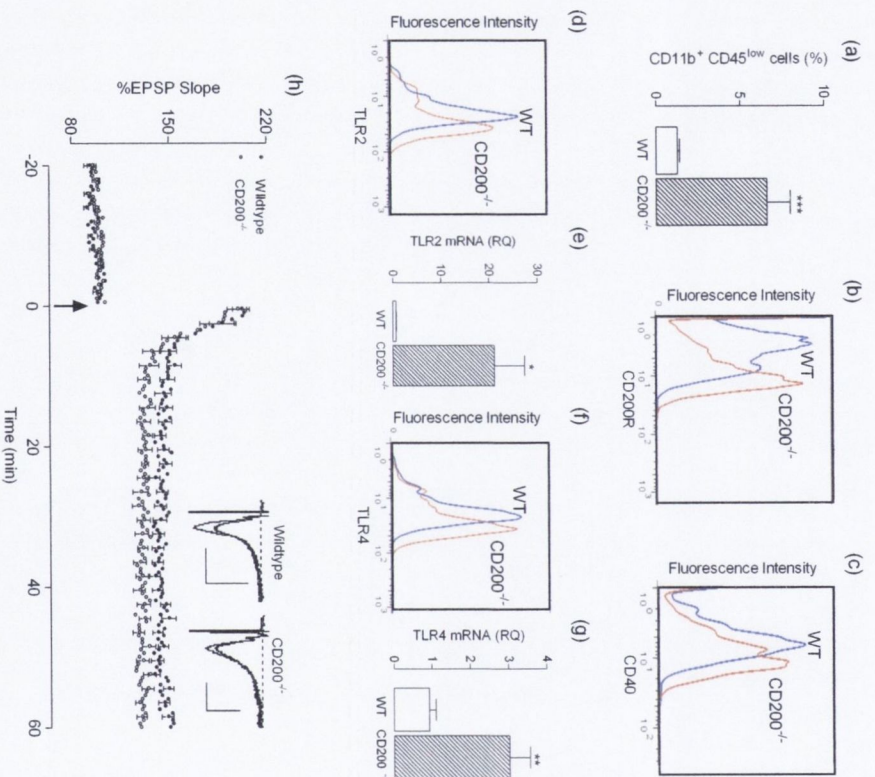


FIGURE 7

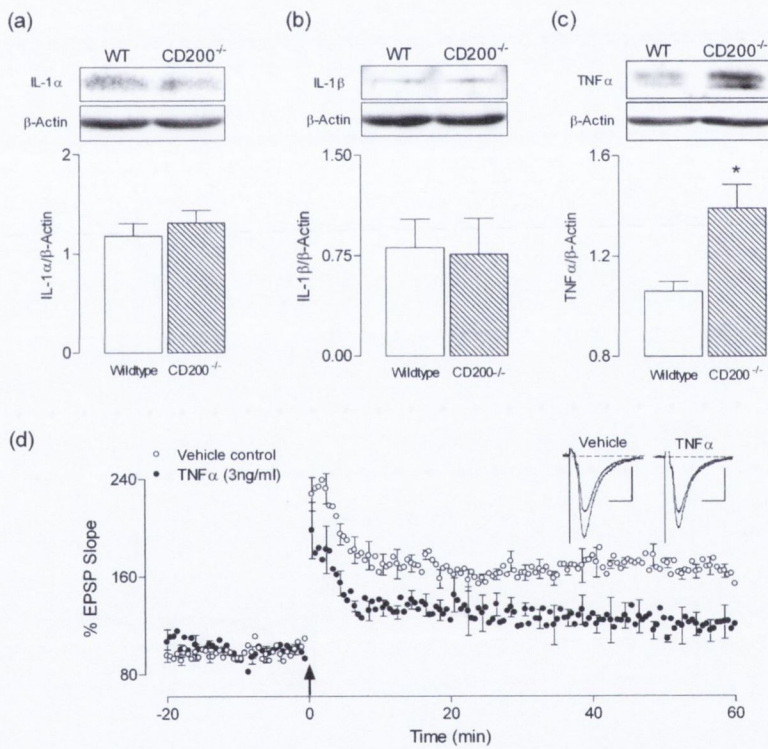


FIGURE 8

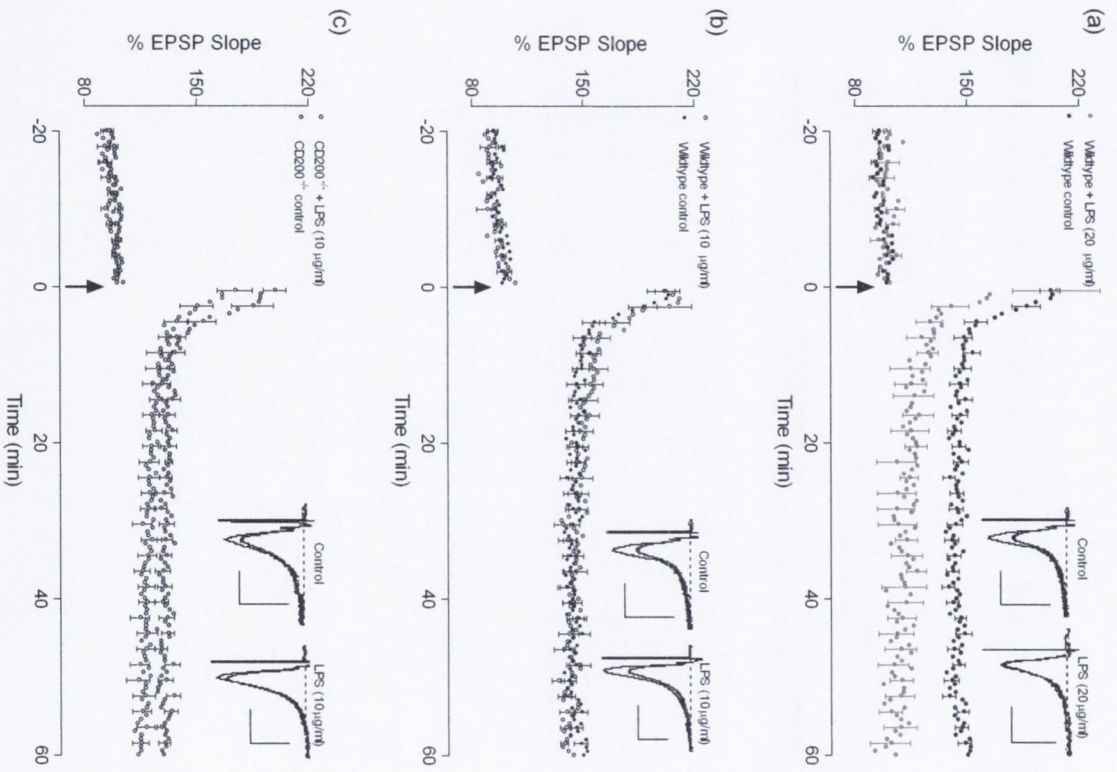


FIGURE 9

